Insights into the biogenesis of the human mitochondrial ribosomal large subunit

–

Characterisation of mL44 and mL45

Dissertation

for the award of the degree

"Doctor rerum naturalium"
of the Georg-August-Universität Göttingen

within the doctoral program: Biomolecules: Structure-Function-Dynamics
of the Georg-August University School of Science (GAUSS)

submitted by

Elisa Hanitsch

from Lutherstadt Wittenberg

Göttingen, 2020

Members of the Thesis Committee

Dr. Ricarda Richter-Dennerlein
(Supervisor and First Referee)

University Medical Center
Department of Cellular Biochemistry
Göttingen, Germany

Prof. Dr. Heike Krebber
(Second Referee)

Georg-August University of Göttingen
Institute for Microbiology and Genetics
Department of Molecular Genetics
Göttingen, Germany

Prof. Dr. Marina Rodnina
(Third Referee)

Max Planck Institute for Biophysical Chemistry
Department Physical Biochemistry
Göttingen, Germany

Members of the Examination Board

Prof. Dr. Michael Meinecke

University Medical Center
Department of Cellular Biochemistry
Göttingen, Germany

Prof. Dr. Ralph Kehlenbach

University Medical Center
Department of Molecular Biology
Göttingen, Germany

Prof. Dr. Henning Urlaub

Max Planck Institute for Biophysical Chemistry
Department Bioanalytical Mass Spectrometry Göttingen,
Germany

Date of oral examination: 04th November 2020

Table of Contents

List of Figures

List of Tables

Abbreviations

Table 1: Abbreviations

A	Adenine
Å	Ångström
A260	Absorbance at 260 nm
ADP	Adenosine diphosphate
AF	assembly factor
Ala	Alanine
Aqua dest.	Aqua destillata
ArfB	Alternative ribosome-rescue factor B
Arg	Arginine
Arg	Arginine
A-site	Aminoacyl - site
Asn	Asparagine
Asp	Aspartic acid
ATP	Adenosine triphosphate
bp	Base pair(s)
BSA	Bovine serum albumin
C	Cytosine
CP	Central protuberance
Cryo-EM	Cryogenic electron microscopy
C-terminus	Carboxyl-terminus
Cys	Cysteine
Del	Deletion
Dig.	Digitonin
DMEM	Dulbecco's modified Eagle's medium
DNA	deoxyribonucleic acid
dNTP	2'-deoxynucleoside-5'-triphosphate
DRP1	Dynamin related protein 1
DTT	Dithiothreitol
Dup	Duplication
E. coli	*Escherichia coli*
EDTA	Ethylendiamintetraacetic acid
ER	Endoplasmic Reticulum
E-site	Exit - site
EtOH	Ethanol
F	Fraction
FAD	Flavin adenine dinucleotide
$FADH_2$	Reduced flavin adenine dinucleotide
FASTKD4	FAST kinase domain-containing protein 4
FCS	Fetal calf serum
Fe-S	Iron-sulfur
FIS1	Mitochondrial fission protein 1
fs	Frame shift
G	Guanine
gDNA	genomic DNA
GDP	Guanosine diphosphate
Gln	Glutamine
Glu	Glutamic acid
GTP	Guanosine triphosphate

h	Helix
H. sapiens	*Homo sapiens*
HEK293T	Human embryonic kidney cell line
HEPES	4-(2-hydroxylethyl)-1-piperazinethanesulfonic acid
His	Histidine
HSP	Heavy strand promoter
H-strand	Heavy strand
IBM	Inner boundary membrane
IMJ	Intermitochondrial junctions
IMM	Inner mitochondrial membrane
IP	Immunoprecipitation
kD	Kilo-Dalton
LB	Lysogeny broth
Leu	Leucine
LFQ	Label free quantification
LRPPRC	Leucine-rich pentatricopeptide repeat containing protein
LSP	Light strand promoter
L-strand	Light strand
LSU	Large subunit
Lys	Lysine
M	Crude mitochondria
MAM	Mitochondria-associated endoplasmic reticulum membrane
Mba1	Multi-copy bypass of AFG3 protein
MCU	Mitochondrial Ca^{2+} uniporter
Met	Methionine
MetOH	Methanol
MFN	Mitofusin
MIA	Mitochondrial import and assembly machinery
MICOS	Mitochondrial contact site and cristae organizing system
MIM	Mitochondrial import complex
MPP	Mitochondrial processing peptidase
mRNA	Messenger ribonucleic acid
MRP	Mitoribosomal protein
mt	Mitochondrial
mtDNA	Mitochondrial deoxyribonucleic acid
mtEFG1	Mitochondrial elongation factor G
mtEFTu	Mitochondrial elongation factor Tu
MTERF1	Mitochondrial termination factor 1
MTFMT	Methionyl-tRNA formyltransferase
mtIF2	Mitochondrial initiation factor 2
mtIF3	Mitochondrial initiation factor 3
mtPAP	Mitochondrial polyA polymerase
mtRF1	Mitochondrial peptide chain release factor 1
mtRF1a	Mitochondrial peptide chain release factor 1-like
NCBI	National Center for Biotechnology Information
NCR	Non-coding region
NTD	N-terminal domain
N-terminal	Amino-terminal
OD	Optical density
OMM	Outer mitochondrial membrane
OPA1	Optic atrophy 1
OXPHOS	Oxidative phosphorylation system
P	Pellet

PAGE	Polyacrylamide gel electrophoresis
PAM	Presequence translocase-associated motor
PBS	Phosphate buffered saline
PCR	polymerase chain reaction
PDB	Protein Data Bank
Pdf	Peptide deformylase
PES	Polypeptide exit site
Phe	Phenylalanine
PK	Proteinase K
PMSF	Phenylmethylsulfonylfluoride
PNPase	Polynucleotide phosphorylase
POLRMT	Mitochondrial DNA-directed RNA polymerase
PPR	Pentatricopeptide repeat
Pro	Proline
P-site	Peptidyl - site
PTC	Peptidyl transferase centre
PVDF	Polyvinylidene fluoride
qMS	Quantitative mass spectrometry
RNA	ribonucleic acid
ROS	Reactive oxygen species
rpm	Rounds per minute
RRF	Ribosome recycling factor
rRNA	Ribosomal ribonucleic acid
S. cerevisiae	*Saccharomyces cerevisiae*
SAM	Sorting and assembly machinery
SDS	Sodium dodecyl sulfate
SILAC	Stable isotope labelling by amino acids in cell culture
siRNA	Small interfering ribonucleic acid
SLIRP	Stem-loop-interacting RNA binding protein
SN	supernatant
SSU	small subunit
T	Thymine
T. brucei	*Trypanosoma brucei*
TAE	Tris/acetate/EDTA buffer
TEFM	Transcription elongation factor
TFAM	Mitochondrial transcription factor A
TFB2M	Mitochondrial transcription factor B2
TIM	Translocase of the inner mitochondrial membrane
TOM	Translocase of the outer mitochondrial membrane
tRNA	Transfer ribonucleic acid
TRNT1	tRNA nucleotidyltransferase 1
U	Uracil
UTR	Untranslated region
v/v	Volume / volume
Val	Valine
VDAC	Voltage-dependent anion-selective channel
WT	Wild type

1. **Abstract**

Due to the presence of high-resolution cryo-EM structures of the human mitoribosome, the understanding about the function and assembly of the intriguing mitochondrial ribonucleoprotein complex increased tremendously during the last years. Even if the human mitoribosome descended from a bacterial ancestor, its structure and composition differs remarkably. During evolution, the RNA content decreased to approximately 50 % of the original bacterial. In contrast, many mitochondrial ribosome specific proteins were recruited and the existing proteins were extended leading to an inverted RNA to protein ratio. Many *in vitro* and *in vivo* studies about the assembly of the 70S bacterial ribosome have been conducted in the past. However, the assembly of the 55S human mitoribosome is not completely solved even if analyses about the biogenesis of the 54S subunit of *Saccharomyces cerevisiae* and the assembly of the mtLSU of *Trypanosoma brucei* contributed to our understanding. The number of mutations in genes encoding for proteins required for the mitochondrial translational apparatus which are implicated in severe early-onset diseases with various clinical phenotypes is growing. Hence, a deep understanding about the complex mechanisms of mitoribosomal assembly is required to shed light into the molecular basis leading to the manifestation of these severe human mitochondrial diseases.

Within this thesis, a new purification protocol was established to obtain 55S human mitoribosomes from HEK293T cells. Therefore, the separation of mitoribosomal complexes on sucrose gradients was optimised in regard of sucrose concentration, buffer conditions and purity of starting material. This was done to ensure a reasonable separation of 28S mtSSU, 39S mtLSU and 55S monosome from each other as well as to improve the stability of the before mentioned complexes. By using the established protocol, 55S human mitoribosomes were successfully isolated for future analyses of the assembly pathway.

In addition, to analyse the biogenesis of the 39S subunit, two proteins of the mtLSU were further characterised. The disease associated protein mL44 was shown to be crucial for *de novo* synthesis of mtDNA-encoded proteins as well as mtLSU assembly. Investigations using a FLAG-tagged variant of mL44 revealed that this protein is probably part of an early assembly intermediate together with bL20m and bL21m. Furthermore, by characterising mL45 it was observed that the mitoribosomal membrane anchor is required for functional mitochondrial translation and hierarchical assembly of the 39S mtLSU.

2. Introduction

2.1 Mitochondria

2.1.1 General aspects

During evolution two billion years ago, ancient eukaryotic cells engulfed α-proteobacteria (Friedman and Nunnari, 2014). Thus, a new organelle emerged: the mitochondrion. During evolution 99% of the genetic information encoded in the mitochondrial genome was outsourced to the nucleus (Richter-Dennerlein et al., 2015). Just 1 % is still encoded by the mitochondrial genome, which is located within the mitochondrial matrix. This innermost compartment is separated from the cytosol by an inner mitochondrial membrane (IMM) (Figure 1), inner membrane space (IMS) and outer mitochondrial membrane (OMM) (Wiedemann and Pfanner, 2017). Each compartment or membrane fulfils specialized functions within mitochondria.
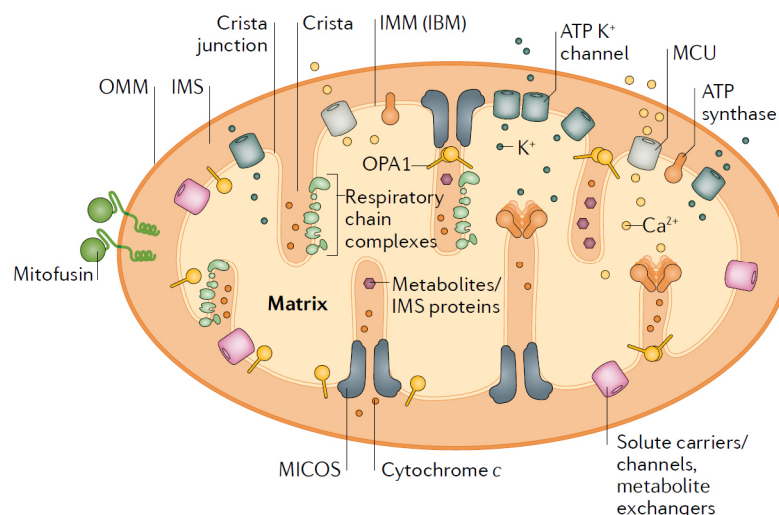
Figure 1: Mitochondrial structure. Abbreviations not mentioned in the text: mitochondrial Ca²⁺ uniporter (MCU), inner boundary membrane (IBM). Picture taken from Giacomello et al., 2020. Reprinted by permission from Springer Nature Customer Service Centre GmbH: Springer Nature, Nature Reviews Molecular Cell Biology, The cell biology of mitochondrial membrane dynamics. Giacomello, M., Pyakurel, A., Glytsou, C., and Scorrano, L. Copyright © 2020, Copyright Clearance Center, Inc. DOI: https://doi.org/10.1038/s41580-020-0210-7

The OMM serves as a barrier to the cytosol, but small hydrophilic molecules are able to diffuse through voltage-dependent anion-selective channels (VDAC)/ porins as reviewed by Benz, 1994. In addition, it is a contact site to the endoplasmic reticulum (ER) via the mitochondria-associated endoplasmic reticulum membrane (MAMs) and to other mitochondria via intermitochondrial junctions (IMJ) (Cogliati et al., 2016; Rowland and Voeltz, 2012).

In contrast, the IMM is highly impermeable to most molecules. The IMM has a much higher protein content than the OMM and is characterized by the presence of a specific phospholipid: cardiolipin (Comte et al., 1976). The characteristic morphology of mitochondria is formed through invaginations of the IMM into cristae. The cristae junctions are mediated by the MICOS complex (mitochondrial contact site and cristae organizing system) and OPA1 (optic atrophy 1), whereas the apex of the cristae is built through dimerization of ATP-synthase complexes (Cogliati et al., 2016; Strauss et al., 2008). These cristae are specialized compartments where most of the respiratory chain complexes are situated (Cogliati et al., 2016).

Depending on the cell type, mitochondria display a variety of different shapes from tubular to spheroid (Bereiter-Hahn and Vöth, 1994). Regulated mitochondrial fusion and fission events are required for proper functionality of the organelle. MFN1 (mitofusin 1), MFN2 and OPA1 are players in mitochondrial fusion, whereas DRP1 (dynamin related protein 1) and FIS1 (mitochondrial fission protein 1) are components of the fission machinery (Chan, 2006).

2.1.2 Import of proteins

Due to the fact that the mitochondrial proteome comprises about 1000 proteins, an import of nuclear-encoded proteins across the mitochondrial double membrane layer is required. Depending on the properties and final destination of the protein to be imported, there are five different pathways currently described, but it is highly likely that there are more existing (Wiedemann and Pfanner, 2017). Four of them are using the translocase of the outer mitochondrial membrane (TOM complex) for translocation of proteins across the OMM.

Presequence pathway: Many mitochondrial proteins are synthesized in the cytosol as precursor proteins, containing mostly cleavable N-terminal presequences. Receptors of the TOM complex recognize these presequences due to their positively charged amphipathic α-helical properties. The preproteins are translocated via the OMM and handed over to the presequence translocase of the inner membrane (TIM23 complex). If a stop transfer signal is present within the cargo, the protein is inserted into the IMM. Otherwise the preprotein is transferred to the presequence translocase-associated motor (PAM), which facilitates the final import into the matrix under ATP consumption, where the mitochondrial processing peptidase (MPP) cleaves off the presequence (Callegari et al., 2020; Harbauer et al., 2014; Schulz et al., 2015; Wiedemann and Pfanner, 2017).

Carrier pathway. Hydrophobic inner membrane carrier proteins containing non-cleavable presequences within the mature protein are imported via the carrier pathway. After translocation via the TOM complex, the proteins are further transported across the IMS by small TIM

chaperones and inserted into the IMM by the TIM22 complex using membrane potential (Rehling et al., 2003; Wasilewski et al., 2017).

β-barrel pathway. β-barrel protein precursors are translocated via the TOM complex, handed over to small TIM chaperones within the IMS and inserted into the OMM by the sorting and assembly machinery (SAM) (Harbauer et al., 2014; Paschen et al., 2003; Wiedemann and Pfanner, 2017).

MIA pathway. Cysteine-rich IMS proteins are imported via the MIA pathway. Therefore, unfolded reduced precursor proteins are imported by the TOM complex and further processed by the mitochondrial import and assembly (MIA) machinery, which inserts disulphide bonds for proper folding (Harbauer et al., 2014).

MIM pathway. The import of α-helical transmembrane proteins of the OMM is not completely solved until now, but it was suggested that these proteins do not use the TOM complex but rather the mitochondrial import complex (MIM) (Harbauer et al., 2014).

2.1.3 Function of mitochondria

Mitochondrial function within eukaryotic cells is diverse as they contribute to Ca^{2+} signalling (Clapham, 2007), ROS production (Shadel and Horvath, 2015), amino acid biosynthesis and biogenesis of lipids. Various pathways of apoptosis are triggered by mitochondria. Amongst them are different mechanisms as: a) release of cytochrome *c* as caspase activator, b) change of redox potential and c) alteration of electron transport and disruption of oxidative phosphorylation system (Green and Reed, 1998). In addition, mitochondria are essential for Fe/S protein and heme biogenesis (Lill and Mühlenhoff, 2008). Several metabolic pathways are situated within the mitochondrial matrix such as the Krebs cycle, urea cycle and β-oxidation.

However, mitochondria are best known for their role in ATP production. As mitochondria are termed "powerhouse of the cell", their main function is to supply the cell with energy. NADH and $FADH_2$ are generated within glycolysis, citric acid cycle and β-oxidation. In order to produce energy in form of ATP by oxidative phosphorylation (OXPHOS), those molecules are oxidized by the respiratory chain complex I and II in the inner mitochondrial membrane. Movement of electrons along the complexes I – IV is linked to pumping of protons from the matrix into the IMS by complex I, III and IV leading to an electrochemical gradient. The driving force of this membrane potential is utilized by the fifth OXPHOS complex to produce ATP (Hosler et al., 2006; Saraste, 1999; Winge, 2012).

The NADH dehydrogenase complex is the first and biggest complex within the OXPHOS system, consisting of 38 nuclear and 7 mtDNA-encoded proteins (Brandt, 2006). Through oxidation of NADH two electrons are transferred to ubiquinone and 4 protons are pumped from the matrix to the IMS. The succinate dehydrogenase (complex II), also part of the citric acid cycle, is the smallest complex within the electron transport chain consisting of just four proteins (Bezawork-Geleta et al., 2017). It catalyses the oxidation of succinate to fumarate and the subsequent transfer of 2 electrons to ubiquinone. The cytochrome c reductase (complex III) passes electrons from ubiquinol to cytochrome c coupled with a proton transfer across the membrane in a process called the Q-cycle (Saraste, 1999). The fourth and final complex of the electron transport chain is called cytochrome c oxidase, which reduces molecular oxygen into water by concomitant pumping of one proton per transferred electron across the IMM (Saraste, 1999). The ATP synthase (complex V) is part of the OXPHOS complex but not of the respiratory chain. Upon flow of protons through the channel of complex V, ATP is produced (Walker, 2013).
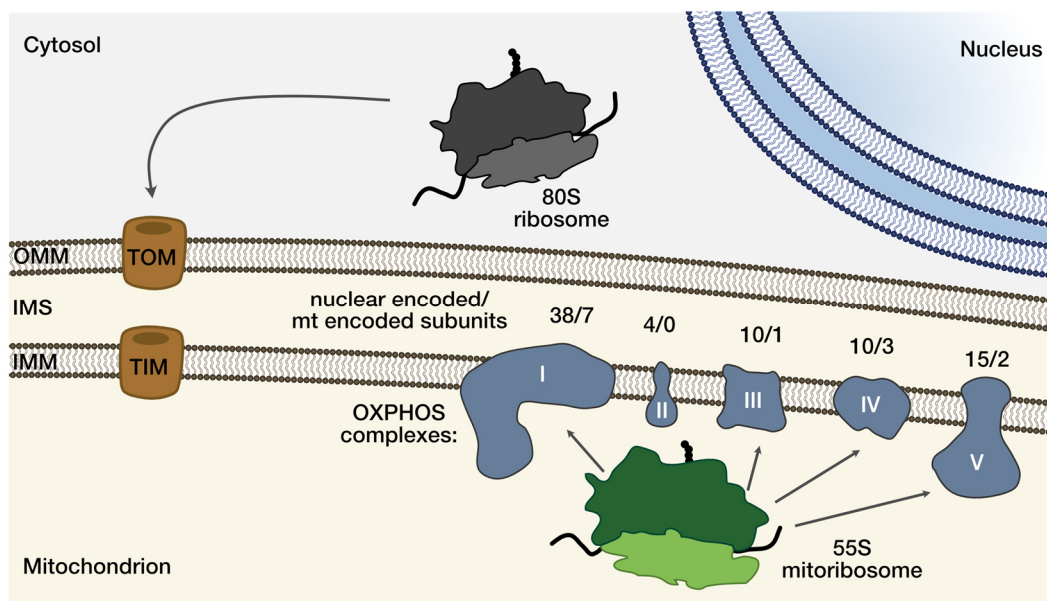
Figure 2: Components of the oxidative phosphorylation system are of dual genetic origin (besides complex II). Most of the proteins are encoded in the nucleus, expressed by 80S cytosolic ribosomes and imported via TOM and TIM complexes. Core components of OXPHOS are still expressed within mitochondria. Numbers above the complexes depict the amount of nuclear and mitochondrial encoded proteins. Picture adapted from (Hanitsch and Richter-Dennerlein, 2020)*.*

The majority of components of the OXPHOS complexes are encoded within the nucleus and transported into mitochondria (Figure 2). Nevertheless, some proteins are expressed within mitochondria (complex I: ND1, ND2, ND3, ND4, ND4L, ND5, ND6, complex III: CYTb, complex IV: COX1, COX2, COX3 and complex V: ATP6, ATP8). One assumption was that the genetic information of these 13 proteins was not transferred to the nucleus due to their high hydrophobicity. In

addition, rRNA components and tRNAs required for final protein expression are also still encoded on the mtDNA. Transport of very hydrophobic protein cargos molecules would be challenging for the cell. For this reason, it was hypothesized that the genetic information of some OXPHOS proteins and parts of the gene expression machinery was maintained within mitochondria during evolution (Kehrein et al., 2013).

2.1.4 Mitochondrial gene expression

2.1.4.1 Mitochondrial genome

Depending on the type of tissue there is a great variance of mtDNA copy number spanning from 1×10^5 (human oocytes) to 3×10^3 (human fibroblasts) (Chen et al., 1995; Hällberg and Larsson, 2014; Kukat et al., 2011). The mtDNA is organized within nucleoids – clusters of DNA and protein, which are closely associated to the IMM (Brown et al., 2011). Per nucleoid just one copy of mtDNA together with the main packaging factor TFAM (mitochondrial transcription factor A) was found to be present (Kukat et al., 2011).

The mitochondrial genome itself is composed of a16.5 kb-sized circular DNA molecule consisting of a heavy (H) and a light (L) strand. Historically, these terms are used due to the fact that one strand has a high guanine content, which leads to a separation of the strands by $CsCl_2$ gradient ultracentrifugation (Berk and Clayton, 1974; Borst, 1972; Gustafsson et al., 2016). The H-strand contains most of the genetic information as it encodes for 2 rRNAs, 14 tRNAs and 8 monocistronic and 2 bicistronic mRNAs giving rise to 12 proteins. On the L-strand, just 1 mRNA and 8 tRNAs are encoded (Figure 3) (Anderson et al., 1981; Ott et al., 2016).
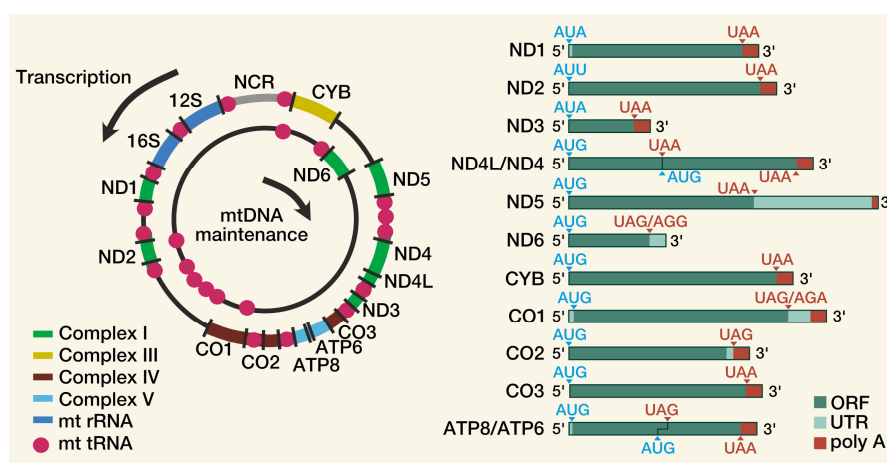
Figure 3: Mitochondrial genome and transcripts. mtDNA consists of H- and L-strand. The mt genome encodes for 22 tRNAs, 2 rRNAs and 11 mRNAs. Just one longer non-coding region (NCR) is present containing regulatory sequences. The transcripts have nearly no 5' untranslated region (UTR) and also no 7-methylguanosine cap. All mRNAs, besides ND6, have a short polyA tail. Just ND5, ND6, CO1,

and CO2 contain a short UTR before their 3'end. Picture adapted from (Hällberg and Larsson, 2014; Richter-Dennerlein et al., 2015)*.*

Codon usage in mitochondria differs from the universal genetic code. Besides AUG, AUA encodes for methionine (Barrell et al., 1979). In addition, AUU also codes for methionine during initiation, but codes for isoleucine during elongation (Fearnley and Walker, 1987). UGA decodes for tryptophan, instead of being a termination codon (Barrell et al., 1979). Furthermore, AGA and AGG do not code for arginine and provoke a -1 ribosomal frameshift leading to the termination of ND6 and COX1 in the stop codon UAG (Temperley et al., 2010a).

2.1.4.2 Transcription and post-transcriptional modifications

Transcription of mtDNA takes place within nucleoids (Pearce et al., 2017). For each strand of the mtDNA exists one promoter: HSP and LSP (Hällberg and Larsson, 2014; Terzioglu et al., 2013). Each of them gives rise to one transcript which has to be further processed. For transcription initiation, the DNA-dependant RNA polymerase POLRMT requires help from other factors in contrast to other structurally related RNA polymerases (D'Souza and Minczuk, 2018). First, TFAM needs to associate with the mtDNA, bends the DNA and recruits POLRMT to the promoter region building the closed pre-initiation complex (Gustafsson et al., 2016; Hillen et al., 2017a; Ramachandran et al., 2017). Next, the mitochondrial transcription factor B2 (TFB2M) binds to POLRMT and melts the initiation region of the promoter, creating the open initiation complex and allowing the polymerase to start transcription (Hillen et al., 2017a; Ramachandran et al., 2017). In order to allow transcription elongation, TFB2M is released and the transcription elongation factor (TEFM) is bound to POLRMT, enhancing its processivity (Hillen et al., 2017b; Minczuk et al., 2011). If transcription is finished, POLRMT and TEFM are released from the mtDNA (Hillen et al., 2017b). However, transcription termination initiated by HSP remains still unsolved, whereas LSP transcription is terminated by binding of the mitochondrial termination factor 1 (MTERF1) (Hillen et al., 2018).

Due to just two promoter areas existing within the mitochondrial genome, there are only two resulting polycistronic transcripts. Besides Cytb/ND5 and ATP6/COIII, all rRNA and protein coding areas are separated by tRNAs (Figure 3). Already in 1981 it was proposed with the "tRNA Punctuation Model" that endonucleolytic cleavage excises the tRNAs and thereby releases the other mRNAs and rRNAs (Ojala et al., 1981). Cleavage of the polycistronic transcript is carried out by mitochondrial RNase P at the 5' end of tRNAs, followed by a cleavage at the 3' end by RNase Z (ELAC2) (Hällberg and Larsson, 2014). Nevertheless, as not all mRNAs are flanked by tRNAs, their release cannot be explained by the aforementioned model and is still subject of ongoing research (D'Souza and Minczuk, 2018).

After release of mRNAs from the polycistronic transcript, 10 of 11 mRNAs are polyadenylated by mitochondrial polyA polymerase (mtPAP) (Hällberg and Larsson, 2014; Nagaike et al., 2005; Tomecki et al., 2004). Polyadenylation is required to stabilize specific mRNAs or to destabilize other ones. In addition, seven mRNAs do not contain a complete stop codon. Their open reading frame is completed by addition of the poly-A tail (Temperley et al., 2010b). Another player in enhancing mt mRNA stability is the leucine-rich pentatricopeptide repeat (PPR)-containing protein (LRPPRC). LRPPRC acts in a complex together with the stem-loop-interacting RNA-binding protein (SLIRP) (Sasarman et al., 2010). Upon blockage of polynucleotide phosphorylase (PNPase) and the helicase SUV3, this complex prevents mRNA from being degraded and stimulates mtPAP for further polyadenylation of mRNAs (Chujo et al., 2012; Ruzzenente et al., 2012). Also FASTKD4 (FAST kinase domain-containing protein 4) modulates mRNA stability in some cases (Wolf and Mootha, 2014).

Mitochondrial tRNAs undergo a variety of post-transcriptional modifications to become fully functional. A complete list of all known factors was summarized by Suzuki and Suzuki, 2014. In brief, the nucleotides of tRNAs are chemically modified and the CCA trinucleotide is added to the 3' end of all mt tRNAs by TRNT1 (tRNA nucleotidyltransferase 1) (Nagaike et al., 2001; Suzuki et al., 2011). Following this addition, tRNAs are ready to be charged with their respective cognate amino acid by aminoacyl-tRNA synthetases (Hällberg and Larsson, 2014). In total, the 22 tRNA recognize 60 sense codons (Suzuki et al., 2011). In mitochondria, just one tRNA is available to decode methionine codons during initiation and elongation in contrast to two distinct cytosolic tRNA[Met]. It was reported that formylation of a cytosine residue at the wobble position (f[5]C34) of the specific tRNA contributes to recognition of all three codons (AUG, AUU, AUA) (Bilbille et al., 2011). Later in translation, Met-tRNA[Met] is used during elongation. A subset of Met-tRNA[Met] is formylated by mitochondrial methionyl-tRNA formyltransferase (MTFMT) and subsequently recruited during translation initiation (Tucker et al., 2011).

The rRNA molecules also undergo excessive post-transcriptional modifications. This will be described in chapter 2.2.2.1. Most of the post-transcriptional processing events of mRNAs, tRNAs and rRNAs are suggested to take place within mitochondrial granules, located in close proximity of nucleoids (Ott et al., 2016).

2.1.4.3 Translation and translational regulation

Translation on mitoribosomes can be divided into four distinct steps (initiation, elongation, termination, ribosome recycling), each requiring a specific subset of regulation factors (Figure 4). Translation initiation in mammalian mitochondria requires the presence of two initiation factors (mtIF2 and mtIF3) instead of three as in bacteria (IF1, IF2, IF3). Detailed mechanisms of translation initiation in mitochondria were revealed by cryo-EM (Koripella et al., 2019; Kummer et al., 2018). In the beginning, mtIF3 binds to 28S mtSSU. In presence of mRNA, a conformational change takes place, to allow binding of fMet-tRNA^{Met}-mtIF2^{GTP} forming the initiation complex. If no mRNA is present, mtIF3 bound to mtSSU blocks association with this complex and the mtLSU (Koripella et al., 2019).

The mRNA binds in proximity of the mitoribosomal PPR protein mS39 located at the entrance of mt mRNA-channel (Amunts et al., 2015; Greber et al., 2015). Another mitoribosomal protein, uS5m, assists to place the mRNA to the aminoacyl (A) and peptidyl (P) site. mtIF2 specifically recognizes fMet-tRNA^{Met} and supports its binding to mtSSU. Upon correct anticodon binding in the P-site, the 39S mtLSU joins, promoted by the mtLSU protein bL12m (Kummer et al., 2018). Association of the mtLSU encourages hydrolysis of GTP to GDP within mtIF2 and the initiation is completed (Kummer et al., 2018). mtIF2^{GDP} and mtIF3 are released concomitantly (Mai et al., 2017). However, very recently a distinct mechanism of translation initiation was proposed by Khawaja et al. They suggested, if mtIF3 is associated with the 28S mtSSU, binding of the initiator tRNA is inhibited. By accommodating mtIF2^{GTP}, mtLSU is recruited, mtIF3 is released and replaced by fMet-tRNA^{Met}. Association of the mRNA was described as final step, which is completely different from the bacterial ancestor of the mitoribosome (Khawaja et al., 2020). Future analyses need to provide evidence for which pathway is more likely to occur.

Before translation elongation can proceed, the N-terminal tail of mL45 has to be removed from the polypeptide exit tunnel in order to enable the growing peptide chain to leave the mitoribosome (Koripella et al., 2020; Kummer et al., 2018). Cryo-EM studies revealed a conformational change of mL45 between initiation and elongation stage, suggesting that this is necessary to anchor the mitoribosome to the inner mitochondrial membrane (Koripella et al., 2020).
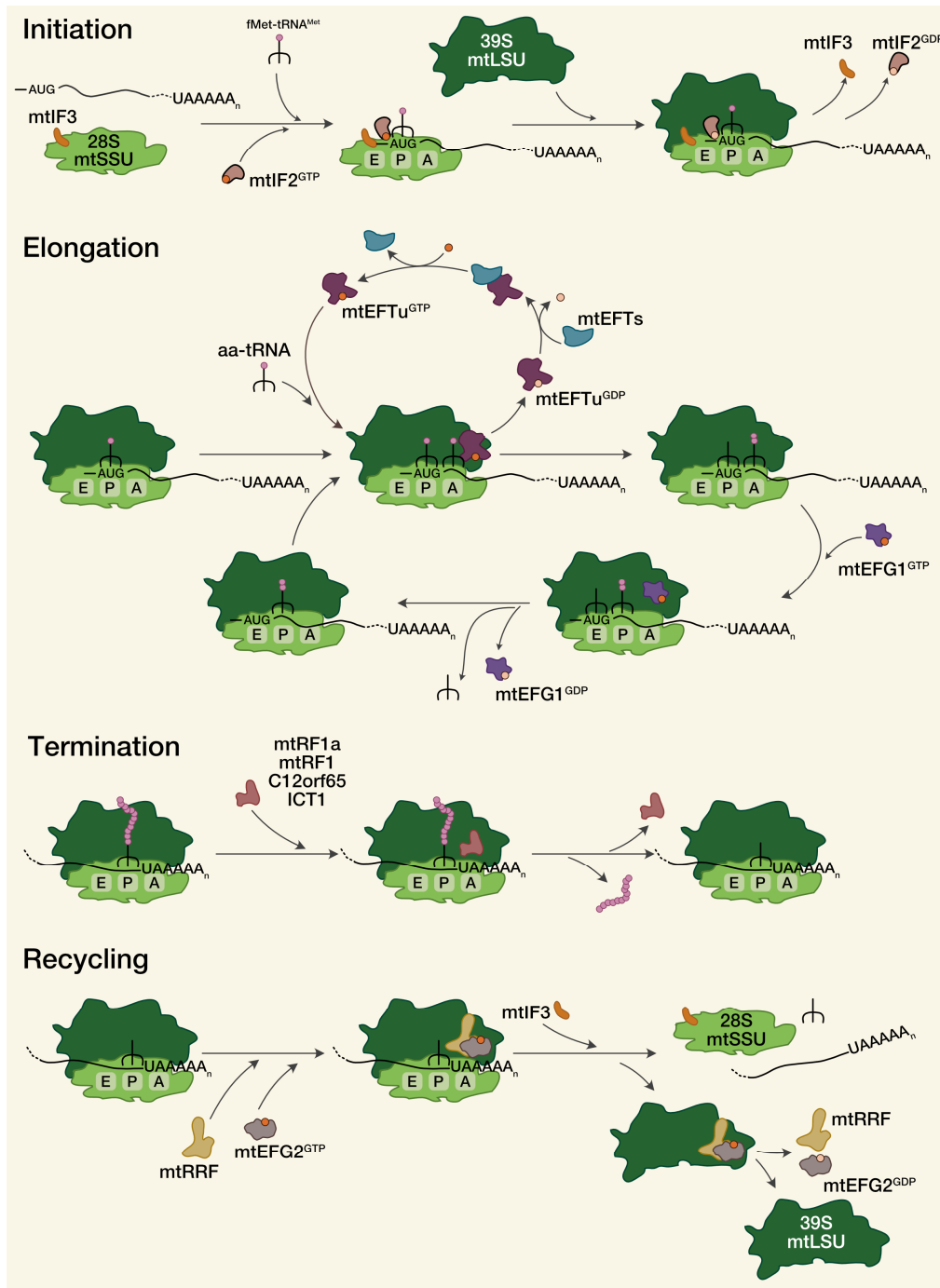
Figure 4: Mitochondrial Translation. Picture adapted from Mai et al., 2017 *including initiation steps described by* Koripella et al., 2019; Kummer et al., 2018*.*

Translation elongation continues upon binding of a complex consisting of mtEFTu coupled with GTP and an aminoacylated tRNA to the A -site of the 55S ribosome. If the anticodon of the tRNA matches the codon presented from the mRNA in the A -site, GTP is hydrolysed and mtEFTu^{GDP} is released. The ribosome catalyses the peptide bond formation between the newly entered aminoacylated tRNA present in the A -site and the peptide chain coming from the P -site. The prolonged peptide chain is now situated in the A -site and the P -site tRNA is deacylated. Upon

binding of mtEFG1^{GTP}, the deacylated tRNA is released to the E -site and the tRNA coupled with the peptide chain fills the P -site, leaving the A -site empty (Hällberg and Larsson, 2014). A specific structure of the mtLSU called the P -site finger supports correct tRNA positioning in the A - and P -site (Greber et al., 2015). To restore the activity of mtEFTu, it builds a complex with mtEFTs, which facilitates dissociation of GDP. Upon association of GTP, mtEFTs is released and mtEFTu^{GTP} is available for the next elongation cycle (Cai et al., 2000).

As reviewed by Chrzanowska-Lightowlers, 2011, this mechanism proceeds until a stop codon encoded on the mRNA reaches the A -site. As there is no matching tRNA, a termination factor binds to release the nascent polypeptide. The termination factor recognizes the stop codon in the A -site by the tripeptide motif (PXT motif) and the α-helical tip. This leads to a conformational change of domain 3 of the termination factor leading to the translocation of the GGQ motif into the peptidyl transferase centre. This enables the release factor to facilitate the hydrolysis of the ester bond between the peptidyl tRNA and the nascent peptide chain (Chrzanowska-Lightowlers et al., 2011). Four release factors have been identified in human mitochondria: mtRF1, mtRF1a, ICT1 (mL62) and C12orf65 (D'Souza and Minczuk, 2018; Huynen et al., 2012; Lind et al., 2013; Richter et al., 2010; Soleimanpour-Lichaei et al., 2007). The question, why the mitoribosome affords four factors for one purpose is subject of still ongoing research.

For recycling of the mitoribosome after translation, the binding of mtRRF and mtEFG2^{GTP} is required. The complex of mtRRF-mtEFG2^{GTP} splits the 55S ribosome into 28S and 39S and releases the mRNA as well as the deacylated tRNA (Rorbach et al., 2008; Tsuboi et al., 2009). GTP consumption and mtIF3 are necessary to dissociate the before mentioned factors from the 39S LSU (Tsuboi et al., 2009).

All of the proteins synthesized from 55S ribosome are highly hydrophobic membrane proteins. For this reason, it is necessary that the newly synthesized polypeptides are released in close proximity of the IMM (Mai et al., 2017) or even co-translationally (Richter-Dennerlein et al., 2015). Therefore, it was suggested that the translational apparatus needs to be situated close to the IMM. By cryo EM tomography it was shown that the mitoribosomal protein (MRP) mL45 mediates this contact between 55S and IMM (Englmeier et al., 2017). Nevertheless, insertion of the synthesized proteins into the IMM is not completely understood in the mammalian system. In yeast, the translocase Oxa1 was described to serve this purpose amongst others (Mai et al., 2017; Stiller et al., 2016). In mammals, OXA1L is the homologue of the yeast Oxa1 and was hypothesized to fulfil this function (Haque et al., 2010). Until now, only an interaction of OXA1L to the 55S ribosome has been shown (Mai, 2016), but functional studies and the concrete interaction partner within the mitoribosome are still missing.

Since proteins of the OXPHOS complexes are of dual genetic origin, a tight regulation of mitochondrial and cytosolic translation is required. For the assembly of cytochrome *c* oxidase, it was shown if COX4 (first nuclear encoded protein to bind in complex IV assembly) is missing, translation of COX1 (mtDNA-encoded) is stalled. Thereby, mt translation is regulated by the presence of nuclear encoded subunits (Richter-Dennerlein et al., 2016). Another feedback mechanism was described for complex I biogenesis, as the nuclear encoded MITRAC15 regulates ND2 expression within mitochondria (Wang et al., 2020). Moreover, factors to regulate cytosolic translation were found to act as well in mitochondria. miR-1 bound to the mt mRNA together with AGO2 stimulates mt translation (Zhang et al., 2014). This was surprising due to the fact that the microRNA miR-1 acts in the cytosol together with AGO2 and GW182 as translational silencing factors and also mediates mRNA degradation (Czech and Hannon, 2011). Future research on mt translation regulation will most likely reveal more regulation pathways.

2.2 Mitochondrial Ribosome

2.2.1 Structure of 55S mitoribosome

The mitochondrial 55S mitoribosome consists of two individually shaped subunits like all ribonucleoprotein complexes termed ribosomes. It is composed of a 39S mt large subunit (LSU) and a 28S mt small subunit (SSU) (O'Brien, 1971). In 2003, a first structure of the mitoribosome at 13.5 Å was published and revealed tremendous differences to the bacterial ribosome as well as the eukaryotic cytosolic ribosome (Sharma et al., 2003) (see Table 2).

Table 2: Overview of ribosomal properties. Table adapted from (Greber and Ban, 2016)

	Bacteria (*Escherichia coli*)	Eukaryotic cytosol	Yeast mitochondria	Mammalian mitochondria
Ribosome	70S	80S	74S	55S
Molecular weight	2.3 MDa	3.3-4.3 MDa	3-3.3 MDa	2.7 MDa
rRNAs	3	4	2	2 + 1 tRNA
Proteins	54	79-80	82	82
Large subunit	50S	60S	54S	39S
rRNAs	23S/5S	26-28S/5.8S/5S	21S	16S + tRNA^{Phe}/tRNA^{Val}
Proteins	33	46-47	46	52
Small subunit	30S	40S	37S	28S
rRNAs	16S	18S	15S	12S
Proteins	21	33	36	30

As mitochondria evolved from a bacterial ancestor, the same is true for the mitochondrial ribosome. It was suggested, that the mitoribosomal evolution happened within two phases: a constructive and a reductive phase. First, mitoribosome-specific proteins were recruited in order to compensate for mutations in mtDNA encoded rRNAs. During the second phase, the rRNA content was reduced (Van Der Sluis et al., 2015). Therefore, the rRNAs of the mitoribosome were reduced to approximately 50 % of the bacterial rRNAs (reviewed by O'Brien, 2003). Shortening of rRNAs happened in all domains, distributed across the complete mitoribosome (Brown et al., 2014). In contrast, the protein content increased by incorporation of specific mitoribosomal proteins and extensions of proteins having homologues in bacteria. Hence, the rRNA core of the mitoribosome is nearly completely covered by proteins (Figure 5) (Amunts et al., 2015; Bieri et al., 2018; Brown et al., 2014; Sharma et al., 2003).
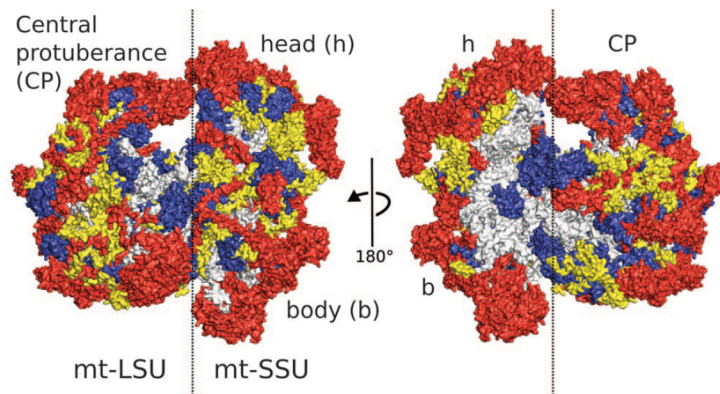
Figure 5: Proteins of the human 55S ribosome. Conserved proteins of 70S and 55S are depicted in blue. Homologous proteins with extensions are shown in yellow and mitoribosome-specific proteins are visualized in red. rRNA is shown in grey. Picture taken from Amunts, A., Brown, A., Toots, J., Scheres, S.H.W., and Ramakrishnan, V. (2015). The structure of the human mitochondrial ribosome. Science (80). 348, 95–98. Reprinted with permission from AAAS. DOI: https://doi.org/10.1126/science.aaa1193

The 36 mitoribosomal-specific proteins do not only protect the RNA but also display various other functions, which will be described later (Amunts et al., 2015; Bieri et al., 2018; Greber et al., 2015). As a result of the RNA compression and protein acquisition, the RNA to protein ratio was inversed between bacterial ribosomes and mitoribosomes (Sharma et al., 2003). Only a small number of the recruited proteins stabilize the 55S ribosome by compensating for the rRNA loss leading to a more porous architecture of the mammalian mitoribosome (Brown et al., 2014; Sharma et al., 2003). Most of the mitoribosomal-specific proteins are clustered around the existing core as described by the onion shape model of the ribosome (Hsiao et al., 2009; Petrov et al., 2019). Due to this structure, the mitoribosome has a lower sedimentation coefficient than its bacterial counterpart even though it has a greater molecular mass (Sharma et al., 2003).

2.2.1.1 Structure of the 39S mtLSU

The 39S mtLSU consists of 52 nuclear encoded mitoribosomal proteins and a 16S rRNA (as reviewed by Bieri et al., 2018). The 50S bacterial LSU contains a 5S rRNA as core structure in the central protuberance (CP), which is absent in mitoribosomes (O'Brien, 2003). In 2014, the Ban and the Ramakrishnan group published high-resolution structures of the porcine and human mtLSU at 3.4 Å resolution. These structures revealed tRNA molecules as architectural features within the CP of the 39S LSU to compensate for the loss of the 5S rRNA (Brown et al., 2014; Greber et al., 2014a). In the human structure, tRNA[Val] was found to be present (Brown et al., 2014) in contrast to the porcine structure where tRNA[Phe] was identified (Greber et al., 2014a). Just these two tRNAs were described to be incorporated into mitoribosomes of different species, as they are

flanking the 12S and 16S rRNA genes (Anderson et al., 1981; Rorbach et al., 2016). Upon loss of tRNA[Val] it was described that the mitoribosome is able to switch to tRNA[Phe] (Rorbach et al., 2016).

In 70S bacterial and 80S cytosolic ribosomes, the CP is built around the 5S rRNA (Greber and Ban, 2016). The 74S yeast mitoribosome does not contain an additional structural RNA element in the CP besides its 21S rRNA (Amunts et al., 2014). Even if the central protuberance of mammalian mitoribosomes is completely remodelled, it maintained its functions to interact with the head of the 28S mtSSU and to tRNAs in the intersubunit space (Brown et al., 2014). During evolution, uL5 and bL25 were lost from the 39S mtLSU CP most likely due to the absence of the 5S rRNA (Brown et al., 2014; Petrov et al., 2019). The structural tRNA is stabilized within the CP via uL18m and bL31m (proteins with bacterial homologues) as well as by mL38, mL40 and mL48 (Figure 6) (Bieri et al., 2018; Brown et al., 2014). The connection of the CP to the body of the 39S is mediated through mL62 (ICT1), mL52 and mL64 (CRIF1) (Brown et al., 2014).
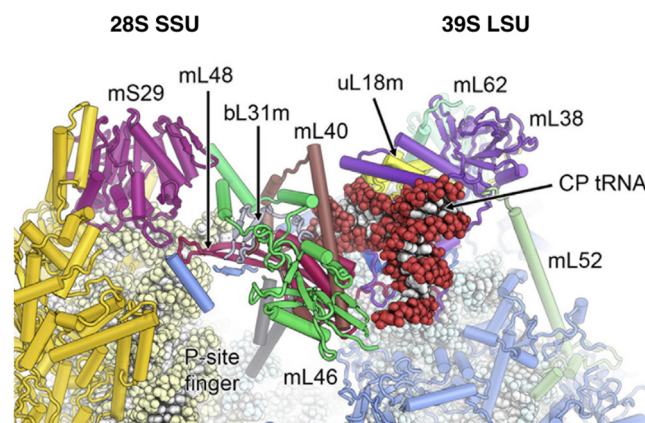
Figure 6: Structure of the remodelled CP in mammalian mitoribosomes. Picture taken from Bieri et al., 2018*. Reprinted from Current Opinion in Structural Biology, 49, Bieri, P., Greber, B.J., and Ban, N., High-resolution structures of mitochondrial ribosomes and their functional implications., 44-53, Copyright (2018), with permission from Elsevier. DOI:* https://doi.org/10.1016/j.sbi.2017.12.009

tRNAs are bound during mt translation at the respective A-, P- or E-site located in the intersubunit space between LSU and SSU. In the past, the presence of an E-site within mitoribosomes was long subject of debates (Mears et al., 2002; Sharma et al., 2003). However, the structures published by the Ban and Ramakrishnan laboratories are showing that the ribosomal E-site is preserved (Brown et al., 2014; Greber et al., 2014a). The tRNA binding sites had to co-evolve together with the highly variable mitochondrial tRNAs (Bieri et al., 2018). Characteristic structures of tRNA binding sites in bacteria are absent in the 55S ribosome. In detail, bL25 and helix H38 of the 16S rRNA are missing at the A-site and uL5 and helix H84 at the P-site (Brown et al., 2014). To stabilize tRNAs located in A- and P-site, the mitoribosome evolved a new structural element: the P-site finger. The P-site finger is a structure protruding from the CP reaching to the A- and P-

site tRNAs (Greber and Ban, 2016). It was hypothesized that mL40 and mL48 are structural components of the P -site finger (Greber et al., 2014a). Even so, additional evidence is required to prove this assumption.
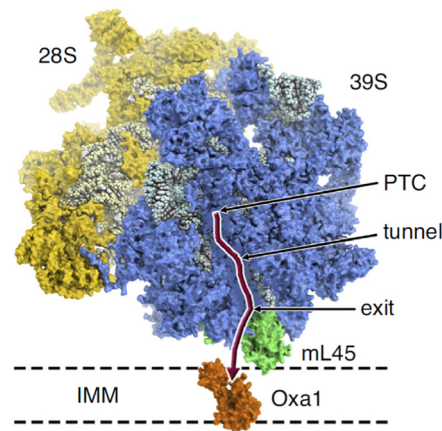
Figure 7: Polypeptide exit tunnel of mammalian 55S mitoribosome. Picture adapted from (Bieri et al., 2018)*. Reprinted from Current Opinion in Structural Biology, 49, Bieri, P., Greber, B.J., and Ban, N., High-resolution structures of mitochondrial ribosomes and their functional implications., 44-53, Copyright (2018), with permission from Elsevier. DOI: https://doi.org/10.1016/j.sbi.2017.12.009*

One evolutionary conserved structure within the 39S mtLSU is the peptidyl transferase centre (PTC) which is mainly formed by the 16S rRNA (Petrov et al., 2019) and bL27m (Greber et al., 2014a) similar to the bacterial ribosome. The highly diverged polypeptide exit tunnel reaches from the PTC to the polypeptide exit site (PES) and was adapted during evolution to the hydrophobic translational products of the mitoribosome (Figure 7). In contrast to the 74S yeast ribosome, the exit tunnel in mammalian mitoribosomes resembles the bacterial one (Amunts et al., 2014; Bieri et al., 2018). Nevertheless, the exit tunnel of the 55S ribosome is prolonged because of the addition of mitochondrial-specific ribosomal proteins or extension of ribosomal proteins (reviewed by Bieri et al., 2018). The tunnel wall comprises hydrophobic residues mostly by uL22m (Brown et al., 2014). The absence of the two rRNA structures (h7 and h24) found in bacteria was compensated by adaptations of uL24m and uL29m, leading to a more protein-rich structure (Brown et al., 2014). The tunnel exit is formed by the conserved proteins uL23m, uL29m, uL22m, uL24m and bL17m as well as by the mitochondria-specific proteins mL39, mL44 and mL45 (Figure 8) (Bieri et al., 2018; Brown et al., 2014; Greber et al., 2014b). As already described, the MRP mL45 mediates the contact between the IMM and the mitoribosome. This contact is most likely built through the helices h2 (S101-K114) and h3 (V116-S128) of mL45 (Englmeier et al., 2017).
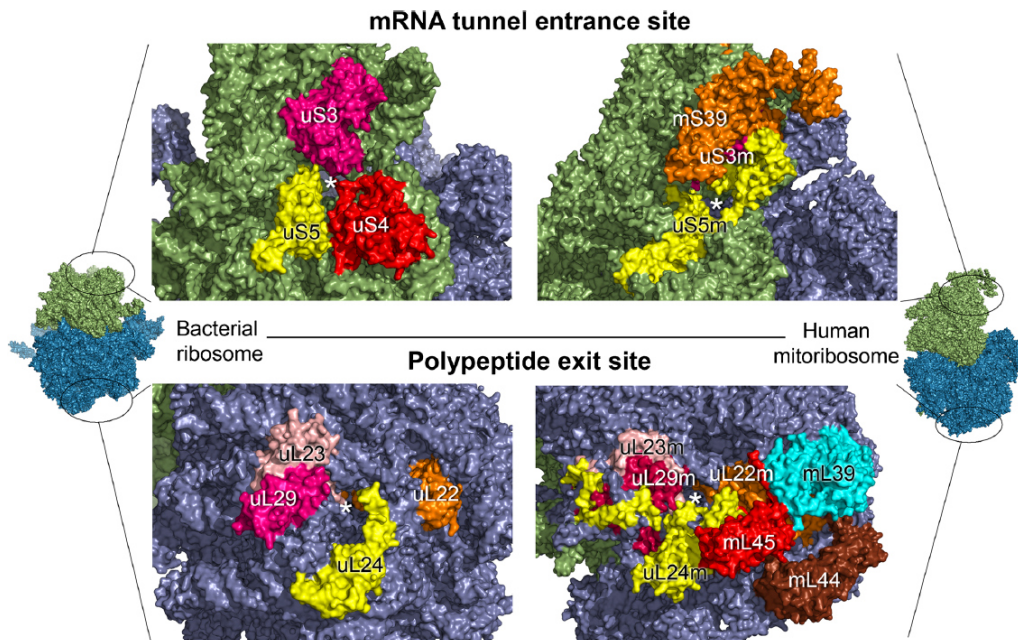
Figure 8: Comparison of bacterial (E. coli PDB 4YBB) and human mitoribosomal (PDB 3J9M) mRNA tunnel entrance site and polypeptide exit site. Asterisks indicate respective tunnel entrance/exit. Green = mtSSU, blue = mtLSU. Picture taken from Mai et al., 2017.

Another feature of the 39S mtLSU is the L7/L12 stalk, which is also larger compared to its bacterial ancestor due to the acquisition of additional ribosomal proteins (Sharma et al., 2003). At this stalk, translational factors bind and GTP is hydrolysed (Brown et al., 2014). In bacteria, L10, L11 and several copies of L12 cluster around h42-44 of the 23S rRNA (Kavran and Steitz, 2007). Within the mitoribosome, homologue proteins are bound around the h42 and h43 of the 16S rRNA (Brown et al., 2014). Additionally, mL53, mL66, uL16m and mL63 are recruited, leading to a less flexible structure (Brown et al., 2014).

2.2.1.2 Structure of the 28S mtSSU

The 28S mtSSU comprises a 12S rRNA and 30 ribosomal proteins (14 mitochondria specific). During translation initiation, the mRNA is bound by the mtSSU and gated through the mRNA channel. This mRNA channel was extensively remodelled during evolution. The bacterial mRNA entrance is characterized by a ring-like structure formed out of uS3, uS4 and uS5 (Figure 8). uS4 is missing in human mitoribosomes as well as the C-terminal domain of uS3. The 28S mRNA entrance side is mainly built by uS5m, which also accoutres the channel with its basic and aromatic residues. However, just single stranded RNA molecules are able to pass the channel even though it was widened during evolution (Amunts et al., 2015). Comparable to cytosolic ribosomes, the 3' end of the 12S rRNA is not involved in translation initiation due to the loss of the Shine-Dalgarno sequence from mitochondrial transcripts (Montoya et al., 1981). Instead, the 3' end interacts with mS37. At the exit of the tunnel, bS1m is situated similar to bacteria, probably supporting mRNA binding (Amunts et al., 2015). In addition, uS7m, uS11m, bS18m and bS21m have been described to be located at the tunnel exit (Figure 9) (Greber et al., 2015).
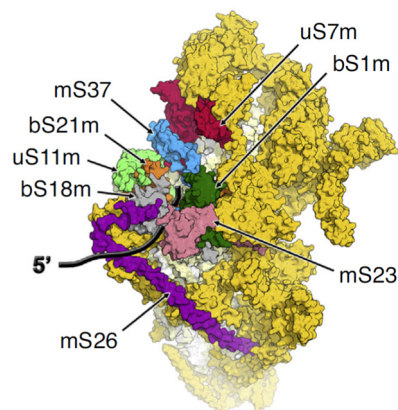
Figure 9: Structure of mtSSU. Proteins enclosing mRNA tunnel exit are labelled. Picture adapted from Bieri et al., 2018. *Reprinted from Current Opinion in Structural Biology, 49, Bieri, P., Greber, B.J., and Ban, N., High-resolution structures of mitochondrial ribosomes and their functional implications., 44-53, Copyright (2018), with permission from Elsevier.*
DOI:https://doi.org/10.1016/j.sbi.2017.12.009

The decoding centre, located within the mtSSU, is entirely built by rRNA as it was shown for bacterial and yeast mitochondrial ribosomes (Amunts et al., 2015; Bieri et al., 2018; Desai et al., 2017; Greber et al., 2015). Therefore, it was hypothesized that decoding was preserved within different species (Greber et al., 2015).

High resolution cryo-EM analyses of the mtSSU revealed that the GTP binding protein mS29 is an integral part of its structure (Amunts et al., 2015; Greber et al., 2015). It is located at the head of the mtSSU and contacts CP proteins via the intersubunit bridges mB1a and mB1b (Figure 6). In total, three protein-protein and six protein-RNA intersubunit bridges mediate the contact between the two ribosomal subunits (Amunts et al., 2015). As these interactions are mainly

situated in the centre of both subunits and are less extensive than in bacteria, the mammalian mitoribosome exhibits a much more flexible structure than its bacterial counterpart (Greber et al., 2015).

2.2.2 Assembly of the 55S mammalian mitoribosome

2.2.2.1 Lessons from the bacterial ancestor

First studies about the assembly of the 70S bacterial ribosome were carried out under harsh ionic conditions and high temperatures (Shajani et al., 2011). Traub and Nomura, 1968, were able to show that a functional 30S SSU can be reconstituted *in vitro* out of synthesized rRNA and purified proteins. By investigating the order of protein addition, they proposed an assembly map based on thermodynamic binding dependencies. A similar approach for the 50S bacterial LSU was carried out by Nierhaus and Dohme, 1979 (Figure 10).
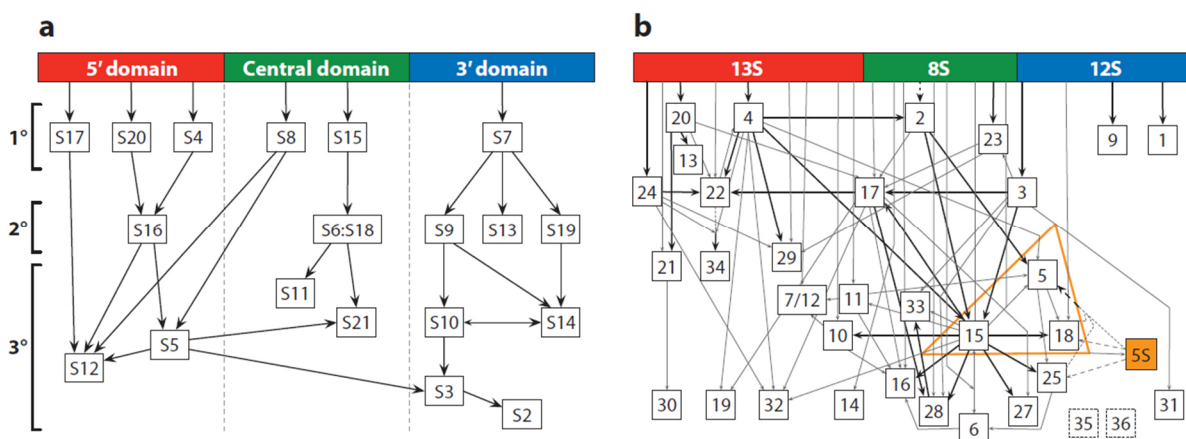
Figure 10: Assembly of the bacterial 30S SSU and 50S LSU in vitro. A) 30S SSU assembly based on thermodynamic binding dependencies described by Nomura. Primary binding proteins (1°) interact directly with the 16S rRNA and are incorporated first, followed by binding of secondary binding proteins (2°), which require interaction with 1°-binders, but not with the rRNA. Last, tertiary binding proteins (3°) are incorporated. Depending on the binding site on the rRNA (red: 5'domain, green: central domain, blue: 3'domain) the ribosomal proteins are ordered. B) 50S LSU assembly visualized by the thermodynamic dependency studies of Nierhaus. Similar to A), proteins are depicted on the map based on their binding position on the 23S rRNA. Proteins required for 5S rRNA binding are situated within the orange triangle. Picture taken from Shajani et al., 2011. Republished with permission of Annual Reviews, Inc. from Assembly of bacterial ribosomes. Shajani, Z., Sykes, M.T., and Williamson, J.R., Annu. Rev. Biochem. 80, 501–526. (2011); permission conveyed through Copyright Clearance Center, Inc. DOI: https://doi.org/10.1146/annurev-biochem-062608-160432

Nevertheless, even if these *in vitro* data were the basis for later research on bacterial ribosome assembly, *in vivo* studies were required to understand the biogenesis under physiological conditions. One of the striking differences evident from *in vivo* data was that the rRNA assembly occurs in a co-transcriptional manner. In addition, many biogenesis factors are required for the

assembly of the bacterial ribosome *in vivo* (reviewed by Davis and Williamson, 2017). The latest assembly map of the 70S was published by Chen and Williamson (2013) using a quantitative mass spectrometry approach. Since then, structures of assembly intermediates obtained by cryo-EM contributed to nowadays understanding of the process.

However, as the structure and composition of the 55S mammalian mitoribosome differs from its ancestor and also from other eukaryotic ribosomes, the knowledge gained about their biogenesis is not directly transferable to draw conclusions about the assembly of the 55S, especially for the 36 MRPs without homologs in bacteria (Greber and Ban, 2016). During the past years, a lot of new insights into the assembly of the 55S mitoribosome have been gained. It was hypothesized that the assembly occurs in a co-transcriptional manner within nucleoids and RNA granules (Antonicka and Shoubridge, 2015; Bogenhagen et al., 2014; Rackham et al., 2016). Factors to orchestrate the hierarchical incorporation of proteins into the growing particle were identified as well as modifying enzymes. In 2018, a first assembly map for the 39S and 28S was published by the laboratory of Bogenhagen.

2.2.2.2 Assembly factors

Many factors are required to assemble and mature the complex structure of the mammalian 55S mitoribosome (Figure 11). After excision of 12S and 16S rRNA from the primary transcript, mt rRNAs undergo modifications as base methylations, pseudouridylations and 2'-O-ribose methylations to complete their functionality and to enhance their stability. However, these modifications are less abundant in the mt rRNA than in bacterial and cytosolic ribosomes (De Silva et al., 2015).

Within the 12S rRNA, two adenines are di-methylated by the methyltransferase TFB1M at position 936 and 937 (Liu et al., 2019; Seidel-Rogol et al., 2003) and two cytosine residues (C839 and C841) are methylated by METTL15 (Chen et al., 2020; Van Haute et al., 2019; Laptev et al., 2020) and NSUN4 (Metodiev et al., 2014), respectively. In addition, TRMT2B methylates one uridine residue at position 429 (Powell and Minczuk, 2020). The GTPase ERAL1 was described as a RNA chaperone to protect the 12S rRNA during mtSSU assembly as it interacts with the 3'loop of the 12S rRNA prior methylation by TFB1M (Dennerlein et al., 2010). In contrast, mtRBFA, which binds at the same site as ERAL1, supports methylation of both adenine residues in the 12S rRNA (Rozanska et al., 2017). The protease CLPP regulates the biogenesis of the mitoribosome by regulation of ERAL1 (Szczepanowska et al., 2016). Additionally, the GTPase C4orf14 (NOA1) is required as a necessary factor for mtSSU assembly (He et al., 2012). For biogenesis of the 28S

mtSSU also the endoribonuclease YBEY is obliged as it recruits uS11m into the growing particle (D'Souza et al., 2019; Summer et al., 2020).

16S rRNA   39S mtLSU   55S mitoribosome   28S mtSSU   12S rRNA

UAAAAA$_n$

AUG

16S rRNA modifications:
TRMT61B: m^{1}A947
MRM1: Gm1145
MRM2: Um1369
MRM3: Gm1370
RPUSD4: Psi1397

16S rRNA regulation:
NGRN, WBSCR16,
RPUSD3, TRUB2,
FASTKD2

mtLSU assembly factors:
DDX28, FASTKD2,
MTERF3, MALSU1,
L0R8F8, mtACP,
mAAA-Protease,
NSUN4-MTERF4,
GTPBP5, GTPBP7,
GTPBP10

55S assembly factors:
DHX30, GRSF1,
MPV17L2

mtSSU assembly factors:
ERAL1, mtRBFA,YBEY
NOA1/C4ORF14, CLPP,
WBSCR16

12S rRNA modifications:
TRMT2B: m^{5}U429
METTL15: m^{4}C839
NSUN4: m^{5}C841
TFB1M: m$^6_2$A936, m$^6_2$A937

Figure 11: Known assembly factors for 55S mitoribosome biogenesis. Picture adapted from Hanitsch and Richter-Dennerlein, 2020.

In contrast to the 12S rRNA, there are three 2'O-ribose methylations of the 16S rRNA at position G1145 (MRM1), U1369 (MRM2) and G1370 (MRM3) (Lee and Bogenhagen, 2014; Rorbach et al., 2014). TRMT61B catalyses the methylation of A947 (Bar-Yaacov et al., 2016) and RPUSD4 is responsible for pseudouridylation of U1397 (Antonicka et al., 2017). Three factors were described to support the stability of the 16S rRNA and to be required for mtLSU assembly, namely the RNA binding proteins MTERF3 and FASTKD2, as well as the RNA helicase DDX28 (Antonicka and Shoubridge, 2015; Popow et al., 2015; Tu and Barrientos, 2015; Wredenberg et al., 2013). However, their exact function still remains elusive. Within a CRISPR death screen, a regulatory model consisting of NGRN, WBSCR16, RPUSD3, RPUSD4, TRUB2 and FASTKD2 was found to coordinate 16S rRNA (Arroyo et al., 2016). In addition, NGRN was reported to contain a Pfam domain, possibly required for RNA binding (Arroyo et al., 2016).

C7orf30 (MALSU1) associates exclusively with the mtLSU as it co-precipitates with proteins of the mtLSU but not of the mtSSU. Loss of MALSU1 leads to atypical assembly of 39S mtLSU and concomitantly to reduced 55S levels, suggesting a role in biogenesis of the mtLSU (Rorbach et al., 2012). In addition, MALSU1 was detected in cryo-EM structures together with L0R8F8 and mt-ACP associated with a late assembly intermediate of the mtLSU. As the complex of MALSU1, L0R8F8 and mt-ACP would sterically prevent binding of the mtSSU to the mtLSU, it was hypothesized to function as an anti-association factor during late mtLSU biogenesis (Brown et al., 2017). The *m*-AAA protease was also described to act during a late assembly step of mtLSU biogenesis, as it processes bL32m prior incorporation into the growing 39S particle (Nolden et al., 2005). Besides methylating 12S rRNA, NSUN4 shares another function with MTERF4. The

NSUN4/MTERF4 complex associates with the mtLSU and prevents subunit joining in order to control that just mature 28S and 39S are used for 55S biogenesis (Metodiev et al., 2014).

Recently, GTPases became the centre of interest regarding mitoribosome assembly. GTPases provide energy by GTP hydrolysis which can be used to facilitate structural changes as well as to incorporate or release proteins into or from pre-existing complexes (Mai et al., 2017). GTPBP7 (MTG1) is involved during a late assembly stage of the 39S mtLSU. It promotes binding of proteins to a late assembly intermediate and interacts with uL19m and mS27, suggesting that it is involved in building the mB6 intersubunit bridge (Kim and Barrientos, 2018). GTPBP10 (OBGH2) was hypothesized to act as well as a late 39S maturation factor as it associates exclusively to the mtLSU and its loss leads to ablation of 55S mitoribosomes (Lavdovskaia et al., 2018; Maiti et al., 2018). As final mtLSU maturation step, interaction of GTPBP5 (OBGH1/MTG2) with the mtLSU was proposed in order to facilitate methylation of G1145 and U1369 and to recruit bL36m to the mtLSU (Maiti et al., 2020).

Additionally, the factors DHX30 (RNA helicase), GRSF1 (RNA-binding protein) and MPV17L2 (IMM protein) are required for proper 55S biogenesis (Antonicka and Shoubridge, 2015; Antonicka et al., 2013; Dalla Rosa et al., 2014). Nevertheless, their exact function during assembly has to be further investigated. The putative GDP/GTP exchange factor WBSCR16 (RCC1L) exists in three isoforms (Reyes et al., 2020). Isoform 1 interacts with the 28S mtSSU and isoform 3 with the mtLSU. Their targets might be GTPBP10, ERAL1 or NOA1.

2.2.2.3 Assembly of the 39S mitochondrial large subunit

A first model for the order of incorporation of mtLSU proteins into the growing particle was suggested by Bogenhagen et al., 2018 (Figure 12).
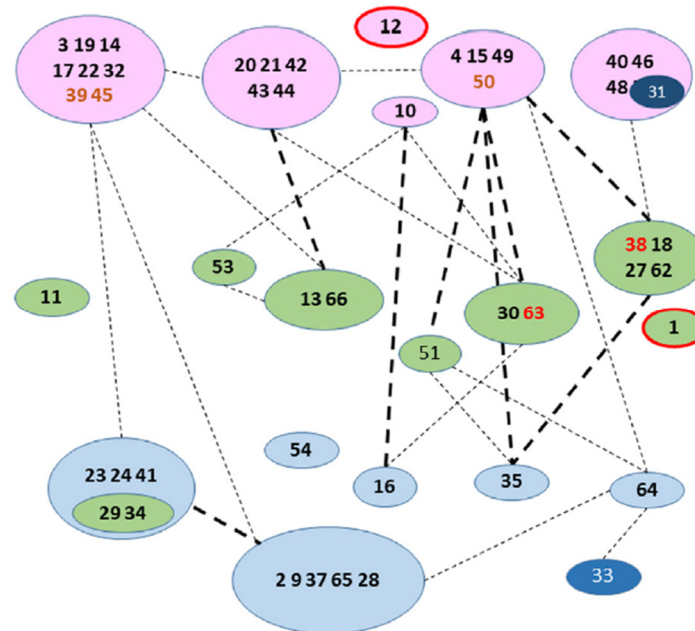
Figure 12: Scheme of 39S LSU assembly. Early binding proteins are shown in red, intermediate binding proteins in green and late binding proteins in blue. Heavy dashed lines show interaction surface areas > 1,000 Å², whereas lighter dashed lines indicate interaction surface areas from 1,000 Å² – 350 Å². Early binding proteins without vast RNA contacts are visualized in bold red. Picture taken from Bogenhagen et al., 2018*. Creative Commons Attribution-Non Commercial-No Derivatives License (CC BY NC ND). DOI: https://doi.org/10.1016/j.celrep.2018.01.066*

Clusters of early binding proteins are recruited to the 16S rRNA core. One cluster contains uL3m, uL14m, bL17m, bL19m, uL22m and bL32m, which mediates the incorporation of mL39 and mL45, which have very little direct rRNA contact. The heterodimer of uL4m/uL15m together with mL49 recruit mL50, which also lacks rRNA interactions (Figure 13).

Assembly of the central protuberance was suggested within two steps. At first, mL40/mL46/mL48 were reported to bind to one side of the tRNA, followed by bL27m/uL18m/mL38/mL62 incorporation. However, the protein bL31m situated in the centre of mL40/mL46/mL48, was designated as a late binding protein. To incorporate this protein at a later stage of assembly, disassembly of the before mentioned proteins would be required.
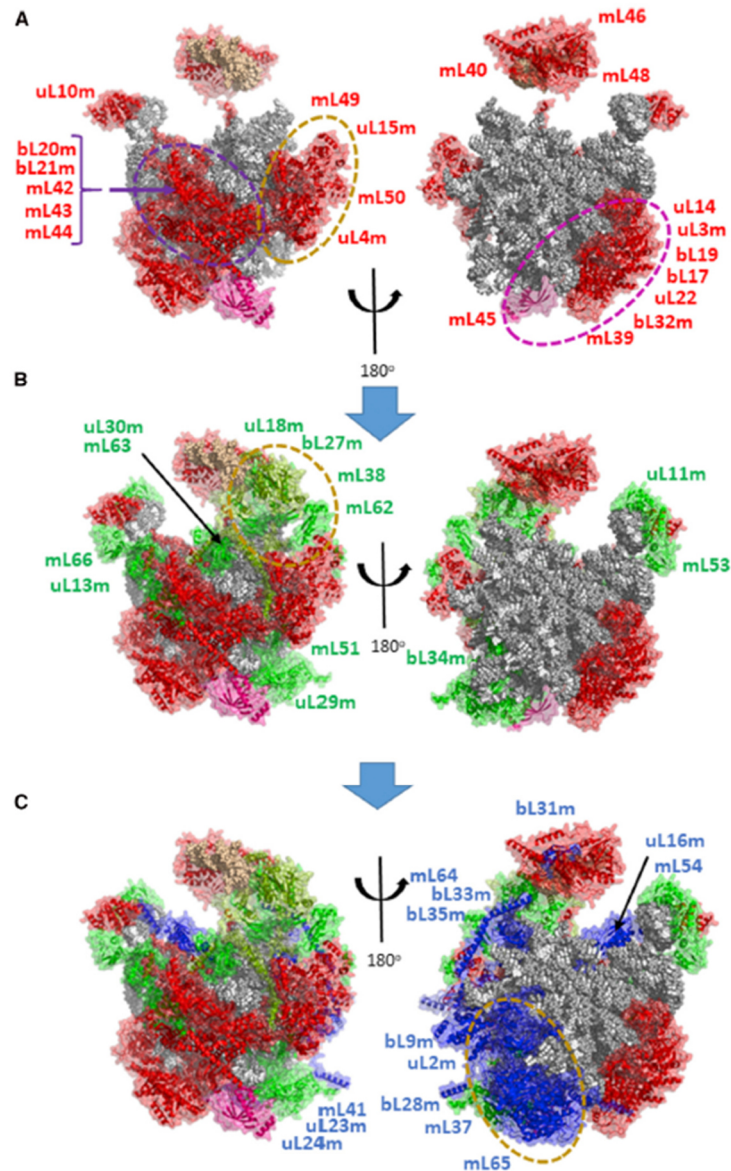
Figure 13: Assembly of the 39S mtLSU. A) Early binding proteins are depicted in red. B) Proteins binding at an intermediate state are coloured green. C) The late binding proteins are visualized in blue. 16S rRNA and structural tRNA are shown as grey spheres. Picture taken from Bogenhagen et al., 2018. *Creative Commons Attribution-Non Commercial-No Derivatives License (CC BY NC ND). DOI:*

The intermediate/late binding proteins mL41, uL23m, uL24m, uL29m and bL34m form parts of the peptide exit tunnel. Other intermediate binding proteins contact either early binding proteins and/or the 16S rRNA as uL13m and mL66, which bind in close proximity to uL10m. The early binding proteins are mainly situated in the periphery of the mtLSU. Instead, late binding proteins are located in the interface such as uL2m, mL37 and mL65. Interestingly, uL2m is not an early binding protein despite its large contact surface to the 16S rRNA.

2.2.2.4 Assembly of the 28S mitochondrial small subunit

Similar to the mtLSU assembly, early binding proteins of the mtSSU bind to the rRNA core of the subunit. The first clusters of proteins bind to the head and lower body of the 12S rRNA (Bogenhagen et al., 2018). The module in the lower body comprises bS16m and mS40, which bind to the 5' end of the 12S rRNA. mS22 interacts then with the before mentioned proteins. In addition, mS34 and mS27 are a part of this cluster, having contact with the 3' end of the 12S rRNA. Incorporation of uS5m follows, probably to mediate the contact between proteins of this cluster (Figure 14).
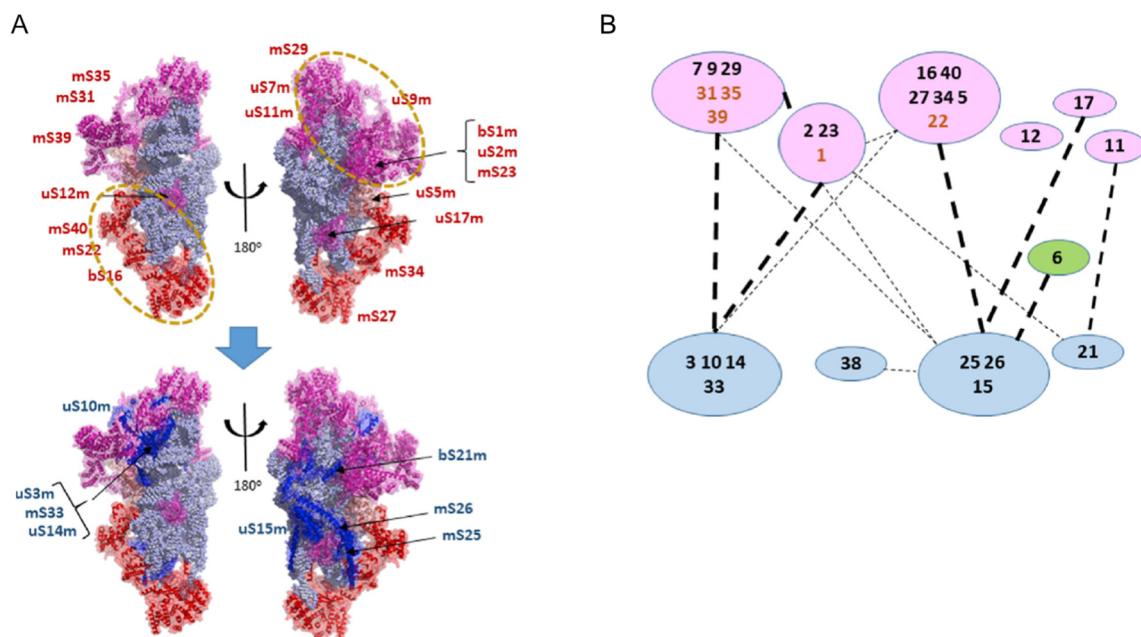
Figure 14: 28S mtSSU assembly. A) Early binding proteins are coloured in red whereas late binding proteins are depicted in blue. The 12S rRNA is visualized as blue spheres. B) Cartoon of mtSSU assembly. Description of dashed lines as indicated in Figure 12. Picture taken from Bogenhagen et al., 2018*. Creative Commons Attribution-Non Commercial-No Derivatives License (CC BY NC ND). DOI: https://doi.org/10.1016/j.celrep.2018.01.066*

The early binding proteins in the head region bind either directly to the rRNA core (uS7m, uS9m, mS29) or to proteins incorporated priorly (mS31, mS35, mS39). A smaller subset of proteins is also binding at an early stage (bS1m, uS2m, mS23), interacting with uS9m and uS5m. uS11m, uS12m and uS17m were also designated as early binding proteins. However, they bind individually to the rRNA core but not to the other protein clusters. It has been suggested that the early binding proteins recruit the late binding proteins. Thereby, the group of uS3m, uS10m, uS14m and mS33 binds to the head group, whereas uS15m, mS25 and mS26 are recruited to the body forming contacts to the bS16m cluster. In total, early binding proteins were described to

bind on the outer surface of the mtSSU. In contrast, late binding proteins are found closer to the LSU contact site (Bogenhagen et al., 2018).

2.2.3 Disease association of 55S mitoribosome

Diseases caused by impaired mitochondrial function have an incidence of about 1 in 5000 as reviewed by Boczonadi and Horvath, 2014. In recent years, more and more patients with mutations in genes encoding for mitoribosomal proteins were identified (Table 3).

Table 3: Disease associated mitoribosomal proteins (MRPs)

MRP	mutation	clinical phenotype	OMIM	Reference
bS1m	c.356A>G, p.(Lys119Arg), deletions of exon 2 and parts of intron 1 and 2	growth retardation, craniofacial dysmorphism, developmental delay	611990	(Pulman et al., 2019)
uS2m	c.328C>T (p.Arg110Cys) c.340G>A (p.Asp114Asn) c.413G>A (p.Arg138His)	sensorineural hearing loss, hypoglycemia	611971	(Gardeitchik et al., 2018)
uS7m	c.550A>G, (p.Met184Val)	congenital sensorineural deafness, progressive hepatic and renal failure, lactic acidemia	611974	(Menezes et al., 2015)
uS14m	c.322C>T (p.Arg108Cys)	perinatal hypertrophic cardiomyopathy, neonatal lactic acidosis, growth retardation, dysmorphism, mental retardation	611978	(Jackson et al., 2019)
bS16m	c.331C>T (p.Arg111*)	agenesis of corpus callosum, mild ventricular dilatation, dysmorphism, lactic acidosis	609204	(Emdadul Haque et al., 2008; Miller et al., 2004)
mS22	c.509G>A (p.Arg170His), c.644T>C (p.Leu215Pro) c.1032_1035dup (p.Leu346Asnfs*21)	agenesis of corpus callosum, skin oedema, hypotonia, hypertrophic cardiomyopathy, lactic acidaemia, hyperammonaemia, tubulopathy, atrial and ventricular septal defects, Cornelia de Lange-like phenotype	605810	(Baertling et al., 2015; Emdadul Haque et al., 2008; Saada et al., 2007; Smits et al., 2011)
mS23	c.119C>G (p.Pro40Arg)	hepatic disease	611985	(Kohda et al., 2016)
mS25	c.215C>T (p.Pro72Leu)	encephalomyopathy, dyskinetic cerebral palsy, partial agenesis of corpus callosum	611987	(Bugiardini et al., 2019)
mS34	c.321+1G>T (p.Val100_Gln107del), c.322-10G>A (p.Asn108Leufs*12, Asn108Glyfs*50) c.37G>A (p.Glu13Lys), c.94C>T (p.Gln32*)	Leigh syndrome	611994	(Lake et al., 2017)
mS39	c.415-2A>G (p.Cys139Glufs*71), c.1747-1748insCT (p.PheSerfs*3)	Leigh syndrome	614918	(Borna et al., 2019)
uL3m	c.950C>G (p.Pro317Arg), deletion	hypertrophic cardiomyopathy, psychomotor retardation	607118	(Galmiche et al., 2011)
bL12m	c.542C>T (p.Ala181Val)	growth retardation, neurological deterioration	602375	(Serre et al., 2013)
uL24m	c.272T>C (p.Leu91Pro)	cerebellar atrophy, choreoathetosis of limbs and face, mental retardation	611836	(Di Nottia et al., 2020)
mL44	c.467T>G (p.Leu156Arg), c.233G>A (p.Arg78Gln)	cardiomyopathy, liver steatosis, pigmentary retinopathy, hemiplegic migraine, Leigh-like lesions in the brain, renal insufficiency, hepatopathy	611849	(Carroll et al., 2013; Distelmaier et al., 2015)

The clinical phenotypes among all patients are quite diverse. However, what they all have in common are early-onset, fatal, multi-system disorders. For this reason, profound knowledge

about the mitoribosome and its assembly are essential to understand the pathological mechanisms leading to those diseases and to determine possible treatment options.

2.3 Scope and aims of the thesis

Aim of this doctoral thesis was to dissect the assembly of the human 39S mtLSU in further detail. Thus, a triple SILAC approach was designed to investigate the biogenesis of the mitoribosome *in vivo*. For this purpose, isolated 55S mitoribosomes were required as an internal standard for mass spectrometry measurements.

Part one of this thesis focuses on the purification of human mitoribosomes. First, the separation of mitoribosomal complexes on sucrose gradients had to be optimized. Therefore, the following questions were addressed:

    i.   Which sucrose concentration has to be used within gradients to achieve the best separation of mitoribosomal particles?

    ii.   Which type and concentration of salt in buffers is required to minimize unspecific protein-protein interactions but keep the ionic strength?

    iii.   Which impact does the concentration of Mg^{2+} ions have on the human mitoribosome integrity?

    iv.   How can the purity of the starting material be improved?

Answers to these questions were used to establish a protocol for isolation of human 55S mitoribosomes. In order to enhance the yield and quality of purified mitoribosomes, the type of detergent for mitochondrial lysis and the purification method of crude mitoribosomes were also investigated.

Within the second part of this thesis, the disease associated protein mL44 and the membrane anchor mL45 were characterized in regard of their impact within the biogenesis of the human 39S mtLSU. In order to do so, the subsequent questions have been asked:

    v.   What is the role of mL44 during 39S mtLSU biogenesis?

    vi.   Does loss of mL44 have an impact on mitochondrial translation and mtLSU assembly?

    vii.   Does the mitoribosome require its membrane anchor to assemble?

    viii.   Do mtLSU submodules assemble in absence of mL45?

    ix.   Is the mtSSU assembly affected upon depletion of mL44 or mL45?

3. Materials and Methods

3.1 Materials

3.1.1 Chemicals

A list of chemicals used in this study together with their manufacturers can be found in Table 4.

Table 4: List of used chemicals in this study.

Chemical name	manufacturer
[^{35}S]-L-methionine	Hartmann Analytic
2-Mercaptoethanol (β-Mercaptoethanol)	AppliChem GmbH
2-Propanol	Roth
Acetic acid	Roth
Acetone	Roth
Acrylamide (2xcrystallized)	Roth
Acrylamide/bisacrylamide (37.5:1) solution	Roth
Agarose NEEO ultra-quality	Roth
Ammonium acetate	Roth
Ammonium chloride (NH$_4$Cl)	MERCK
Ammonium hydroxide solution	Sigma-Aldrich
Ammonium persulfate (APS)	Roth
Ampicillin	AppliChem GmbH
Anti-FLAG M2 Affinity Gel	Sigma-Aldrich
Bacto™ Agar	BD
Bacto™ Peptone	BD
Bacto™ Tryptone	BD
Bacto™ Yeast Extract	BD
Bis-acrylamide (2X)	SERVA
Blasticidine S HCl	ThermoFisher Scientific
BPB (Bromophenol blue)	MERCK
BSA (Bovine Serum Albumin)	Sigma Life Science
Calcium chloride dihydrate	Roth
Chloramphenicol	Sigma Life Science
Chloroform	Roth
CNBr activated Sepharose 4B	GE Healthcare
cOmplete™ Protease inhibitor cocktail tablets	Roche
Coomassie Brilliant Blue R-250	Serva
Developing solution Developer G153	Agfa
Digitonin	Calbiochem
di-Potassium hydrogen phosphate	Roth

Chemical name	manufacturer
di-Sodium hydrogen phosphate dihydrate	AppliChem GmbH
DMSO (dimethyl sulphoxide)	MERCK
DNase I	Thermo Scientific
dNTP Mix	Thermo Scientific
DTT (1.4-Dithiothreitol)	Roth
EDTA (Ethylendiamine tetraacetic acid)	Roth
Emetine	Invitrogen
Ethanol	Roth
Ethidium Bromide (0.025%)	Roth
FBS (fetal bovine serum)	Biochrom
Fixing solution Rapid Fixer G354	Agfa
FLAG-peptide	Sigma-Aldrich
Formaldehyde	Sigma-Aldrich
GeneJuice® Transfection Reagent	Novagen
GeneRuler DNA Ladder Mix	Thermo Scientific
Glycerol	Sigma-Aldrich
Glycine	Roth
HEPES (4-(2-hydroxyethyl)-1-piperazineethanesulfonic acid)	Roth
Hydrochloric acid 37% w/v	Roth
Hydrogen peroxide	Sigma-Aldrich
Hygromycine B	Life Technologies
L-Glutamine 200mM (100X)	gibco
Lipofectamine RNAiMAX	Invitrogen
Magnesium chloride heptahydrate	MERCK
Manganese (II) chloride tetrahydrate	Roth
Methanol	Roth
MOPS (Morpholinopropanesulfonic acid)	Roth
NP-40 (Nonidet P40, 4-Nonylphenyl-polyethylene glycol)	Sigma Life Science
Nupage 20x running buffer	Invitrogen
NuPage LDS Sample buffer 4x	Invitrogen
Opti-MEM™	gibco
Penicillin Streptomycin	gibco
Phenol	Roth
Phosphatase alkaline	Roche
Pierce™ ECL Western Blotting Substrate	Life Technologies
Plasmocin™	invivogen
PMSF (Phenylmethyl sulphonyl fluoride)	Roth
Ponceau S (C.I. 27195)	Roth
Potassium chloride	Roth
Potassium dihydrogen phosphate	Roth
Potassium hydroxide	Roth

Chemical name	manufacturer
Precision Plus Protein™ All Blue Prestained Standards (10-250kD)	Bio-Rad
Protein-A sepharose	GE healthcare
Proteinase K	Roth
RiboLock RNase Inhibitor	Thermo Scientific
Roti-Quant® Reagent	Roth
Rubidium Chloride	Roth
SDS (sodium dodecyl sulfate)	Roth
Silver nitrate	Roth
Sodium acetate	Roth
Sodium azide	Sigma-Aldrich
Sodium carbonate	MERCK
Sodium chloride	Roth
Sodium Deoxycholate	Roth
Sodium dihydrogen phosphate	Roth
Sodium hydrogen carbonate	MERCK
Sodium hydroxide	AppliChem GmbH
Sodium pyruvate solution	Sigma Life Science
Sodium tetraborate	Sigma-Aldrich
Sodium Thiosulfate	Sigma Chemical Co.
Sucrose, D (+)	Roth
Taq DNA Polymerase	Invitrogen
TCA (Trichloroacetic acid)	Roth
TEMED (Tetramethylethylendiamine)	Roth
Trehalose	Roth
Tricine	Roth
TRIS (Tris(hydroxymethyl)aminomethane)	Roth
Tris(2-carboxyethyl)-phosphine hydrochloride (TCEP)	Sigma-Aldrich
tri-Sodium Citrate Dihydrate	Roth
Triton X-100	Roth
TRIzol™ Reagent	Ambion
Tween-20	Roth
Uridine	Sigma-Aldrich

3.1.2 Recipes of used buffers and solutions

Buffers were prepared as stated in Table 5 with Aqua dest. and autoclaved or sterile filtrated if indicated.

Table 5: Composition of used buffers and solutions in this study.

Buffer	Recipe
15 % sucrose buffer	15 % (w/v) sucrose, 100 mM NH_4Cl, 8mM $MgCl_2$, 20 mM Tris/HCl pH 7.5, 5 mM DTT
30 % gradient buffer	30 % (w/v) sucrose, 100 mM NH_4Cl, 10 mM $MgCl_2$, 20 mM Tris/HCl pH 7.4, cOmplete™ Protease inhibitor cocktail tablet 1/50 ml
30 % sucrose buffer	15 % (w/v) sucrose, 100 mM NH_4Cl, 8mM $MgCl_2$, 20 mM Tris/HCl pH 7.5, 5 mM DTT
5 % gradient buffer	5 % (w/v) sucrose, 100 mM NH_4Cl, 10 mM $MgCl_2$, 20 mM Tris/HCl pH 7.4, cOmplete™ Protease inhibitor cocktail tablet 1/50 ml
acrylamide Mix	45 % (w/v) acrylamide, 1.5 % (w/v) bis-acrylamide (32:1), sterile filtrated
anode buffer	0.2 M Tris, pH 8.9
blocking solution	5% (w/v) milk powder in TBS-T
cathode buffer	0.1 M tricine, 0.1% (w/v) SDS, 0.1M Tris, pH 8.25
cell culture cultivation medium	DMEM (Dulbecco's modified Eagle's medium), 10% (v/v) FBS, 2 mM L-glutamine, 1 mM sodium pyruvate, 50 µg/ml uridine, 100 units/ml penicillin, 100 µg/ml streptomycin, sterile filtrated
Coomassie staining solution	0.25 % (w/v) Coomassie Brilliant Blue R-250, 10 % (v/v) acetic acid, 40 % (v/v) ethanol
coupling buffer	0.1 M $NaHCO_3$ pH 8.3, 0.5 M NaCl
destainer	40% ethanol (v/v), 10% acetic acid (v/v)
developing solution	6 % (w/v) Na_2CO_3, 0.0185 % (v/v) formaldehyde, 16 µM $Na_2S_2O_3$
fixation solution / Stop solution	50 % (v/v) methanol, 12 % (v/v) acetic acid
FLAG-IP dilution buffer	20 mM Tris/HCl pH 7.4, 100 mM NH_4Cl, 10 % (v/v) glycerol, 20 mM $MgCl_2$, 1 mM PMSF, cOmplete™ Protease inhibitor cocktail tablet 1/50 ml
FLAG-IP lysis buffer	20 mM Tris/HCl pH 7.4, 100 mM NH_4Cl, 10 % (v/v) glycerol, 20 mM $MgCl_2$, 1 % (w/v) digitonin, 1 mM PMSF, 0.08 U/µl RiboLock RNase Inhibitor, cOmplete™ Protease inhibitor cocktail tablet 1/50 ml
FLAG-IP wash buffer with or without glycerol	20 mM Tris/HCl pH 7.4, 100 mM NH_4Cl, 20 mM $MgCl_2$, 1 mM PMSF, cOmplete™ Protease inhibitor cocktail tablet 1/50 ml, supplemented with or without 10 % (v/v) glycerol
freezing medium	DMEM (Dulbecco's modified Eagle's medium), 18 % (v/v) FBS, 9 % (v/v) DMSO, sterile filtrated
gel buffer	1 M Tris, 0.1 % (w/v) SDS, pH 8.45, autoclaved
high sucrose cushion buffer	60 % (w/v) sucrose, 100 mM NH_4Cl, 8mM $MgCl_2$, 20 mM Tris/HCl pH 7.5, 5 mM DTT
homogenisation buffer	300 mM trehalose, 10 mM KCl, 10 mM HEPES pH 7.4, 1 mM PMSF, with or without 0.2 % (w/v) BSA, autoclaved
impregnation solution	0.8 mM $Na_2S_2O_3$

Buffer	Recipe
isolation dilution buffer/storage Buffer	100 mM NH_4Cl, 8mM $MgCl_2$, 20 mM Tris/HCl pH 7.5, 5 mM DTT
isolation lysis buffer	100 mM NH_4Cl, 8mM $MgCl_2$, 20 mM Tris/HCl pH 7.5, 1 % (v/v) Triton X-100, 5 mM DTT
LB medium (lysogeny broth)	1 % (w/v) tryptone, 0.5 % (w/v) NaCl, 1 % (w/v) yeast extract, autoclaved
mitoplast dilution buffer	3 % (w/v) sucrose, 100 mM NH_4Cl, 10 mM $MgCl_2$, 20 mM Tris/HCl pH 7.5, 0.08 U/µl RiboLock RNase Inhibitor, cOmplete™ Protease inhibitor cocktail tablet 1/50 ml
mitoplast Lysis buffer	3 % (w/v) sucrose, 100 mM NH_4Cl, 10 mM $MgCl_2$, 20 mM Tris/HCl pH 7.5, 1 % (w/v) digitonin, 0.08 U/µl RiboLock RNase Inhibitor, cOmplete™ Protease inhibitor cocktail tablet 1/50 ml
NP-40 lysis buffer	50 mM Tris/HCl pH 7.4, 130 mM NaCl, 2 mM $MgCl_2$, 1 % NP-40 (v/v), 1 mM PMSF, 1x PI-Mix
PBS (Phosphate buffered saline)	0.14 M NaCl, 2.7 mM KCl, 0.01 M Na_2HPO_4, 1.8 mM KH_2PO_4, pH 7.4, autoclaved
RF1 buffer	100 mM RbCl, 50 mM $MnCl_2$, 30 mM Na-acetate, 10 mM $CaCl_2$, 15% (w/v) glycerol; pH adjustment to 5.8 with Acetic acid; sterile filtrated
RF2 buffer	10 mM RbCl, 50 mM $MnCl_2$, 10 mM MOPS, 75 mM $CaCl_2$, 15% (w/v) glycerol; pH adjustment to 6.8 with NaOH; sterile filtrated
SDS sample buffer	10 % (v/v) glycerol, 2 % (w/v) SDS, 0.01 % (w/v) bromophenol blue, 63 mM Tris/HCl, pH 6.8, 5 mM DTT
silver solution	0.2 % (w/v) $AgNO_3$, 0.026 % formaldehyde
sucrose cushion buffer	34 % (w/v) sucrose, 100 mM NH_4Cl, 8mM $MgCl_2$, 20 mM Tris/HCl pH 7.5, 5 mM DTT
TAE buffer	40 mM Tris/acetate pH 8.0, 2 mM EDTA
TBS-T (Tris buffered saline - Tween20)	20 mM Tris/HCl (pH 7.5), 125 mM NaCl, 0.1 % (v/v) Tween20
transfer buffer	20 mM Tris, 0.02 % (w/v) SDS, 150 mM glycine, 20 % (v/v) ethanol

3.1.3 Disposables and kits

All disposables and kits used in this study are listed in Table 6.

Table 6: Used disposables and kits.

Item	Manufacturer
Amicon® Ultra-0.5 Centrifugal Filter Devices 100K	Merck Millipore
Amicon® Ultra-15 Centrifugal Filter Devices 100K	Merck Millipore
Amicon® Ultra-4 Centrifugal Filter Devices 100K	Merck Millipore
Blotting paper	Heinemann Labortechnik
Bottle Top Filter 500 ml, 45 mm neck	Corning
Cell culture flask Nunc™ EasYFlask™ Nunclon™ Delta Surface 25cm², 75cm²	Thermo Scientific
Cellstar® Cell Culture Dishes, PS, 145/20 mm	Greiner Bio-One
Cellstar® Cell Culture Plate 6, 12, 24, 96 Well	Greiner Bio-One
Cellstar® Tubes 50 ml, 15 ml	Greiner Bio-One
Centrifuge bottles polypropylene with caps (29 x 104 mm), 50 ml	Beckman Coulter
CryoPure Tube 1.6 ml	Sartstedt
Disposable hypodermic needle Sterican® 21G x 3 1/8"/ ∅ 0.80 x 80 mm, 14G x 3 1/8"/ ∅ 2.10 x 80 mm	B. Braun
Econo-Pac® Disposable Chromatography Columns, 10 ml	Bio-Rad
Fast digestion enzymes	Thermo Fisher
First Strand cDNA Synthesis Kit	Thermo Scientific
Graduated filter tips 1000 µl, 300 µl, 20 µl, 10 µl	Greiner Bio-One
Immobilon®-P membrane, PVDF, 0.45 µm	Merck Millipore
KOD Hot Start DNA Polymerase	Novagen
MColorpHast™ pH indicator stripes pH 5.0-10.0	Merck Millipore
Micro tube 1.5 ml protein Low binding	Sarstedt
Micro tubes 2.0 ml, 1.5 ml	Sarstedt
Multiply®- Pro cup 0.2 ml	Sarstedt
Nitrocellulose membrane Amersham™ Protran™ 0.2µm NC	GE Healthcare Life Science
NuPAGE™ 4-12% Bis-Tris Midi Gel	Invitrogen
Open-top centrifuge tubes polyallomer (13x51 mm)	Seton
Open-top centrifuge tubes polyallomer (25x89 mm)	Seton
Open-top polyclear™ centrifuge tubes (14x89 mm)	Seton
Pipette tips 1000 µl, 200 µl, 10 µl	Sarstedt
QuickExtract™ DNA Extraction Solution	Lucigen
Rapid DNA Ligation Kit	Thermo Scientific
Reaction tubes 0.6 ml	Biozym
SafeSeal tube 5 ml	Sarstedt
SensiMix™ SYBR Low-ROX Kit	Bioline
Spin columns Mobicol "classic"	MoBiTec
Super RX-N Fuji Medical X-ray film	Fujifilm
Syringe Omnifix® Luer Lock Solo 50ml, 10 ml	B. Braun
TOPO TA Cloning® Kit for Sequencing	Invitrogen
Wizard® *Plus* SV Minipreps DNA Purification System	Promega
Wizard® SV Gel and PCR Clean-Up System	Promega

3.1.4 Instruments and equipment

Instruments and equipment used in this doctoral work are stated in Table 7.

Table 7: Instruments and equipment:

Instrument/Equipment	Model	Manufacturer/Supplier
Centrifuge	5418	Eppendorf
	5427R	Eppendorf
	5804R	Eppendorf
	Avanti J-26XP	Beckman Coulter
	Sorvall RC 6 Plus	Thermo Scientific
	Optima L-90K	Beckman Coulter
	Optima Max-XP	Beckman Coulter
	Universal 320	Hettich
	Kendro Megafuge 1.0	Heraeus®
Electrophoresis	Blotting chamber PerfectBlue™ "Semi-Dry" Electro Blotter Sedec™ M	peqlab
	Power Supply EV3020, EV2650	Consort
	Novex™ XCell™ SureLock™ Mini-Cell	Invitrogen
	XCell4 SureLock Midi-Cell	Invitrogen
	Wide Mini-Sub® Cell GT	Bio-Rad
	PowerPac HC™ Power Supply	Bio-Rad
Miscellaneous	GeneTouch Thermal Cycler	BIOER
	Gradient Station™	Biocomp
	Homogenisator Potter-Elvehjem with PTFE pistil 15ml	Sartorius
	Homogenisator Potter-Elvehjem with PTFE pistil 2ml	Omnilab
	Homogenisator Potter-Elvehjem with PTFE pistil 5ml	Omnilab
	Incubator Heraeus® Hera cell 150	Thermo Scientific
	Light microscope	Zeiss
	Pipettes	Gilson
	Sterile Hood Heraeus® Hera safe	Thermo Scientific
	Thermomixer comfort	Eppendorf
	Vortex-Genie 2	Scientific Industries
	Storage Phosphor screen	GE Healthcare
	Synergy H1 microplate reader	BioTek
	Nanodrop™ One^C Microvolume UV-Vis Spectrophotometer	Thermo Scientific
	Homogenisator machine homogen^{plus}	schuett-biotec.de
	Rocking table RS-RR10	PHOENIX instrument
	Fisherbrand™ Glass Funnel Filter with Sintered Glass Disc	Fisherbrand™
	Accu-jet® pro	Brand
	X-ray cassette 24x30	rego X-ray GmbH
	Magnetic stirrer MR3001	HEIDOLPH

Instrument/Equipment	Model	Manufacturer/Supplier
Rotor	JA-20	Beckman Coulter
	MLS-50	Beckman Coulter
	SS-34	Sorvall
	SW 32 Ti	Beckman Coulter
	SW 41 Ti	Beckman Coulter
	TLA-55	Beckman Coulter
Scanner	Developing machine Curix 60	AGFA
	Typhoon FLA 9500 Phoshpoimager	GE Healthcare

3.1.5 Cells and microorganisms

Human cell lines used in this study are listed in Table 8.

Table 8: Cell lines used in this study.

Cell line	Source
Flp-In™ T-REx™ 293 (HEK293T WT)	ThermoFisher Scientific, R78007
Flp-In™ T-REx™ 293 mL44$^{-/-}$	This study
Flp-In™ T-REx™ 293 mL44$^{-/-}$_mL44-FLAG (mL44 Rescue)	This study
Flp-In™ T-REx™ 293 mL45$^{-/-}$	This study
Flp-In™ T-REx™ 293 mL45$^{-/-}$_mL45-FLAG (mL45 Rescue)	This study

Table 9 shows the bacterial cell lines used in this doctoral work.

Table 9: Bacterial cell lines used in this study.

Bacterial cell line	Source
E. coli TOP10 One Shot® Chemicallly Competent Cells	Invitrogen
E. coli XL1-Blue	Stratagene

3.1.6 Antibodies

Primary antibodies were purchased from ProteinTech Europe (Manchester, United Kingdom), Merck KGaA (Darmstadt, Germany), Bio-Techne GmbH (Wiesbaden, Germany), Santa Cruz Biotechnology, Inc. (Heidelberg, Germany) or abcam (Cambridge, United Kingdom). Home-made antibodies were obtained by injecting purified proteins or synthetic peptides into rabbits and subsequent serum retrieval. A complete list of primary antibodies used in this doctoral work is shown in Table 10. Secondary antibodies coupled with HRP (goat-anti-rabbit and goat-anti-mouse) were purchased from Dianova GmbH (Hamburg, Germany).

Table 10: List of primary antibodies used in this study.

Protein	Antibody	Company
uL1m	Anti-MRPL1 rabbit polyclonal	home-made
uL3m	Anti-MRPL3 rabbit polyclonal	ProteinTech (16584-1-AP)
uL10m	Anti-MRPL10 rabbit polyclonal	ProteinTech (16652-1-AP)
bL12m	Anti-MRPL12 rabbit polyclonal	ProteinTech (14795-1-AP)
uL13m	Anti-MRPL13 rabbit polyclonal	ProteinTech (16241-1-AP)
bL20m	Anti-MRPL20 rabbit polyclonal	ProteinTech (16969-1-AP)
bL21m	Anti-MRPL21 rabbit polyclonal	ProteinTech (16978-1-AP)
uL23m	Anti-MRPL23 rabbit polyclonal	home-made
uL24m	Anti-MRPL24 rabbit polyclonal	ProteinTech (16224-1-AP)
bL32m	Anti-MRPL32 rabbit polyclonal	home-made
mL39	Anti-MRPL39 rabbit polyclonal	home-made
mL44	Anti-MRPL44 rabbit polyclonal	ProteinTech (16394-1-AP)
mL45	Anti-MRPL45 rabbit polyclonal	ProteinTech (15682-1-AP)
mL45	Anti-MRPL45 rabbit polyclonal	home-made
mL62	Anti-ICT1 rabbit polyclonal	ProteinTech (10403-1-AP)
uS7m	Anti-MRPS7 rabbit polyclonal	Sigma-Aldrich (HPA023007)
uS14m	Anti-MRPS14 rabbit polyclonal	ProteinTech (16301-1-AP)
uS15m	Anti-MRPS15 rabbit polyclonal	ProteinTech (17006-1-AP)
bS16m	Anti-MRPS16 rabbit polyclonal	ProteinTech (16735-1-AP)
mS22	Anti-MRPS22 rabbit polyclonal	ProteinTech (10984-1-AP)
mS25	Anti-MRPS25 rabbit polyclonal	ProteinTech (15277-1-AP)
mS27	Anti-MRPS27 rabbit polyclonal	ProteinTech (17280-1AP)
mS29	Anti-DAP3 rabbit polyclonal	ProteinTech (10276-1-AP)
mS40	Anti-MRPS18b rabbit polyclonal	ProteinTech (16139-1-AP)
GTPBP7	Anti-MTG1 rabbit polyclonal	novusbio (NBP2-19428)
GTPBP10	Anti-GTPBP10 rabbit polyclonal	novusbio (NBP1-85055)
GAPDH	Anti-GAPDH mouse monoclonal	Santa Cruz (sc-32233)
COX2	Anti-COX2 mouse monoclonal	abcam (ab110258)
FLAG	Anti-FLAG mouse monoclonal	Sigma-Aldrich (F1804)
SDHA	Anti-SDHA mouse monoclonal	ThermoFisher (459200)
Sec61β	Anti-Sec61β rabbit polyclonal	kindly provided by AG Schwappach
RPL3	Anti-RPL3 mouse monoclonal	ProteinTech (66130-1-lg)
NGRN	Anti-NGRN rabbit polyclonal	ProteinTech (14885-1-AP)
NSUN4	Anti-NSUN4 rabbit polyclonal	ProteinTech (16320-1-AP)
Calnexin	Anti-Calnexin mouse monoclonal	ProteinTech (66903-1-lg)
PHB2	Anti-Prohibitin 2 rabbit polyclonal	ProteinTech (12295-1-AP)
YME1L	Anti-YME1L rabbit polyclonal	ProteinTech (11510-1-AP)
TIM23	Anti-TIM23 rabbit polyclonal	home-made
TOM70	Anti-TOM70 rabbit polyclonal	home-made
MFN2	Anti-MFN2 rabbit polyclonal	ProteinTech (12186-1-AP)

3.1.7 Plasmids and oligonucleotides

Oligonucleotides used in this doctoral work were purchased from Microsynth SEQLAB (Göttingen, Germany) and are listed in Table 11.

Table 11: Oligonucleotides used in this study.

Oligonucleotide name	sequence	function
EK#11	ATGGCGTCCGGGCTGGTAAG	forward primer to amplify region of mL44 $^{-/-}$
EK#12	CGGCTTCTCTGAACGGCGCA	reverse primer to amplify region of mL44 $^{-/-}$
RRD#132	GCAGGAAGTGAGAGCAGTGTG	forward primer to amplify region of mL45$^{-/-}$
RRD#133	CTCACACATCTTAGTAGAGCCAAC	revers primer to amplify region of mL45$^{-/-}$

Plasmids used in this study were either bought from Fisher Scientific GmbH (Schwerte, Germany) or isolated from *E. coli* (XL1-blue). For details of used plasmids check Table 12.

Table 12: Plasmids used in this study.

Plasmid	Function	Source
pOG44	expression of Flp recombinase	Invitrogen
pcDNA5/FRT/TO	insertion of tetracycline inducible constructs into FRT sites in Flp-In™ host cell line	Invitrogen
pCR™4-TOPO®	for rapid cloning of Taq-polymerase generated PCR products for sequencing	Invitrogen
pcDNA5-mL44-FLAG clone 3-2	tetracycline inducible expression of FLAG-tagged variant of mL44 protein	provided by Dr. Ricarda Richter-Dennerlein
pcDNA5-mL45-FLAG clone 4-2	tetracycline inducible expression of FLAG-tagged variant of mL45 protein	provided by Dr. Ricarda Richter-Dennerlein

3.1.8 Software

Software used in this doctoral work is listed in Table 13.

Table 13: Used Software.

Software	Producer
Adobe® Illustrator® CS6	Adobe Systems, San Jose, CA, USA
Adobe® Photoshop® CS6	Adobe Systems, San Jose, CA, USA
Affinity Designer	Serif (Europe) Ltd., Nottingham, United Kingdom
Genious® 11.1.4	Biomatters Ltd., Auckland, New Zealand
ImageJ 1.50i	Rasband, W.S., U. S. National Institutes of Health, Bethesda, MD, USA,
ImageQuant TL	GE Healthcare BioSciences AB, Uppsala, Sweden
Mendeley	Elsevier, Amsterdam, Netherlands
Microsoft® Office	Microsoft Corporation, Redmond, WA, USA
Papers	Mekentosj, Aalsmeer, Netherlands

3.2 Methods

3.2.1 Molecular biology techniques

3.2.1.1 Polymerase chain reaction (PCR)

For amplification of DNA fragments via PCR the KOD Hot Start DNA Polymerase (Novagen®) was used according to the manufacturer's instructions. Primers were designed in respect to which DNA area had to be amplified and the melting temperature adjusted. To set up the reaction, 25 mM $MgSO_4$, 2 mM dNTPs, 10 µM forward primer, 10 µM reverse primer, template DNA, 1 µl polymerase (1 U/µl) and 5 µl 10x reaction buffer (part of the KOD Hot Start DNA Polymerase Kit) were mixed and the total reaction volume was adjusted with Aqua dest. to 50 µl. Depending on the purpose either 10 ng plasmid DNA or 2 µl of a reverse transcription reaction was used as template. The reaction mixture was placed into the Thermal Cycler (GeneTouch) and the PCR was started by activation of the polymerase at 95°C for 2 min, followed by a denaturing step at 95°C for 20 s. The annealing temperature was calculated depending on the used primers and applied for 10 s. Length of extension at 70°C was chosen corresponding to the size of the DNA fragment to be amplified. Denaturation, annealing and extension were repeated in cycles for 20 to 40 times. The obtained PCR product was analysed via agarose gel electrophoresis.

3.2.1.2 Agarose gel electrophoresis

To analyse or purify DNA, agarose gel electrophoresis was used. To cast a gel, agarose (Roth) was dissolved in TAE-buffer by heating, to obtain a 1 % (w/v) or 1.5 % (w/v) solution depending on the size of the DNA fragment to be purified. The melted agarose was cooled down to approximately 50°C before adding ethidium bromide (Roth) up to a concentration of 1 µg/ml. Samples were mixed with either 50 % glycerol (v/v) or 10 % Fast Digest Green Buffer (Thermo Scientific), loaded onto the gel next to the molecular weight marker (GeneRuler DNA Ladder Mix) and were run for 10 min at 120 V. To finally visualize the DNA fragments, they were exposed to UV-light.

3.2.1.3 Purification of PCR products

PCR products were either directly purified by using the Wizard® SV Gel and PCR Clean-Up System (Promega) or first loaded onto an agarose gel, the respective DNA band excised and then purified as recommended by the company.

3.2.1.4 Determination of DNA/RNA concentrations

To measure the DNA or RNA concentration within a solution, 1 µl of the samples was analysed by determining the absorption at 260 nm with the Nanodrop™ One^C Microvolume UV-Vis Spectrophotometer (Thermo Scientific).

3.2.1.5 Molecular cloning

For molecular cloning, the plasmid DNA and the PCR product, which should be inserted into the plasmid, were subjected to restriction digestion with Fast digestion enzymes (Thermo Fisher). Conditions for digestion were chosen according to the manufacturer's instructions. Two Micrograms of insert and 4 µg of vector DNA were digested for 30 min at 37°C, each in 40 µl total reaction volume (DNA, 2 µl restriction enzyme A, 2 µl restriction enzyme B, 4 µl 10x Fast Digest Buffer, adjusted to the final volume with Aqua dest.). To avoid re-ligation, the vector was dephosphorylated by adding 2 µl alkaline phosphatase (Roche) and 4 µl 10x buffer (supplied from alkaline phosphatase kit) and incubated for 45 min at 37°C. Vector and insert DNA were purified as described before and ligation was set up usually in a 1:6 (vector : insert) molar ratio using the Rapid DNA Ligation Kit (Thermo Scientific). To carry out the reaction 50 ng vector and an appropriate amount of insert were mixed with 5x ligation buffer, 1 µl T4 DNA-Ligase, adjusted to a total reaction volume of 20 µl with Aqua dest. and incubated for 30 min at 22°C. Four microliter from this reaction were used to transform 100 µl chemically competent *E. coli (*XL1-blue). Single clones were picked on the next day, inoculated in LB-media containing 100 µg/ml ampicillin and incubated for 37°C over night shaking. Plasmid DNA was isolated by using Wizard® *Plus* SV Minipreps DNA Purification System (Promega). To analyse, whether the isolated plasmids contained the desired insert, a test digestion was performed with approximately 150 ng of plasmid DNA followed by an agarose gel electrophoresis of the samples. Positive clones were chosen and sent for sequencing (Microsynth SEQLAB Göttingen).

3.2.1.6 Transformation of chemically competent E. coli

In order to bring plasmid DNA into bacteria, transformation via heat shock was performed. For this reason, 4 µl DNA was added to 100 µl of chemically competent *E. coli* (XL1-blue) cells, incubated for 30 min on ice followed by a heat shock at 42°C for 1 min. Cells were rested on ice for 2 min prior adding of 900 µl of pre-warmed LB-media and subsequent incubation at 37°C for 1 h shaking. The bacterial suspension was centrifuged at 8,000xg for 1 min at room temperature, the bacterial pelleted was resuspended in 100 µl LB-media and finally plated onto LB-agar-plates (15 g/l agar) containing ampicillin (final concentration: 100 µg/ml) as selective antibiotic.

3.2.1.7 RNA isolation from cultured cells

RNA isolation from cultured cells was performed as described previously by (Chomczynski and Sacchi, 2006). HEK293T cells were seeded into a 6-well cell culture plate and harvested upon 80 % confluency with PBS supplemented with 1 mM EDTA. Cells were centrifuged at 1,000xg for 5 min at room temperature. The cell pellet was carefully resuspended with 500 µl TRIzol™ Reagent (Ambion) and incubated for 5 min at room temperature. Next, 100 µl chloroform were added and the sample was shaken by hand for 15 s followed by an incubation for 3 min at room temperature. Subsequently, the sample was centrifuged at 12,000xg for 15 min at 4°C to separate the RNA from DNA and proteins. The upper aqueous phase containing the RNA was transferred into a new reaction tube and 250 µl isopropanol were added and incubated for 10 min at room temperature to precipitate the RNA. The RNA was pelleted by centrifugation at 12,000xg for 10 min at 4°C, washed once with 80 % (v/v) ethanol and dried by several short centrifugation steps followed by removal of the supernatant. Finally, 10 µl Aqua dest. supplemented with 0.5 µl RiboLock RNase Inhibitor (Thermo Scientific) were added to the RNA pellet and incubated over night at 4°C for complete dissolving. The concentration of the RNA was determined as described before. For long-term storage, the RNA was kept at -80°C.

3.2.1.8 cDNA preparation

Complementary DNA was prepared from RNA via reverse transcription by using the First strand cDNA synthesis kit (Thermo Scientific) according to the specifications of the manufacturer. All steps were carried out in a thermal cycler. To set up the reaction, 1 µg of mRNA was used, 1 µl of 100 µM oligo $(dT)_{18}$ were added and the total volume was adjusted to 11 µl with Aqua dest.. The mixture was incubated at 65°C for 5 min and afterwards cooled down on ice for 2 min. Upon addition of 4 µl 5x reaction buffer, 1 µl RiboLock RNase Inhibitor (20 U/µl), 2 µl 10 mM dNTP Mix and 2 µl M-MuLV Reverse Transcriptase, the reaction was incubated at 37°C for 60 min and next at 70°C for 5 min. The obtained cDNA was either used directly for PCR or stored at -20°C.

3.2.1.9 Isolation of genomic DNA from cultured cells

For isolation of genomic DNA from cultured HEK293T cells the QuickExtract™ DNA Extraction Solution (Lucigen) was used according to the manufacturer's instructions. For this purpose, cells were seeded into a 96-well cell culture plate and cultured until they reached confluency. Cells were harvested and mixed with 50 µl QuickExtract Solution, vortexed for 15 s followed by an incubation at 65°C for 10 min. After another 15-s vortex step the sample was incubated at 98°C for 5 min and diluted with 100 µl Aqua dest. The extracted genomic DNA was stored until usage at -20°C. To sequence specific areas of the gDNA a PCR with respective primers was carried out.

The PCR product was purified and sent in for sequencing (Microsynth SEQLAB Göttingen). Analysis of the obtained sequences was performed by using the Genious® Software.

3.2.1.10 TOPO® sequencing

For sequencing of heterozygous HEK293T$^{-/-}$ cell lines TOPO® sequencing was applied. The linearized plasmid pCR™4-TOPO® included in the TOPO TA Cloning® Kit for Sequencing (Invitrogen) has a covalently bound Topoisomerase I and 3' thymidine overhangs. The sequence which should be analysed, was amplified via PCR by using *Taq* polymerase according to the manufacturer's instructions to obtain a deoxyadenosine at the 3' end. To set up the TOPO® cloning reaction, 4 µl of the respective PCR product were mixed with 1 µl of TOPO® vector and 1 µl salt solution followed by an incubation for 5 minutes at room temperature. Afterwards the sample was cooled down on ice to stop the reaction. Transformation was performed by adding 2 µl of the reaction into a vial of One Shot® chemically competent *E. coli* (TOP10). Bacterial cells were incubated on ice for 10 min, the heat-shock was performed for 30 s at 42°C and the cells were again placed on ice. Next, 250 µl of pre-warmed S.O.C. medium was added and cells were shaken at 200 rpm at 37°C for 1 h. Finally, 50 µl of cells were plated on a prewarmed LB-plate containing 100 µg/ml ampicillin and incubated at 37°C overnight. Twenty single colonies were picked and further processed as described in 3.2.1.5. Each colony contained just one variant of the sequence of the heterozygous HEK293T$^{-/-}$ cell line and the sequencing results were analysed by using the Genious® Software.

3.2.2 Cell culture techniques

3.2.2.1 Cell culture maintenance

Human embryonic kidney cell lines (Flp-In™ T-REx™ 293: WT / mL44$^{-/-}$ / mL44 Rescue / mL45$^{-/-}$ / mL45Rescue) were maintained in cell culture cultivation medium (see Table 5) at 37°C in a humidified atmosphere enriched with 5% CO_2. When confluent, cells were passaged. For this purpose, cells were harvested with PBS supplemented with 1 mM EDTA and centrifuged at 1000xg for 5 min at room temperature. The cell pellet was resuspended with cell culture cultivation medium and an appropriate number of cells was seeded into a 75cm² cell culture flask for further cultivation or into cell culture dishes for expansion. The same procedure was applied to harvest cells for further experiments. For long-term storage of cells in liquid nitrogen, obtained cell pellets were resuspended in freezing medium (compare Table 5). Cells were tested on a regular basis upon Mycoplasma contamination. If a contamination was detected cells were treated with plasmocin (Invivogen) for 2 weeks and tested again.

3.2.2.2 Generation of stable inducible expression cell lines

The HEK293T knock-out cell lines mL44^{-/-} and mL45^{-/-} generated via CRISPR/Cas9 technology were kindly provided by Dr. Ricarda Richter-Dennerlein. Both knock-out cell lines were made in a WT background carrying the Flp-In™ T-REx™ cassette. To rescue the respective phenotypes both cell lines were transfected with plasmids carrying the genetic information of the FLAG-tagged copy of the protein to generate stable inducible expression cell lines as described by (Mick et al., 2012; Richter-Dennerlein et al., 2016). Three days prior to transfection knock-out cells were seeded into a 6-well cell culture plate to reach a cell confluency of approximately 50 % on the day of transfection. For transfection, serum free media (Opti-MEM™ - gibco) was mixed with the transfection reagent (GeneJuice® - Novagen) according to the manufacturer's instructions and incubated for 5 min at room temperature. Afterwards 0.9 µg pOG44 and 0.1 µg pcDNA5/FRT/TO containing the respective construct was added to the transfection mix and another 15-min incubated at room temperature. This mixture was added to the cells which were maintained in cell culture cultivation medium without penicillin and streptomycin. Selection of positive clones having the desired insert started two days after transfection with 100 µg/ml hygromycin B and 5 µg/ml blasticidin S. Approximately four weeks after start of the selection single clones could be isolated. After induction with tetracycline for 24 h analysis of expression could be carried out via western blot.

3.2.2.3 Tetracycline titration

To test which concentration of tetracycline was required to get an expression level of the FLAG-tagged version of the protein similar to the endogenous one, a tetracycline titration was performed. For this purpose, cells were seeded into a 6-well cell culture plate and different concentrations of tetracycline (250 ng/ml, 100 ng/ml, 10 ng/ml, 1 ng/ml, 0.1 ng/ml, 0 ng/ml) were applied in cell culture cultivation medium. After 24 h cells were harvested and tested for expression by Western Blot.

3.2.2.4 [^{35}S] de novo synthesis of mitochondrial encoded proteins

To assess the *de novo* synthesis of mitochondrial encoded proteins a [^{35}S]Methionine labelling was carried out according to protocols by (Chomyn, 1996; Lavdovskaia et al., 2018).Therefore, cells were seeded into 25 cm² cell culture flasks. On the day of the experiment, the cell culture cultivation medium was removed from the cells and replaced by DMEM without methionine, cysteine and FCS. Cell were incubated for 10 min at 37°C. This washout step was done twice to remove unlabelled methionine. To inhibit cytosolic translation, cells were treated for 10 min at 37°C with media containing 100 µg/ml emetine and 10 % (v/v) FCS. Afterwards, cells were

incubated at 37°C with 200 µCi/ml [^{35}S]Methionine for 1 h and then harvested. The obtained cell pellet was washed four times with PBS and cells were lysed. Proteins were separated via SDS-PAGE and signals from radiolabelled proteins were visualized using the Typhoon FLA 9500 Phosphoimager (GE Healthcare).

3.2.3 Isolation of mitochondria

Isolation of crude mitochondria was carried out as described previously by (Callegari et al., 2016). In brief, HEK293T cells were harvested with PBS supplemented with 1 mM EDTA and pelleted at 1,000xg for 5 min at room temperature. The cellular pellet was solubilized in homogenization buffer with 0.2 % (w/v) BSA and incubated for 5 min on ice. To disrupt the cell membrane the cells were homogenized 20 times with a motor-driven potter at 800 rpm. The homogenate was subjected to several differential centrifugation steps in a tabletop centrifuge. At first, the homogenate was centrifuged at 400xg for 10 min at 4°C to remove the cellular debris. The supernatant was collected and the cellular pellet homogenized once or twice again. To pellet the mitochondria all obtained supernatants were combined and spun at 11000xg for 10 min at 4°C. The crude mitochondria were washed once in homogenization buffer without BSA and PMSF and subjected to another clarifying spin. Afterwards, the mitochondria were solubilized again and centrifuged at 400xg for 2 min at 4°C to remove eventual contaminations with cellular debris. The obtained supernatant contained the crude mitochondria which could be used for further processing or analyses.

For large scale isolation of mitochondria, the centrifugation steps were adapted due to the larger sample volumes: The slow spin was carried out at 1,000xg for 10 min at 4°C and the fast spin was performed at 20,000xg for 30 min at 4°C in a SS34 Rotor in a Sorvall RC 6 Plus centrifuge. All other conditions remained the same.

3.2.4 Mitochondrial or mitoplast lysate preparation

For lysis of mitochondria or mitoplasts the organelles were dissolved in mitoplast lysis buffer (mitochondrial concentration: 2 mg/ml, detergent/protein ratio 5:1) and incubated for 20 min on ice with occasional vortexing. To pellet the non-soluble parts, the solution was centrifuged for 15 min at 16,000xg at 4°C and the supernatant was transferred into a new reaction tube and was further processed by sucrose gradient centrifugation.

3.2.5 Protein co-immunoprecipitation

For investigation of protein-protein interactions, protein co-immunoprecipitation was performed according to (Dennerlein et al., 2015) with some modifications. Specific HEK293T cell lines expressing FLAG-tagged variants of proteins were induced for 24 h with corresponding concentrations of tetracycline and mitochondria were isolated from these cell lines as described before. Mitochondria were resuspended in FLAG-IP lysis buffer (detergent to protein ratio 5:1) and incubated for 30 min on ice with concomitant vortexing. The lysate was centrifuged for 10 min at 16,000xg at 4°C and the supernatant was transferred to a precooled low binding tube and diluted 1:1 with FLAG-IP dilution buffer. Anti-FLAG M2 affinity gel beads (1 mg protein/30 µl gel suspension containing 50 % beads) were washed three times with FLAG-IP wash buffer with glycerol, prior to loading of the sample onto the beads and subsequent binding of the FLAG-tagged protein and its interaction partners on a rotating wheel at 4°C for 1 h. To remove the unbound and not interacting proteins of the target protein, the beads were washed for 10 times with FLAG-IP Wash buffer with glycerol by centrifugation at 5,000xg for 30 s at 4°C and subsequent buffer exchange. If the co-immunoprecipitated complexes together with the FLAG-tagged protein were further separated via sucrose gradient centrifugation, the beads were washed 7 times with FLAG-IP wash buffer with glycerol and 3 times with FLAG-IP wash buffer without glycerol to avoid sinking of the sample into the gradient. After washing of the beads, the target protein and the co-immunoprecipitated complexes were eluted within a 30-min incubation step at 4°C at 1,000 rpm shaking in the presence of FLAG peptide (20 µg of FLAG peptide/1 mg of initial mitochondria) diluted 1:20 in FLAG-IP wash buffer with or without glycerol. The eluate containing the FLAG-tagged protein and its interaction partners was either subjected to sucrose gradient centrifugation or directly analysed via SDS-PAGE followed by western blotting.

3.2.6 Sucrose gradient centrifugation

To separate mitoribosomal complexes from each other, sucrose gradient centrifugation was performed as described by Lavdovskaia et al., 2018, with some changes. Therefore, 5-30 % linear sucrose gradients were casted. The top half-fill position of the centrifugation tube (14x89 mm, SETON) was marked by using the SW41 marker block. Half of the tube was filled with 5 % gradient buffer. By using a syringe and a needle the 30 % gradient buffer was carefully layered below the low percentage sucrose solution until the tube was completely filled. The tubes were closed with short rubber caps used for isokinetic sucrose gradient centrifugation. Linear sucrose gradients were prepared by using the program "Rotor: SW41, caps: short, 5-30% sucrose 1 step gradient" of the Gradient Station™ (BioComp) according to the manufacturer's instructions. Prior to usage,

prepared gradients were left for stabilization for 1 h at 4°C. For separation of mitoribosomal complexes either 300 µl of immunoprecipitation eluate or 300 µl of lysed mitochondria or mitoplasts were loaded on top of a 5-30 % gradient. If the sample volume was less than 300 µl, the volume was filled up with either FLAG-IP dilution buffer or mitoplast dilution buffer. The loaded sample volume was withdrawn from the gradient before. Gradients were centrifuged for 15 h at 79,000xg at 4 °C (Ultracentrifuge: Optima L-90K, Rotor: SW41Ti, Beckman Coulter). After the centrifugation, the gradients were fractionated by using the Gradient Station™ (BioComp) with the following settings: speed 0.3, distance 5.15 mm, fractions 16. These settings were leading to a fraction volume of approximately 730 µl. Fractions were precipitated and analysed via SDS-PAGE followed by western blotting.

3.2.7 Protein analysis

3.2.7.1 Protein precipitation

To concentrate proteins within fractions after sucrose gradient centrifugation, proteins were precipitated with ethanol. Therefore, to each fraction the 2.5-fold 100 % ethanol (ice cold) and the 1/3-fold 3 M sodium acetate pH 6.5 of the sample volume were added. Samples were frozen at -20°C for at least 2 h. Afterwards, proteins were pelleted for 15 min at 20,817xg at 4 °C and subsequently washed once with 80 % (v/v) ethanol before being dissolved in SDS sample buffer containing 50 mM DTT.

3.2.7.2 Cell lysate preparation

Harvested HEK293T cells were solubilized with an appropriate volume of NP40 lysis buffer and vortexed for 30 s at room temperature. After a clarifying spin at 600xg for 2 min at 4°C the supernatant was transferred into a new reaction tube and the protein concentration was determined. Samples can be stored at -20°C (in SDS sample buffer) or for long term storage at -80°C.

3.2.7.3 Bradford assay

Protein quantification was performed as described by (Bradford, 1976). Therefore, samples were mixed with Roti-Quant®reagent (Roth) and the absorbance was measured with a micro plate reader at 595 nm. With the help of a standard curve of different dilutions of 0.1 % (w/v) BSA the protein concentration of the sample was calculated.

3.2.7.4 SDS-PAGE

In order to separate proteins according to their size samples were subjected to SDS-PAGE. Due to the size of mitoribosomal proteins Tricine-SDS-PAGE was chosen as best option for protein separation according to (Schägger, 2006). Gel pouring stations and running chambers were custom made by the mechanical service department. For best resolution, either 10 – 18 % or 8 – 14 % gradient acrylamide gels were casted as dissolving gel overlaid by a 4 % stacking gel. SDS sample buffer was added to the samples. Prior to the electrophoresis, samples were incubated for 15 min at 37°C shaking. As a marker, the Precision Plus Protein™ All Blue Prestained Standard (Bio-Rad) was used. Gel electrophoresis was performed in cathode and anode buffer for 16 h overnight at 80 V and 25 mA. After electrophoresis, the proteins were visualized via gel staining or western blotting followed by immunostaining.

3.2.7.5 Silver staining

Silver staining is an easy possibility to stain proteins in the nanogram range. The staining procedure was performed as described by (Chevallet et al., 2006) with some changes. All steps were performed at room temperature on a rocking table. The gel was fixed in fixation solution for at least 1 h. Afterwards the gel was washed twice with 50 % (v/v) ethanol and once with 30 % (v/v) ethanol for 20 min respectively. This step was performed to remove the acetic acid which would lead to a decomposition of sodium thiosulphate present in the impregnation solution and subsequently to silver sulphite formation. The ethanol washing steps were followed by gel impregnation with impregnation solution for exactly 60 s. Next, the gel was washed three times with Aqua dest. for each 20 s to remove the sodium thiosulphate from the gel surface. The gel was then impregnated for 20 min with silver solution and subsequently washed three times for 20 s with Aqua dest.. To visualize the proteins, the gel was treated with developing solution for approximately 5 min until the bands were clearly visible. This was followed by two further washing steps for 2 min with Aqua dest. and finally, the developing was stopped by placing the gel into stop solution. The stained gel was stored in 5 % (v/v) acetic acid solution.

3.2.7.6 Western blot

For further analyses, proteins were required to be transferred from polyacrylamide gel to nitrocellulose membrane (GE Healthcare Life Science) or PVDF membrane (Merck Millipore) by semi-dry blotting. For this purpose, the membranes were either activated with methanol (PVDF) or Aqua dest. (nitrocellulose). Before blotting, membranes, blotting paper (Heinemann Labortechnik) and the gel were equilibrated in transfer buffer. All components were assembled

into the blotting chamber and transfer of the proteins from gel onto membrane occurred within 2 h at 250 mA and 25 V.

3.2.7.7 Membrane staining

After blotting, the membranes were stained to visualize all immobilized proteins. In brief, nitrocellulose membranes were stained with Ponceau S for 5 min at room temperature on a rocking table. To remove unbound Ponceau S, the membranes were washed shortly several times with Aqua dest. before drying.

For staining of PVDF membranes, Coomassie Brilliant Blue R-250 (Serva) was used. Prior to staining, the membrane was activated with methanol, then stained with Coomassie staining solution for approximately 5 min, followed by several washing steps with destainer and then dried.

3.2.7.8 Immunostaining

Dried membranes were activated either with Aqua dest. (nitrocellulose) or methanol (PVDF) followed by a washing step with TBS-T. Membranes were incubated for at least one hour at room temperature with blocking solution to avoid unspecific binding of antibodies. The membranes were incubated overnight with primary antibodies, which are prepared in blocking solution plus 0.2 % sodium azide. On the next day, the membranes were washed three times for 10 min with TBS-T on a rocking table to remove unbound antibodies. Membranes were then incubated with secondary antibodies coupled with HRP for 1.5 h. Subsequent detection of the antibody-protein complexes was performed after three additional washing steps with TBS-T, (each for 10 min) by using the Pierce™ ECL Western Blotting Substrate (Life Technologies) according to the manufacturer's instructions. The chemiluminescence signals were visualized by using X-ray films (Agfa). For quantification, X-ray films were scanned and signals were quantified by using the software ImageQuant TL (GE Healthcare). This procedure was required, as some antibodies against mitoribosomal proteins were not possible to detect by using fluorescence protein coupled secondary antibodies, due to their low abundance.

3.2.8 Antibody purification

To purify an antibody, the protein against which the antibody was generated needed to be coupled to CNBr activated sepharose. For this reason, CNBr activated sepharose was soaked on a glass funnel filter with sintered glass disc for 15 min in 1 mM HCl, followed by a washing step with 1 mM HCl. The pH of the beads was adjusted to 8 by rinsing with coupling buffer. Beads were transferred into a 50-ml tube, mixed with the protein dissolved in coupling buffer and incubated in an end over end shaker for 2 h at room temperature. Afterwards, beads were washed first with coupling buffer and second with 0.1 M Tris/HCl pH 8, prior to an overnight blocking step with 0.1 M Tris/HCl pH 8 at 4°C. On the next day, beads were transferred into a column and washed for three times with 0.1M sodium acetate / 0.5M NaCl pH 5 and another three times with 0.1 M Tris/HCl / 0.5 M NaCl pH 8. For purification of the respective antibody, beads were washed with TBS. Next, the antibody serum was diluted 1:1 with TBS and passed over the column containing the beads coupled with the corresponding protein to bind for two times. This was followed by another washing step with TBS before elution was performed via pH shift by using 100 mM glycine/HCl pH 2.5. A total of six fractions containing the purified antibody were collected and mixed with 0.1 M Tris pH 8. The beads were regenerated with 10 mM Tris pH 7.5 until the pH reached 7.5, which was tested by using pH indicator stripes. Finally, the beads were washed with TBS complemented with 0.02 % sodium azide before they were stored at 4°C.

3.2.9 Preparation of competent cells

Preparation of transformation competent *E. coli* with divalent cations was performed as described previously by (Hanahan, 1983) with some changes. XL1-blue cells were inoculated as a pre-culture in LB medium overnight at 37°C and continuous shaking. On the following day, the pre-culture was diluted 1:100 with LB medium and grown at 37°C while shaking to mid-log phase (OD_{600}=0.2-0.3). Cells were incubated on ice for 15 min, pelleted at 900xg for 10 min at 4°C and subsequently resuspended in sterile RF1 buffer and further incubated on ice for 30 min. After this, bacteria were again pelleted at 900xg for 10 min at 4°C and the obtained pellet was resuspended in cold RF2 buffer, followed by a 15-min incubation step on ice. The competent cells were aliquoted, snap frozen in liquid nitrogen and stored at -80°C.

4. Results

4.1 Purification of mammalian mitoribosomes

4.1.1 Introduction

Within this doctoral thesis the assembly of the 39S mtLSU should be further investigated. Therefore, a triple SILAC approach (Figure 15) was set up in collaboration with Prof. Dr. Henning Urlaub to analyse the biogenesis of the mitoribosome similar as already described by Chen and Williamson (2013) for the assembly of the bacterial ribosome.
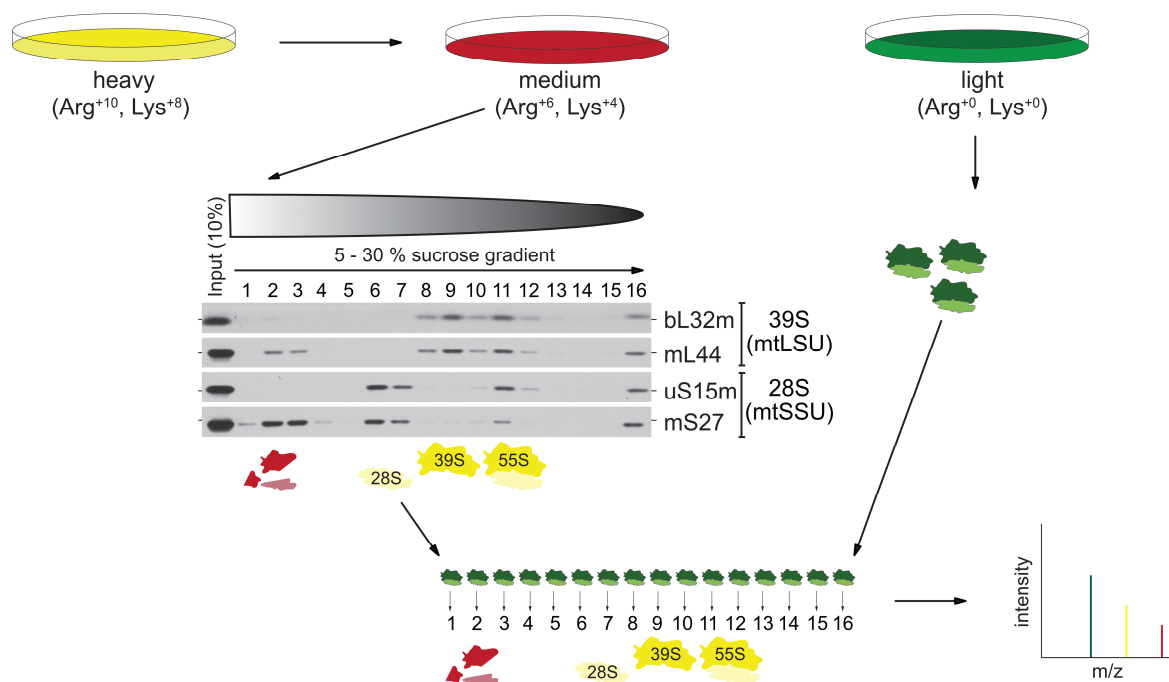
Figure 15: Triple SILAC approach. HEK293T WT cells were grown for at least 10 days in heavy SILAC medium (Arg+10, Lys+8) and then shifted into medium SILAC medium (Arg+6, Lys+4). Cells were harvested at different points of time; mitochondria isolated and mitoribosomal complexes separated by sucrose gradient ultracentrifugation. Gradients were fractionated and an internal standard of lightly labelled purified mitoribosomes (Arg+0, Lys+0) was added into each fraction. Fractions were subjected to MS analysis.

After separation of mitoribosomal particles on sucrose density gradients, the behaviour of every mitoribosomal protein (MRP) in each fraction of the gradient will be investigated by quantitative mass spectrometry. This approach will reveal the order and time point of incorporation of individual MRPs, their ability to form submodules and to finally create a map for the assembly of the mitoribosome. Even if an assembly map for the mammalian 55S mitoribosome was suggested recently (Bogenhagen et al., 2018), the biogenesis of the mitochondrial ribosome is not solved in

detail. Data used in the aforementioned publication were gained by SILAC analysis of the complete 55S mitoribosome. In contrast, the planned triple SILAC approach aims to determine each MRP and assembly factor in each fraction along the gradient in a quantitative way at different time points. For this, purified mitoribosomes lightly labelled (Arg^{+0}, Lys^{+0}) were used as an internal standard, which were spiked into each fraction at each time point. To obtain the required human 55S mitoribosomes, different parameters of the separation of mitoribosomal complexes on sucrose gradients had to be optimized in order to establish a method for mitoribosome purification. Additionally, purified mitoribosomes were not only required for this specific SILAC study but also for functional assays and structural analyses in the future to address the mammalian mitoribosome assembly. Some protocols for mitoribosome isolations were already published but did not fit to our requirements. (Aibara et al., 2018; Carroll, 2017; O'Brien and Kalf, 1967; Spremulli, 2007). Hence, a new protocol to purify 55S mitoribosomes from human cells had to be determined.

4.1.2 Optimization of separation of mitoribosomal complexes on sucrose gradients

To analyse assembly intermediates and to purify mitoribosomes, the separation of mitoribosomal complexes on sucrose gradients had to be improved in regard of sucrose concentration, buffer conditions and purity of starting material.

4.1.2.1 Sucrose concentration

First of all, the impact of different sucrose concentrations on mitoribosome separation on sucrose gradients was tested. Therefore, mitochondria were isolated from HEK293T WT cells and lysed as described in chapter 3.2.3 and 3.2.4. The cleared lysate was loaded either on top of a 5-30 % sucrose gradient or on top of a 10-30 % gradient and sucrose gradient ultracentrifugation was performed according to 3.2.6. Gradients were fractionated, fractions were ethanol precipitated and further analysed by SDS-PAGE and western blot with specific antibodies for mtLSU or mtSSU. In a 5-30 % gradient the 55S ribosome migrates in fraction 12/13, the 39S mtLSU in fraction 10 and the 28S mtSSU in fraction 7/8. In contrast, in a 10-30 % gradient the 55S particle is in fraction 9/10, the 39S in fraction 7 and the 28S in fraction 5/6. Ribosomal complexes including assembly intermediates are better separated in the lower dense fractions using a 5-30% sucrose gradient instead of a 10-30 % gradient (Figure 16). For this reason, a 5-30 % sucrose gradient was used for further investigations.
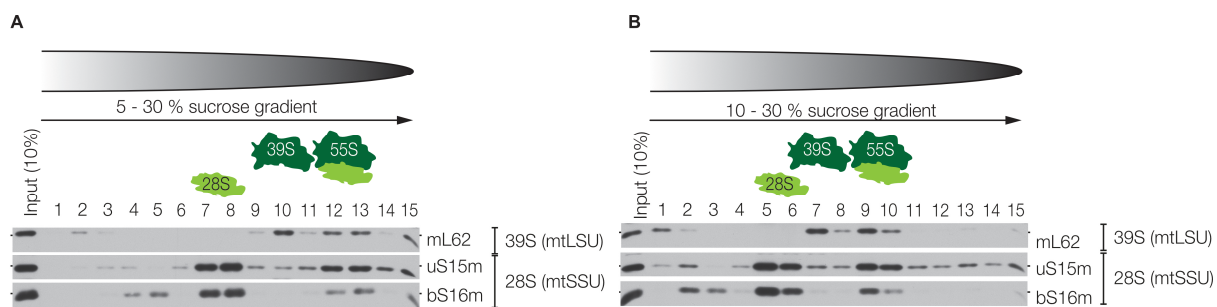
Figure 16: Impact of sucrose concentration on complex separation. Mitochondrial lysate (0.5 mg) was subjected to sucrose gradient ultracentrifugation. Collected fractions (1-16) were precipitated and analysed by SDS-PAGE and western blot using specific antibodies for mtLSU (mL62) and mtSSU (uS15m, bS16m). Input = 50 µg lysed mitochondria. A) 5-30% sucrose gradient. B) 10-30% sucrose gradient.

4.1.2.2 Type and concentration of salt

As a next step, the type of salt used in buffers for sucrose gradients was analysed. Sodium chloride needs to be avoided as it dissociates bacterial 70S ribosomes (Hardy and Turnock, 1971). Usually, potassium chloride is used as salt in buffers for separation of mitoribosomal complexes in order to reduce unspecific protein-protein-interactions and to keep the ionic strength (Carroll, 2017). However, studying the assembly and function of bacterial ribosomes ammonium chloride is commonly used. In the following, both salts were compared in their attribute on complex separation and 55S maintenance. As described before, mitochondrial lysates were subjected to sucrose gradient ultracentrifugation in buffers containing either 100 mM KCl or 100 mM NH_4Cl. Under both conditions, the 55S ribosome was preserved, however, a better separation of 39S from 55S was observed in the presence of NH_4Cl (Figure 17). Hence, in the following experiments NH_4Cl was the salt of choice.
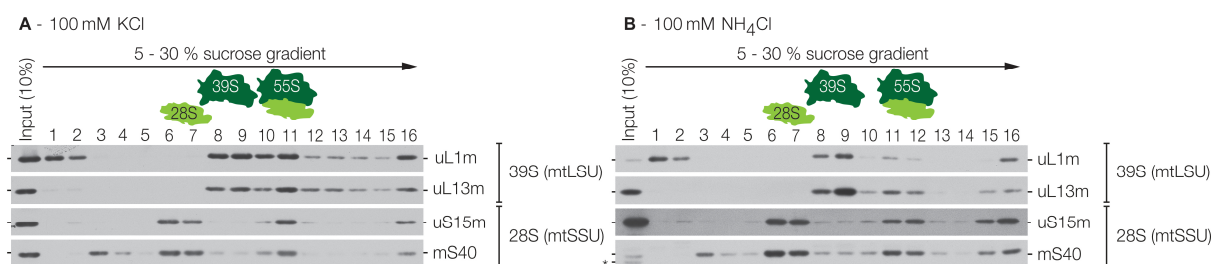
Figure 17: Difference between KCl and NH_4Cl in regard of separation of ribosomal complexes. Sample preparation was performed as indicated in Figure 16. Input = 50 µg lysed mitochondria. Asterisk indicates residual signals from previous antibody decorations.

Next, the optimal salt concentration was determined. High salt concentrations are used to minimize unspecific protein-protein interactions and to dissociate translational factors from the bacterial ribosome (Goyal et al., 2017; Spitnik-Elson and Atsmon, 1969). In contrast to eukaryotic ribosomes, 70S ribosomes accept high salt concentrations while still keeping their integrity

(Schweet and Heintz, 1966). As the mammalian mitoribosome is closely related to the bacterial ribosome, higher salt concentrations were tested in order to improve the purification of mitoribosomes. To check whether 55S mitoribosomes can cope with high salt concentrations, mitoribosomal particles were separated by sucrose gradient ultracentrifugation in buffer containing either 100 mM NH_4Cl or 300 mM NH_4Cl. Using 300 mM NH_4Cl a loss of the 55S monosome together with an increase in free 39S and 28S particles was observed (Figure 17). As the mammalian mitoribosome was found to dissociate at higher salt concentrations, 100 mM NH_4Cl was finally used for further purifications.
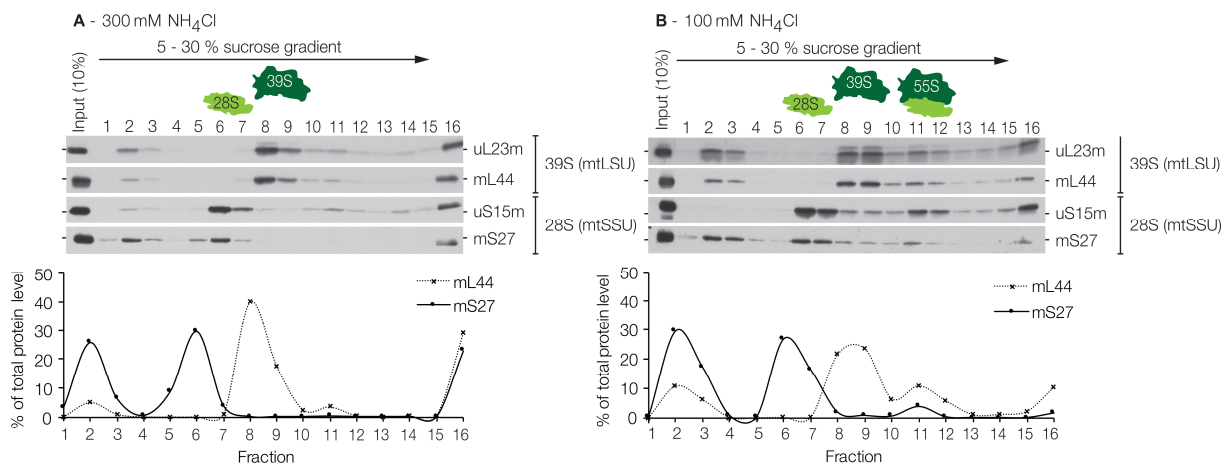
Figure 18: Impact of salt concentration on mitoribosome stability. Sample preparation was performed as indicated in Figure 16. Input = 50 µg lysed mitochondria. Proteins of mtLSU (mL44) and mtSSU (mS27) were quantified and the protein distribution across the gradient in comparison to the total protein level was calculated.

4.1.2.3 Impact of Mg^{2+} concentration on mitoribosome integrity

For isolation of mitochondria, buffers are often supplemented with EDTA in order to reduce protease activity by chelating Mg^{2+} and Ca^{2+} ions (Carroll, 2017). This chelating agent needs to be strictly avoided as it was shown already by (Lamfrom and Glowacki, 1962) that Mg^{2+} is required to maintain the structural integrity of 70S ribosomes. In contrast, high Mg^{2+} concentrations do not have a positive influence on translation in bacteria (Noah and Wollenzien, 1998). In order to determine the appropriate Mg^{2+} concentration for separating mitoribosomal complexes without dissociation of the 55S monosome, different Mg^{2+} concentrations were tested in buffers for mitochondrial lysis and sucrose gradient centrifugation. Isolated mitochondria were lysed in different buffers containing 20 mM, 10 mM, 8 mM, 6 mM, 4 mM or 2 mM $MgCl_2$. Ribosomal particles were separated by sucrose gradient centrifugation using the mentioned magnesium concentrations. The 55S ribosome was intact in the presence of 20 mM $MgCl_2$, 10 mM $MgCl_2$ or 8 mM $MgCl_2$. Using 6 mM $MgCl_2$ a slight reduction in the level of 55S ribosome in fraction 11 and 12 was detected, especially visible for the mtSSU protein mS27. Reducing the $MgCl_2$ concentration

further to 4 mM, the dissociation of 55S particles was even more pronounced and using 2 mM MgCl$_2$ 55S ribosomes were not detectable. Thus 8 mM MgCl$_2$ is required to prevent 55S dissociation and was used for further experiments
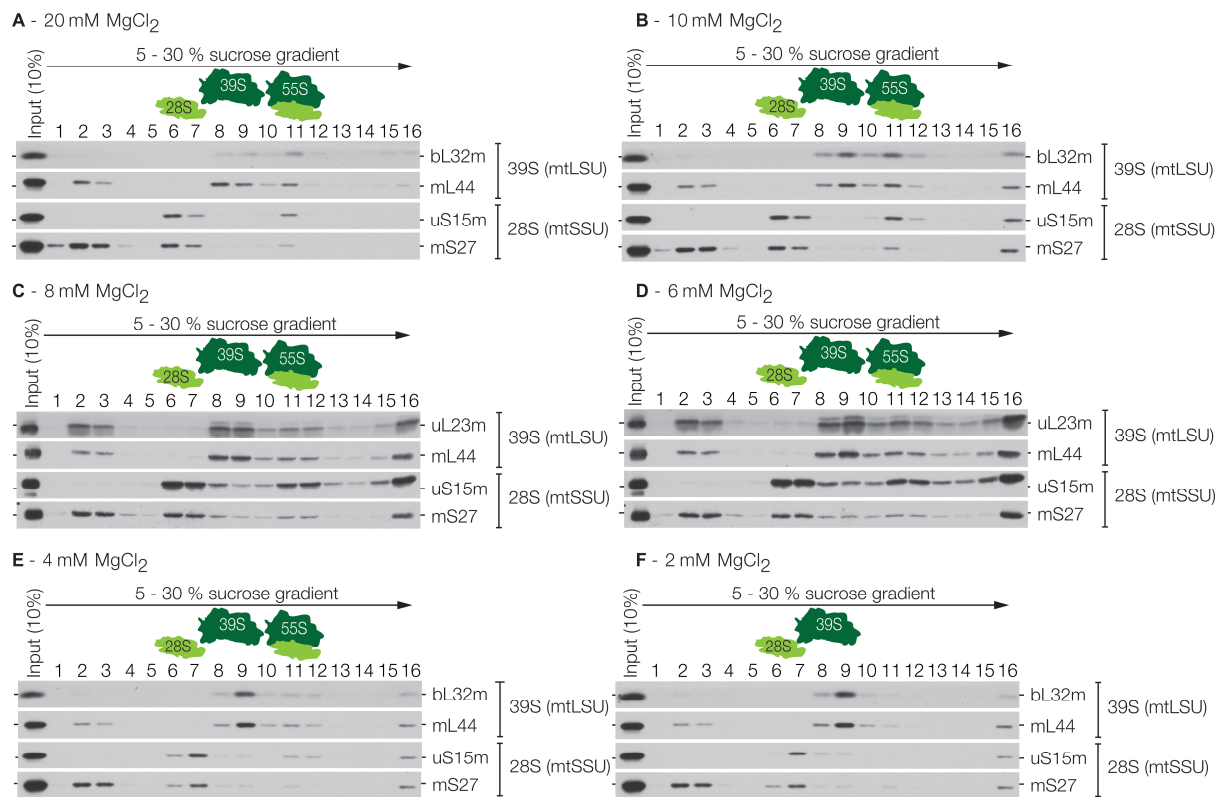
Figure 19: Impact of different Mg^{2+} concentrations on mitoribosome stability. Sample preparation was performed as indicated in Figure 16. Input = 50 µg lysed mitochondria.

4.1.2.4 Improvements on purity of starting material

Mitochondria are isolated as described in 3.2.3. These mitochondrial samples contain still contaminants such as endoplasmic reticulum (ER) and cytosolic proteins. The ER and mitochondria are in close relationship as reviewed by De Brito and Scorrano, 2010. Cytosolic ribosomes (80S) are bound to a portion of ER. An initial experiment was performed by Dr. Ricarda Richter-Dennerlein: mitochondria were isolated, lysed and the lysate was loaded on a 10-30% sucrose gradient. Obtained fractions were precipitated with ethanol and fractions 3-15 were analysed by mass spectrometry in the group of Prof. Dr. Henning Urlaub, Department of Bioanalytical Mass Spectrometry, Max Planck Institute for Biophysical Chemistry (Göttingen). Samples were subjected to LC/MS, analysed via MaxQuant (version 1.6.0.1) and LFQ (label free quantification) values were calculated. The LFQ intensity for each analysed fraction for two mitoribosomal proteins is plotted in Supp. Figure 1A. The 55S monosome is situated in fraction 9. For this reason, fraction 9 was further analysed (Supp. Table 1). In total, 805 proteins were

detected by MS analysis. Out of these, 72 of 82 mitoribosomal proteins were found with low abundance. In contrast, the sarcoplasmic/endoplasmic reticulum calcium ATPase 2 and the ER protein Calnexin were identified with higher abundances. In addition, 47 proteins of the cytosolic ribosome were detected. As beforehand mentioned, purified mammalian mitoribosomes are required for further analyses and thus contamination with 80S ribosomes needs to be minimized. A possibility to eliminate associated cytosolic ribosomes is to strip mitochondria from the outer membrane using low concentration of digitonin in order to produce mitoplasts (Spremulli, 2007). If the digitonin concentration is well chosen, the outer mitochondrial membrane (OMM) is disrupted and can be removed together with proteins of the inter membrane space (IMS) by Proteinase K treatment leaving the inner mitochondrial membrane (IMM) and the matrix still intact (Figure 20).
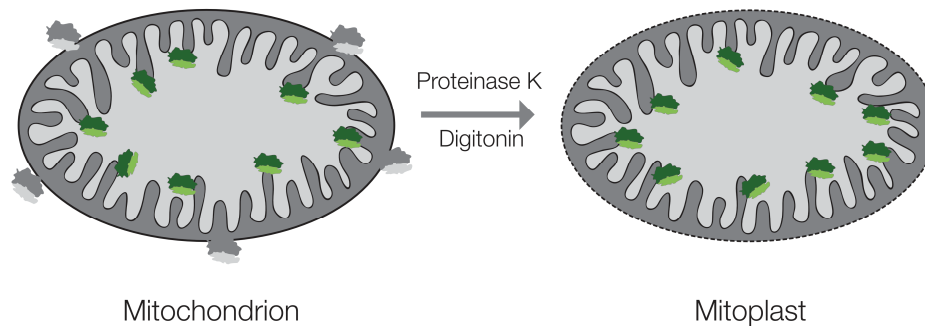
Figure 20: Difference mitochondrion and mitoplast.

In order to define the best digitonin concentration, mitochondria were isolated and treated with different concentrations of the detergent to rupture the OMM. Samples were incubated for 30 min and further subjected to Proteinase K treatment (0.5 µg Proteinase K/100 µg mitochondria). If just the OMM is disrupted but not the IMM, proteins of the matrix are shielded by the IMM from a Proteinase K digestion. If the samples are centrifuged afterwards for 5 min at 12000xg, mitoplasts are pelleted, separated from digested proteins of the OMM and IMS in the supernatant. Without digitonin treatment 80S proteins are pelleted together with mitochondria. Using 0.01%, 0.05% and 0.1 % digitonin the IMM protein TIM23 is still intact, but the OMM protein MFN2 is digested by Proteinase K as well as the ER marker Sec61β and the 60S protein RPL3 (Figure 21A). Thus, under these conditions, the IMM of the mitoplasts stays intact while the OMM, ER and 80S ribosomes are removed. If the digitonin concentration is increased up to 0.2 %, the amount of proteins decreases in the mitoplast pellet suggesting that the IMM starts to get ruptured as well. Hence, mitoribosomal proteins in the matrix are also not protected well enough. Thus, for the preparation of mitoplasts 0.1% digitonin will be applied to 4 mg/ml mitochondrial suspension (protein:detergent = 4:1) followed by Proteinase K digestion with 5 µg protease/ 1 mg protein.
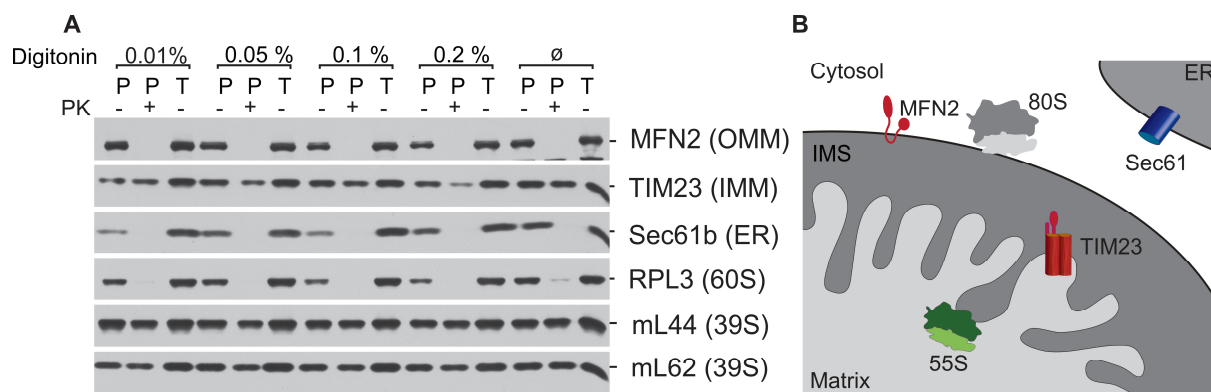
Figure 21: A) Determination of digitonin concentration for preparation of mitoplasts. Mitochondria were isolated and treated with different concentrations of digitonin. Samples were treated with Proteinase K (PK) as indicated and subjected to centrifugation. P = pellet fraction, T = total sample. All samples were further analysed by SDS-PAGE and western blot with specific antibodies for mtLSU, cytosolic ribosomes, ER, IMM and OMM. B) Localisation of proteins tested in A).

Finally, mitoplasts prepared as described above, were lysed and loaded onto a 5-30% sucrose gradient to separate mitoribosomal particles. Obtained fractions were given to our collaborators for MS-analysis. LFQ intensities for all 16 fractions for 2 mitoribosomal proteins are shown in Supp. Figure 1B. Fraction 11 with the assembled 55S ribosome was further investigated (Supp. Table 2). By MS-analysis 510 proteins were identified in this fraction. Overall, 80 of 82 mitoribosomal proteins have been detected with a 10-fold enrichment to the previous experiment. In contrast, just 36 cytosolic proteins were identified and contaminations with ER proteins (e.g. Calnexin and sarcoplasmic/endoplasmic reticulum calcium ATPase 2) were strongly reduced.

The parameters for the separation of mitoribosomal complexes by density gradient centrifugation could be significantly improved. Using mitoplasts instead of crude mitochondria increase the purity of the starting material. The optimal buffer composition was determined with $100\,mM\,NH_4Cl$ and $8\,mM\,MgCl_2$; and a sucrose gradient of 5-30% provides a reasonable separation in the lower dense fractions.

4.1.3 Mammalian mitoribosome isolation

4.1.3.1 Establishing a protocol for mammalian mitoribosome isolation

For the isolation of mitochondrial ribosomes from HEK293T cells, available protocols for bovine mitoribosome (Spremulli, 2007) and bacterial ribosome isolation (Rodnina and Wintermeyer, 1995) were tested and adjusted. First, mitoplasts from HEK293T cells were lysed in buffer containing 100 mM KCl, 20 mM MgCl$_2$, 20 mM HEPES/KOH pH 7.4, 3 mM β-mercaptoethanol, 1x protease inhibitor cocktail (Roche), 0.08 U/μl RiboLock RNase Inhibitor and 2 % digitonin (5 g digitonin:1 g protein). The lysate was subjected to centrifugation for 15 min at 20000xg to pellet the membrane fraction. The cleared lysate was loaded onto a 1 M sucrose cushion and ribosomes were pelleted using a SW41Ti rotor at 148,000xg for 15 h at 4°C. As the mitochondrial inner membrane comprises many large protein complexes, e.g. OXPHOS complexes, a lot of these were pelleted together with the mitoribosome. For subsequent separation of the 55S from the 28S and 39S, the sample was loaded onto a 10-30% sucrose gradient and centrifuged at 79,000xg for 15 h at 4°C using a SW41Ti rotor. Collected fractions were analysed by silver staining and western blotting (Figure 22).
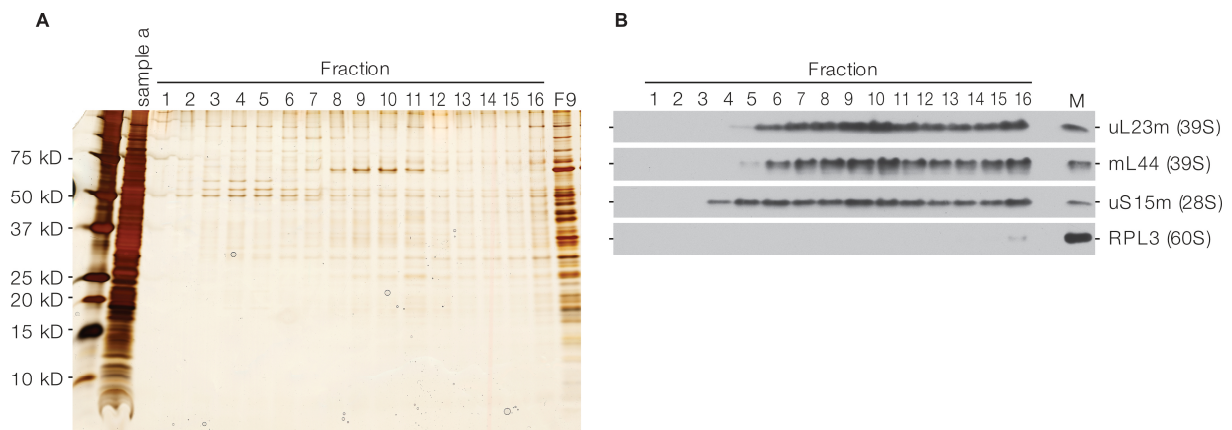
Figure 22: Mitoribosome isolation. From initial 60 plates of HEK293T cells, 20.5 mg mitoplasts were isolated. A) Sample a = 5 % of crude mitoribosomes. The remaining 95 % were loaded onto the 10-30 % sucrose gradient. For analysis, 1% of fraction material was loaded on a 10-18% Tris-Tricine gel and a silver staining was performed. Fraction 9 was pelleted to enhance the ribosomal concentration. F9 = 10 % of pelleted fraction 9. B) To analyse the composition of the pelleted fraction 9, 30 % of the total F9 were separated again on a 10-30 % sucrose gradient. Samples were separated by SDS-PAGE followed by western blotting using specific antibodies against mitoribosomal proteins and possible contaminants. M=10 μg crude mitochondria.

Fractions corresponding to 55S ribosomal particles were pelleted. Within the fractions no distinct peaks corresponding to mtLSU, mtSSU or 55S were detectable. Sample A was taken after the sucrose cushion prior loading of the material on the sucrose gradient. A sample of the pelleted fraction 9 was also analysed. Mitoribosomal proteins have mostly a molecular weight of less than 50 kD. The silver staining of the pelleted fraction 9 showed many proteins with a higher molecular weight reflecting contaminations with non-ribosomal proteins potentially caused by the use of the mild detergent digitonin, which maintains other large mitochondrial complexes.

Therefore, different detergents for lysing mitoplasts were tested to increase the efficiency and to reduce other mitochondrial complexes. Initially, sodium deoxycholate was used as solubilizing agent in mitoribosome isolation protocols (O'Brien and Kalf, 1967). Unfortunately, this detergent tends to precipitate upon addition of $MgCl_2$ or other divalent cations (Rehm and Letzel, 2016). As the presence of Mg^{2+} ions is crucial for the integrity of 55S mitoribosomes (see Figure 19), sodium deoxycholate was not suitable to use. In the protocol for bovine mitoribosome isolation by Spremulli, 2007, 0.16 mg Triton X-100 for 1 mg protein was used for solubilisation. However, the solubilisation capacity of Triton X-100 has a saturation of 0.38 mg Triton X-100 per 1 mg protein (Nicholson and McMurray, 1986) and the solvent-to-protein ratio should be 2-4:1 for Triton X-100 (Rehm and Letzel, 2016).

Thus, 2.5 mg Triton X-100:1 mg protein and 5 mg digitonin:1 mg protein were compared for lysis. Mitoplasts (33 mg) were lysed in buffer containing 100 mM NH_4Cl, 8 mM $MgCl_2$, 20 mM Tris/HCl pH 7.5, 2 U DNase/5 mg protein, 10 μM $CaCl_2$, 0.5 mM TCEP and the respective detergent (1 % Triton X-100/2 % digitonin). The cleared lysate was loaded onto a 1 M sucrose cushion, centrifuged as described previously and further subjected to 5-30 % sucrose gradient ultracentrifugation to separate the ribosomal particles.

The absorption of nucleic acids at 260 nm corresponds to 12S and 16S rRNA of the mitochondrial ribosome and thus three peaks are expected for 28S, 39S and 55S within the gradient. By using digitonin, no well-defined peaks corresponding to the mitoribosomal particles were obtained (Figure 23A). In contrast, using Triton X-100 as detergent revealed clear and distinct peaks for 39S mtLSU and 55S monosome and higher A260 values suggesting that more mitoribosomes were isolated (Figure 23B). Hence, Triton X-100 was further used as detergent for further experiments.
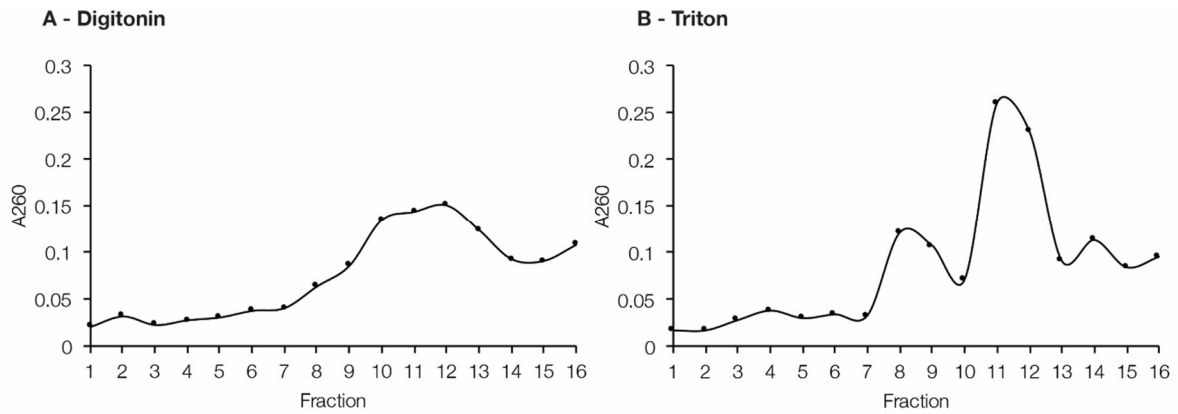
Figure 23: Mitoribosome isolation. Lysis of mitoplasts with 100 mM NH₄Cl, 8 mM MgCl₂ and A) 2 % digitonin B) 1 % Triton X-100. From all taken fractions, the absorption at A260 was measured and plotted over the fractions.

Since the crude ribosomal pellet was hard to dissolve a two-step sucrose cushion was applied to avoid pelleting (suggestion by Prof. Dr. Marina Rodnina). The mitoribosomes will accumulate in the interphase between 1 M and 1.7 M sucrose cushion. To check, whether the two-step sucrose cushion has an advantage over pelleting, both methods were compared.

After lysis of mitoplasts and subsequent centrifugation, proteins of the mitoribosome and other big complexes within the IMM are enriched in the supernatant fraction. Smaller portions are still in the pellet, besides residual amounts of cytosolic ribosomes, which were not completely removed by stripping of the OMM of mitochondria (Figure 24 A). The cleared lysate was loaded either A) onto a two-step sucrose cushion (20 ml sample/11 ml 1 M sucrose cushion solution/10 ml 1.67 M sucrose cushion solution) or B) on top of a single sucrose cushion (27 ml diluted sample/11 ml 1 M cushion solution) and centrifuged as described previously. The pelleted crude ribosome sample B was dissolved in wash buffer (100 mM NH₄Cl, 8 mM MgCl₂, 20 mM Tris/HCl pH 7.5, 5 mM DTT) supplemented with 1 % DMSO. From the two-step cushion sample A the interlayer between the two sucrose cushions was taken and buffer exchange was performed by ultrafiltration using Amicon® Ultra-15 Centrifugal Filter Devices 100K (Merck).

Samples of the interlayer (A) showed mitoribosomal proteins, a reduction of YME1L, but still contaminations with PHB2. Even with a two-step sucrose cushion, some proteins pelleted - amongst them a bigger portion of YME1L but also mitoribosomal proteins. Samples of the resuspended pellet B showed no reduction in the level of YME1L meaning that other big complexes cannot be separated with this method.
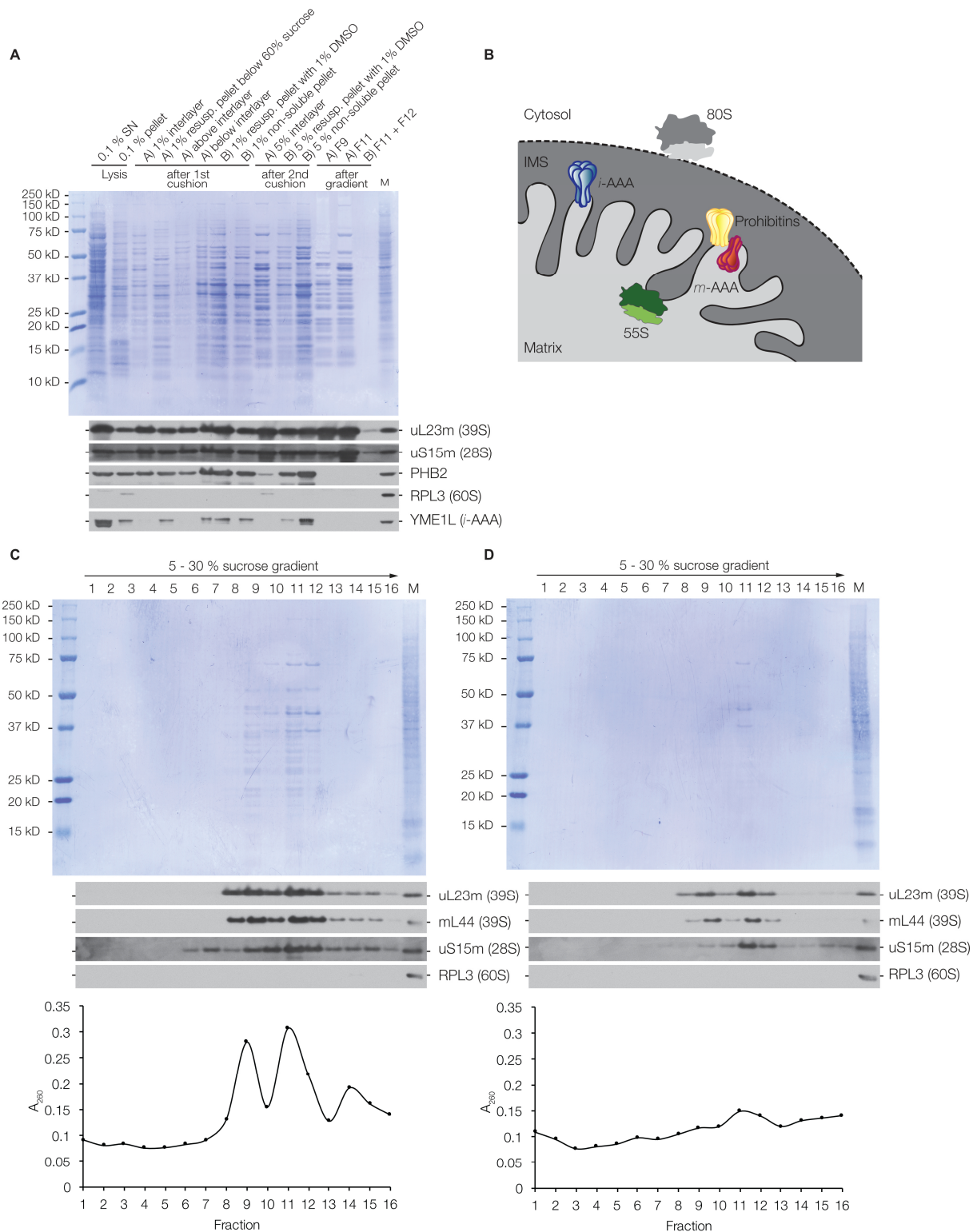
Figure 24: Mitoribosome isolation comparing non-pelleting versus pelleting of crude ribosomes. Buffer conditions: 100 mM NH₄Cl, 8 mM MgCl₂, 1 % Triton. Mitochondria were isolated from 120 plates of HEK293T cells and in total 66 mg of mitoplasts were obtained. A) Samples during experiment. 0.1 % of SN/pellet = 0.1 % of supernatant/pellet after lysis of 66 mg mitoplasts. F9/11/11+12 = 33 % of final fraction 9/11/11+12. B) Simplified presentation of protein complex localisation. Protein distribution over sucrose gradient and absorption at A_{260} plotted over the fractions of the two-step sucrose cushion (C) and pelleted sample (D). M= 10 µg crude mitochondria.

To improve the purity, both samples were subjected to a second sucrose cushion (A: two-step sucrose cushion: 6 ml sample/ 4.5 ml 1.1 M sucrose cushion/ 1.5 ml 1.75 M sucrose cushion; B: single sucrose cushion: 6.5 ml sample/ 4.5 ml 1.1 M sucrose cushion). Afterwards, the pelleted sample (B) was again dissolved in wash buffer containing 1 % DMSO or the two-step cushion sample (A) was ultra-filtrated for buffer exchange and sample volume reduction. Here, sample A showed a strong reduction of the PHB2 level. In contrast, the resuspended sample B was still contaminated with YME1L and PHB2. It has to be mentioned, that it was not possible to dissolve the pellet completely, as already described before. By analysing this non-soluble pellet, it became apparent that bigger portions of PHB2 and YME1L stayed insoluble together with mitoribosomal proteins. It can be concluded that substantial amounts of mitoribosomes get lost with this method.

To separate the crude mitoribosomes into 28S mtSSU, 39S mtLSU and assembled 55S complexes, samples were loaded on 5-30 % linear sucrose gradients, centrifuged and fractionated. For mitoribosomal fractions of sample A buffer exchange and sample volume reduction was applied by ultrafiltration. In contrast, 55S fraction of sample B was pelleted at 181,000xg for 6 h using a TLA55 rotor. The two-step sucrose cushion sample revealed well resolved peaks for 39S mtLSU and 55S monosome (Figure 24C). Proteins of the large and small mitoribosomal subunit are enriched in fraction 11, whereas RPL3 as cytosolic ribosome marker and PHB2 and YME1L as marker for other large mitochondrial protein complexes were not detected in contrast to 10 µg crude isolated mitochondria (Figure 24A). Based on the assumption by Spremulli, 2007, that 1 A_{260} equals 32 pmol of 55S, 4.5 nmol of 55S ribosomes were isolated from 33 mg mitoplasts. The Coomassie Blue staining revealed mainly proteins below 50 kD characteristic for mitoribosomal proteins. In comparison, by pelleting the material, the purification and separation of mitoribosomal particles was inefficient du to precipitations (Figure 24D). The 55S fractions 11 and 12 were combined, but from 33 mg mitoplasts just 1.4 nmol of 55S ribosomes were isolated, which is compared to the non-pelleted sample a loss in yield of 69 %. (Figure 24A).Although the purification of mitoribosomes over two two-step sucrose cushions improved the isolation efficiency significantly, the amount of lost material was still relatively high, thus for next isolations only one two-step cushion followed by a sucrose gradient was applied.

Finally, the sucrose gradient centrifugation step required optimization. With the help of Lukas Schulte and Uma Lakshmi Dakshinamoorthy from the laboratory of Holger Stark (Max-Planck-Institute for Biophysical Chemistry, Göttingen) by using their sucrose gradient estimator CowGraCE (Schulte, 2018) the sucrose gradient centrifugation was changed from 5-30 % linear sucrose gradient and 15 h run time at 79,000xg to 15-30 % linear sucrose gradient and 16 h 10 min run time at 115,605xg. With these settings the lowest overlap of subunit peaks and an optimal separation of the ribosomal particles was possible.

4.1.3.2 Final protocol for mammalian mitoribosome purification

After alteration of various parameters within the protocol for mitoribosome purification, the final strategy was applied:

Mitochondria were isolated from 98 plates of HEK293T cells as described in section 3.2.3. Mitoplasts were prepared by using 0.2 % digitonin (protein:detergent ratio 4:1) and 5 µg Proteinase K per 1 mg mitochondria. Following this, 68 mg mitoplasts were solubilized in a buffer containing 1 % Triton X-100, 100 mM NH_4Cl, 8 mM $MgCl_2$, 20 mM Tris/HCl pH 7.5, 5 mM DTT and membranes are separated by centrifugation. The cleared lysate was loaded onto a two-step sucrose cushion (20 ml sample/ 11 ml 1 M sucrose cushion solution/ 5 ml 1.75 M sucrose cushion solution) containing the same buffer conditions without detergent and centrifuged using a SW32Ti rotor for 15 h at 148,000xg at 4°C. Afterwards, the sample was fractionated and RNA and protein distribution over the fractions analysed (Figure 25A/B). Fraction 1-4 corresponded to material on top of the 1 M sucrose cushion after centrifugation, fraction 5 included the upper 2/3 of the 1 M sucrose cushion and fraction 6 the lower 1/3 of the 1 M sucrose cushion. Fraction 7 contained the interlayer between the two sucrose cushions and the complete 1.75 M sucrose cushion without the small pellet on the bottom. Within this pellet proteins of large complexes like *i*-AAA (YME1L) protease and Prohibitins (PHB2) were detected, but just smaller portions of mitoribosomal proteins. Mitoribosomes were enriched in fraction 7 and this material was subjected to ultrafiltration using Amicon® Ultra-15 Centrifugal Filter Devices 100K (Merck) in order to reduce the sucrose concentration and the sample volume. Within the ultrafiltration, some material pelleted in the filter devices (sample PA) and was analysed. A similar protein composition as in the pellet after the two-step sucrose cushion was detected (sample PS).

The cleared crude mitoribosome sample was subjected to 15-30 % linear sucrose gradient ultracentrifugation using a SW41Ti rotor at 115,605xg for 16 h 10 min at 4°C. Collected fractions corresponding to 28S, 39S and 55S particles were concentrated and sucrose removed by ultrafiltration with Amicon® Ultra-4 Centrifugal Filter Devices 100K (Merck). The RNA profile of the fractions revealed well separated distinct peaks for mitoribosomal particles (Figure 25C). The Coomassie Blue staining showed protein bands mainly below 50 kD corresponding to mitoribosomal proteins which have mainly a molecular weight less than 50 kD (Figure 25B). Immunodetection of proteins of the mitoribosome showed a clear enrichment in comparison to a 10 µg mitochondria control in contrast to RPL3, YME1L and PHB2.
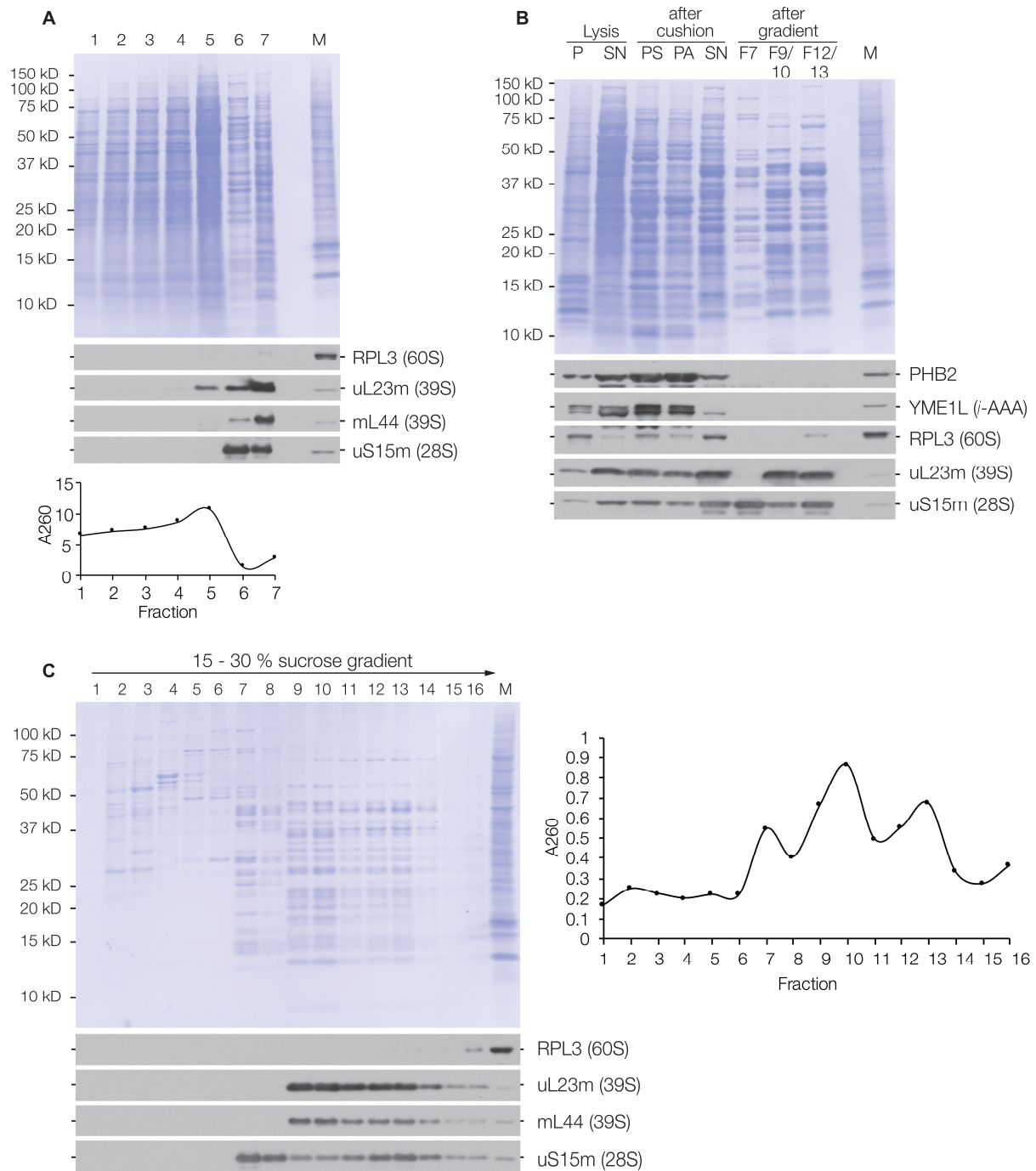
Figure 25: Mammalian mitoribosome isolation. 68 mg mitoplast were lysed and loaded onto a two-step sucrose cushion. From a total sample plus cushion volume of 36 ml, per fraction 20 µl were analysed via SDS-PAGE (A). B) Samples during experiment analysed via SDS-PAGE followed by Coomassie Blue staining and western blotting: 0.1 % of SN/pellet = 0.1 % of supernatant/pellet after lysis. 1 % of PS/PA/SN, PS = resuspended pellet after centrifugation, PA = resuspended pellet from Amicon filter, SN = crude mitoribosomes. From the finally purified ribosomal samples were analysed: 9 % of fraction 7 (F7), 7 % of fraction 9 (F9) and 8 % of the combined fraction 12/13 (F12/13). M = 10 µg crude mitochondria C) A total of 1% per fraction was analysed. Protein and RNA distribution over sucrose gradient are visualized.

To check the final purity of the isolated 55S monosomes, 5 µl of sample (633 pmol of 55S) were analysed by mass spectrometry, which was performed by Dr. Andreas Linden, Department of Bioanalytical Mass Spectrometry headed by Prof. Dr. Henning Urlaub, Max Planck Institute for Biophysical Chemistry (Göttingen). Purified 55S mitoribosomes were subjected to LC/MS, analysed via MaxQuant (version 1.6.0.1) and iBAQ values were calculated (Supp. Table 3). Finally, 82/82 mitoribosomal proteins were detected and most of them with a high abundance. However, 62 of 80 cytosolic ribosomal proteins were measured as well, but with a much lower abundance.
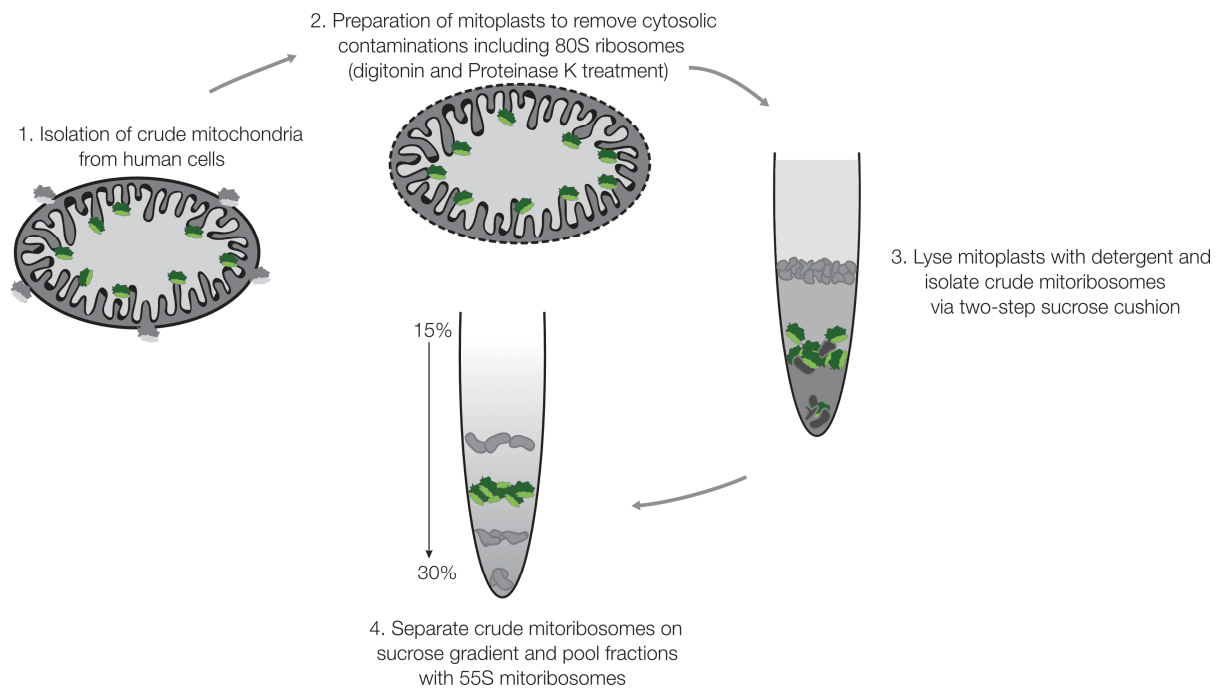
Figure 26: Flowchart mammalian mitoribosome isolation.

In conclusion, a protocol for mitoribosome isolation from HEK293T cells was successfully established and the final strategy is visualized in the flowchart (Figure 26). In total, from 98 plates of HEK293T cells 188 mg of mitochondria were obtained. By further processing, 68 mg of mitoplasts were isolated. Finally, 30 nmol of 28S mtSSU from fraction 7, 74 nmol of 39S mtLSU from fraction 9/10 and 34 nmol of 55S ribosomes from fraction 12/13 were isolated.

For the quantitative mass spectrometry approach of the assembly of the mitoribosome, lightly labelled 55S mitoribosomes were isolated as standard for 240 gradient fractions (5 time points, 16 fractions each, n = 3). In total, 251 nmol mitoribosomes were purified, which was sufficient to add 633 pmol of 55S ribosomes into each fraction. The final experiment was performed together with Elena Lavdovskaia and MS analysis is currently performed by Dr. Andreas Linden. The data analysis is still ongoing and will shed new light into the biogenesis of the mitochondrial ribosome.

4.1.4 Discussion

Within this thesis, a new purification procedure has been established to obtain 55S human mitoribosomes from HEK293T cells different from the already published protocols (Aibara et al., 2018; Carroll, 2017; O'Brien and Kalf, 1967; Spremulli, 2007). The first mitoribosomes were isolated from rat liver (O'Brien and Kalf, 1967). Additionally, mitoribosomes were obtained from livers of *Bos Taurus* or *Sus scrofa* (Greber et al., 2014b; Spremulli, 2007) or HEK293T cells (Aibara et al., 2018; Brown et al., 2014).

The buffer conditions needed to be taken into careful consideration and parameters had to be adjusted as each component can be crucial for the integrity of the 55S mitoribosome. Of special importance is the type of salt used in purification buffers. As already described by Carroll (2017) salts within the buffers are required to stabilize the ionic strength, by reducing unspecific protein-protein interactions in order to keep the integrity of the ribosomes. Using sodium chloride for bacterial ribosome isolation, no 70S ribosomes are obtained (Beller and Davis, 1971; Hardy and Turnock, 1971; Phillips et al., 1969). As mitoribosomes evolved from bacterial ribosomes it is reasonable to avoid this salt in buffers for mitoribosome purification (Carroll, 2017). Various protocols for mitoribosome isolation use potassium chloride in a range of 50-100 mM in purification buffers (Aibara et al., 2018; Brown et al., 2014; Carroll, 2017; Greber et al., 2014b; O'Brien and Kalf, 1967; Spremulli, 2007). In contrast, ammonium chloride is usually used for bacterial ribosome isolation. It was shown that bacterial ribosomes are more active in presence of NH_4Cl instead of KCl (Zamir et al., 1971). The same was stated for 74S yeast mitoribosome (Pfisterer and Buetow, 1981). Thus, KCl was replaced by 100 mM NH_4Cl and the stability of assembled 55S complexes were analysed. By using ammonium chloride, a better separation of mitoribosomal particles and a well resolved monosome peak was obtained. However, the activity of the purified mitoribosomes was not investigated and requires further analyses.

Bacterial 70S ribosomes are able to keep their integrity in a wide range of salt concentrations other than eukaryotic 80S ribosomes which aggregate (Schweet and Heintz, 1966). Conversely, for dissociation of 80S ribosomes from peas 500 mM NH_4Cl can be used (Lin et al., 1975). If high salt concentrations are applied to 50S bacterial ribosomes, translational factors dissociate (Goyal et al., 2017). In a well-established protocol from Rodnina and Wintermeyer, 1995, 500 mM NH_4Cl are used within the 1.1 M sucrose cushion for 70S bacterial ribosome purification leading to the question whether an improvement of 55S mitoribosome isolation with higher salt conditions is possible. Apparently, 300 mM NH_4Cl lead to a drastic reduction of 55S monosome and increased levels of 39S and 28S. Mammalian mitoribosomes seems to be unstable under high salt conditions

and dissociate into their subunits. In conclusion, just 100 mM NH_4Cl were used for purifications. However, higher salt concentrations could be considered to isolate dissociated subunits.

To purify assembled 55S mitoribosomes the concentration of Mg^{2+} ions in preparation buffers has to be carefully evaluated. Already Lamfrom et al. stated in 1962 that 70S ribosomes dissociate in absence of Mg^{2+} ions. However, high concentrations of Mg^{2+} ions do not have a positive influence on 70S ribosomes (Carroll, 2017; Noah and Wollenzien, 1998). Carroll (2017) suggested 10-20 mM Mg^{2+} to be added in buffers for mitoribosome purifications. Spremulli (2007) used buffers including 20 mM $MgCl_2$ for purification of 55S ribosomes and buffers including 2 mM $MgCl_2$ for purification of ribosomal subunits. Therefore, magnesium concentrations were tested in a range from 2 mM to 20 mM for suitability in mitoribosome purification. As high magnesium concentrations might have negative effects on mitoribosomes (statement by Prof. Dr. Marina Rodnina), the magnesium concentration was titrated to a minimum. The best yield of 55S monosomes was obtained using 8 mM $MgCl_2$. If the magnesium concentration was lower than 6 mM, the 55S started to dissociate into 39S and 28S subunits.

To reduce contaminations with 80S cytosolic ribosomes purified mitoplasts were used instead of crude isolated mitochondria for mitoribosome purification, which is in contrast to other published protocols (Brown et al., 2014; Greber et al., 2014a; O'Brien and Kalf, 1967). The biggest difference between all other procedures and the one described here is the avoidance of pelleting ribosomes. Instead, the interlayer between a two-step sucrose cushion was used where the mitoribosomal fraction is enriched. This improved the yield and the quality of purified mitoribosomes in the end as confirmed by mass spectrometry. Although the purification strategy shows an improvement compared to the already published protocols, the activity of the isolated mitoribosomes needs to be investigated in the future.

4.2 Characterization of the disease associated protein mL44 and the membrane anchor mL45 within the biogenesis of the human 39S mtLSU

The mammalian mitoribosome consists of 82 proteins, amongst these 50 proteins belonging to the 39S mtLSU (Greber and Ban, 2016). This doctoral work focuses on the assembly of the 39S mtLSU. To shed light into this, two different proteins of the mtLSU were further characterized – the disease associated mL44 and the mitoribosomal membrane anchor mL45.

4.2.1 Influence of the disease associated mitoribosomal protein mL44 on 39S mtLSU biogenesis

4.2.1.1 Introduction

The mitochondria-specific mL44 was shown to be an integral protein in the structure of the large subunit of the porcine and human mitoribosome (Brown et al., 2014; Greber et al., 2014a). mL44 is situated in proximity to the polypeptide exit tunnel, but not as close as in yeast where this protein directly forms the tunnel exit together with uL22m, uL23m, uL24m and mL50 (Bieri et al., 2018). Recently it was suggested that mL44 is incorporated early in assembly together with bL20m, bL21m, mL42 and mL43 (Bogenhagen et al., 2018). Also in yeast, mL44 is assembled early (Zeng et al., 2018).

As already mentioned in section 2.3, mL44 is a disease-associated protein. Carroll et al. described in 2013 two patients with infantile cardiomyopathy. Exome sequencing revealed a mutation in the *Mrpl44* gene at position c.467T>G (p.Leu156Arg) in both patients, predicted to giving rise to an improper folded mL44 protein. Further biochemical analyses uncovered a combined respiratory chain deficiency of complex I and IV for patient 1 in heart and skeletal muscle, whereas complex II and III were not affected. For patient 2 they showed just reduced levels of complex IV in fibroblasts. Hence, they suggested that the mL44 mutation affects OXPHOS complexes in a tissue specific manner. The authors suggested that in patient fibroblasts, the assembly of the 39S mtLSU was impaired. However, assembly intermediates were not visible and mitochondrial translation was comparable to WT. Consequently, the authors hypothesized that mL44 is required for the stability or assembly of the newly synthesized mtDNA-encoded proteins (Carroll et al., 2013).

Distelmaier et al. identified in 2015 another two unrelated patients with hypertrophic cardiomyopathy caused by mL44 deficiency. One of their patients had in addition to the previous reported homozygous mutation a heterozygous variation at position c.233G>A (p.Arg78Gln). Patient 1 showed in fibroblasts an isolated complex IV defect and patient 2 in heart tissue a

moderate complex I and a severe complex IV deficiency. These data support Carroll's et al. suggestion that mutated mL44 gives rise to a tissue specific phenotype (Distelmaier et al., 2015).

Carroll et al. speculated that the structural important mL44 is not directly required for *de novo* synthesis of mtDNA encoded proteins. However, siRNA mediated depletion of mL44 revealed a reduction in [35S]Methionine *de novo* mitochondrial protein synthesis. To clarify this discrepancy and to define the role of mL44 in mtLSU biogenesis and mitochondrial translation mL44 was characterised in more detail in the next sections.

4.2.1.2 Impact of loss of function of mL44

To understand the function of mL44 and to assess the order of protein binding during mtLSU assembly, the consequences of loss of function of mL44 were investigated. Therefore, the HEK293T mL44-/- cell line obtained from Dr. Ricarda Richter-Dennerlein was further characterized. By applying CRISPR/Cas9 technology using the guide RNA [AAGCTGGTCCCTCCGGTTCG] the knock-out cell line was generated according to Ran et al., 2013. Sequence analysis of the knock-out cell line using TOPO® sequencing as described in 3.2.1.10 unveiled three different mutations (Figure 27). Each mutation was leading to a frameshift resulting in a premature stop codon and the presence of truncated versions of mL44. Instead of the normal length mL44 protein comprising 332 aa (amino acids), the mutated forms consisted of only a) 30 aa, b) 89 aa and c) 89 aa.
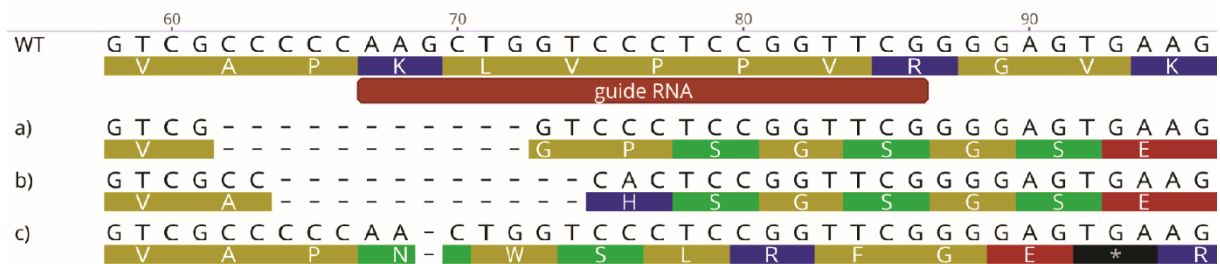
Figure 27: Sequence analysis of mL44-/- cell line. The coding sequence of mL44 consists of 996 bp (base pairs). WT = wild type sequence of MRPL44. a) Mutation allele 1: mL44_c.61_71del b) Mutation allele 2: mL44_c.65_66+68_76del c) Mutation allele 3: mL44_c.69del.

To analyse the impact of mL44 ablation on mitochondrial *de novo* protein synthesis, a [^{35}S]Methionine labelling was performed as described previously (3.2.2.4). In the mL44$^{-/-}$ cell line a complete depletion of mitochondrial translation was observed compared to wild type (WT), even if residual amounts of mL44 protein were detected (Figure 28). In order to show that defects are specific due to the loss of mL44 and not caused by an off-target effect, a rescue cell line was generated. The mL44$^{-/-}$ cell line was transfected with pOG44 and pcDNA5/FRT/TO encoding a C-terminal FLAG tagged variant of mL44. Clones with successful integration of mL44^{FLAG} into the Flp-In cassette were selected with hygromycin. For convenience, this cell line is called mL44$^{-/-}$R. The expression of exogenous mL44^{FLAG} and mitochondrial translation competence was tested by [^{35}S]Methionine *de novo* synthesis and subsequent western blotting. The expression of mL44^{FLAG} completely restored the translation phenotype indicating that the knockout is specific, and the FLAG tagged variant of mL44 is also functional. Thus, mL44 is required for mitochondrial translation.
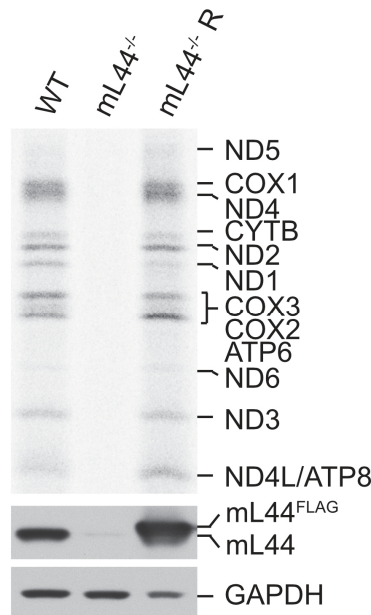
Figure 28: Loss of mitochondrial translation in mL44$^{-/-}$ cells. Mitochondrial translation was tested by the incorporation of [^{35}S]Methionine into de novo synthesized mtDNA-encoded proteins while cytosolic translation was blocked with emetine. Samples (50 µg) were analysed by SDS-PAGE followed by autoradiography (upper panel) and western blotting (lower panel). GAPDH was used as a loading control. WT: HEK293T wild type, mL44$^{-/-}$R: mL44$^{-/-}$expressing mL44^{FLAG}(n=3).

Depletion of mL44 leads to a complete loss of mitochondrial translation suggesting that the function or biogenesis of the mitoribosome is disturbed. To dissect the consequences of mL44 loss further, protein steady state levels of mitoribosomal proteins and assembly factors were tested by western blotting. If mL44 is missing, most protein levels of the tested LSU proteins were diminished (uL1m, uL3m, bL20m, bL21m, uL23m, mL39, mL45, mL62) or even not detectable (uL13m). One of the tested proteins, uL10m, remained stable whereas bL12m was even

upregulated (Figure 29). Surprisingly, ablation of mL44 leads to reduction of some mtSSU proteins (uS14m, mS22, mS25), no change in mS27 level and increase in uS7m. All tested assembly factors were also decreased (GTPBP7, GTPBP10, MALSU1, NSUN4).
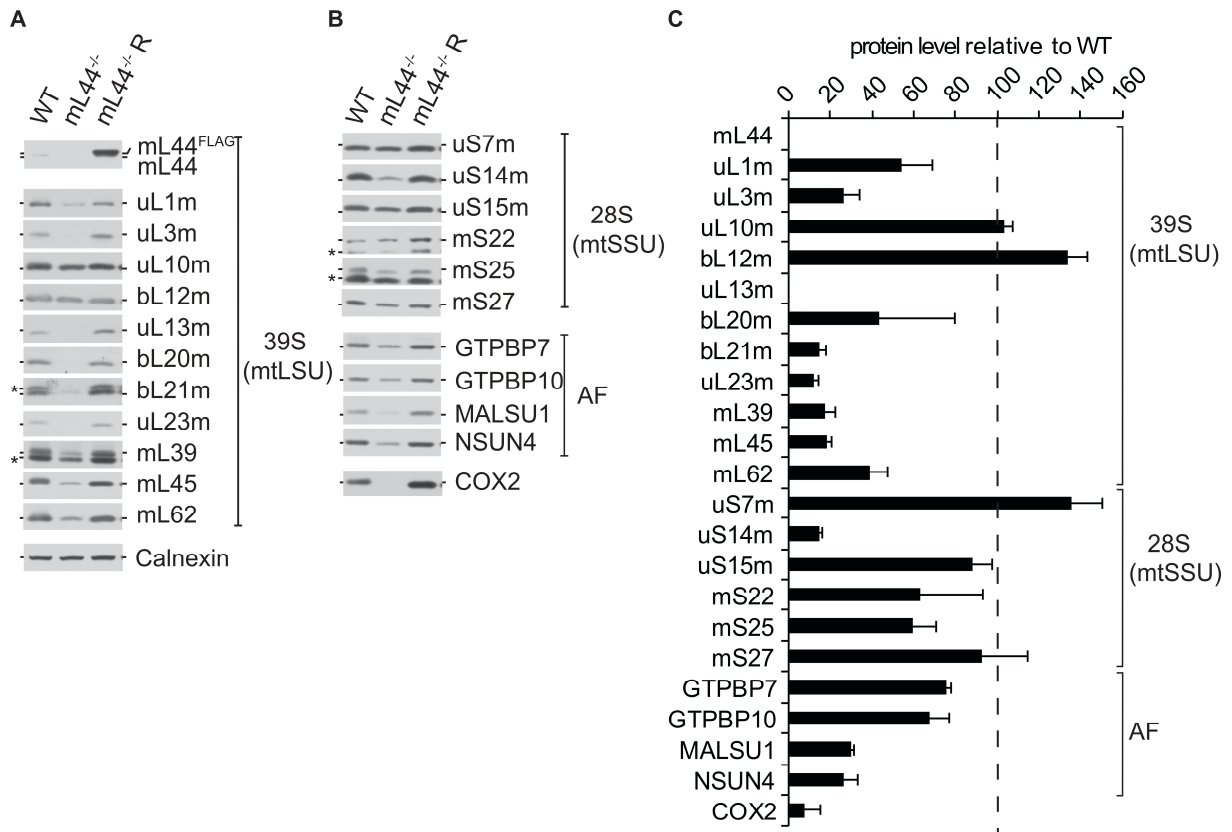
Figure 29: Protein steady state analysis of cell lysates obtained from HEK293 WT cells, HEK293T mL44$^{-/-}$ cells or HEK293T mL44$^{-/-}$R. A, B) Cell lysates (50 μg) were tested by western blotting using antibodies against MRPs of the mtLSU and mtSSU, and of assembly factors (AF). Calnexin was used as a loading control. * indicates residual signals of preceding antibody decorations. C) Protein levels in mL44$^{-/-}$ were quantified using ImageQuant TL software and calculated relative to wild type (WT).

To analyse whether mitoribosomes or subcomplexes are formed in the absence of mL44, mitoplast lysates were separated by sucrose gradient ultracentrifugation. For all tested mitoribosomal proteins of the mtLSU, no assembled 39S mtLSU and 55S particle were detected (Figure 30A). In contrast, 28S mtSSU assembly seemed to be unaffected (Figure 30B). The level of assembled 28S is higher than in WT control, as 28S is not used to form monosomes (Figure 30D). All tested assembly factors accumulate upon ablation of mL44 in the lower dense fractions (Figure 30C).
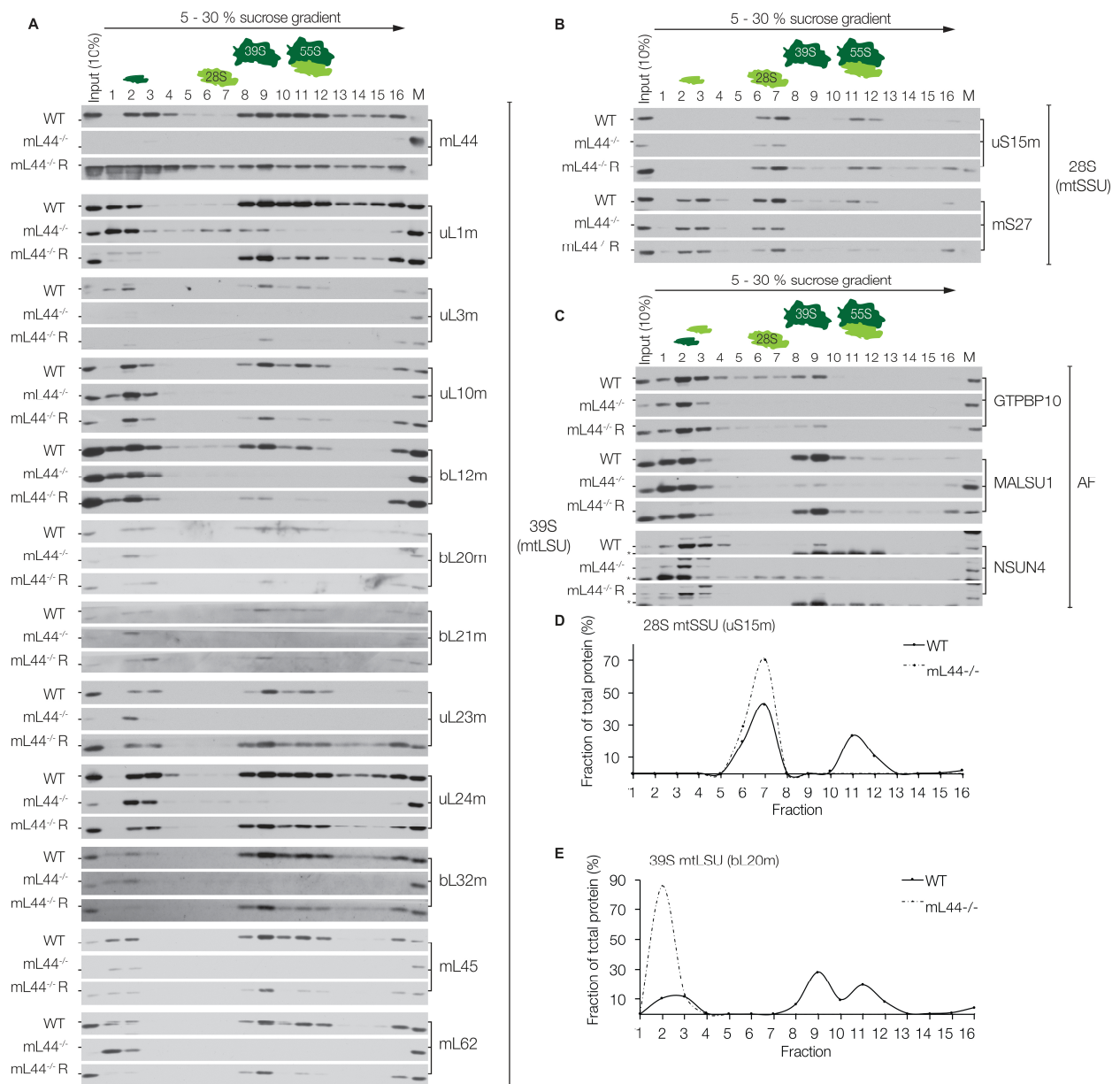
Figure 30: Effect of mL44 ablation on mitoribosome biogenesis. Lysates of 500 µg mitoplasts isolated from HEK293T WT, HEK293T mL44-/- or HEK293T mL44-/-R were separated on 5-30% sucrose gradients, fractionated and analysed via SDS-PAGE and immunostaining of mitoribosomal proteins (A, B) and assembly factors (AF, C). D, E) Quantification of bL20m and uS15m across sucrose gradient for comparison of WT and mL44-/- using the software ImageJ. M = 10 µg HEK293T WT mitochondria, 10 % Input of loaded material = 50 µg lysed mitoplasts. (n=3)

Assembly intermediates accumulated in the lower dense fractions in absence of mL44. For better visualization of this effect, one protein of the mtLSU, bL20m, was quantified across the gradient (Figure 30E). Differences in signal patterns of proteins are corresponding probably to more than one assembly intermediate. For uL1m, bL32m, mL45 and mL62 signals in fraction 1 and 2 of the sucrose gradient were detected. These could correspond to very initial subparticles or to a free pool of these proteins. The behaviour of mL45 and its interaction partners will be discussed in

section 4.2.2. No signals close to the position of 39S particle in WT control were observed upon mL44 ablation corresponding to nearly complete assembled mtLSU. These data provide evidence that mL44 is binding early in assembly.

The protein distribution of uL10m and bL12m in the lower dense fractions showed a similar pattern. As cross-linking mass spectrometry experiments revealed inter-protein crosslinks between uL10m and bL12m (Greber et al., 2014b), we suggest that they form a subcomplex. Future analyses are required to define this complex.

In conclusion, mtLSU and monosome assembly is mL44 dependent, whereas mtSSU assembly is independent of mL44. Together with data from steady state analysis it is shown that mL44 loss is leading to a destabilization of mtLSU. Many of the tested mtLSU proteins show signals in the lower dense fractions corresponding to early assembly intermediates or distinct submodules.

4.2.1.3 Characterization of an early assembly intermediate containing mL44

bL20m, bL21m, uL23m and uL24m showed a protein distribution in the sucrose gradient similar to mL44 in WT (Figure 30A). Nevertheless, the question remained whether they all form one complex together with mL44 or whether there are distinct small assembly intermediates. To answer this question, FLAG-immunoprecipitation experiments followed by sucrose gradients were performed according to 3.2.5. Therefore, the HEK293T mL44$^{-/-}$R cell line was used. As expected, using mL44^{FLAG} as a bait, which is a structural component of the 55S ribosome, assembly intermediates containing mL44, as well as fully assembled mtLSU and monosome were co-immunoprecipitated. This is illustrated by the co-isolation of proteins of the 39S mtLSU (bL20m, bL21m, mL45, mL62) and 28S mtSSU (uS14m, mS25, mS27) as well as one tested assembly factor (GTPBP10) (Figure 31A). Specifically, bL20m, bL21m and GTPBP10 were enriched in the elution fraction, suggesting the presence of an assembly intermediate.

To test this hypothesis further, eluates of FLAG-immunoprecipitation experiments were subjected to sucrose gradient centrifugation. Besides signals in fractions corresponding to 39S and 55S particles, also an assembly intermediate in the lower dense fractions was observed (Figure 31B, C). mL44 is interacting with bL20m, bL21m and GTPBP10 but not with uL23m, uL24m as previously suggested. To dissect the composition of this subcomplex detected in fraction 2 and 3 further, samples were analysed by mass spectrometry in the group of Prof. Dr. Henning Urlaub, Department of Bioanalytical Mass Spectrometry, Max Planck Institute for Biophysical Chemistry (Göttingen). Samples were subjected to LC/MS, analysed via MaxQuant (version 1.6.0.1) and iBAQ values were calculated (Supp. Table 4) by Dr. Andreas Linden. The proteins mL43, mL42, bL21m, bL20m and mL50 were detected with a high abundance, suggesting that they interact with mL44 in this subcomplex. GTPBP10 was detected as well, but with a lower abundance. The results of the

sucrose gradient experiments and MS-analysis (Figure 30A and Figure 31B, C) indicate that there are distinct early assembly intermediates, of which uL23m and uL24m seem to build another subcomplex without mL44.
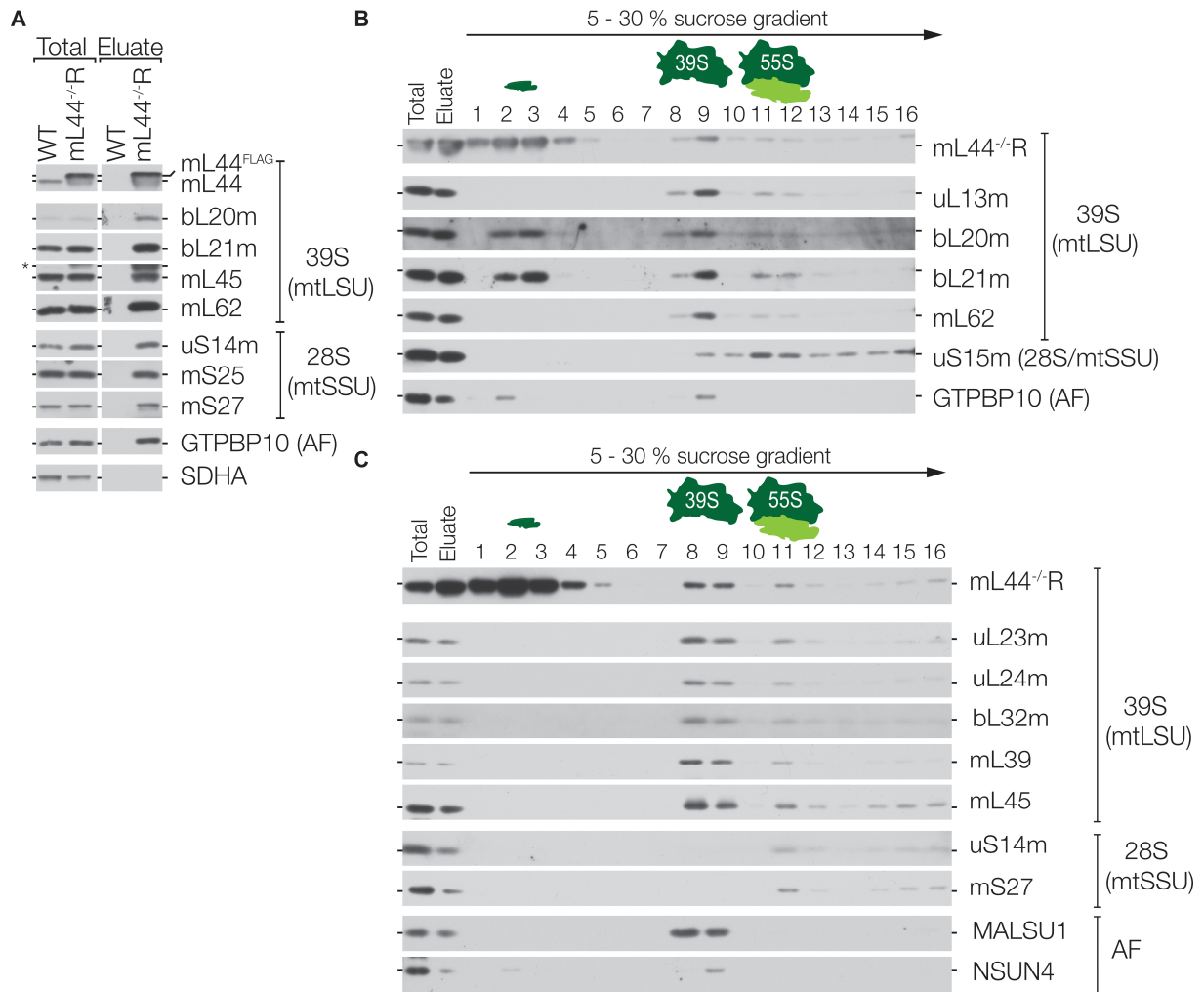
Figure 31: Interactome of mL44. A) Isolated mitochondria (1 mg) from HEK293T WT (negative control) and mL44-/-R cells were used for FLAG-co-immunoprecipitation. Analysis of samples by SDS-PAGE and western blotting using the indicated antibodies against mtLSU, mtSSU and assembly factors (AF). To exclude unspecific protein binding during IP, SDHA was used as negative control. Total = 3 % of mitochondrial lysate prior IP, Eluate = 100% of immunoprecipitated sample (n=3) B, C) Isolated mitochondria (B: 3 mg, C: 2.4 mg) were lysed, subjected to FLAG-co-immunoprecipitation and mitoribosomal particles further separated by 5-30% sucrose density gradient centrifugation. Analysis of samples by immunoblotting. Total = 1 % of FLAG-IP input, Eluate = 20 % of FLAG -IP eluate. Asterisk indicate residual signals from previous antibody decorations.

4.2.1.4 Stability of mitoribosomal proteins

As already described in chapter 2.1.4.2 a subset of Met-tRNA^{Met} is formylated. After progression of translation, this initial formyl group is cleaved by the enzyme peptide deformylase (Pdf). The drug actinonin can prevent this cleavage by inhibition of Pdf (Lee et al., 2004). It was already shown that treatment of cells with 150 µM actinonin leads to a reversible, time dependent depletion of MRPs, 12S rRNA and 16S rRNA (Richter et al., 2013). However, the authors showed the effect of actinonin just for two MRPs: uL13m and uS15m. To get further insights into the stability of other MRPs, HEK293T WT cells were seeded and treated for different periods of time with 150 µM actinonin.

protein	half-life [h]
uL1m	19.00
mL44	13.85
uL3m	9.85
uL23m	9.5
mL62	9.1
uL13m	8.75
mL54	8.25

protein	half-life [h]
mS27	>24
mS22	12.80
bS16m	11.50
uS15m	11.00
mS40	10.00
uS14m	8.75
GTPBP10	13.75
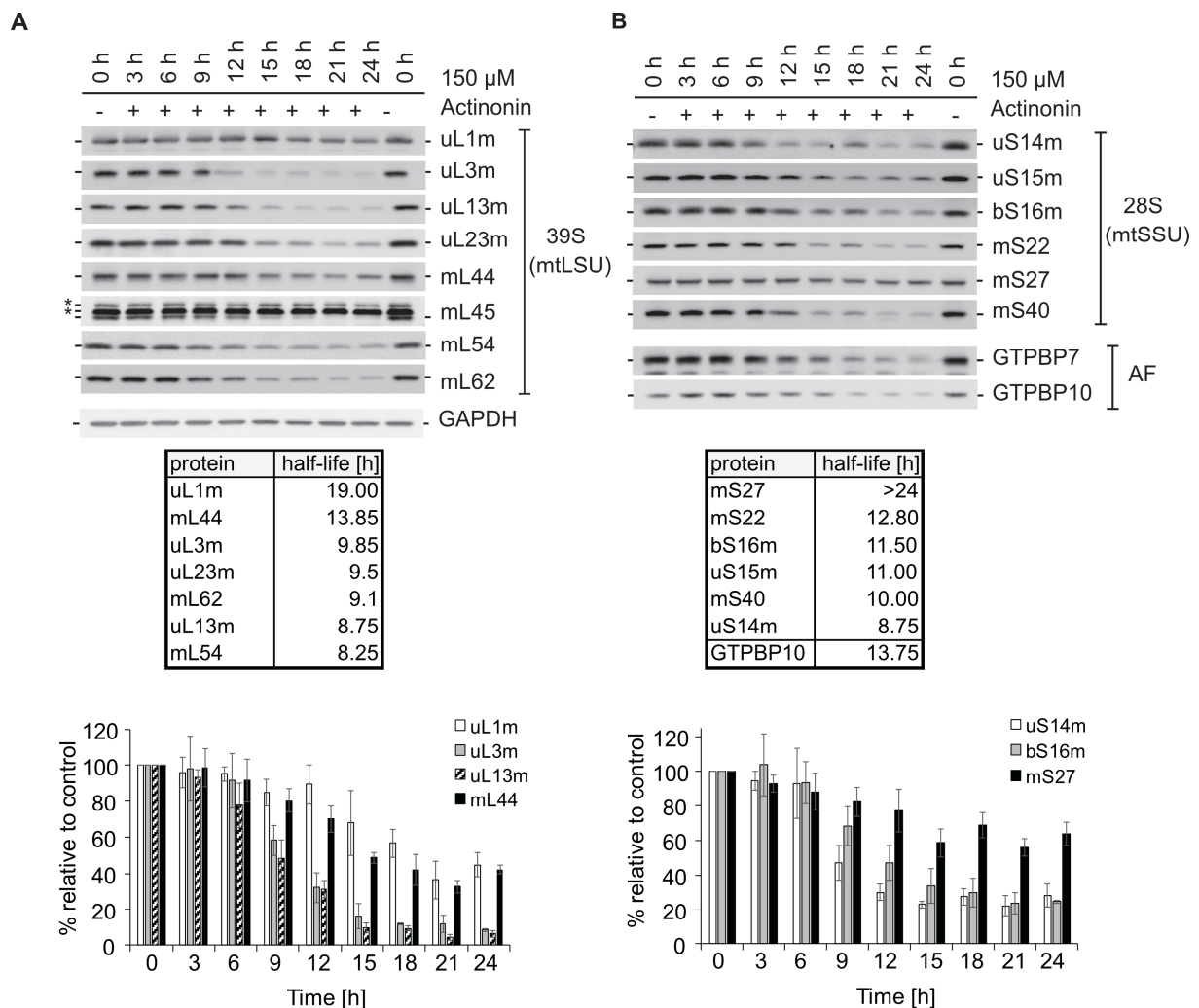
Figure 32: Influence of actinonin on steady state levels of proteins of A) mtLSU B) mtSSU and AFs. Cells were treated with 150 µM actinonin, harvested at distinct time points as indicated, lysed and analysed via SDS-PAGE and western blotting. Quantification of protein levels relative to untreated control was performed using the software ImageJ (n=3, mean±SEM). GAPDH served as loading control. The half-life of the adjacent proteins was determined as the time until the initial protein levels have been depleted by 50%. (Supp. Figure 2). Asterisks indicate unspecific antibody signals.

Actinonin treatment of cells lead to a decrease in protein levels of all tested proteins of mtLSU, mtSSU and AFs (Figure 32). However, some proteins were more stable than others. After 19 h still 50 % of the uL1m protein level was detectable. Also, mL44 was more stable than uL3m, uL23m, mL62, uL13m and mL54. However, the most stable protein was mS27. Within the tested time frame just a reduction of 40 % from the initial protein level was observed (Figure 32B, Supp. Figure 2) suggesting that it has crucial functions within mitochondria and consequently is required to be more stable.

4.2.1.5 Discussion

mL44 is a mitochondria specific ribosomal protein with no homologues in bacterial and cytosolic ribosomes. It is a protein consisting of 332 amino acids, of which the first 30 N-terminal residues probably serve as targeting signal for mitochondrial import. Within its structure two domains are predicted: a RNase III-like domain and a double-stranded RNA-binding domain (Carroll et al., 2013). However, the residues important for RNase function are not present in mL44. Hence, it is most likely not performing the function of RNase III, which is observed in prokaryotes (Koc et al., 2001).

By using for the first time a mL44$^{-/-}$ cell line, it was shown in this doctoral thesis that mL44 is required for the assembly of the 39S mtLSU. In contrast, absence of mL44 has no impact on 28S mtSSU assembly. This is in agreement with data provided from Carroll et al., 2013. Within the investigated patient cell lines, the authors suggested an assembly defect of the mtLSU as well. The underlying mutation in those patients was identified as a substitution of leucine at position 156 to arginine. Structural analyses revealed that this specific leucine is surrounded by other hydrophobic amino acids, building a "hydrophobic pocket" (Brown et al., 2014). Due to incorporation of the basic amino acid arginine, they hypothesized that the mutation prevents binding of mL44 to the 39S due to its changed structure. However, even if Carroll et al. described "a dramatic loss" of mtLSU in their patient cell line, still substantial amounts of LSU proteins uL13m and mL44 were detectable by western blot analyses, suggesting the presence of a pool of 39S. This could be the reason, why no translation defect was observed. One can hypothesize that these residual mitoribosomes are capable of translation.

Mutational analyses of yeast mitoribosomes revealed that mL44 is an essential protein for mitochondrial protein synthesis in *S. cerevisiae* (Zeng et al., 2018). By creating a mL44 deletion strain the authors observed a significant loss of 21S rRNA implying an important structural role of mL44 within the yeast 74S ribosome. As shown in this doctoral study, *de novo* synthesis of mtDNA-encoded proteins in human cells was completely abolished upon loss of mL44 (Figure 28)

giving evidence that mL44 is a structural component of the 39S mtLSU and indeed required for functional translation similar to the yeast mL44 homologue.

In our analyses, upon ablation of mL44 most mtLSU proteins were diminished (Figure 29). The upregulated or stable mitoribosomal proteins are fulfilling most likely other functions within the cell. uL10m was described to act on cyclinB1/Cdk1 activity and thereby influencing cell growth (Li et al., 2016). By binding of bL12m on POLRMT it increases mitochondrial transcription and it was hypothesized that bL12m is part of a feedback loop for coordination of mitochondrial gene expression and ribosome biogenesis (Nouws et al., 2016; Surovtseva et al., 2011; Wang et al., 2007). mS27 is a pentatricopeptide repeat domain (PPR) protein and was suggested to be a translational regulator (Davies et al., 2012). An additional role of the disease associated protein uS7m was not described until now, but it might have also another function, as it is not depleted in the mL44$^{-/-}$ cell line. One can hypothesize that cells are trying to cope with the loss of mL44 and therefore upregulating transcriptional activators as bL12m.

Upon actinonin treatment of cells, all tested proteins were diminished (Figure 32). One of the least reduced proteins was uL1m, which was described as part of the flexible L1 stalk in the porcine structure of the 39S mtLSU (Greber et al., 2014a). Nevertheless, its exact localization was not resolved until now. In bacteria, the L1 stalk was indicated to facilitate translocation of tRNAs from the P- to the E-site (Fei et al., 2008). Brown et al. (2014) were able to show in their cryo EM structure of the human mtLSU that parts of the E-site tRNA interact with the L1 stalk, suggesting a similar role for the mitoribosomal L1 stalk as for the bacterial. Probably, uL1m is protected by surrounding structures as the bacterial L1 shown by Nikulin et al., 2003 and reacts for this reason less sensitive upon treatment with actinonin. Another hypothesis for enhanced stability of uL1m would be that it fulfils additional functions within mitochondria as described for mS27, which was the most stable protein during actinonin treatment.

By comparing the half-life of proteins after treatment with actinonin, it became apparent that also mL44 was not as strongly affected by this drug as other proteins. Why does mL44 seem to be more stable? Structurally it is located quite exposed to the surface, in close proximity to the polypeptide exit tunnel (Brown et al., 2014; Greber et al., 2014a). As exemplified for other mitoribosomal proteins as bL12m (Nouws et al., 2016; Surovtseva et al., 2011; Wang et al., 2007), it might be that mL44 has a dual function that requires a higher stability.

Upon ablation of mL44, especially uL13m was not detectable. During actinonin treatment, uL13m was also very unstable. It is located in close proximity to mL44, facing the matrix (Brown et al., 2014). uL13m does not show signals in lower dense fractions in WT sucrose gradient analyses

(Figure 17). For this reason, it is suggested not to be part of an early submodule. Loss of mL44 seems to destabilize uL13m. No interaction of mL44[FLAG] with uL13m in fraction 2/3 of sucrose gradients after co-immunoprecipitation experiments was observed despite their adjacent localization (Figure 31B). For this reason, one might assume that mL44 has to be assembled prior uL13m incorporation. This is in agreement with Bogenhagen's assembly map of the 39S mtLSU.

Additionally, mL44 interacts directly with bL20m, bL21m, uL22m, mL42, mL43, mL50 and mL51 (Brown et al., 2014). The steady state levels of bL20m and bL21m were determined in absence of mL44. Both proteins showed reduced levels, but not as strong as uL13m. bL20m and bL21m are located in close proximity to mL44 (Figure 33). For bL20m inter-protein crosslinks to mL44 were described (Greber et al., 2014b).
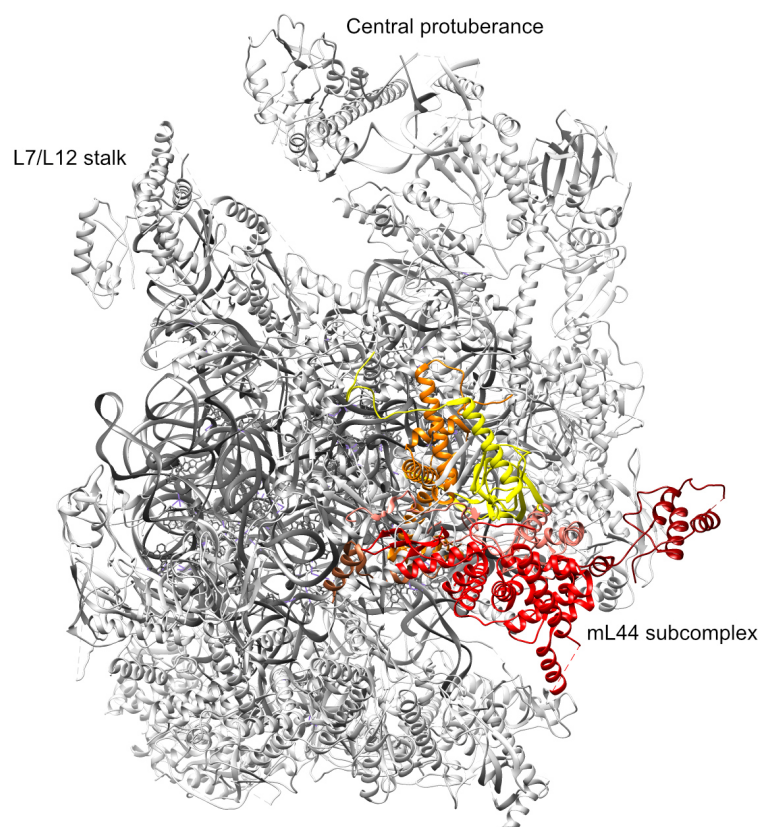
Figure 33: Structure of human 39S mtLSU visualized with UCSF Chimera (PDB: 3J7Y). 16S rRNA (dark grey), bL20m (orange), bL21m (yellow), mL42 (brown), mL43 (salmon), mL44 (red), mL50 (dark red).

In bacteria, bL20 and bL21 are components of the first submodule which is bound to the 23S rRNA. Subsequently, uL13 binds to bL20 (Chen and Williamson, 2013; Nierhaus and Dohme, 1979). Within human mitochondria, bL20m and bL21m were found to be in a complex together with mL44 (Figure 31B). Dissecting this complex by mass spectrometry the mitochondria-specific ribosomal proteins mL42, mL43 and mL50 were identified, indicating that binding of uL13m to

the growing mtLSU is not only dependent on the presence of bL20m, but on the previously formed subcomplex consisting of bL20m, bL21m, mL42, mL43, mL50 and mL44.

Additionally, to bL20m, bL21m, mL42, mL43 and mL50 in the submodule of mL44, the assembly factor GTPBP10 was detected (Figure 31B). In contrast, presence of uL23m and uL24m was excluded (Figure 31C). Inter-protein cross links between mL45 and uL23m as well as uL24m, but not with mL44 were observed by Greber et al., 2014b. Within the structure of the 39S mtLSU, uL23m and uL24m are further apart from mL44 suggesting the presence of distinct mtLSU assembly modules. However, the question remains whether there is really an interaction of GTPBP10 with the mL44 subcomplex. The assembly factor GTPBP10 acts late during mtLSU biogenesis, probably having a function in quality control (Lavdovskaia et al., 2018; Maiti et al., 2018). Elena Lavdovskaia (PhD student in the GGNB program Molecular biology of cells) provided evidence that GTPBP10 is interacting with other late assembly factors like MALSU1, MTERF4 and NSUN4. Pull-down experiments using GTPBP10[FLAG] as bait followed by sucrose gradient analysis revealed no interaction with mL44 in the early dense fractions. Interactions of GTPBP10 with this early assembly intermediate might be very transient and for this reason not easy to detect. The bacterial homologue of GTPBP10 ObgE is interacting with the peptidyl transferase centre on the 50S LSU (Feng et al., 2014). However, ObgE has a second homologue in humans called GTPBP5 (OBGH1) (Hirano et al., 2006). As the peptidyl transferase centre of 55S mitoribosomes is evolutionary conserved, it can be speculated that one ObgE homologue could also bind in its proximity. As it was implied that GTPBP5 is involved in PTC maturation late during mtLSU biogenesis, a localisation of GTPBP5 close to the PTC would be required (Maiti et al., 2020). Hence, GTPBP10 might interact with the mtLSU at a different structure. However, to finally answer the question whether an interaction of GTPBP10 and mL44, situated in the shell of the 39S mtLSU, would be structurally possible, structural analyses using cryo-EM or protein-protein cross linking approaches would be beneficial.

The assembly factors NSUN4 and MALSU1 do not interact with the early mL44 assembly intermediate. This is not surprising as both were found to fulfil their function late in ribosome biogenesis (Brown et al., 2017; Metodiev et al., 2014). In addition, MALSU1 is binding to uL14m at the intersubunit interface of the mtLSU, which is on the opposite site of mL44 (Brown et al., 2017).

Carroll et al, 2013 proposed that the homozygous mutation identified in their patients was leading to instability of mL44. However, reduced amounts of 39S mtLSU were still detected in the patient derived cell lines. In contrast to the complete loss of uL13m in the mL44$^{-/-}$ cell line shown in this doctoral study, uL13m was just diminished in patient fibroblasts. By comparing the protein steady

state levels of different mt-encoded proteins of the respiratory chain, Carroll et al. detected a more severe phenotype in heart and skeletal muscle cells in contrast to fibroblasts of patients. One can hypothesize that this could be due to differences in the energy demand of various cell types, as high energy demanding tissues are usually more severely affected by mitochondrial disorders (Frazier et al., 2019).

In order to understand the effects of the L156R mutation in the *Mrpl44* gene on 39S mtLSU biogenesis and the interaction of mutated mL44 to other MRPs, a cell line was generated via site-directed mutagenesis containing the mutated form of mL44. This cell line should serve as a tool to explore the effect of the L156R mutation within mL44. Will this mutated protein still interact with bL20m and GTPBP10? Will there be an accumulation of the assembly intermediate containing mL44[L156R]? To answer these questions, this cell line is currently analysed by Venkatapathi Challa, a PhD student in the research group of Dr. Ricarda Richter-Dennerlein. Using the mL44[L156R] cell line, the mt translation will be examined to clarify the discrepancy between the unaffected mitochondrial *de novo* synthesis of proteins observed in patient fibroblasts and the severely depleted translation in mL44^{-/-} cells.

4.2.2 Dissecting the role of the membrane anchor mL45 in mitoribosome biogenesis

4.2.2.1 Introduction

Like mL44, mL45 is a mitochondria specific ribosomal protein without having a homologue in bacteria (Greber et al., 2014b). mL45 contains a TIM44-like domain on its C-terminus, which is oriented on the mtLSU similar to the membrane binding structure of TIM44 itself. In addition, mL45 shows homologies to the yeast mitoribosome membrane anchor Mba1 (multi-copy bypass of AFG3 protein), suggesting that mL45 is mediating the contact between the 55S mammalian mitoribosome and the IMM (Figure 34) (Greber et al., 2014b).
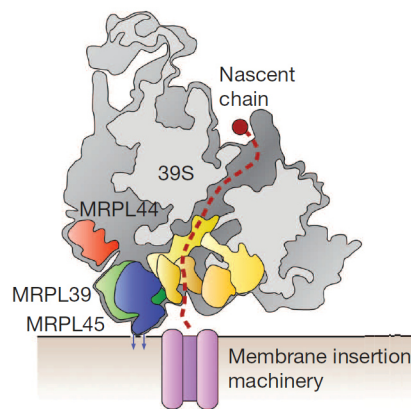
Figure 34: Localisation of mL45. Proteins are labelled by using the old mitoribosomal nomenclature. MRPL39 = mL39, MRPL44 = mL44, MRPL45 = mL45. Picture taken from Greber et al., 2014b*. Reprinted by permission from Springer Nature Customer Service Centre GmbH: Springer Nature, Nature, Architecture of the large subunit of the mammalian mitochondrial ribosome. Greber, B.J., Boehringer, D., Leitner, A., Bieri, P., Voigts-Hoffmann, F., Erzberger, J.P., Leibundgut, M., Aebersold, R., and Ban, N.; Copyright © 2014. Copyright Clearance Center, Inc.*
DOI: https://doi.org/10.1038/nature12890

This assumption was confirmed in 2017 by the group of Prof. Dr. Friedrich Förster. They were able to show that the 55S ribosome is anchored by mL45 via cryoelectron tomography (Englmeier et al., 2017). In contrast to the mitoribosome of *Saccharomyces cerevisiae*, the mammalian mitoribosome is connected to the IMM only by one contact. The second contact which is built through a rRNA interaction with the IMM in yeast, is missing in human (Englmeier et al., 2017). Bogenhagen suggested, that mL45 is binding early during assembly. However, within this doctoral project the question should be addressed, whether the mitoribosome requires its membrane anchor to assemble, whether mtLSU submodules can still assemble in the absence of mL45 and whether the assembly of the mtSSU is independent of the membrane anchor of the mtLSU.

4.2.2.2 Loss of function of mL45

In order to answer these questions, a HEK293T mL45^{-/-} cell line kindly provided by Dr. Ricarda Richter-Dennerlein was analysed. This knock-out cell line was obtained by using the CRISPR/Cas9 technology. The underlying mutations within the mL45^{-/-} cells were investigated by applying TOPO® sequencing. BLAST search against the wildtype variant of mL45 revealed three different mutations. The gene *Mrpl45* encoding for the protein mL45 is located on the chromosomal position 17q21.2 (Zody et al., 2006) and comprises 1553 bases according to the NCBI reference sequence (NM_032351.6). Karyotype analysis of HEK293T cells unveiled in most cases a triplicate of chromosome 17 (Stepanenko and Dmitrenko, 2015; Stepanenko et al., 2015). Hence, all three *Mrpl45* gene copies were affected in the present knock-out cell line. For allele 1, a deletion of 27 bp in frame was found. According to this, a truncated version of the protein, missing 9 amino acids, is built. Allele 2 is altered by a 4 bp deletion, leading to a frameshift, an altered amino acid sequence and a premature stop codon. Within allele 3, 2 bp were missing, having similar consequences as the mutation in allele 2.
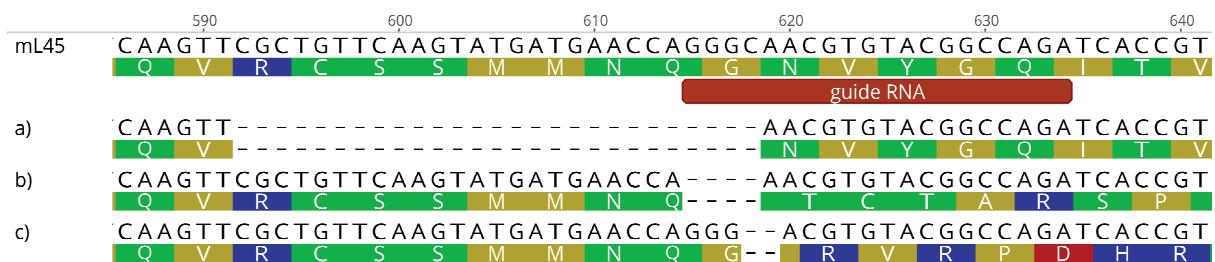
Figure 35: Sequence determination of HEK293T mL45^{-/-} at the guide RNA target sequence. The sequence at the top resembles the MRPL45/mL45 wild type. Numbers indicate base positions of Mrpl45 open reading frame. The guide RNA to create the knock-out is marked in red. Sequence of guide RNA: 5'-[GGGCAACGTGTACGGCCAGA]-3'. The three lower panels visualize the mutations: a) mL45_c.592_618del b) mL45_c.615_618del c) mL45_c.618_619del.

To determine the influence of ablation of mL45 on mitochondrial translation, a [35S]Methionine labelling was performed. Due to the absence of the mitoribosomal anchor protein, the mitochondrial translation was completely abolished (Figure 36). To verify that this translational defect is specifically caused by loss of mL45, the knock-out cell line was rescued by transfection with pOG44 and pcDNA5/FRT/TO carrying the gene for a C-terminal FLAG-tagged wildtype variant of mL45. For selection of clones having successfully integrated mL45[FLAG] into the Flp-In cassette, cells were treated with hygromycin. The successful established cell line called mL45^{-/-} R showed a wildtype-like phenotype, proving that deficiencies of the knock-out cell line are specifically resulting from loss of mL45.
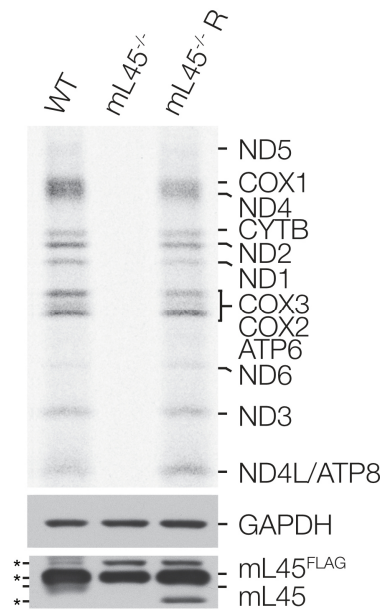
Figure 36: Ablation of mL45 leads to mitochondrial translation deficiency. To test mitochondrial translation, cells were grown for 1 h in media containing [35S]Methionine. Simultaneously, cytosolic translation was blocked with emetine. De novo synthesized mtDNA-encoded proteins were detected by autoradiography (upper panel). Samples (50 µg) were analysed by SDS-PAGE and immunoblotting (lower panel). GAPDH was used as loading control. Asterisk indicates unspecific antibody binding due to usage of homemade mL45 antibody. Cells were induced with 100 ng/µl tetracycline for 24 h prior labelling (n = 3).

Besides the translation defect, cells lacking mL45 showed also reduced steady state levels of various MRPs (Figure 37). Some proteins of the 39S mtLSU were slightly reduced (uL1m, bL20m, bL21m, mL39). Protein levels of others were stronger affected (uL3m, uL23m, mL44, mL62) and uL13m was completely lost. As mentioned in section 4.2.1, the mtLSU protein uL13m was also depleted in the mL44$^{-/-}$ cell line (Figure 29A) and was one of the less stable proteins during actinonin treatment (Figure 32A). Therefore, it is not surprising that uL13m is not detectable in mL45$^{-/-}$ cells, as it seems to be one of the least stable proteins. As suggested in 4.2.1, bL20m and bL21m are building a complex together with mL44. Thus, it seems reasonable, that bL20m and bL21m were stronger affected by depletion of mL44 than by loss of mL45. Nevertheless, steady state levels of some proteins were not affected (uL10m, bL12m) probably for the same reason as in mL44 deficient cells.

The 28S mtSSU protein levels compared to a WT control of uS14m (11 %), uS15m (56%), mS22 (40 %) and mS25 (36 %) were stronger reduced in mL45$^{-/-}$ cells (Figure 37B) than in cells lacking mL44 (uS14m: 14 %, uS15m: 88 %, mS22: 63 %, mS25: 59 %), suggesting that loss of mL45 has a more severe impact on the complete mitoribosome. The uS7m and mS27 protein levels were not affected.

Most of the tested assembly factors (GTPBP10, MALSU1, NSUN4) were diminished upon loss of mL45 (Figure 37B).
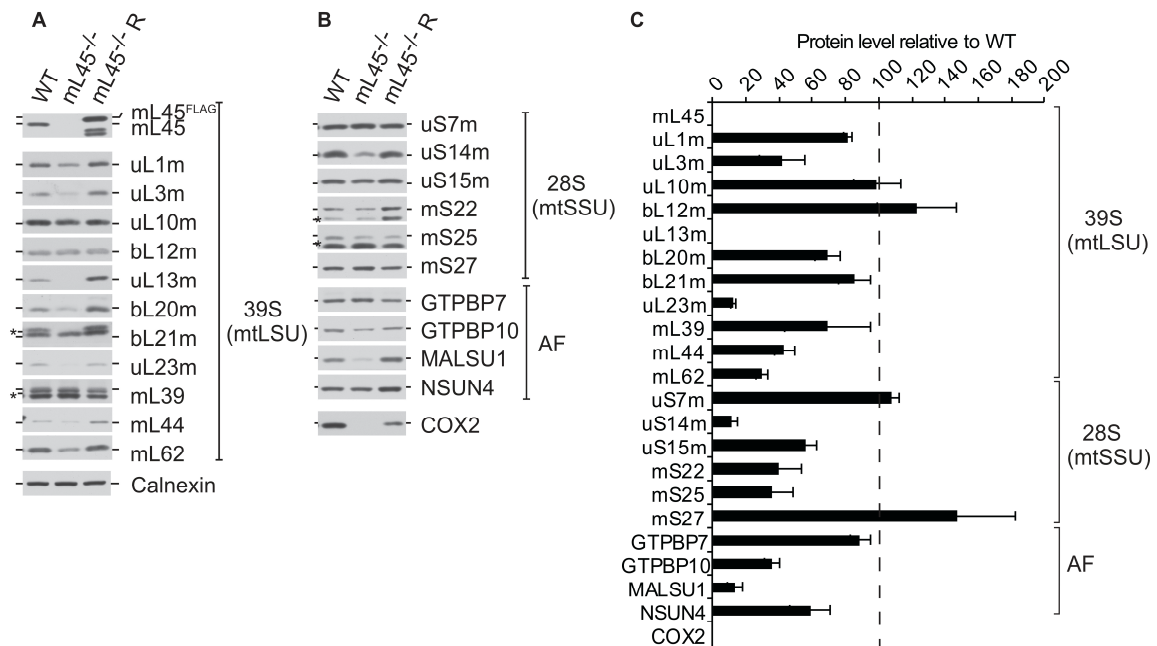
Figure 37: Analysis of protein steady state levels of cell lysates from HEK293T WT, mL45$^{-/-}$ or mL45$^{-/-}$R. Cells were treated for 24 h with 100 ng/μl tetracycline prior analysis. A and B) Samples (50 μg) were tested by immunoblotting using antibodies against MRPs of the mtLSU, mtSSU and of assembly factors (AF). C) Protein levels of mL45$^{-/-}$ cell line were quantified using the software ImageQuant TL and calculated relative to wild type (WT). Calnexin served as loading control (n=3, mean ± SEM). mL45 antibody used during this experiment: ProteinTech (15682-1-AP). Asterisks indicates residual signals from previous antibody decorations.

To determine whether mitoribosomal particles or subcomplexes are formed in absence of mL45, lysates from mitoplast preparations from HEK293T WT, mL45$^{-/-}$, mL45$^{-/-}$ R were subjected to sucrose gradient ultracentrifugation. Upon loss of mL45, no 39S mtLSU and no monosome was present (Figure 38A). Although a similar profile of tested mtSSU proteins in sucrose gradients compared to WT samples was observed (Figure 38B, C), steady state levels were in some cases severely reduced (Figure 37B, C). These data suggest that 28S mtSSU assembly is in some degree affected by the loss of mL45. All tested assembly factors accumulate in the lower dense fractions if mL45 is missing (Figure 38D).
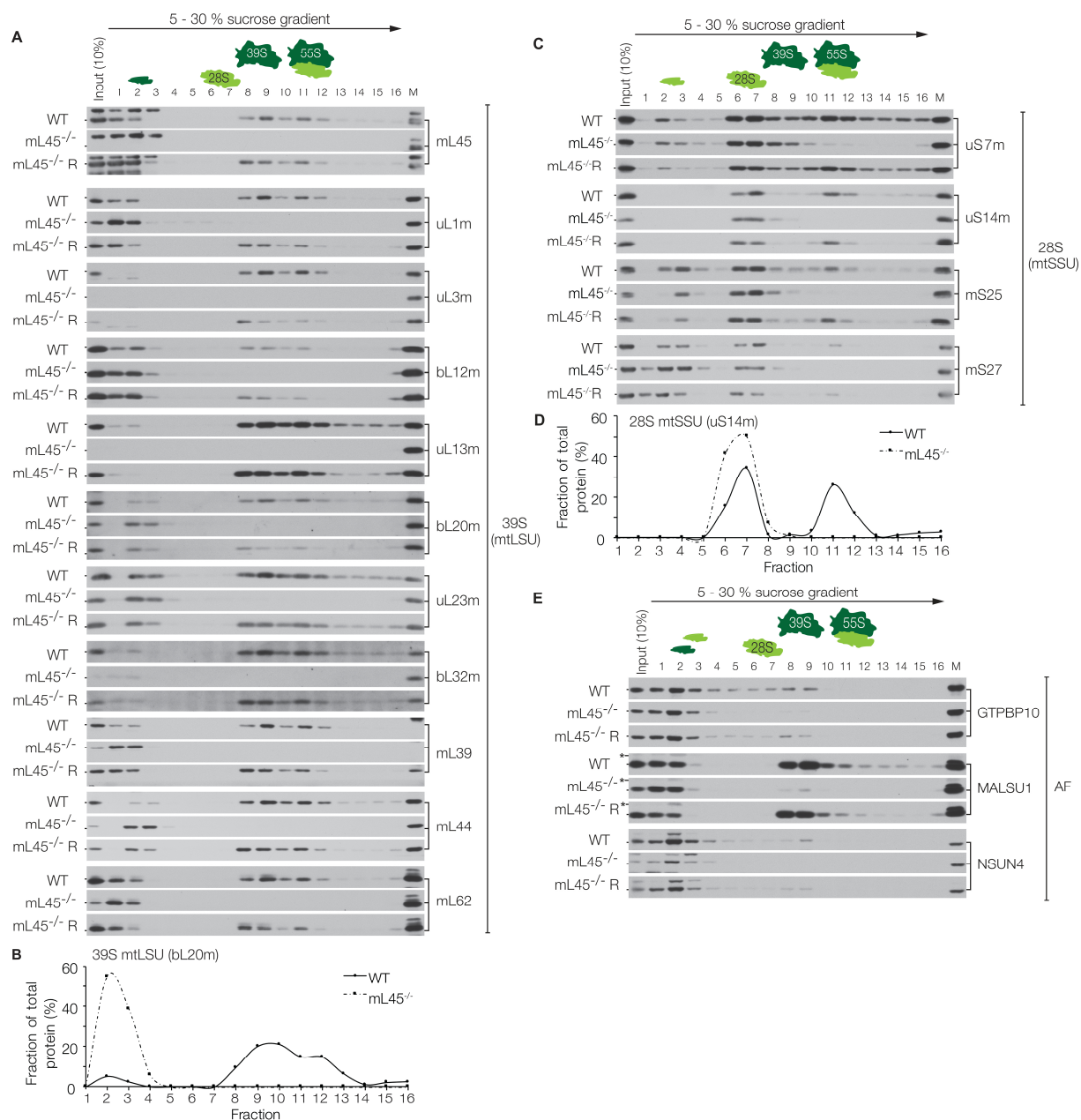
Figure 38: Impact of loss of mL45 on mitoribosome assembly. Mitoplasts (500 μg) obtained from HEK293T WT, mL45⁻/⁻ or mL45⁻/⁻ R were lysed and ribosomal particles were separated via sucrose density gradient centrifugation. A, B, D) Fractions were analysed via SDS-PAGE and western blotting using indicated antibodies. C, E) Selected markers for mtSSU (uS14m) and mtLSU (bL20m) were quantified by using the software ImageJ and plotted relative to the total protein level across the gradient. M = 10 μg HEK293T WT mitochondria, 10 % Input of loaded material = 50 μg mitoplast lysate (n = 3).

As there is neither a 39S mtLSU particle nor an assembly intermediate close to its density built, proteins of the mtLSU accumulate in the lower dense fractions (Figure 38A, E). Thus, mL45 needs to be incorporated early during mitoribosome biogenesis and its loss prevents further 39S assembly. As already described in section 4.2.1, there are different sedimentation profiles in these early fractions for distinct assembly intermediates. As the proteins bL20m and mL44 were not

found to be in a complex together with mL45 (Figure 31C), their accumulation upon mL45 ablation suggests that this submodule can be formed and is also stable if the mitoribosomal membrane anchor is missing. In addition, the subcomplex in fraction two and three containing uL23m remained stable in absence of mL45. The sedimentation profile of uL1m, bL12m, bL32m, mL39 and mL62 looked similar to the one of mL45 in the first three fractions of the gradient. By taking the structural information of the localisation of those proteins into consideration, uL1m, bL12m and mL62 are very unlikely to build a subcomplex together with mL45.

4.2.2.3 Interactome of mL45

To determine the composition of mL45 complexes, FLAG-immunoprecipitation experiments were performed followed by sucrose gradient centrifugation. In initial experiments, the HEK293T mL45[FLAG] cell line was used. Using mL45[FLAG] as a bait, proteins of the mtLSU and mtSSU were co-purified. This indicates that mL45[FLAG] is functional and able to be incorporated into the 39S mtLSU, which can form 55S particles (Figure 39). Some proteins were more enriched in the elution fraction than others. The L7/L12 stalk protein bL12m co-immunoprecipitated with mL45[FLAG] in lower portions whereas the central protuberance protein mL62 was enriched in the elution fraction.
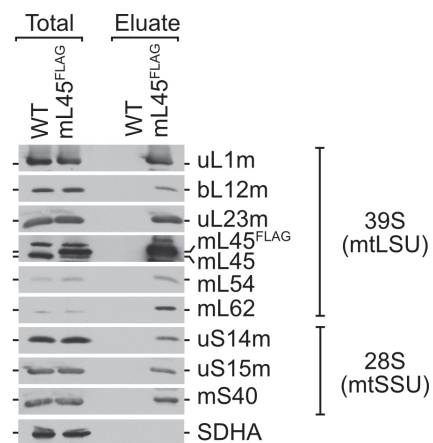
Figure 39: mL45[FLAG] immunoprecipitation Isolated mitochondria (1 mg) from HEK293T WT (negative control) or mL45[FLAG] cells were lysed and subjected to FLAG co-immunoprecipitation Samples were analysed by SDS-PAGE followed by immunoblotting using the indicated antibodies. SDHA served as negative control to exclude unspecific binding during immunoprecipitation. Total = 3 %, Eluate = 100 %, (n = 3). Cells were induced with 0.25 µg/ml tetracycline for 24 h prior analysis.

However, under these conditions mL45[FLAG] was strongly overexpressed. Therefore, the HEK293T mL45^{-/-}R cell line was used in subsequent analyses, to obtain physiological levels of mL45[FLAG] expression. By analysing fractions after FLAG-co-immunoprecipitations of mL45^{-/-}R followed by sucrose gradient centrifugation, signals from proteins corresponding to the 39S and 55S particles were observed (Figure 40). Despite that the sedimentation profiles in mitoplast gradients (Figure 38A) looked similar for bL32m and mL62 to the one of mL45, no signals in the first fractions

corresponding to an assembly intermediate were observed. Just mL39 was found in a complex with mL45 in fraction one and two. Surprisingly, uL23m and uL24m were also not present in this complex, despite the fact that inter-protein crosslinks for these proteins to mL45 were reported (Greber et al., 2014b) and that they are closely localised to mL45 (Bieri et al., 2018). These data indicate that mL45 forms a submodule together with mL39.
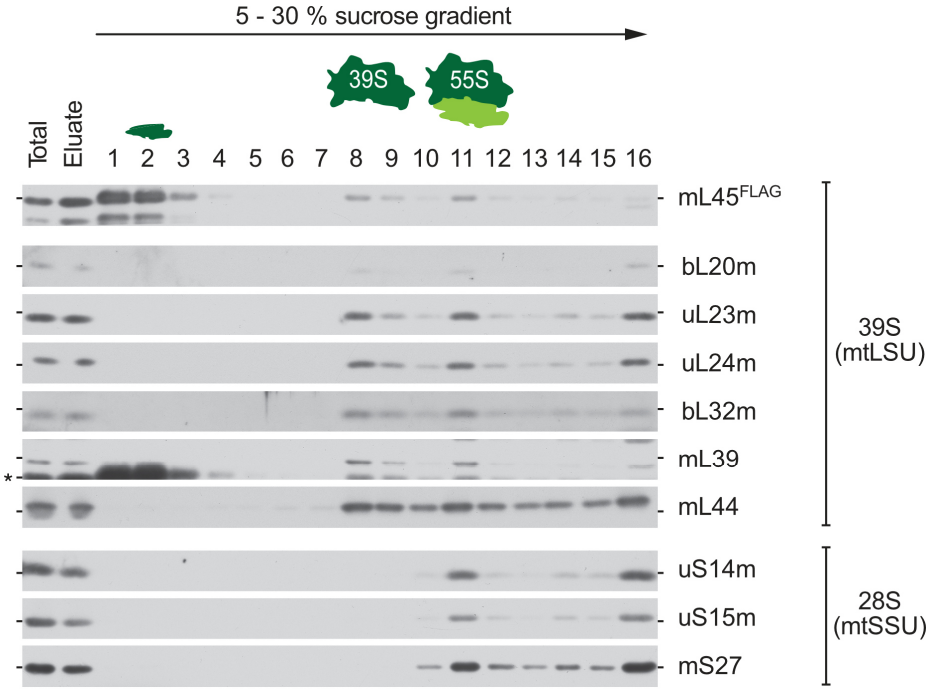
Figure 40: Separation of mL45^{FLAG} containing particles by sucrose density centrifugation. HEK293T mL45$^{-/-}$R cells were induced with 100 ng/ml tetracycline for 24 h prior mitochondria isolation. Mitochondria (2.4 mg) were lysed and subjected to FLAG-immunoprecipitation followed by sucrose gradient centrifugation. Fractions were ethanol precipitated and analysed by SDS-PAGE followed by western blotting using the indicated antibodies of mtLSU and mtSSU. Total = 1 % of FLAG-IP input, Eluate = 20 % of FLAG-IP eluate (n=1). Asterisk indicates residual signals from previous antibody decorations.

4.2.2.4 Discussion mL45

Recently, new insights about the function of the N-terminal domain (NTD) of mL45 became available. The NTD of mL45 comprises approximately 80 amino acids, reaches from L38 to N115 and is present basically in its primary structure (Kummer et al., 2018). Kummer et al. illustrated by high-resolution structural analyses that during translation initiation, the polypeptide exit tunnel is blocked by residue 38 – 64 of the NTD of mL45 and concluded that it has to be removed to enable synthesis of the nascent peptide chain. In addition, mutational analyses revealed that the NTD is necessary for functional mt translation. However, knock-out of mL45 only led to reduced mt translation.

Koripella et al. (2020) suggested, based on their latest cryo-EM structure of the 55S mitoribosome, that an adenine residue (A2725) of the 16S rRNA located between helices 73 and 74 could mediate the interaction of the nascent polypeptide chain and R40 of the NTD of mL45. By comparing structures of the initiation and elongation complex, they observed a conformational change of R61 – D73 within mL45, which they hypothesized as preparative steps for removal of the NTD of mL45 from the polypeptide exit tunnel. Furthermore, the authors were able to show another conformational change of residues T101 - Y128. The positively charged residues within this area were suggested to mediate the contact of the 55S mitoribosome to the negatively charged IMM (Englmeier et al., 2017). For this reason, charged amino acids in the segment spanning from 118 – 136 of mL45 were exchanged for alanine in a study of Mai (2016) but did not prevent binding of mL45 to the IMM. Deletion of residue 1 – 117 of mL45 described in the same study, did not inhibit anchoring of the mitoribosome to the IMM, as well. However, Koripella et al. proposed that the conformational change of T101 - Y128 of mL45 is required to anchor the mitoribosome to the IMM. In contrast, earlier publications stated that the mitoribosome interacts with the IMM independently of a nascent chain (Greber et al., 2014b; Liu and Spremulli, 2000). This arises the question, whether the mitoribosome is only anchored to the IMM during translation elongation, which would be surprising.

Ablation of mL45 led to a complete loss of assembled mtLSU and subsequently to depletion of 55S mitoribosomes (Figure 38). In contrast, mtSSU assembly was just partially affected due to ablation of mL45. Thus, it is tempting to speculate that membrane attachment of the mtLSU during biogenesis is crucial as the absence of the membrane anchor mL45 is leading to severe defects. To exclude effects based on the loss of mL45 in regard of integrity of the mitoribosomal structure, mutational analyses of the residues T101 – Y128 of mL45 would be required. This would clarify as well, under which circumstances the mtLSU is anchored to the IMM.

Within this doctoral study, it was shown that mL45 is required for mt translation and stability of most MRPs (Figure 36,Figure 37). Upon mL45 ablation, we observed a complete loss of mtDNA-encoded proteins, which is in contrast to previously published data by Kummer et al., 2018. As the authors did not perform FACS sorting after CRISPR/Cas9 transformation, cells probably represent a mixed population of mL45 mutants and wild type cells leading to an incomplete depletion and subsequently just to a reduced mt translation. siRNA mediated depletion analyses of mL45 carried out by the research group of Prof. Dr. Antoni Barrientos revealed similar tendencies in protein steady state levels (Kim and Barrientos, 2018) in comparison to the data shown here. Most of the tested mtLSU proteins were either diminished (uL14m, bL19m, mL66) or lost (uL16m) (Kim and Barrientos, 2018). Just bL12m remained stable, as well as bL36m (Kim and Barrientos, 2018). However, within a study of the same laboratory, siRNA mediated depletion of mL45 lead to a severe reduction of bL36m levels (Maiti et al., 2018), which one would expect as bL36m is incorporated late during assembly (Brown et al., 2017). Nevertheless, it is not finally solved whether mL45 depletion has an influence on bL36m. bL12m was also stable in mL45$^{-/-}$ cells (Figure 37A), probably due to additional functions of this protein on transcription regulation within mitochondria (Nouws et al., 2016; Surovtseva et al., 2011; Wang et al., 2007). By siRNA mediated depletion of mL45 no effect on the mtSSU proteins bS18m, mS27 and mS40 was observed, but a reduction of protein levels of the assembly factors MALSU1, GTPBP5, GTPBP7 and GTPBP10 (Kim and Barrientos, 2018; Maiti et al., 2018). This is in agreement with data of this study, in which a decrease of protein steady state levels of GTPBP10, MALSU1 and NSUN4 was observed as well (Figure 37B). The biogenesis factors might be less stable upon loss of mL45 as they are interacting with the mtLSU at a later assembly stage, which is not reached if mL45 is missing.

Most of the tested proteins of the mtSSU (uS14m, uS15m, mS22, mS25) in mL45$^{-/-}$ revealed reduced steady state levels implying a cross talk between mtLSU and mtSSU. As the 28S mtSSU is not as strongly affected upon loss of mL45 as the 39S mtLSU, the effect of siRNA-mediated depletion of mL45 might not be severe enough to reveal these changes.

Bogenhagen et al., 2018, already suggested that mL45 is binding early during assembly to mediate the IMM contact. The authors described mL45 in an early assembly intermediate together with uL3m, uL14m, bL17m, bL19m, uL22m, bL32m and mL39. Our data also provide evidence, that mL45 is assembling early during mtLSU biogenesis. However, data of this thesis did not show a complex of mL45 together with bL32m in the light dense fractions after separation of ribosomal particles from FLAG co-immunoprecipitated samples or any other indication that bL32m may assemble early in this process (Figure 40). This is not surprising as the yeast homologue bL32m is assembled at a late stage (Nolden et al., 2005; Zeng et al., 2018) and its bacterial counterpart

bL32 was found to bind at an intermediate assembly step (Chen and Williamson, 2013). Consequently, it is suggested that bL32m is not binding to an early assembled submodule containing mL45.

However, mL39 was present in fraction one and two from FLAG-immunoprecipitated samples, subjected to sucrose gradient centrifugation, leading to the assumption of a module containing mL45 and mL39, which is supported by inter-protein crosslinking data between mL39 and mL45 from Greber et al. (2014b). Inter-protein crosslinks were also obtained for mL45 to uL23m and uL24m (Greber et al., 2014b), but these proteins were not detected in the submodule consisting of mL39 and mL45. Thus, uL23m and uL24m might assemble in a distinct subcomplex despite their close proximity to mL45.

The 54S yeast mtLSU proteins mL43, mL44, mL50, mL57, mL58, which are located in close proximity to the exit tunnel and which form a "membrane-facing protuberance", assemble early during biogenesis in order to tether the growing ribosomal particle to the IMM (Zeng et al., 2018). The yeast mitoribosome is anchored to the IMM via two contact sites: the 21S rRNA segment 96-ES1 and the IMM ribosome receptor protein Mba1, which is interacting with proteins of a so called "membrane-facing protuberance" (Pfeffer et al., 2015; Zeng et al., 2018). As already mentioned, the structural homologue of Mba1 in human mitochondria is mL45 (Greber and Ban, 2016). As mL45 is the only anchor of the 55S mitoribosome to the IMM, one can hypothesize that it has to be assembled early during mitoribosome biogenesis in order to provide a platform for 39S mtLSU assembly as suggested for the biogenesis of the yeast mtLSU (Zeng et al., 2018).

5. Discussion

By using a quantitative mass spectrometry approach, Chen and Williamson, 2013, proposed an *in vivo* assembly map for the bacterial 70S ribosome. Proteins of the 50S subunit bind during the whole subunit biogenesis at every domain of the 23S rRNA (Chen and Williamson, 2013). The first group of proteins (L20, L21, L22, L24) is binding directly to the 5' domain of the 23S rRNA. Also, the second (L1, L3, L4, L13, L15, L17, L23) and third group (L5, L18, L29, L34) are binding mostly immediate to the rRNA. The fourth group of binding proteins consists of L14 (binds to the rRNA) and L2, L19, L32 (bind to already present proteins). Within the fifth group are L6, L9, L11, L28 and L33 assembling onto the 23S rRNA and at last L7/L12, L10, L16, L25, L27, L30, L31, L35 and L36 are incorporated to finish the LSU assembly (Figure 41) (Chen and Williamson, 2013).
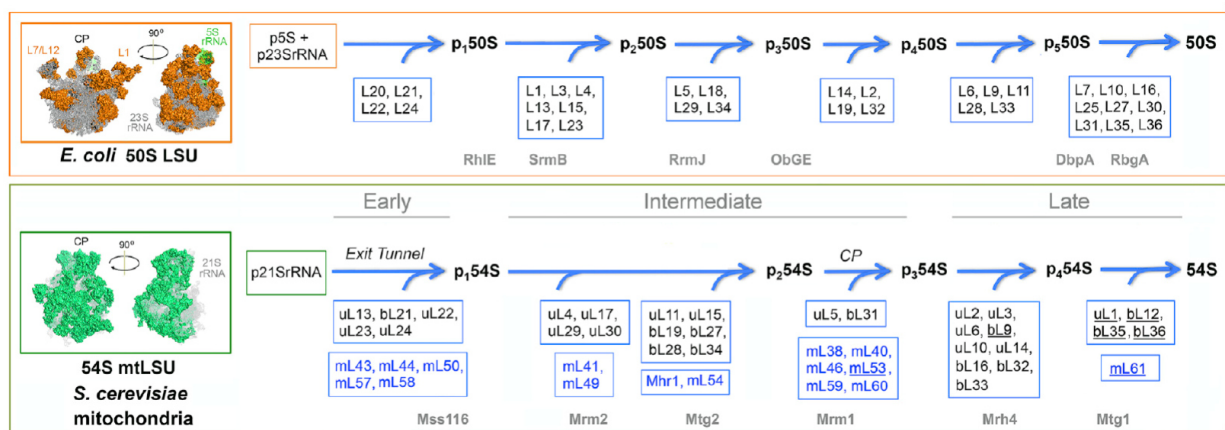
Figure 41: Assembly of the bacterial 50S LSU and the S. cerevisiae 54S mtLSU. Proteins of the yeast mtLSU, which are conserved in bacteria are shown in black, while mitochondrial ribosome specific proteins are visualized in blue. Known assembly factors of the 54S particle are depicted in grey and their bacterial orthologs/paralogs are shown on the bottom of the E. coli panel. Picture adapted from Zeng et al., 2018*. Reprinted from Cell Metabolism, 27, Zeng, R., Smith, E., and Barrientos, A.: Mitoribosome Large Subunit Assembly Proceeds by Hierarchical Incorporation of Protein Clusters and Modules on the Inner Membrane. 645-656, Copyright (2018), with permission from Elsevier. DOI: https://doi.org/10.1016/j.cmet.2018.01.012*

Upon loss of various assembly factors, biogenesis of the bacterial LSU was trapped, leading to late assembly intermediates (Jomaa et al., 2014; Li et al., 2013; Ni et al., 2016). Structural analyses of these immature particles revealed predominantly a lack of assembled central protuberance (CP) consistent with the mainly late incorporation of CP proteins (L5, L16, L18, L25, L27, L31, L33, L35) into the LSU (Davis and Williamson, 2017; Korepanov et al., 2012). Interestingly, the peptidyl transferase centre was also in an immature assembly stage, giving rise to the hypothesis of a very late maturation of this catalytical core (Davis and Williamson, 2017).

In contrast to the bacterial ribosome, mitoribosomes of different species consist of an increased number of proteins but variable rRNA contents (Figure 42). Despite their tremendous structural differences, the assembly mechanisms are hypothesized to follow basically a similar path (Jaskolowski et al., 2020).
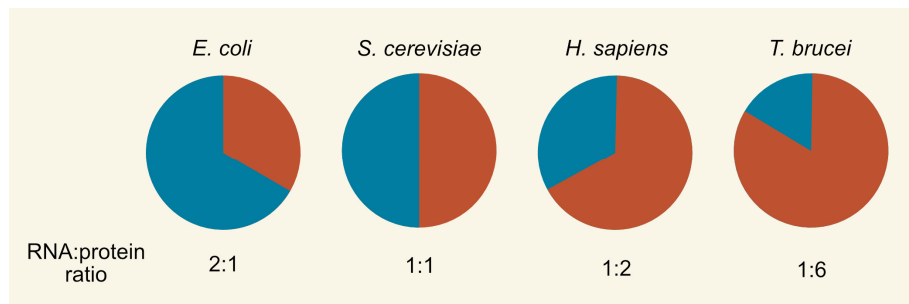
Figure 42 Comparison of RNA:protein ratios of different species (Jaskolowski et al., 2020). *Blue = RNA, orange = protein.*

Like for the assembly of the bacterial ribosome, a stepwise incorporation of protein modules was described for the 54S yeast mtLSU (Figure 41) (Zeng et al., 2018). Proteins having homologs in bacteria, are incorporated at comparable stages during biogenesis.

The CP in yeast was remodelled during evolution due to the absence of an additional structural RNA component (Amunts et al., 2014). Box et al. (2017) suggested the existence of a subcomplex consisting of proteins of the CP (mL38, uL5, bL27, mL46, mL40). Within mutational analyses of Zeng et al. (2018), CP proteins remained stable, proposing that they form an independent protein complex, which is incorporated into the growing mtLSU. Recent studies of the biogenesis of the mtLSU of *Trypanosoma brucei* implicated the presence of a pre-assembled CP as well (Jaskolowski et al., 2020). On the contrary, Bogenhagen et al. (2018) described proteins forming the CP (Figure 43) to be incorporated at an early (mL40, mL46, mL48, bL31m) or intermediate (uL18m, bL27m, mL38, mL62) assembly stage.

Th mtLSU MRP mL62 was detected in fraction one and two from sucrose gradients of mitoplast lysates from HEK293T WT cells (Figure 30). mL62 was previously described to be incorporated late during mtLSU biogenesis (Richter, 2010). It would be one possibility that mL62 along with other proteins of the CP and the structural tRNA^{Val} forms a subcomplex similar to the ones observed in *S. cerevisiae* and *T. brucei*, which can be detected in light dense fractions of a sucrose density gradient. However, mL62 also belongs to the release factor family and might be involved in translation termination and ribosome rescue pathways (Akabane et al., 2014; Richter et al., 2010), like its bacterial homologue ArfB (alternative ribosome-rescue factor B), which was just recently reported to rescue stalled ribosomes (Chan et al., 2020). Thus, mL62 in fractions one and

two might represent different populations e.g. a free pool available from ribosome rescue or a submodule of the CP, respectively. To dissect this hypothesis, immunoprecipitation experiments of mL62 followed by sucrose gradient centrifugation would be necessary to analyse the composition and existence of a subcomplex present in fraction one and two.
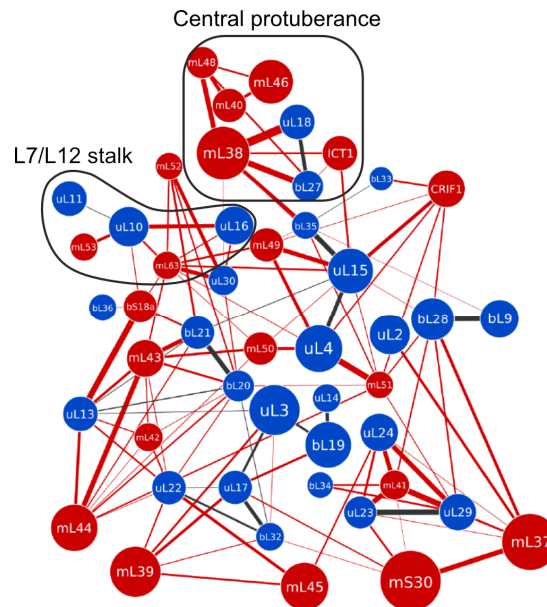
Figure 43: Protein interactions within 39S mtLSU. Black lines indicate conserved interactions from the bacterial ancestor, whereas red lines represent mitoribosome specific connections. blue = proteins having homologs in bacteria, red = mitochondrial ribosome specific proteins. ICT1 = mL62, CRIF1 = mL64. Encircled are proteins of L7/L12 stalk and central protuberance. Due to the high flexibility of the L7/L12 stalk, bL12m was not modelled. Picture adapted from Brown, A., Amunts, A., Bai, X. -c. X.-C.C., Sugimoto, Y., Edwards, P.C., Murshudov, G., Scheres, S.H.W.W., and Ramakrishnan, V. (2014). Structure of the large ribosomal subunit from human mitochondria. Science (80). 346, 718–722. Reprinted with permission from AAAS. DOI: https://doi.org/10.1126/science.1258026

Based on a cryo-EM analysis of another late stage assembly intermediate from *T. brucei*, assembly of the L7/L12 stalk is suggested to happen late during mtLSU biogenesis (Tobiasson et al., 2020). The authors identified an assembly intermediate lacking the CP and the L7/L12 stalk. Instead, a total of 16 assembly factors were found to be associated. Thus, a model was proposed where dissociation of assembly factors enables rRNA folding, conformational changes and at last binding of uL10m and four copies of bL12m. Also in the yeast mtLSU, uL10m and bL12m are incorporated late similar to homologs in bacteria (Chen and Williamson, 2013; Zeng et al., 2018). However, within the assembly map of the human mtLSU uL10m and bL12m are designated early binding proteins (Bogenhagen et al., 2018), which is in discrepancy to the bacterial, yeast and trypanosomal mtLSU assembly.

Data of this doctoral study show comparable sedimentation profiles for uL10m and bL12m in sucrose gradients (Figure 30). In addition, uL10m and bL12m are stable upon ablation of the early

binding proteins mL44 and mL45 (Figure 29, Figure 37), leading to the assumption that proteins of the L7/L12 stalk might form an independent subcomplex as described for the CP of *S. cerevisiae* and *T. brucei,* which is incorporated at a late biogenesis stage (Jaskolowski et al., 2020; Zeng et al., 2018). This pre-assembled submodule could be detectable in the light dense fractions of sucrose gradients. Similar approaches as mentioned to dissect the submodule containing mL62 would be required to investigate the existence and composition of the complex containing uL10m and bL12m and would shed light into the biogenesis of the L7/L12 stalk.

The 39S human mtLSU consists of 52 proteins. Out of these, there are 30 proteins having homologs in bacteria whereas 22 are mitoribosomal specific. Three proteins (uL5, uL6, bL25) are existing in the bacterial 50S LSU but not in the 39S mtLSU (Ban et al., 2014; Greber and Ban, 2016). Even if the mitoribosomal proteins conserved in bacteria are following a comparable assembly path, the order of incorporation of the mito-specific proteins remains not completely solved. Based on the observations of the biogenesis of the mtLSU of *T. brucei* it was proposed that ribosomes with a high protein content assemble at first their "protein shell" at an early stage, probably independent from rRNA maturation steps (Jaskolowski et al., 2020). Data of this doctoral thesis support this theory as the mitochondrial ribosome specific protein mL44, which is located on the surface of the mtLSU particle, is assumed to be assembled with bL20m, bL21m, mL42, mL43 and mL50 early during biogenesis. By using a SILAC approach containing purified mitoribosomes, we want to address this issue further. The future analysis of these data will give intriguing new insights into the assembly of the 39S mtLSU and will enable us to understand the order of incorporation of mitoribosomal specific proteins in the background of assembly maps of other species.

6. Bibliography

Aibara, S., Andréll, J., Singh, V., and Amunts, A. (2018). Rapid Isolation of the Mitoribosome from HEK Cells. J. Vis. Exp. 1–9.

Akabane, S., Ueda, T., Nierhaus, K.H., and Takeuchi, N. (2014). Ribosome Rescue and Translation Termination at Non-Standard Stop Codons by ICT1 in Mammalian Mitochondria. PLoS Genet. *10*, 1–14.

Amunts, A., Brown, A., Bai, X.C., Llácer, J.L., Hussain, T., Emsley, P., Long, F., Murshudov, G., Scheres, S.H.W., and Ramakrishnan, V. (2014). Structure of the yeast mitochondrial large ribosomal subunit. Microsc. Microanal. *20*, 1252–1253.

Amunts, A., Brown, A., Toots, J., Scheres, S.H.W., and Ramakrishnan, V. (2015). The structure of the human mitochondrial ribosome. Science (80-.). *348*, 95–98.

Anderson, S., Bankier, A.T., Barrell, B.G., de Bruijn, M.H.L., Coulson, A.R., Drouin, J., Eperon, I.C., Nierlich, D.P., Roe, B.A., Sanger, F., et al. (1981). Sequence and organization of the human mitochondrial genome. Nature *290*, 457–465.

Antonicka, H., and Shoubridge, E.A. (2015). Mitochondrial RNA Granules Are Centers for Posttranscriptional RNA Processing and Ribosome Biogenesis. Cell Rep. *10*, 920–932.

Antonicka, H., Sasarman, F., Nishimura, T., Paupe, V., and Shoubridge, E.A. (2013). The mitochondrial RNA-binding protein GRSF1 localizes to RNA granules and is required for posttranscriptional mitochondrial gene expression. Cell Metab. *17*, 386–398.

Antonicka, H., Choquet, K., Lin, Z., Gingras, A., Kleinman, C.L., and Shoubridge, E.A. (2017). A pseudouridine synthase module is essential for mitochondrial protein synthesis and cell viability. EMBO Rep. *18*, 28–38.

Arroyo, J.D., Jourdain, A.A., Calvo, S.E., Ballarano, C.A., Doench, J.G., Root, D.E., and Mootha, V.K. (2016). A Genome-wide CRISPR Death Screen Identifies Genes Essential for Oxidative Phosphorylation. Cell Metab. *24*, 875–885.

Baertling, F., Haack, T.B., Rodenburg, R.J., Schaper, J., Seibt, A., Strom, T.M., Meitinger, T., Mayatepek, E., Hadzik, B., Selcan, G., et al. (2015). MRPS22 mutation causes fatal neonatal lactic acidosis with brain and heart abnormalities. Neurogenetics *16*, 237–240.

Ban, N., Beckmann, R., Cate, J.H.D., Dinman, J.D., Dragon, F., Ellis, S.R., Lafontaine, D.L.J., Lindahl, L., Liljas, A., Lipton, J.M., et al. (2014). A new system for naming ribosomal proteins. Curr. Opin. Struct. Biol. *24*, 165–169.

Bar-Yaacov, D., Frumkin, I., Yashiro, Y., Chujo, T., Ishigami, Y., Chemla, Y., Blumberg, A., Schlesinger, O., Bieri, P., Greber, B., et al. (2016). Mitochondrial 16S rRNA Is Methylated by tRNA Methyltransferase TRMT61B in All Vertebrates. PLoS Biol. *14*, 1–21.

Barrell, B.G., Bankier, A.T., and Drouin, J. (1979). A different genetic code in human mitochondria. Nature *282*, 189–194.

Beller, R.J., and Davis, B.D. (1971). Selective dissociation of free ribosomes of Escherichia coli by sodium ions. J. Mol. Biol. *55*, 477–485.

Benz, R. (1994). Permeation of hydrophilic solutes through mitochondrial outer membranes: review on mitochondrial porins. BBA - Rev. Biomembr. *1197*, 167–196.

Bereiter-Hahn, J., and Vöth, M. (1994). Dynamics of mitochondria in living cells: Shape changes, dislocations, fusion, and fission of mitochondria. Microsc. Res. Tech. *27*, 198–219.

Berk, A.J., and Clayton, D.A. (1974). Mechanism of mitochondrial DNA replication in mouse L-cells: Asynchronous replication of strands, segregation of circular daughter molecules, aspects of topology and turnover of an initiation sequence. J. Mol. Biol. *86*, 801–824.

Bezawork-Geleta, A., Rohlena, J., Dong, L., Pacak, K., and Neuzil, J. (2017). Mitochondrial Complex II: At the Crossroads. Trends Biochem. Sci. *42*, 312–325.

Bieri, P., Greber, B.J., and Ban, N. (2018). High-resolution structures of mitochondrial ribosomes and their functional implications. Curr. Opin. Struct. Biol. *49*, 44–53.

Bilbille, Y., Gustilo, E.M., Harris, K.A., Jones, C.N., Lusic, H., Kaiser, R.J., Delaney, M.O., Spremulli, L.L., Deiters, A., and Agris, P.F. (2011). The Human Mitochondrial tRNAMet: Structure/Function Relationship of a Unique Modification in the Decoding of Unconventional Codons. J. Mol. Biol. *406*, 257–274.

Boczonadi, V., and Horvath, R. (2014). Mitochondria: Impaired mitochondrial translation in human disease. Int. J. Biochem. Cell Biol. *48*, 77–84.

Bogenhagen, D.F., Martin, D.W., and Koller, A. (2014). Initial steps in RNA processing and ribosome assembly occur at mitochondrial DNA nucleoids. Cell Metab. *19*, 618–629.

Bogenhagen, D.F., Ostermeyer-Fay, A.G., Haley, J.D., and Garcia-Diaz, M. (2018). Kinetics and Mechanism of Mammalian Mitochondrial Ribosome Assembly. Cell Rep. *22*, 1935–1944.

Borna, N.N., Kishita, Y., Kohda, M., Lim, S.C., Shimura, M., Wu, Y., Mogushi, K., Yatsuka, Y., Harashima, H., Hisatomi, Y., et al. (2019). Mitochondrial ribosomal protein PTCD3 mutations cause oxidative phosphorylation defects with Leigh syndrome. Neurogenetics *20*, 9–25.

Borst, P. (1972). Mitochondrial Nucleic Acids. Annu. Rev. Biochem. *41*, 333–376.

Box, J.M., Kaur, J., and Stuart, R.A. (2017). MrpL35, a mitospecific component of mitoribosomes, plays a key role in cytochrome c oxidase assembly. Mol. Biol. Cell *28*, 3489–3499.

Bradford, M.M. (1976). A rapid and sensitive method for the quantitation of microgram quantities of protein utilizing the principle of protein-dye binding. Anal. Biochem. *72*, 248–254.

Brandt, U. (2006). Energy converting NADH:quinone oxidoreductase (complex I). Annu. Rev. Biochem. *75*, 69–92.

De Brito, O.M., and Scorrano, L. (2010). An intimate liaison: Spatial organization of the endoplasmic reticulum-mitochondria relationship. EMBO J. *29*, 2715–2723.

Brown, A., Amunts, A., Bai, X. -c. X.-C.C., Sugimoto, Y., Edwards, P.C., Murshudov, G., Scheres, S.H.W.W., and Ramakrishnan, V. (2014). Structure of the large ribosomal subunit from human mitochondria. Science (80-.). *346*, 718–722.

Brown, A., Rathore, S., Kimanius, D., Aibara, S., Bai, X.C., Rorbach, J., Amunts, A., and Ramakrishnan, V. (2017). Structures of the human mitochondrial ribosome in native states of assembly. Nat.

Struct. Mol. Biol. *24*, 866–869.

Brown, T.A., Tkachuk, A.N., Shtengel, G., Kopek, B.G., Bogenhagen, D.F., Hess, H.F., and Clayton, D.A. (2011). Superresolution Fluorescence Imaging of Mitochondrial Nucleoids Reveals Their Spatial Range, Limits, and Membrane Interaction. Mol. Cell. Biol. *31*, 4994–5010.

Bugiardini, E., Mitchell, A.L., Rosa, I.D., Horning-Do, H.T., Pitmann, A.M., Poole, O. V., Holton, J.L., Shah, S., Woodward, C., Hargreaves, I., et al. (2019). MRPS25 mutations impair mitochondrial translation and cause encephalomyopathy. Hum. Mol. Genet. *28*, 2711–2719.

Cai, Y.C., Bullard, J.M., Thompson, N.L., and Spremulli, L.L. (2000). Interaction of mitochondrial elongation factor Tu with aminoacyl-tRNA and elongation factor Ts. J. Biol. Chem. *275*, 20308–20314.

Callegari, S., Richter, F., Chojnacka, K., Jans, D.C., Lorenzi, I., Pacheu-Grau, D., Jakobs, S., Lenz, C., Urlaub, H., Dudek, J., et al. (2016). TIM29 is a subunit of the human carrier translocase required for protein transport. FEBS Lett. *590*, 4147–4158.

Callegari, S., Cruz-Zaragoza, L.D., Rehling, P., and Rehling, P. (2020). From TOM to the TIM23 complex - Handing over of a precursor. Biol. Chem. *401*, 709–721.

Carroll, A.J. (2017). Isolation of Mitochondrial Ribosomes. pp. 267–280.

Carroll, C.J., Isohanni, P., Pöyhönen, R., Euro, L., Richter, U., Brilhante, V., Götz, A., Lahtinen, T., Paetau, A., Pihko, H., et al. (2013). Whole-exome sequencing identifies a mutation in the mitochondrial ribosome protein MRPL44 to underlie mitochondrial infantile cardiomyopathy. J. Med. Genet. *50*, 151–159.

Chan, D.C. (2006). Mitochondrial Fusion and Fission in Mammals. Annu. Rev. Cell Dev. Biol. *22*, 79–99.

Chan, K.H., Petrychenko, V., Mueller, C., Maracci, C., Holtkamp, W., Wilson, D.N., Fischer, N., and Rodnina, M. V. (2020). Mechanism of ribosome rescue by alternative ribosome-rescue factor B. Nat. Commun. *11*, 1–11.

Chen, S.S., and Williamson, J.R. (2013). Characterization of the ribosome biogenesis landscape in E. Coli using quantitative mass spectrometry. J. Mol. Biol. *425*, 767–779.

Chen, H., Shi, Z., Guo, J., Chang, K.J., Chen, Q., Yao, C.H., Haigis, M.C., and Shi, Y. (2020). The human mitochondrial 12S rRNA m4C methyltransferase METTL15 is required for mitochondrial function. J. Biol. Chem. *295*, 8505–8513.

Chen, X., Prosser, R., Simonetti, S., Sadlock, J., Jagiello, G., and Schon, E.A. (1995). Rearranged mitochondrial genomes are present in human oocytes. Am. J. Hum. Genet. *57*, 239–247.

Chevallet, M., Luche, S., and Rabilloud, T. (2006). Silver staining of proteins in polyacrylamide gels. Nat. Protoc. *1*, 1852–1858.

Chomczynski, P., and Sacchi, N. (2006). The single-step method of RNA isolation by acid guanidinium thiocyanate-phenol-chloroform extraction: Twenty-something years on. Nat. Protoc. *1*, 581–585.

Chomyn, A. (1996). [18] In vivo labeling and analysis of human mitochondrial translation products. pp. 197–211.

Chrzanowska-Lightowlers, Z.M.A., Pajak, A., and Lightowlers, R.N. (2011). Termination of protein synthesis in mammalian mitochondria. J. Biol. Chem. *286*, 34479–34485.

Chujo, T., Ohira, T., Sakaguchi, Y., Goshima, N., Nomura, N., Nagao, A., and Suzuki, T. (2012). LRPPRC/SLIRP suppresses PNPase-mediated mRNA decay and promotes polyadenylation in human mitochondria. Nucleic Acids Res. *40*, 8033–8047.

Clapham, D.E. (2007). Calcium Signaling. Cell *131*, 1047–1058.

Cogliati, S., Enriquez, J.A., and Scorrano, L. (2016). Mitochondrial Cristae: Where Beauty Meets Functionality. Trends Biochem. Sci. *41*, 261–273.

Comte, J., Maǐsterrena, B., and Gautheron, D.C. (1976). Lipid composition and protein profiles of outer and inner membranes from pig heart mitochondria. Comparison with microsomes. BBA - Biomembr. *419*, 271–284.

Czech, B., and Hannon, G.J. (2011). Small RNA sorting: Matchmaking for argonautes. Nat. Rev. Genet. *12*, 19–31.

D'Souza, A.R., and Minczuk, M. (2018). Mitochondrial transcription and translation: Overview. Essays Biochem. *62*, 309–320.

D'Souza, A., Van Haute, L., Powell, C., Rebelo- Guiomar, P., Rorbach, J., and Minczuk, M. (2019). YbeY is required for ribosome small subunit assembly and tRNA processing in human mitochondria.

Dalla Rosa, I., Durigon, R., Pearce, S.F., Rorbach, J., Hirst, E.M.A., Vidoni, S., Reyes, A., Brea-Calvo, G., Minczuk, M., Woellhaf, M.W., et al. (2014). MPV17L2 is required for ribosome assembly in mitochondria. Nucleic Acids Res. *42*, 8500–8515.

Davies, S.M.K., Lopez Sanchez, M.I.G., Narsai, R., Shearwood, A.M.J., Razif, M.F.M., Small, I.D., Whelan, J., Rackham, O., and Filipovska, A. (2012). MRPS27 is a pentatricopeptide repeat domain protein required for the translation of mitochondrially encoded proteins. FEBS Lett. *586*, 3555–3561.

Davis, J.H., and Williamson, J.R. (2017). Structure and dynamics of bacterial ribosome biogenesis. Philos. Trans. R. Soc. B Biol. Sci. *372*.

Dennerlein, S., Rozanska, A., Wydro, M., Chrzanowska-Lightowlers, Z.M.A., and Lightowlers, R.N. (2010). Human ERAL1 is a mitochondrial RNA chaperone involved in the assembly of the 28S small mitochondrial ribosomal subunit. Biochem. J. *430*, 551–558.

Dennerlein, S., Oeljeklaus, S., Jans, D., Hellwig, C., Bareth, B., Jakobs, S., Deckers, M., Warscheid, B., and Rehling, P. (2015). MITRAC7 Acts as a COX1-Specific Chaperone and Reveals a Checkpoint during Cytochrome c Oxidase Assembly. Cell Rep. *12*, 1644–1655.

Desai, N., Brown, A., Amunts, A., and Ramakrishnan, V. (2017). The structure of the yeast mitochondrial ribosome. Science (80-.). *355*, 528–531.

Distelmaier, F., Haack, T.B., Catarino, C.B., Gallenmüller, C., Rodenburg, R.J., Strom, T.M., Baertling, F., Meitinger, T., Mayatepek, E., Prokisch, H., et al. (2015). MRPL44 mutations cause a slowly progressive multisystem disease with childhood-onset hypertrophic cardiomyopathy. Neurogenetics *16*, 319–323.

Emdadul Haque, M., Grasso, D., Miller, C., Spremulli, L.L., and Saada, A. (2008). The effect of mutated mitochondrial ribosomal proteins S16 and S22 on the assembly of the small and large ribosomal subunits in human mitochondria. Mitochondrion *8*, 254–261.

Englmeier, R., Pfeffer, S., and Förster, F. (2017). Structure of the Human Mitochondrial Ribosome Studied in Situ by Cryoelectron Tomography. Structure *25*, 1574-1581.e2.

Fearnley, I.M., and Walker, J.E. (1987). Initiation Codons in Mammalian Mitochondria: Differences in Genetic Code in the Organelle. Biochemistry *26*, 8247–8251.

Fei, J., Kosuri, P., MacDougall, D.D., and Gonzalez, R.L. (2008). Coupling of Ribosomal L1 Stalk and tRNA Dynamics during Translation Elongation. Mol. Cell *30*, 348–359.

Feng, B., Mandava, C.S., Guo, Q., Wang, J., Cao, W., Li, N., Zhang, Y., Zhang, Y., Wang, Z., Wu, J., et al. (2014). Structural and Functional Insights into the Mode of Action of a Universally Conserved Obg GTPase. PLoS Biol. *12*.

Frazier, A.E., Thorburn, D.R., and Compton, A.G. (2019). Mitochondrial energy generation disorders: Genes, mechanisms, and clues to pathology. J. Biol. Chem. *294*, 5386–5395.

Friedman, J.R., and Nunnari, J. (2014). Mitochondrial form and function. Nature *505*, 335–343.

Galmiche, L., Serre, V., Beinat, M., Assouline, Z., Lebre, A.S., Chretien, D., Nietschke, P., Benes, V., Boddaert, N., Sidi, D., et al. (2011). Exome sequencing identifies MRPL3 mutation in mitochondrial cardiomyopathy. Hum. Mutat. *32*, 1225–1231.

Gardeitchik, T., Mohamed, M., Ruzzenente, B., Karall, D., Guerrero-Castillo, S., Dalloyaux, D., van den Brand, M., van Kraaij, S., van Asbeck, E., Assouline, Z., et al. (2018). Bi-allelic Mutations in the Mitochondrial Ribosomal Protein MRPS2 Cause Sensorineural Hearing Loss, Hypoglycemia, and Multiple OXPHOS Complex Deficiencies. Am. J. Hum. Genet. *102*, 685–695.

Giacomello, M., Pyakurel, A., Glytsou, C., and Scorrano, L. (2020). The cell biology of mitochondrial membrane dynamics. Nat. Rev. Mol. Cell Biol. *21*, 204–224.

Goyal, A., Belardinelli, R., and Rodnina, M. V. (2017). Non-canonical Binding Site for Bacterial Initiation Factor 3 on the Large Ribosomal Subunit. Cell Rep. *20*, 3113–3122.

Greber, B.J., and Ban, N. (2016). Structure and Function of the Mitochondrial Ribosome. Annu. Rev. Biochem. *85*, 103–132.

Greber, B.J., Boehringer, D., Leibundgut, M., Bieri, P., Leitner, A., Schmitz, N., Aebersold, R., and Ban, N. (2014a). The complete structure of the large subunit of the mammalian mitochondrial ribosome. Nature *515*, 283–286.

Greber, B.J., Boehringer, D., Leitner, A., Bieri, P., Voigts-Hoffmann, F., Erzberger, J.P., Leibundgut, M., Aebersold, R., and Ban, N. (2014b). Architecture of the large subunit of the mammalian mitochondrial ribosome. Nature *505*, 515–519.

Greber, B.J., Bieri, P., Leibundgut, M., Leitner, A., Aebersold, R., Boehringer, D., and Ban, N. (2015). The complete structure of the 55S mammalian mitochondrial ribosome. Science (80-.). *348*, 303–308.

Green, D.R., and Reed, J.C. (1998). Mitochondria and Apoptosis. Science (80-.). *281*, 1309–1312.

Gustafsson, C.M., Falkenberg, M., and Larsson, N.-G. (2016). Maintenance and Expression of Mammalian Mitochondrial DNA. Annu. Rev. Biochem. *85*, 133–160.

Hällberg, B.M., and Larsson, N.G. (2014). Making proteins in the powerhouse. Cell Metab. *20*, 226–240.

Hanahan, D. (1983). Studies on transformation of Escherichia coli with plasmids. J. Mol. Biol. *166*, 557–580.

Hanitsch, E., and Richter-Dennerlein, R. (2020). Biogenese der mitochondrialen Proteinsynthesemaschine. BioSpektrum *26*, 16–19.

Haque, M.E., Elmore, K.B., Tripathy, A., Koc, H., Koc, E.C., and Spremulli, L.L. (2010). Properties of the C-terminal tail of human mitochondrial inner membrane protein Oxa1L and its interactions with mammalian mitochondrial ribosomes. J. Biol. Chem. *285*, 28353–28362.

Harbauer, A.B., Zahedi, R.P., Sickmann, A., Pfanner, N., and Meisinger, C. (2014). The protein import machinery of mitochondria - A regulatory hub in metabolism, stress, and disease. Cell Metab. *19*, 357–372.

Hardy, S.J.S., and Turnock, G. (1971). Stabilization of 70S ribosomes by spermidine. Nat. New Biol. *229*, 17–19.

Van Haute, L., Hendrick, A.G., D'Souza, A.R., Powell, C.A., Rebelo-Guiomar, P., Harbour, M.E., Ding, S., Fearnley, I.M., Andrews, B., and Minczuk, M. (2019). METTL15 introduces N4-methylcytidine into human mitochondrial 12S rRNA and is required for mitoribosome biogenesis. Nucleic Acids Res. *47*, 10267–10281.

He, J., Cooper, H.M., Reyes, A., Di Re, M., Kazak, L., Wood, S.R., Mao, C.C., Fearnley, I.M., Walker, J.E., and Holt, I.J. (2012). Human C4orf14 interacts with the mitochondrial nucleoid and is involved in the biogenesis of the small mitochondrial ribosomal subunit. Nucleic Acids Res. *40*, 6097–6108.

Hillen, H.S., Morozov, Y.I., Sarfallah, A., Temiakov, D., and Cramer, P. (2017a). Structural Basis of Mitochondrial Transcription Initiation. Cell *171*, 1072.e10-1081.e10.

Hillen, H.S., Parshin, A. V., Agaronyan, K., Morozov, Y.I., Graber, J.J., Chernev, A., Schwinghammer, K., Urlaub, H., Anikin, M., Cramer, P., et al. (2017b). Mechanism of Transcription Anti-termination in Human Mitochondria. Cell *171*, 1082-1093.e13.

Hillen, H.S., Temiakov, D., and Cramer, P. (2018). Structural basis of mitochondrial transcription. Nat. Struct. Mol. Biol. *25*, 754–765.

Hirano, Y., Ohniwa, R.L., Wada, C., Yoshimura, S.H., and Takeyasu, K. (2006). Human small G proteins, ObgH1, and ObgH2, participate in the maintenance of mitochondria and nucleolar architectures. Genes to Cells *11*, 1295–1304.

Hosler, J.P., Ferguson-Miller, S., and Mills, D.A. (2006). Energy transduction: Proton transfer through the respiratory complexes. Annu. Rev. Biochem. *75*, 165–187.

Hsiao, C., Mohan, S., Kalahar, B.K., and Williams, L.D. (2009). Peeling the onion: Ribosomes are ancient molecular fossils. Mol. Biol. Evol. *26*, 2415–2425.

Huynen, M.A., Duarte, I., Chrzanowska-Lightowlers, Z.M.A., and Nabuurs, S.B. (2012). Structure based hypothesis of a mitochondrial ribosome rescue mechanism. Biol. Direct *7*, 1–10.

Jackson, C.B., Huemer, M., Bolognini, R., Martin, F., Szinnai, G., Donner, B.C., Richter, U., Battersby, B.J., Nuoffer, J.M., Suomalainen, A., et al. (2019). A variant in MRPS14 (uS14m) causes perinatal hypertrophic cardiomyopathy with neonatal lactic acidosis, growth retardation, dysmorphic features and neurological involvement. Hum. Mol. Genet. *28*, 639–649.

Jaskolowski, M., Ramrath, D.J.F., Bieri, P., Niemann, M., Mattei, S., Calderaro, S., Leibundgut, M., Horn, E.K., Boehringer, D., Schneider, A., et al. (2020). Structural Insights into the Mechanism of Mitoribosomal Large Subunit Biogenesis. Mol. Cell *79*, 629-644.e4.

Jomaa, A., Jain, N., Davis, J.H., Williamson, J.R., Britton, R.A., and Ortega, J. (2014). Functional domains of the 50S subunit mature late in the assembly process. Nucleic Acids Res. *42*, 3419–3435.

Kavran, J.M., and Steitz, T.A. (2007). Structure of the Base of the L7/L12 Stalk of the Haloarcula marismortui Large Ribosomal Subunit: Analysis of L11 Movements. J. Mol. Biol. *371*, 1047–1059.

Kehrein, K., Bonnefoy, N., and Ott, M. (2013). Mitochondrial protein synthesis: Efficiency and accuracy. Antioxidants Redox Signal. *19*, 1928–1939.

Khawaja, A., Itoh, Y., Remes, C., Spåhr, H., Yukhnovets, O., Höfig, H., Amunts, A., and Rorbach, J. (2020). Distinct pre-initiation steps in human mitochondrial translation. Nat. Commun. *11*, 1–10.

Kim, H.J., and Barrientos, A. (2018). MTG1 couples mitoribosome large subunit assembly with intersubunit bridge formation. Nucleic Acids Res. *46*, 8435–8453.

Koc, E.C., Burkhart, W., Blackburn, K., Moyer, M.B., Schlatzer, D.M., Moseley, A., and Spremulli, L.L. (2001). The large subunit of the mammalian mitochondrial ribosome: Analysis of the complement of ribosomal proteins present. J. Biol. Chem. *276*, 43958–43969.

Kohda, M., Tokuzawa, Y., Kishita, Y., Nyuzuki, H., Moriyama, Y., Mizuno, Y., Hirata, T., Yatsuka, Y., Yamashita-Sugahara, Y., Nakachi, Y., et al. (2016). A Comprehensive Genomic Analysis Reveals the Genetic Landscape of Mitochondrial Respiratory Chain Complex Deficiencies. PLoS Genet. *12*, 1–31.

Korepanov, A.P., Korobeinikova, A. V., Shestakov, S.A., Garber, M.B., and Gongadze, G.M. (2012). Protein L5 is crucial for in vivo assembly of the bacterial 50S ribosomal subunit central protuberance. Nucleic Acids Res. *40*, 9153–9159.

Koripella, R.K., Sharma, M.R., Haque, M.E., Risteff, P., Spremulli, L.L., and Agrawal, R.K. (2019). Structure of Human Mitochondrial Translation Initiation Factor 3 Bound to the Small Ribosomal Subunit. IScience *12*, 76–86.

Koripella, R.K., Sharma, M.R., Bhargava, K., Datta, P.P., Kaushal, P.S., Keshavan, P., Spremulli, L.L., Banavali, N.K., and Agrawal, R.K. (2020). Structures of the human mitochondrial ribosome bound to EF-G1 reveal distinct features of mitochondrial translation elongation. Nat. Commun. *11*, 3830.

Kukat, C., Wurm, C.A., Spåhr, H., Falkenberg, M., Larsson, N.G., and Jakobs, S. (2011). Super-resolution microscopy reveals that mammalian mitochondrial nucleoids have a uniform size and frequently contain a single copy of mtDNA. Proc. Natl. Acad. Sci. U. S. A. *108*, 13534–13539.

Kummer, E., Leibundgut, M., Rackham, O., Lee, R.G., Boehringer, D., Filipovska, A., and Ban, N. (2018). Unique features of mammalian mitochondrial translation initiation revealed by cryo-EM. Nature *560*, 263–267.

Lake, N.J., Webb, B.D., Stroud, D.A., Richman, T.R., Ruzzenente, B., Compton, A.G., Mountford, H.S., Pulman, J., Zangarelli, C., Rio, M., et al. (2017). Biallelic Mutations in MRPS34 Lead to Instability of the Small Mitoribosomal Subunit and Leigh Syndrome. Am. J. Hum. Genet. *101*, 239–254.

Lamfrom, H., and Glowacki, E.R. (1962). Controlled dissociation of rabbit reticulocyte ribosomes and its effect on hemoglobin synthesis. J. Mol. Biol. *5*, 97–108.

Laptev, I., Shvetsova, E., Levitskii, S., Serebryakova, M., Rubtsova, M., Zgoda, V., Bogdanov, A., Kamenski, P., Sergiev, P., and Dontsova, O. (2020). METTL15 interacts with the assembly intermediate of murine mitochondrial small ribosomal subunit to form m4C840 12S rRNA residue. Nucleic Acids Res. 1–13.

Lavdovskaia, E., Kolander, E., Steube, E., Mai, M.M.Q., Urlaub, H., and Richter-Dennerlein, R. (2018). The human Obg protein GTPBP10 is involved in mitoribosomal biogenesis. Nucleic Acids Res. *46*, 8471–8482.

Lee, K.W., and Bogenhagen, D.F. (2014). Assignment of 2′-O-methyltransferases to modification sites on the mammalian mitochondrial large subunit 16 S ribosomal RNA (rRNA). J. Biol. Chem. *289*, 24936–24942.

Lee, M.D., She, Y., Soskis, M.J., Borella, C.P., Gardner, J.R., Hayes, P.A., Dy, B.M., Heaney, M.L., Philips, M.R., Bornmann, W.G., et al. (2004). Human mitochondrial peptide deformylase, a new anticancer target of actinonin-based antibiotics. J. Clin. Invest. *114*, 1107–1116.

Li, H.B., Wang, R.X., Jiang, H.B., Zhang, E.D., Tan, J.Q., Xu, H.Z., Zhou, R.R., and Xia, X.B. (2016). Mitochondrial ribosomal protein L10 associates with Cyclin B1/Cdk1 activity and mitochondrial function. DNA Cell Biol. *35*, 680–690.

Li, N., Chen, Y., Guo, Q., Zhang, Y., Yuan, Y., Ma, C., Deng, H., Lei, J., and Gao, N. (2013). Cryo-EM structures of the late-stage assembly intermediates of the bacterial 50S ribosomal subunit. Nucleic Acids Res.

Lill, R., and Mühlenhoff, U. (2008). Maturation of iron-sulfur proteins in eukaryotes: Mechanisms, connected processes, and diseases. Annu. Rev. Biochem. *77*, 669–700.

Lin, C.-Y., Chia, S.L.-L., Travis, R.L., and Key, J.L. (1975). Studies on Pea Ribosomal Proteins. Plant Physiol. *56*, 39–43.

Lind, C., Sund, J., and Åqvist, J. (2013). Codon-reading specificities of mitochondrial release factors and translation termination at non-standard stop codons. Nat. Commun. *4*.

Liu, M., and Spremulli, L. (2000). Interaction of mammalian mitochondrial ribosomes with the inner membrane. J. Biol. Chem. *275*, 29400–29406.

Liu, X., Shen, S., Wu, P., Li, F., Liu, X., Wang, C., Gong, Q., Wu, J., Yao, X., Zhang, H., et al. (2019). Structural insights into dimethylation of 12S rRNA by TFB1M: indispensable role in translation of mitochondrial genes and mitochondrial function. Nucleic Acids Res. *47*, 7648–7665.

Mai, N. (2016). The role of MRPL45 and OXA1L in human mitochondrial protein synthesis.

Mai, N., Chrzanowska-Lightowlers, Z.M.A., and Lightowlers, R.N. (2017). The process of mammalian mitochondrial protein synthesis. Cell Tissue Res. *367*, 5–20.

Maiti, P., Kim, H.J., Tu, Y.T., and Barrientos, A. (2018). Human GTPBP10 is required for

mitoribosome maturation. Nucleic Acids Res. *46*, 11423–11437.

Maiti, P., Antonicka, H., Gingras, A., Shoubridge, E., and Barrientos, A. (2020). Human GTPBP5 (MTG2) fuels mitoribosome large subunit maturation by facilitating 16S rRNA methylation. Nucleic Acids Res. *5*, 1–20.

Mears, J.A., Cannone, J.J., Stagg, S.M., Gutell, R.R., Agrawal, R.K., and Harvey, S.C. (2002). Modeling a minimal ribosome based on comparative sequence analysis. J. Mol. Biol. *321*, 215–234.

Menezes, M.J., Guo, Y., Zhang, J., Riley, L.G., Cooper, S.T., Thorburn, D.R., Li, J., Dong, D., Li, Z., Glessner, J., et al. (2015). Mutation in mitochondrial ribosomal protein S7 (MRPS7) causes congenital sensorineural deafness, progressive hepatic and renal failure and lactic acidemia. Hum. Mol. Genet. *24*, 2297–2307.

Metodiev, M.D., Spåhr, H., Loguercio Polosa, P., Meharg, C., Becker, C., Altmueller, J., Habermann, B., Larsson, N.G., and Ruzzenente, B. (2014). NSUN4 Is a Dual Function Mitochondrial Protein Required for Both Methylation of 12S rRNA and Coordination of Mitoribosomal Assembly. PLoS Genet. *10*, 1–11.

Mick, D.U., Dennerlein, S., Wiese, H., Reinhold, R., Pacheu-Grau, D., Lorenzi, I., Sasarman, F., Weraarpachai, W., Shoubridge, E.A., Warscheid, B., et al. (2012). MITRAC links mitochondrial protein translocation to respiratory-chain assembly and translational regulation. Cell *151*, 1528–1541.

Miller, C., Saada, A., Shaul, N., Shabtai, N., Ben-Shalom, E., Shaag, A., Hershkovitz, E., and Elpeleg, O. (2004). Defective mitochondrial translation caused by a ribosomal protein (MRPS16) mutation. Ann. Neurol. *56*, 734–738.

Minczuk, M., He, J., Duch, A.M., Ettema, T.J., Chlebowski, A., Dzionek, K., Nijtmans, L.G.J., Huynen, M.A., and Holt, I.J. (2011). TEFM (c17orf42) is necessary for transcription of human mtDNA. Nucleic Acids Res. *39*, 4284–4299.

Montoya, J., Ojala, D., and Attardi, G. (1981). Distinctive features of the 5′-terminal sequences of the human mitochondrial mRNAs. Nature *290*, 465–470.

Nagaike, T., Suzuki, T., Tomari, Y., Takemoto-Hori, C., Negayama, F., Watanabe, K., and Ueda, T. (2001). Identification and Characterization of Mammalian Mitochondrial tRNA nucleotidyltransferases. J. Biol. Chem. *276*, 40041–40049.

Nagaike, T., Suzuki, T., Katoh, T., and Ueda, T. (2005). Human mitochondrial mRNAs are stabilized with polyadenylation regulated by mitochondria-specific poly(A) polymerase and polynucleotide phosphorylase. J. Biol. Chem. *280*, 19721–19727.

Ni, X., Davis, J.H., Jain, N., Razi, A., Benlekbir, S., McArthur, A.G., Rubinstein, J.L., Britton, R.A., Williamson, J.R., and Ortega, J. (2016). YphC and YsxC GTPases assist the maturation of the central protuberance, GTPase associated region and functional core of the 50S ribosomal subunit. Nucleic Acids Res.

Nicholson, D.W., and McMurray, W.C. (1986). Triton solubilization of proteins from pig liver mitochondrial membranes. Biochim. Biophys. Acta - Biomembr. *856*, 515–525.

Nierhaus, K.H., and Dohme, F. (1979). Total Reconstitution of 50 S Subunits from Escherichia Coli Ribosomes. Methods Enzymol. *59*, 443–449.

Nikulin, A., Eliseikina, I., Tishchenko, S., Nevskaya, N., Davydova, N., Platonova, O., Piendl, W., Selmer, M., Liljas, A., Drygin, D., et al. (2003). Structure of the L1 protuberance in the ribosome. Nat. Struct. Biol. *10*, 104–108.

Noah, J.W., and Wollenzien, P. (1998). Dependence of the 16S rRNA decoding region structure on Mg2+, subunit association, and temperature. Biochemistry *37*, 15442–15448.

Nolden, M., Ehses, S., Koppen, M., Bernacchia, A., Rugarli, E.I., and Langer, T. (2005). The m-AAA protease defective in hereditary spastic paraplegia controls ribosome assembly in mitochondria. Cell *123*, 277–289.

Di Nottia, M., Marchese, M., Verrigni, D., Mutti, C.D., Torraco, A., Oliva, R., Fernandez-Vizarra, E., Morani, F., Trani, G., Rizza, T., et al. (2020). A homozygous MRPL24 mutation causes a complex movement disorder and affects the mitoribosome assembly. Neurobiol. Dis. *141*, 104880.

Nouws, J., Goswami, A. V., Bestwick, M., McCann, B.J., Surovtseva, Y. V., and Shadel, G.S. (2016). Mitochondrial ribosomal protein L12 Is required for POLRMT stability and exists as two forms generated by alternative proteolysis during import. J. Biol. Chem. *291*, 989–997.

O'Brien, T.W. (1971). The General in Mammalian Occurrence of 55 S Ribosomes Liver Mitochondria. J. Biol. Chem. *246*, 3409–3417.

O'Brien, T.W. (2003). Properties of Human Mitochondrial Ribosomes. IUBMB Life *55*, 505–513.

O'Brien, T.W., and Kalf, G.F. (1967). Ribosomes from Rat Liver Mitochondria II. Partial Characterization. J. Biol. Chem. *242*, 2180–2185.

Ojala, D., Montoya, J., and Attardi, G. (1981). tRNA punctuation model of RNA processing in human mitochondria. Nature *290*, 470–474.

Ott, M., Amunts, A., and Brown, A. (2016). Organization and Regulation of Mitochondrial Protein Synthesis. Annu. Rev. Biochem. *85*, 77–101.

Paschen, S.A., Waizenegger, T., Stan, T., Preuss, M., Cyrklaff, M., Hell, K., Rapaport, D., and Neupert, W. (2003). Evolutionary conservation of biogenesis of. *426*, 862–866.

Pearce, S.F., Rebelo-Guiomar, P., D'Souza, A.R., Powell, C.A., Van Haute, L., and Minczuk, M. (2017). Regulation of Mammalian Mitochondrial Gene Expression: Recent Advances. Trends Biochem. Sci. *42*, 625–639.

Petrov, A.S., Wood, E.C., Bernier, C.R., Norris, A.M., Brown, A., and Amunts, A. (2019). Structural patching fosters divergence of mitochondrial ribosomes. Mol. Biol. Evol. *36*, 207–219.

Pfeffer, S., Woellhaf, M.W., Herrmann, J.M., and Förster, F. (2015). Organization of the mitochondrial translation machinery studied in situ by cryoelectron tomography. Nat. Commun. *6*.

Pfisterer, J., and Buetow, D.E. (1981). In vitro reconstruction of the mitochondrial translation system of yeast. Proc. Natl. Acad. Sci. U. S. A. *78*, 4917–4921.

Phillips, L.A., Hotham-Iglewski, B., and Franklin, R.M. (1969). Polyribosomes of Escherichia coli. I. Effects of monovalent cations on the distribution of polysomes, ribosomes and ribosomal subunits. J. Mol. Biol. *40*, 279–288.

Popow, J., Alleaume, A.M., Curk, T., Schwarzl, T., Sauer, S., and Hentze, M.W. (2015). FASTKD2 is an RNA-binding protein required for mitochondrial RNA processing and translation. Rna *21*, 1873–1884.

Powell, C.A., and Minczuk, M. (2020). TRMT2B is responsible for both tRNA and rRNA m5U-methylation in human mitochondria. RNA Biol. *17*, 451–462.

Pulman, J., Ruzzenente, B., Bianchi, L., Rio, M., Boddaert, N., Munnich, A., Rötig, A., and Metodiev, M.D. (2019). Mutations in the MRPS28 gene encoding the small mitoribosomal subunit protein bS1m in a patient with intrauterine growth retardation, craniofacial dysmorphism and multisystemic involvement. Hum. Mol. Genet. *28*, 1445–1462.

Rackham, O., Busch, J.D., Matic, S., Siira, S.J., Kuznetsova, I., Atanassov, I., Ermer, J.A., Shearwood, A.M.J., Richman, T.R., Stewart, J.B., et al. (2016). Hierarchical RNA Processing Is Required for Mitochondrial Ribosome Assembly. Cell Rep. *16*, 1874–1890.

Ramachandran, A., Basu, U., Sultana, S., Nandakumar, D., and Patel, S.S. (2017). Human mitochondrial transcription factors TFAM and TFB2M work synergistically in promoter melting during transcription initiation. Nucleic Acids Res. *45*, 861–874.

Ran, F.A., Hsu, P.D., Wright, J., Agarwala, V., Scott, D.A., and Zhang, F. (2013). Genome engineering using the CRISPR-Cas9 system. Nat. Protoc. *8*, 2281–2308.

Rehling, P., Model, K., Brandner, K., Kovermann, P., Sickmann, A., Meyer, H.E., Kühlbrandt, W., Wagner, R., Truscott, K.N., and Pfanner, N. (2003). Protein insertion into the mitochondrial inner membrane by a twin-pore translocase. Science *299*, 1747–1751.

Rehm, H., and Letzel, T. (2016). Der Experimentator: Proteinbiochemie/Proteomics (Berlin, Heidelberg: Springer Berlin Heidelberg).

Reyes, A., Favia, P., Vidoni, S., Petruzzella, V., and Zeviani, M. (2020). RCC1L (WBSCR16) isoforms coordinate mitochondrial ribosome assembly through their interaction with GTPases. PLOS Genet. *16*, e1008923.

Richter-Dennerlein, R., Dennerlein, S., and Rehling, P. (2015). Integrating mitochondrial translation into the cellular context. Nat. Rev. Mol. Cell Biol. *16*, 586–592.

Richter-Dennerlein, R., Oeljeklaus, S., Lorenzi, I., Ronsör, C., Bareth, B., Schendzielorz, A.B., Wang, C., Warscheid, B., Rehling, P., and Dennerlein, S. (2016). Mitochondrial Protein Synthesis Adapts to Influx of Nuclear-Encoded Protein. Cell *167*, 471-483.e10.

Richter, R. (2010). The functions of ICT1 and mtRbfA in the human mitochondrial ribosome. Newcastle University.

Richter, R., Rorbach, J., Pajak, A., Smith, P.M., Wessels, H.J., Huynen, M.A., Smeitink, J.A., Lightowlers, R.N., and Chrzanowska-Lightowlers, Z.M. (2010). A functional peptidyl-tRNA hydrolase, ICT1, has been recruited into the human mitochondrial ribosome. EMBO J. *29*, 1116–1125.

Richter, U., Lahtinen, T., Marttinen, P., Myöhänen, M., Greco, D., Cannino, G., Jacobs, H.T., Lietzén, N., Nyman, T.A., and Battersby, B.J. (2013). A mitochondrial ribosomal and RNA decay pathway blocks cell proliferation. Curr. Biol. *23*, 535–541.

Rodnina, M. V., and Wintermeyer, W. (1995). GTP consumption of elongation factor Tu during translation of heteropolymeric mRNAs. Proc. Natl. Acad. Sci. U. S. A. *92*, 1945–1949.

Rorbach, J., Richter, R., Wessels, H.J., Wydro, M., Pekalski, M., Farhoud, M., Kühl, I., Gaisne, M., Bonnefoy, N., Smeitink, J.A., et al. (2008). The human mitochondrial ribosome recycling factor is essential for cell viability. Nucleic Acids Res. *36*, 5787–5799.

Rorbach, J., Gammage, P.A., and Minczuk, M. (2012). C7orf30 is necessary for biogenesis of the large subunit of the mitochondrial ribosome. Nucleic Acids Res. *40*, 4097–4109.

Rorbach, J., Boesch, P., Gammage, P.A., Nicholls, T.J.J., Pearce, S.F., Patel, D., Hauser, A., Perocchi, F., and Minczuk, M. (2014). MRM2 and MRM3 are involved in biogenesis of the large subunit of the mitochondrial ribosome. Mol. Biol. Cell *25*, 2542–2555.

Rorbach, J., Gao, F., Powell, C.A., D'Souza, A., Lightowlers, R.N., Minczuk, M., and Chrzanowska-Lightowlers, Z.M. (2016). Human mitochondrial ribosomes can switch their structural RNA composition. Proc. Natl. Acad. Sci. U. S. A. *113*, 12198–12201.

Rowland, A.A., and Voeltz, G.K. (2012). Endoplasmic reticulum–mitochondria contacts: function of the junction. Nat. Rev. Mol. Cell Biol. *13*, 607–615.

Rozanska, A., Richter-Dennerlein, R., Rorbach, J., Gao, F., Lewis, R.J., Chrzanowska-Lightowlers, Z.M., and Lightowlers, R.N. (2017). The human RNA-binding protein RBFA promotes the maturation of the mitochondrial ribosome. Biochem. J. *474*, 2145–2158.

Ruzzenente, B., Metodiev, M.D., Wredenberg, A., Bratic, A., Park, C.B., Cámara, Y., Milenkovic, D., Zickermann, V., Wibom, R., Hultenby, K., et al. (2012). LRPPRC is necessary for polyadenylation and coordination of translation of mitochondrial mRNAs. EMBO J. *31*, 443–456.

Saada, A., Shaag, A., Arnon, S., Dolfin, T., Miller, C., Fuchs-Telem, D., Lombes, A., and Elpeleg, O. (2007). Antenatal mitochondrial disease caused by mitochondrial ribosomal protein (MRPS22) mutation. J. Med. Genet. *44*, 784–786.

Saraste, M. (1999). Oxidative phosphorylation at the fin de siecle. Science (80-.). *283*, 1488–1493.

Sasarman, F., Brunel-Guitton, C., Antonicka, H., Wai, T., and Shoubridge, E.A. (2010). LRPPRC and SLIRP Interact in a Ribonucleoprotein Complex That Regulates Posttranscriptional Gene Expression in Mitochondria. Mol. Biol. Cell *21*, 1315–1323.

Schägger, H. (2006). Tricine-SDS-PAGE. Nat. Protoc. *1*, 16–22.

Schulte, L. (2018). New Computational Tools for Sample Purification and Early-Stage Data Processing in High-Resolution Cryo-Electron Microscopy.

Schulz, C., Schendzielorz, A., and Rehling, P. (2015). Unlocking the presequence import pathway. Trends Cell Biol. *25*, 265–275.

Schweet, R., and Heintz, R. (1966). Protein Synthesis. Annu. Rev. Biochem. *35*, 723–758.

Seidel-Rogol, B.L., McCulloch, V., and Shadel, G.S. (2003). Human mitochondrial transcription factor B1 methylates ribosomal RNA at a conserved stem-loop. Nat. Genet. *33*, 23–24.

Serre, V., Rozanska, A., Beinat, M., Chretien, D., Boddaert, N., Munnich, A., Rötig, A., and Chrzanowska-Lightowlers, Z.M. (2013). Mutations in mitochondrial ribosomal protein MRPL12 leads to growth retardation, neurological deterioration and mitochondrial translation deficiency. Biochim. Biophys. Acta - Mol. Basis Dis. *1832*, 1304–1312.

Shadel, G.S., and Horvath, T.L. (2015). Mitochondrial ROS Signaling in Organismal Homeostasis. Cell *163*, 560–569.

Shajani, Z., Sykes, M.T., and Williamson, J.R. (2011). Assembly of bacterial ribosomes. Annu. Rev. Biochem. *80*, 501–526.

Sharma, M.R., Koc, E.C., Datta, P.P., Booth, T.M., Spremulli, L.L., and Agrawal, R.K. (2003). Structure of the mammalian mitochondrial ribosome reveals an expanded functional role for its component proteins. Cell *115*, 97–108.

De Silva, D., Tu, Y.T., Amunts, A., Fontanesi, F., and Barrientos, A. (2015). Mitochondrial ribosome assembly in health and disease. Cell Cycle *14*, 2226–2250.

Van Der Sluis, E.O., Bauerschmitt, H., Becker, T., Mielke, T., Frauenfeld, J., Berninghausen, O., Neupert, W., Herrmann, J.M., and Beckmann, R. (2015). Parallel structural evolution of mitochondrial ribosomes and OXPHOS complexes. Genome Biol. Evol. *7*, 1235–1251.

Smits, P., Saada, A., Wortmann, S.B., Heister, A.J., Brink, M., Pfundt, R., Miller, C., Haas, D., Hantschmann, R., Rodenburg, R.J.T., et al. (2011). Mutation in mitochondrial ribosomal protein MRPS22 leads to Cornelia de Lange-like phenotype, brain abnormalities and hypertrophic cardiomyopathy. Eur. J. Hum. Genet. *19*, 394–399.

Soleimanpour-Lichaei, H.R., Kühl, I., Gaisne, M., Passos, J.F., Wydro, M., Rorbach, J., Temperley, R., Bonnefoy, N., Tate, W., Lightowlers, R., et al. (2007). mtRF1a Is a Human Mitochondrial Translation Release Factor Decoding the Major Termination Codons UAA and UAG. Mol. Cell *27*, 745–757.

Spitnik-Elson, P., and Atsmon, A. (1969). Detachment of ribosomal proteins by salt. I. Effect of conditions on the amount of protein detached. J. Mol. Biol. *45*, 113–124.

Spremulli, L.L. (2007). Large-Scale Isolation of Mitochondrial Ribosomes From Mammalian Tissues. In Mitochondria Practical Protocols, pp. 265–276.

Stepanenko, A.A., and Dmitrenko, V. V. (2015). HEK293 in cell biology and cancer research: Phenotype, karyotype, tumorigenicity, and stress-induced genome-phenotype evolution. Gene *569*, 182–190.

Stepanenko, A., Andreieva, S., Korets, K., Mykytenko, D., Huleyuk, N., Vassetzky, Y., and Kavsan, V. (2015). Step-wise and punctuated genome evolution drive phenotype changes of tumor cells. Mutat. Res. *771*, 56–69.

Stiller, S.B., Höpker, J., Oeljeklaus, S., Schütze, C., Schrempp, S.G., Vent-Schmidt, J., Horvath, S.E., Frazier, A.E., Gebert, N., Van Der Laan, M., et al. (2016). Mitochondrial OXA Translocase Plays a Major Role in Biogenesis of Inner-Membrane Proteins. Cell Metab. *23*, 901–908.

Strauss, M., Hofhaus, G., Schröder, R.R., and Kühlbrandt, W. (2008). Dimer ribbons of ATP synthase shape the inner mitochondrial membrane. EMBO J. *27*, 1154–1160.

Summer, S., Smirnova, A., Gabriele, A., Toth, U., Fasemore, A.M., Förstner, K.U., Kuhn, L., Chicher, J., Hammann, P., Mitulović, G., et al. (2020). YBEY is an essential biogenesis factor for mitochondrial ribosomes. Nucleic Acids Res. 1–25.

Surovtseva, Y. V., Shutt, T.E., Cotney, J., Cimen, H., Chen, S.Y., Koc, E.C., and Shadel, G.S. (2011). Mitochondrial ribosomal protein L12 selectively associates with human mitochondrial RNA polymerase to activate transcription. Proc. Natl. Acad. Sci. U. S. A. *108*, 17921–17926.

Suzuki, T., and Suzuki, T. (2014). A complete landscape of post-transcriptional modifications in mammalian mitochondrial tRNAs. Nucleic Acids Res. *42*, 7346–7357.

Suzuki, T., Nagao, A., and Suzuki, T. (2011). Human mitochondrial trnas: Biogenesis, function, structural aspects, and diseases. Annu. Rev. Genet. *45*, 299–329.

Szczepanowska, K., Maiti, P., Kukat, A., Hofsetz, E., Nolte, H., Senft, K., Becker, C., Ruzzenente, B., Hornig-Do, H., Wibom, R., et al. (2016). CLPP coordinates mitoribosomal assembly through the regulation of ERAL 1 levels . EMBO J. *35*, 2566–2583.

Temperley, R., Richter, R., Dennerlein, S., Lightowlers, R.N., and Chrzanowska-Lightowlers, Z.M. (2010a). Hungry codons promote frameshifting in human mitochondrial ribosomes. Science (80-.). *327*, 301.

Temperley, R.J., Wydro, M., Lightowlers, R.N., and Chrzanowska-Lightowlers, Z.M. (2010b). Human mitochondrial mRNAs-like members of all families, similar but different. Biochim. Biophys. Acta - Bioenerg. *1797*, 1081–1085.

Terzioglu, M., Ruzzenente, B., Harmel, J., Mourier, A., Jemt, E., López, M.D., Kukat, C., Stewart, J.B., Wibom, R., Meharg, C., et al. (2013). MTERF1 Binds mtDNA to prevent transcriptional interference at the light-strand promoter but is dispensable for rRNA gene transcription regulation. Cell Metab. *17*, 618–626.

Tobiasson, V., Gahura, O., Aibara, S., Baradaran, R., and Zíková, A. (2020). Interconnected assembly factors regulate the biogenesis of mitoribosomal large subunit in trypanosomes. BioRxiv 1–32.

Tomecki, R., Dmochowska, A., Gewartowski, K., Dziembowski, A., and Stepien, P.P. (2004). Identification of a novel human nuclear-encoded mitochondrial poly(A) polymerase. Nucleic Acids Res. *32*, 6001–6014.

Traub, P., and Nomura, M. (1968). Structure and function of E. coli ribosomes. V. Reconstitution of functionally active 30S ribosomal particles from RNA and proteins. Proc. Natl. Acad. Sci. U. S. A. *59*, 777–784.

Tsuboi, M., Morita, H., Nozaki, Y., Akama, K., Ueda, T., Ito, K., Nierhaus, K.H., and Takeuchi, N. (2009). EF-G2mt Is an Exclusive Recycling Factor in Mammalian Mitochondrial Protein Synthesis. Mol. Cell *35*, 502–510.

Tu, Y.T., and Barrientos, A. (2015). The Human Mitochondrial DEAD-Box Protein DDX28 Resides in RNA Granules and Functions in Mitoribosome Assembly. Cell Rep. *10*, 854–864.

Tucker, E.J., Hershman, S.G., Köhrer, C., Belcher-Timme, C.A., Patel, J., Goldberger, O.A., Christodoulou, J., Silberstein, J.M., McKenzie, M., Ryan, M.T., et al. (2011). Mutations in MTFMT underlie a human disorder of formylation causing impaired mitochondrial translation. Cell Metab. *14*, 428–434.

Walker, J.E. (2013). The ATP synthase: The understood, the uncertain and the unknown. Biochem. Soc. Trans. *41*, 1–16.

Wang, C., Richter-Dennerlein, R., Pacheu-Grau, D., Liu, F., Zhu, Y., Dennerlein, S., and Rehling, P. (2020). MITRAC15/COA1 promotes mitochondrial translation in a ND2 ribosome–nascent chain complex. EMBO Rep. *21*, 1–12.

Wang, Z., Cotney, J., and Shadel, G.S. (2007). Human mitochondrial ribosomal protein MRPL12

interacts directly with mitochondrial RNA polymerase to modulate mitochondrial gene expression. J. Biol. Chem. *282*, 12610–12618.

Wasilewski, M., Chojnacka, K., and Chacinska, A. (2017). Protein trafficking at the crossroads to mitochondria. Biochim. Biophys. Acta - Mol. Cell Res. *1864*, 125–137.

Wiedemann, N., and Pfanner, N. (2017). Mitochondrial Machineries for Protein Import and Assembly. Annu. Rev. Biochem. *86*, 685–714.

Winge, D.R. (2012). Sealing the Mitochondrial Respirasome. Mol. Cell. Biol. *32*, 2647–2652.

Wolf, A.R., and Mootha, V.K. (2014). Functional Genomic Analysis of Human Mitochondrial RNA Processing. Cell Rep. *7*, 918–931.

Wredenberg, A., Lagouge, M., Bratic, A., Metodiev, M.D., Spåhr, H., Mourier, A., Freyer, C., Ruzzenente, B., Tain, L., Grönke, S., et al. (2013). MTERF3 Regulates Mitochondrial Ribosome Biogenesis in Invertebrates and Mammals. PLoS Genet. *9*.

Zamir, A., Miskin, R., and Elson, D. (1971). Inactivation and reactivation of ribosomal subunits: Amino acyl-transfer RNA binding activity of the 30 s subunit of Escherichia coli. J. Mol. Biol. *60*, 347–364.

Zeng, R., Smith, E., and Barrientos, A. (2018). Yeast Mitoribosome Large Subunit Assembly Proceeds by Hierarchical Incorporation of Protein Clusters and Modules on the Inner Membrane. Cell Metab. *27*, 645-656.e7.

Zhang, X., Zuo, X., Yang, B., Li, Z., Xue, Y., Zhou, Y., Huang, J., Zhao, X., Zhou, J., Yan, Y., et al. (2014). MicroRNA directly enhances mitochondrial translation during muscle differentiation. Cell *158*, 607–619.

Zody, M.C., Garber, M., Adams, D.J., Sharpe, T., Harrow, J., Lupski, J.R., Nicholson, C., Searle, S.M., Wilming, L., Young, S.K., et al. (2006). DNA sequence of human chromosome 17 and analysis of rearrangement in the human lineage. Nature *440*, 1045–1049.

7. Supplementary
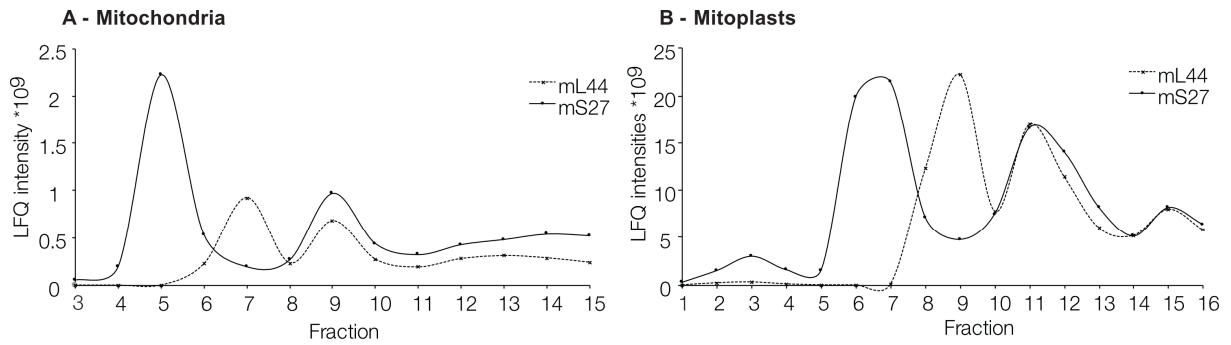
Supp. Figure 1: Localisation of 55S monosome in a 10-30% sucrose gradient (A) and 5-30% sucrose gradient (B). LFQ intensities for two specific mtLSU (mL44) and mtSSU (mS27) proteins were plotted over the gradient fractions.
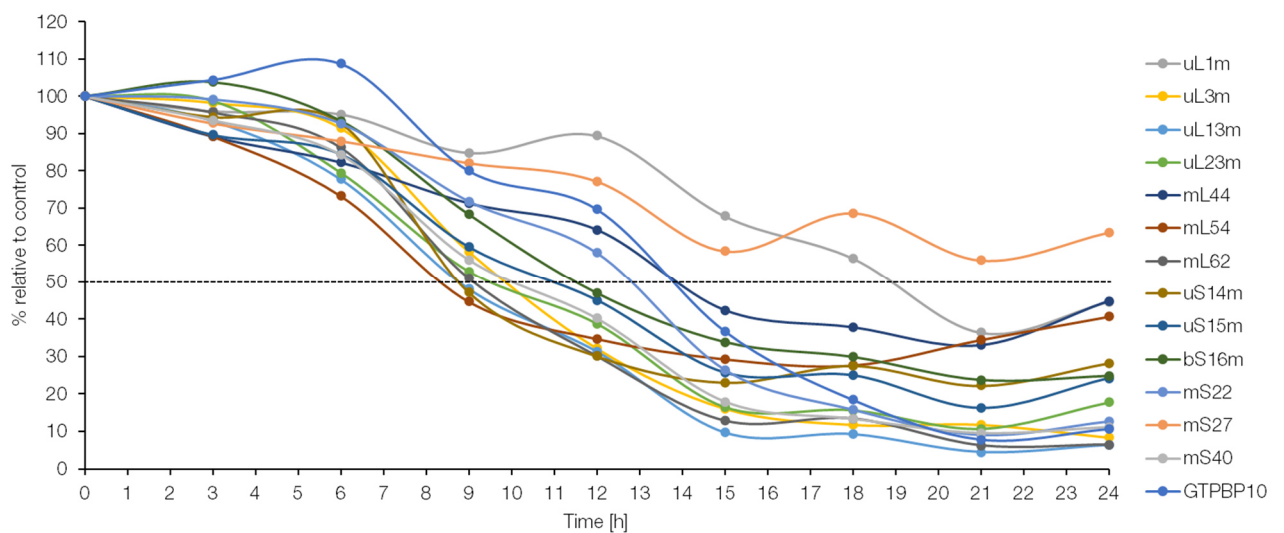
Supp. Figure 2: Quantification of protein levels after actinonin treatment (150 μM). Mean of protein levels of mtLSU, mtSSU and AF relative to control (GAPDH) was plotted over time (n=3).

Supp. Table 1: MS-analysis of fraction 9 from a 10-30% sucrose gradient (lysate of mitochondria was separated). Mitoribosomal proteins are coloured in green, whereas cytosolic ribosomal proteins are visualized in grey.

#	Majority protein IDs	Gene names	LFQ intensity 9
1	V9HW31;P06576;Q0QEN7;H0YH81;F8W079	HEL-S-271;ATP5B	54132000000
2	V9HW26;P25705;K7EK77	HEL-S-123m;ATP5A1	50967000000
3	CON__P00761	N/A	36826000000
4	L0R5A1	CSF2RB	10425000000
5	H6VRG2	KRT1	8061500000
6	Q8TAS0;P36542;B4DL14;B4DFE6	ATP5C1	7871300000
7	Q99623;J3KPX7;F5GY37;B4DW05;F5GWA7;F5H3X6	PHB2	6529100000
8	P05141;Q6NVC0	SLC25A5	6324600000
9	CON__P13645;P13645	KRT10	5343300000
10	A8K401;P35232;Q6FHP5;Q53FV0;Q6PUJ7;C9JW96;C9JZ20;E7ESE2;E9PCW0	PHB;HEL-S-54e	4396700000
11	Q5ST80;Q53HQ0;O75955;Q6IB58;A0A140T9R1;A2VCL5;A0A140T9W4;A2AB10	FLOT1	3869400000
12	A0A024QZ62;Q14254;Q6FG43;E7EMK3;J3QLD9;Q9BTI6;K7EKW9	hCG_1998851;FLOT2	3419200000
13	Q6IBR0;P04843;Q53EP4;B4DL99;B7Z4L4;B4DNJ5	RPN1	3358700000
14	P30049	ATP5D	3309000000
15	Q16891;B9A067;B4DKR1;B4DQY2;B4DT20	IMMT	3133900000
16	A0A0S2Z3L2;P16615;H7C5W9	ATP2A2	2921600000
17	P27824	CANX	2914700000
18	P35527;CON__P35527;K7EQQ3	KRT9	2749700000
19	P35908	KRT2	2687000000
20	P05023;B7Z3V1	ATP1A1	2307200000
21	A0A024RBH2;Q07065;B3KVX6;Q8TB01;Q6NWZ1	CKAP4	2196800000
22	**Q9BZE1;S4R369**	**MRPL37**	**1895300000**
23	A0A024QZ30;P31040;D6RFM5;Q0QF12;B4DYN5;B3KT34;A0A087X1I3	SDHA	1870600000
24	P21796;B3KTS5	VDAC1	1638300000
25	**A8K5D5;P49406;B4DIG4;S4R3W9;A0A0A0MRF4**	**MRPL19**	**1622200000**
26	Q14789	GOLGB1	1566000000
27	**Q96EY7;B2RDU4**	**PTCD3**	**1561800000**
28	Q9NVI7	ATAD3A	1547700000
29	B7Z4V2;V9HW84;P38646;Q8N1C8;B7Z4T3;B7Z1V7	HEL-S-124m;HSPA9	1535200000
30	A0A0A0MR02;A0A024QZT0;P45880;A0A024QZN9;B4DKM5;Q5JSD1	VDAC2	1526500000
31	I3L1P8;Q6IBH0;Q02978	SLC25A11	1483500000
32	A0A0C4DGS1;A0A024RAD5;P39656;U3KQ84	DDOST	1461100000
33	Q9UJZ1;A0A087WYB4;Q6ZNW0;F2Z2I8	STOML2	1436800000
34	Q9P035;H3BS72;H3BPZ1	PTPLAD1	1433200000
35	E5RHW4;O94905	ERLIN2	1382400000
36	Q3MIH3;P62987;M0R2S1;J3QS39;J3QTR3;F5H6Q2;F5GYU3;F5H2Z3;F5H265;Q5UGI3;B4DV12;F5H388;F5H747;F5GXK7;J3QKN0;Q5U5U6;Q5PY61;Q9UFQ0;Q96C32;Q96MH4;L8B4I8;L8B196;Q96H31;L8B4R0;A8K674;L8B4Z6;L8B4M0;L8B4J3;Q66K58;Q59EM9;P0CG47;P0CG48;M0R1V7;Q49A90;M0R1M6	UBA52;UBB;RPS27A;UBC;DKFZp434K0435;UbC	1366600000
37	B2RE46;P04844;B4DJL0	RPN2	1365200000
38	B3KNK9;Q8NBJ4	GOLPH2;GOLM1	1352100000
39	H3BRG4;P22695;H3BSJ9;H3BP04	UQCRC2	1344700000
40	P48047;Q53HH2;H7C0C1	ATP5O	1339200000
41	**E7ESL0;J3KQY1;Q9NWU5**	**MRPL22**	**1335900000**
42	**G5E9W7;G5E9V5;P82650;Q8NBL6;Q59GX8**	**MRPS22**	**1330500000**
43	**Q7Z2W9;A0A024R5G7;B4DXI4;F5H7V8**	**MRPL21**	**1296100000**
44	A0A024R3X4;P10809;B3GQS7;B7Z597;B7Z4F6;B7Z5E7	HSPD1	1283900000
45	**Q9NYK5;C9JG87**	**MRPL39**	**1249800000**
46	**Q9BYD1;E5RJI7**	**MRPL13**	**1249100000**
47	O00461;F8W785	GOLIM4	1234100000
48	Q53HT6;Q53GT2;P51572;C9JSP1;C9JQ75;C9J0M4;C9JMD7	BCAP31	1209300000
49	**P82675**	**MRPS5**	**1154000000**
50	**Q96DV4;B2R894**	**MRPL38**	**1129100000**
51	**Q9NX20**	**MRPL16**	**1120600000**
52	**Q9BYD2;Q5SZR1**	**MRPL9**	**1100900000**
53	E5KNY5;P42704;B4DSR0	LRPPRC	1071000000
54	Q2TB59;A0A024R0C3;Q13423;E9PCX7	NNT	1064500000
55	Q8TBK5;Q8N5Z7;A0A024RBK3;Q9HBB3;Q02878;B2R4K7;B4DRX3	RPL6	1016300000
56	**Q92665**	**MRPS31**	**994780000**
57	A8KA83;Q9P0L0	VAPA	993520000
58	H6VRG0;H6VRF8;H6VRG1;P04264;CON__P04264;H6VRG3;H6VRF9	KRT1	990050000
59	**G5EA06;A0A024RAJ1;Q92552;D6RH20;B4DT94;D6RJC7;Q6PKB3**	**MRPS27**	**970380000**
60	Q96JZ5;A0A024QYS2;Q9HD45;Q8WUB5;Q5TB53	SMBP;TM9SF3	962030000
61	A0A024R6I3;Q53GF9;P49755;G3V2K7;B4DL12	TMED10	943770000
62	**Q9NVS2;Q5QPA5**	**MRPS18A**	**941650000**
63	**H0Y9G6;E7ETU7;B4DKM0;P09001;B4DW56;D6RC14;E9PF06**	**MRPL3**	**935830000**
64	**Q9P015;B2R739;E5RIZ4;E5RHF4**	**MRPL15**	**932280000**
65	**P82933;Q86WV4**	**MRPS9**	**929430000**
66	A4D1N4;C9JRZ6;Q9NX63;B7Z1X9;F8WAR4	CHCHD3	926690000
67	A0A024R663;Q86UP2	KTN1	895450000
68	V9HWB4;P11021	HEL-S-89n;HSPA5	892250000

69	V9HW80;P55072;Q96IF9;Q0IIN5;Q9NTC4	HEL-S-70;VCP;DKFZp434K0126	862650000
70	**Q13084;A2IDC6;A2IDC7;Q4TT37**	**MRPL28**	**860500000**
71	Q6I9V5;P12236;Q59EI9	SLC25A6	858950000
72	Q71UA6;Q15758;Q59ES3;M0QXM4;B4DE27	SLC1A5	850710000
73	**Q53G19;Q9Y3B7**	**MRPL11**	**814870000**
74	P31930;B4DUL5	UQCRC1	785170000
75	Q53GR7;Q9UJS0;B7Z2E2	SLC25A13	777890000
76	**H0Y6Y8;B1AL05;Q8N983;H0YBU8**	**MRPL43**	**766870000**
77	B2R774;A0A024R2A7;P49257;Q53FS4	LMAN1	763350000
78	**A0A024RD78;Q6P1L8**	**MRPL14**	**752920000**
79	A0A0C4DFM1;A0A024QYR3;Q92544;B4DH88;B4DKC1;B4DYH6	TM9SF4	751230000
80	**Q96A35;X6RJ73**	**MRPL24**	**747810000**
81	**Q9BYC9**	**MRPL20**	**744840000**
82	Q53GK6;Q53G99;Q53G76;Q1KLZ0;P60709;B4E335;Q8WVW5;P63261;B4DVQ0;B4DW52;B4E3A4;I3L3I0;I3L1U9;G5E9R0;E7EVS6;I3L4N8;B3KWQ3;Q6PJ43;B7ZAP6;B3KUD3	PS1TP5BP1;ACTB;ACTG1	736420000
83	P62424;Q9BY74;Q5T8U2;Q5T8U3	RPL7A;RP-L7a	727980000
84	**A0A024R7C5;Q9BYD3;K7ES61;K7ELQ0;X6RAY8**	**MRPL4**	**721410000**
85	Q6IB11;O00264	PGRMC1	721380000
86	A0A024R2Q4;P61313;E7EQV9;E7ENU7;B4DLP4	RPL15	707320000
87	**A0PJ79;Q9BYD6;H0Y8N7**	**MRPL1**	**706410000**
88	Q10471;G3V1S6;B7Z6K2;B7Z462	GALNT2	702960000
89	P38606;B7Z2V6	ATP6V1A	702790000
90	**Q8N5N7**	**MRPL50**	**691680000**
91	Q6IAA8;F5GX19;F5H3Y3;H0YFI1;F5H479	LAMTOR1	687000000
92	**A0A024R473;Q9H9J2**	**MRPL44**	**677830000**
93	Q96HS1	PGAM5	638020000
94	Q53XM7;O95292;Q6ZSP7;B4DNS4;Q6ZR82	VAPB	635190000
95	B3KTM6;A2RUM7;Q59GX9;P46777;Q5T7N0	RPL5	629410000
96	A0A024R4X0;P00387;B1AHF3;Q6ZVI6	CYB5R3	628550000
97	**P82663;E7EPW2**	**MRPS25**	**617990000**
98	Q0QEW2;H0YHA7;A0A024QZD1;J3QQ67;Q07020;G3V203;F8VUA6;F8VYV2;B4DDY5;A0A075B7A0	RPL18	613730000
99	Q8N766	EMC1	613560000
100	A0A087WXM6;J3QQT2;J3KRX5;A0A024R261;A0A0A6YYL6;P18621;J3KRB3;A0A087WWH0;J3QS96;J3QLC8;A0A0A0MRF8;A0A087WY81	RPL17;hCG_24487	604030000
101	Q59GY2;P36578;B4DMJ6;Q53G74;H3BM89;B4DMJ2;B4DFI6	RPL4	600620000
102	A0A024R3J7;P46977	hCG_2032701;STT3A	599300000
103	**A0A087X2D5;B4DEF8;Q9BRJ2;A0A0G2JMS5;A0A087WU62**	**MRPL45**	**587380000**
104	**Q9BUN6;Q53H77;Q9NP92;Q53GN7**	**MRPS30**	**585220000**
105	G3V3D2;G3V5V8;G3V5H6;G3V2V4;G3V287;G3V4A9;G3V2E1;B3KP74;A8KAE2;Q6FI63;A8K3L6;V9HVY9;Q9P0W8	SPATA7;HEL-S-296	579080000
106	**D6RAN8;Q9P0M9;H7C5U8**	**MRPL27**	**577320000**
107	Q6IPH7;E7EPB3;A0PJ62;B7Z6S8;P50914;A8K3Q9	RPL14	572600000
108	P0DMV9;P0DMV8;A8K5I0;A0A0G2JIW1;Q59EJ3;B4DNT8;B4DI39;B4DWK5;B4DFN9;B4E1S9;B4DVU9;B4E388;V9GZ37;B3KTT5	HEL-S-103;HSPA1A	566320000
109	A0A024R2F9;Q9BTV4;A0A0S2Z5N2;Q8TEP9	TMEM43;FLJ00144	563010000
110	**Q9HD33**	**MRPL47**	**558160000**
111	B2R8G6;A0A024R7P2;Q14318;B7Z6M0;M0R2K9	FKBP8	556100000
112	A0A024QYR8;Q99805;B3KSG9	TM9SF2	548080000
113	A4D1U5;Q53H12;E9PC15;B4E2Z8;E9PG39;B4DR72;A0A0G2JLG5	FLJ10842;AGK	546890000
114	Q6IBH6;P61254;J3QRI7;J3QQQ9;J3QQV1;J3QRC4;J3KTJ8;A0A024RBF6	RPL26;KRBA2;hCG_26523	542050000
115	A0A024R6C9;P36957;Q6IBS5;Q86TQ8;Q86TW7;Q86SW4	DLST	528630000
116	**A0A024R578;Q13405;H0YDP7;Q59GE9**	**MRPL49**	**522400000**
117	**Q5T653;A0A024RD44;C9IY40**	**MRPL2**	**521800000**
118	B4DY23;Q54A51;P35613;B4DNE1;A0A087X2B5;A0A087WUV8;I3L192	hEMMPRIN;BSG	516580000
119	Q9Y6C9;Q53G34;E9PIE4	MTCH2	509260000
120	B4DL07;P28288;B4DZ22	ABCD3	504040000
121	E4W6B6;B2R4D8;A0A024R1V4;P61353;K7ELC7;K7EQQ9	RPL27	501740000
122	D3DUJ0;Q8TA92;Q9Y4W6	AFG3L2	499920000
123	A0A140VK65;P21281;Q59HF3;H0YC04	ATP6V1B2	487970000
124	**B0S7P4;Q9Y676;A0A0G2JIC6**	**MRPS18B**	**487500000**
125	M0R117;B4DM74;Q02543;M0R3D6;B4DM94;M0R1A7;B4DUV3;Q53HD3;B2R4C0;M0R0P7;Q32XH3	RPL18A	477630000
126	**Q8IXM3**	**MRPL41**	**476940000**
127	Q07021;A8K651	C1QBP	476530000
128	Q9NZI8;D3DTW3	IGF2BP1	474390000
129	Q0VAB1;A0A024R0M6;Q3ZCQ8;M0R2F8;M0R0C3;M0R003	TIMM50	466380000
130	P50402;Q5HY57	EMD	465300000
131	K7EJT5;K7EP65;K7EKS7;K7ELC4;K7EMH1;K7ERI7;Q7Z4W8;P35268	RPL22	464260000
132	**B2R9J4;A0A024RCB2;A6NJD9;A8MVT4;A8MYK1;Q16540;H7C2P7**	**MRPL23**	**461580000**
133	C9J3L8;C9J5W0;B2R6N9;E9PAL7;C9IZQ1;P43307	SSR1	457040000
134	Q5VVD0;P62913;Q08ES8;Q5VVC8;Q5VVC9	RPL11	447900000
135	B4E106		444720000
136	P40429;Q9BSQ6;Q5QTS3;Q53H34;M0QYS1;Q8J015;Q0VGL3;B4DNC8	RPL13A;RPL13a	441210000
137	P39023;Q8TBW1;Q96QL0;B3KS36;Q9NY85;G5E9G0;Q49AJ9;Q9BT63;H7C422;B5MCW2;H7C3M2	RPL3;rpl3	437510000
138	O14654	IRS4	432430000

139	A8K5H7;Q96TA2;Q96I63;Q9Y2Q2;Q9NQ51	YME1L1;FTSH	431180000
140	Q9Y512	SAMM50	430600000
141	B2R6K4;A0A024R056;P62873;F6UT28;B1AKQ8	GNB1	423530000
142	O95202;D3DVQ1	LETM1	413770000
143	**Q9Y3D9;J3QLR8**	**MRPS23**	**408370000**
144	B3KQF0;A0A0S2Z5M1;Q9UGP8;B3KNE7	SEC63	400880000
145	E5KRK5;P28331;B4DJ81;Q9P1A0	NDUFS1	397450000
146	H7BY10;K7EJV9;K7ERT8;A8MUS3;P62750;K7EMA7	RPL23A	396450000
147	Q9Y277;E5RJN6;E5RHZ6	VDAC3	396200000
148	Q8IYS2;B2RXJ9	KIAA2013;LOC728138	395050000
149	**A8K9D2;Q9H0U6**	**MRPL18**	**394820000**
150	Q96CS3;B4E2M8	FAF2	393850000
151	E9KL44;P40939;B4DRH6;B4DDZ5	HADHA	393450000
152	P18124;A0A024R814;A8MUD9;O95036	RPL7;WUGSC:H_RG05 4D04.1	392240000
153	Q9H9B4;D6RFI0;D6RDG7;S4R2X2	SFXN1	392110000
154	B3KM97;Q9NZ01;B3KSQ1;M0R3C3	TECR	390660000
155	**Q8TCC3;B8ZZV5**	**MRPL30**	**385070000**
156	Q92896;H3BM42	GLG1	371380000
157	A8KAL2;Q8TBA6;B4E1D4	GOLGA5	369010000
158	**A0A024RDM4;Q9BQC6**	**MRP63;MRPL57**	**368000000**
159	P62917;B4DVG7;E9PKZ0;E9PKU4;G3V1A1	RPL8	366830000
160	V9HW22;P11142;E9PKE3;Q53GZ6;Q96IS6;B3KTV0;Q53HF2;E9PNE6;A8K7Q2	HEL-S-72p;HSPA8	364830000
161	**A0A024R7J4;M0R226;Q9BQ48**	**MRPL34**	**363360000**
162	Q53HW2;A8K4Z4;A0A024RBS2;P05388;Q6NSF2;F8VWS0;Q53HK9;F8VU65;B4E3D5;F8VW21;F8V ZS0;F8VPE8;G3V210	RPLP0	351520000
163	CON__P13647;P13647	KRT5	348290000
164	O75306;B7Z792;Q53HG2	NDUFS2	347910000
165	A0A024RBC7;P20020;E7ERY9;Q59H63	ATP2B1	340680000
166	O94826;B4DZ87	TOMM70A	336400000
167	**S4R360;J3KPP0;A0A024RBG3;S4R2Z7;Q9Y6G3**	**MRPL42**	**335770000**
168	CON__P04259;B4DKV4		328370000
169	A0A024R3R5;Q14739;C9JXK0	LBR	328120000
170	Q14165;F5H1S8	MLEC	327730000
171	**A0A024R8L0;J3QLS3;Q9Y2R9;J3QQS1;J3QKW2;J3KSI8**	**MRPS7**	**326160000**
172	P51571;A6NLM8	SSR4	325270000
173	Q8WVM8;Q53GW1;B7Z738;B7Z5N7	SCFD1	321870000
174	Q5U0I6;P62820;B7Z8M7;E7END7	RAB1A	321650000
175	**A4D1V4;Q9BYC8**	**MRPL32**	**321150000**
176	P54709;D3DNF9	ATP1B3	321020000
177	**Q96EL2**	**MRPS24**	**315010000**
178	O75947	ATP5H	310020000
179	Q5JPE7;J3KN36;P69849;Q1LZN2	NOMO2;NOMO3	308290000
180	Q6LAP8;D9HTE9;P53007;B4DP62	SLC25A1	305360000
181	**F5H702;Q96GC5;F5H8D0**	**MRPL48**	**304390000**
182	Q8NCF7;A0A024RBE8;B2RE88;A0A024RBH9;Q00325;Q53HC3;F8VVM2	SLC25A3	299110000
183	Q53Z07;P32969;D6RAN4;H0Y9V9;E7ESE0;B4E1M5;B4DLV8	RPL9	296460000
184	P42766;F2Z388;A4D2M5;A0A024R866	RPL35;LOC154880	295130000
185	B3KVY9;Q8TB61	SLC35B2	295040000
186	A8K3M3;P18031;B4DSN5	PTPN1	294930000
187	Q6IAX2;P46778;Q59GK9	RPL21	290590000
188	Q8NEW0	SLC30A7	285840000
189	Q53T76;A0A140VJK2;P43304;A8K1Z2	GPD2	284680000
190	CON__P02533;P02533;A0A024R1X6	KRT14	284040000
191	A0A140VK05;Q92667;B4DN86	AKAP1	283990000
192	P05556	ITGB1	280380000
193	D6RFL1	CANX	280310000
194	Q8IXI1;H3BST5;I3L2C6	RHOT2	275990000
195	Q96A33;A0A087WYW6	CCDC47	275860000
196	**Q9NRX2;E9PKV2**	**MRPL17**	**275380000**
197	B4DWN1;A8K7T4;Q12907;D6RBV2;D6RIU4;D6RDX1	LMAN2	273080000
198	Q9H845;Q9H9W4;H0Y8Z9;Q9BUX5	ACAD9	271780000
199	O95831;E9PMA0	AIFM1	269910000
200	A0A0S2Z5V7;Q8TCT9;A0A075B6F6;A0A0S2Z6F0	HM13	269230000
201	B2R6E5;A8K3B4;Q59ED7;P16435;Q63HL4;H0Y4R2;B4DKM8;B4DJI8;E7EMD0;B4DDH3;B4E305	POR;DKFZp686G0423 5	268610000
202	A0A0S2Z3Y1;Q08380;B4DVE1;B4DWA8;B3KP88;B4DDG4;B4DI70	LGALS3BP	267750000
203	D3DR65;O75477;B2RDK6;B4DPN7;B0QZ43	SPFH1;ERLIN1	263850000
204	B3KRY3;A0A024RDY3;P11279	LAMP1	262050000
205	A0A024R7V6;P61019;A0A0A1HAW1;E9PKL7	RAB2;RAB2A	257600000
206	A0A0S2Z2Z3;O75027;B4DGL8;A0A087WW65;B3KM98	ABCB7	255010000
207	A0A158RFU6;P51149;B4DPH9;C9J8S3;C9J4V0;C9J592;C9J4S4	RAB7A	254720000
208	O75381;B7Z4Z4	PEX14	254350000
209	A0A024QYX0;Q15125;C9J719;C9JJ78	EBP	239100000
210	A0A140VJW5;P14868;D3DP78;Q53T60	DARS	238220000
211	Q5U676;O94766;G3V150;B4DNL8	B3GAT3	237860000
212	**J3KS15;Q14197**	**ICT1**	**236350000**

213	P30050;Q59FI9;D3DS95	RPL12;hCG_21173	232820000
214	Q6FGX3;Q53ET8;A0A024R5H8;A0A024R5J5;P20340;F5H3K7	RAB6A	232280000
215	Q14573;Q59ES2;A6H8K3	ITPR3	230930000
216	E9KL35;P63244;J3KPE3;D6RAC2;H0YAF8;H0Y8W2;H0YAM7;D6REE5;D6RHH4;D6R9Z1;D6R9L0	GNB2L1	229080000
217	**Q53FX9;P82912;Q53GJ8;H0YL99**	**MRPS11**	**228640000**
218	Q7Z7H5	TMED4	227890000
219	P55084;B4DY96;F5GZQ3;B5MD38;D6W539;B4DDC9	HADHB	227720000
220	**B4DEH0;Q7Z7H8**	**MRPL10**	**224700000**
221	A0A024RDH8;P49207	RPL34	223510000
222	C9K025;P18077;F8WBS5;F8WB72	RPL35A	223050000
223	E9PN17;O75964	ATP5L	221750000
224	F5GZS6;J3KPF3;P08195;B4E2Z3;A0A024R599	SLC3A2	221530000
225	O75976	CPD	220660000
226	E7EQZ4;Q16637;A0A076L8Z0;B4DP61	SMN1	220080000
227	X5MFE4;Q29840;D5H3U2;D5H3U1;B2R7U3;B1PKY1;A9YWM1;A0A1C3PHG3;A0A0U5KK56;A0A0S4XRD4;A0A0S4XQY1;A0A0S4XQY0;A0A0S4XQR9;A0A0S4XQP0;Q5SRN5;P04439;A0A060VHD0;X5MPH3;A0A060VCY5;X5MFD7;A7MAP4;A0A0S4XRT2;A0A1C3PHA9;A0A0U5Q331;A0A1C3PH98;A0A0S4XQR6;A0A0S4XQM8;A0A0S4XRI6;A0A0S4XRI5;A0A0S4XQV7;X5MBH2;S5CRT1;R9WYX8;M1KE04;I2E8C4;E7BBA1;D1MYY8;C7U1K2;C7E539;C6H0N8;B6VA02;B6ECH6;B6ECH2;A7MAK2;A0A0N9E2I7;A0A0F6SCZ8;D0AB29;A5PHP7;A0A143Y4D5;Q5SRN7;Q861B7;F6IQV7;B4E2X4;A0A0K3AQ92;X5MI21;A0A0D6K972;A0A0D6K9K6;A0A060VCY6;A0A125R6G4;I0J2M4;A1Z1D7;C5IWY0;A0A0S4XR96;A0A0K3ATN2;X5D2K4;A0ZXY8;E1B2D6;G8FQ53;Q4A1H0;L7X986;W6CHX3;B7VBV1;J7SBK9;Q6IVJ9;A0A0D6K9L8;U5YMP4;F6IQV8;F6IQV6;A0A060VG34;A0A060VHC2;Q2A688;A0A0N9HRK5;G5CJS3;B7VCC4;D0W032;A0A1C3L6B0;E1Y422;A0A0N9QHU3;A0A0N9MPC4;Q7YPW4;A7DZQ5;A0A078N1N5;A0A060VD16;A0A0U5PYZ0;A0A0S2IKY1;A0A0D6E067;D6CIB2;A7L858;A5I8L2;A0A0S2C4N3;A0A0U5LBS5;Q5ND69;A0A0D6K9K8;X5MI15;A0A0D6K9L7;Q5MCQ6;A0A0S4XRG0;Q5S3G3;H2DMX5;F4NCR9;D9UB10;D7GM35;D5H3U4;D5H3U3;D0V0C4;C5IWZ2;A0A1C3PHG8;A0A1C3PH91;A0A0U5IHQ3;A0A0S4XQW9;A0A0S4XQU8;A0A0K0TQ18;Q5ZGM8;Q5SUL5;M4QEH4;I3ZN77;C5IWX4;A0A1C3PHC8;A0A0U5Q1Q2;A0A0U5PXM5;A0A0U5PXL2;A0A0U5PXI8;A0A0S4XRW0;A0A0S4XRG6;A0A0S4XR94;A0A0S4XQX0;A0A0S4XQT2;A0A0G2JIF2;P13746;P30455;P30443;B4DVC4;A0A0N9MQ43;B7ZAP7;A0A060VG42;A0A060VCZ1;A0A060VCW6;A0A060VD08;A0A0S2IIT2;D9UB11;A0A0U5PU71;D5H3U6;A0A0U5IHK3;A0A1C3PHH2;Q95HA5;A0A1C3PHF2;A0A1C3PH97;A0A0U5Q0S0;A0A0U5PZ31;A0A0S4XR33;A0A0S4XQX6;Q59GJ2;A0A0G2JL56;V6CKU4;W8NKP1;W6CJ57;W0G8I7;S5U3G8;S0F2B1;R4NJ42;R4KXX0;Q9TQP8;Q6F3E3;Q4W6C0;M9TNT6;M5ETC1;M5A8I6;M4TCH1;J7I2U3;I3VB21;I3TBB8;H2D5G2;G0UE14;G0M6G1;F8T1H2;F8LSY2;F8LSV3;F8LSV2;F2XI31;E3WH33;E1Y7G0;D3YFD2;D1MZT7;D0VFI1;C7C6D3;C7C695;C6H0N6;B6VA01;B3VE19;B2ZRD4;B2DFW7;B1Q4X5;B1Q4X2;A9IW15;A8E0Y3;A5PHT9;A2Q117;A0JHM7;A0A140CTI6;A0A125RL90;A0A0P0HDI3;A0A0N9QNI4;A0A0H3WB50;A0A097PED7;A0A060GTH2;A0A060GQ71;R9UTP9;R7RVB7;R7RV73;L7UVL0;K7SHJ4;H6SSQ0;G8ZKX4;E0WN91;C7U2Z0;C7ENH9;B6ECH3;A7WPI8;A0A078BPG3;A0A078BNH2;Q0E7X7;D9UAY2;D6CIC1;D5LN74;D5H3U5;B1PT16;A0A143Y239;A0A1EAW8;Q0E7X3;A0A0G2JI36;G9FTK2;G0Z6Y6;A0A0D6K959;A0A0D6K978;B7VF83;U5YMQ3;U5YMP9;U5YML8;U5YKF9;U5YKC8;U5YJQ0;U5YJP8;U5YJK1;U5YJJ6;F6IQZ1;F6IQZ0;F6IQY5;F6IQY1;F6IQY0;F6IQX7;F6IQX6;F6IQX4;F6IQX3;F6IQX2;F6IQX1;F6IQX0;F6IQW9;F6IQW8;F6IQW6;F6IQW5;F6IQW4;F6IQW0;F6IQV9;A0A076JXB7;A0A076JS26;Q95IG4;F6IQS9;F6IQR9;A0A090KKK5;A0A060VCX2;A0A090KKC3;L8B936;A0A142J2B1;A0A173ADK6;X5LKD6;Q2A689;A0A1C3PHF4;A0A0U5Q074;D9UB05;A0A0F7NGH0;Q2LC93;A0A0S4XRV2;I4EPX9;P16188;V9N3G0;V9N2X1;V9N2U2;U5IQK9;S4TZI2;S4TZE1;R9R080;R4QGE9;R4I501;R4I3H2;Q9MYA8;Q9GJM2;Q95IY8;Q8HWS5;Q6UJZ9;Q5XLD1;Q5JZM7;Q5FYV2;Q2WBP4;Q1M2R8;O78081;M9PNR0;M9PAA7;M9PAA4;M9P8Z4;M9P8Q7;M4N7U4;M4N6L9;M4N6H6;M1SQT4;M1FYE6;M1FYE3;M1FWW6;M1FUQ9;M1F5P2;M1F4C0;L7PHV2;L7PHU7;L7PH13;L7PH07;L7PEX4;L7PEW5;L0BVP5;K9LDJ0;K9LCM8;K9LC07;K9LC01;K9L7Y8;K7WPD7;K7P600;K7P5W6;K7P5V7;K7P5U2;K7P5E0;K7P5B6;K7P562;K7P558;J9UP83;J9TNR8;J9PWV5;J9PWL3;J7GM07;J7FNZ2;J7F8L2;J7F4Y9;I6SJ64;I6RGW8;I6RGW0;I6QU16;I6NS25;I6NS19;I3UI58;I3UI55;I3UI47;I3QHQ4;I2B305;I2B2Z9;I1W1L8;H9BQ78;H6UV72;H6UV69;H6UV68;H6UV64;H2DML9;H2EBE80;H2BDP5;G9I2J6;G9HW64;G9HW24;G9HRL1;G3DR81;G1EPH8;G1EPG4;G1EPD3;G1EPB3;G1EPB1;G1EP98;G1EP96;G1EP95;G1EP93;G1EP88;G1EP78;G1EP71;G1EP55;G1EP53;G1EP50;G1EP19;G1EP18;G1EP05;G1ENY5;G0ZMG9;G0ZMG4;G0ZMG3;G0ZMF4;G0ZDS9;G0WVA6;G0WVA0;F8RHD6;F8RHD1;F8RHC4;F8RHC3;F8RHC2;F8RHB9;F8R8I1;F8R119;F8R116;F8R115;F8R110;F8R103;F6KRP1;F6KRM4;F6KRL8;F6KRK7;F4YU26;F4YU20;F2X609;F2X604;F2X5Y9;F2X5Y4;F2X5Y0;F2X5X9;F2VP64;F2VP60;F2VP51;F2VNJ4;F2VNJ2;F2VNJ1;F2VNH3;F2VNH2;F2VNH0;F2VNG0;F2VNF7;F2VNF2;F2VNE0;F2VND5;F2VND0;F2VNC4;E9LY14;E9LY02;E9LY00;E8ZF52;E7BY93;E7BY85;E5DCM4;E5DCM2;E5DCM1;E5DCM0;E3SWG4;E3SG86;E3SG82;E2DH82;E2DH80;E2DH75;E2DH72;E2D5M3;E2D5L9;E2D5L6;E2D5K9;E0YTI8;E0YTI1;E0YTG4;E0YTG3;E0X9K3;E0X9K2;E0WBY8;E0WBY5;E0WBX4;E0WBX1;E0WBW7;D9IFQ7;D7NSP9;D7NSP0;D7NSN9;D7NPL2;D7NPA6;D7NPA3;D7NP98;D7NP92;D7NP85;D7NNU1;D7NNT9;D7NNT6;D7NNT3;D7NNS2;D7NNR5;D7NNP4;D7NNN7;D7NNM6;D6MLN9;D6MLN8;D6MLN3;D6MLM4;D6MLL1;D6MLK2;D6MLJ4;D6MLJ1;D6MLI3;D6MLI63;D6ML56;D6ML55;D6ML54;D6ML46;D6ML44;D6ML42;D6ML40;D6ML35;D6ML33;D6ML18;D6ML17;D6ML16;D6ML10;D6ML09;D6ML06;D6ML01;D6MKY9;D6MJF7;D5M8G4;D5M8G1;D5M8E9;D5M8E4;D5L9A3;D5G2J2;D5FZI6;D5FIG9;D5FIG8;D5FHQ9;D5FHN7;D5FHM5;D5FHM3;D5FHK5;D5FHG0;D5FHF9;D3U484;D3U454;D3U442;D3JT97;D2SSL9;D0RAY3;D0EZK0;D0EZJ9;C9WEL9;C9WEL6;C9WEL3;C9WEL2;C9WEL1;C9E1E8;C9E1E7;C8XTP8;C8XTP7;C8XTP2;C8XTN9;C8XTN8;C8XTN7;C8CH66;C7E580;C6K4J6;C6K4I6;C6K4I1;C6K4H8;C6K4H3;C6K4H0;C6K4G4;C6K4G0;C6K4F7;C6K4E3;C5J029;C5J027;C5IZR4;C5IZQ6;C5IZQ3;C4PFZ1;C4PFY9;C0M144;B8YCR7;B1PQ33;A7E1C1;A4USG8;A3RKJ9;A2VBX5;A0A1C3MVU6;A0A141AZ45;A0A140FAH7;A0A120GW98;A0A109VDQ9;A0A109V340;A0A109NRD9;A0A109NR90;A0A0X7YV65;A0A0X7YKZ5;A0A0X7YKV3;A0A0X7YJN3;A0A0X7YJM6;A0A0N7A621;A0A0N7A4M1;A0A0M3STX8;A0A0K0KRW3;A0A0K0KRU1;A0A0K0KR22;A0A0K0KR17;A0A0G2R1G8;A0A0G2R0Y0;A0A0G2R0U8;A0A0G2R0R4;A0A0E3DD69;A0A0E3DD27;A0A0E3DD21;A0A0E3DC02;A0A0D4CZE3;A0A0A7C8N8;A0A0A7C8C9;A0A0A7C890;A0A0A7C876;A0A0A7C7S7;A0A0A7C730;A0A0A7C533;A0A0A7C516;A0A0A7C4K5;A0A0A7C4I1;A0A0A7C4H1;A0A0A7C421;A0A0A7C3Y0;A0A0A7C3W4;A0A0A7C3V6;A0A0A7C3V2;A0A0A7C3Q5;F4NC94;Q3BK35;B4DVB9;F2XI28;E0WMN2;A0A078BBY8;W6SIV4;G4V593;V5L1W2;F2XI30;A0A110BIQ6;A0A076L0P9;I0DFI9;S0F2I4;J7JHS1;E0WN90;X4YT82;U6BZQ8;M9T819;I0DHJ2;C0MP56;A0A142J2I0;W8SKC0;H6SSQ1;B2DFW8;R4NLT9;L7Y4K8;I7B4Y2;C9E9Y0;A0A0K2GVF7;T2MJM6;E0WN84;E0WMN1;D0RB02;M5EE32;A9QUT7;A1KWT0;A0A0D6K9D3;I2GAD6;F6IQX5;U5YKF4;U5YMI0;U5YMM6;F6IQY4;F6IQY8;F6IQW7;F6IQY9;U5YMI4;U5YME5;F6IQW3;F6IQW2;F6IQW1;L8B932;I3ZN78;C5IWZ0;C5IWY9;Q95J07;E3UN97;B6ETN7;B2MVI0;A0A1B1LKE5;A0A0U5PXQ4;A0A0S4XQY3;A0A0S4XQM2;A0A0S4XRL3;P30459;F2VYI1;D6MKY7;A8DA04;M4YQG8;M4SNZ1;M1FXT8;K0A058;I6NWN3;I6M537;H9C5F8;G1EPG0;G1ENC7;F8R8I0;F8R107;F6KRJ5;E2GJD4;E2GJD3;E0YTJ0;D7NNS8;D6MLK6;D6ML50;D6ML04;D5FZV4;D5FIG2;C9E846;C8CH74;C6K4H6;C	HLA-A;HLA;HLA-A*01;HLA-B;HLA-DQB1	218270000

	5IZR2;A0A186VNF4;A0A120GWA1;A0A0G2R1L2;R9QZR4;Q6V117;Q45FD6;Q05G01;M9WP47;M9P8G3;L7PH16;K7P5R4;K7P560;H9C5F6;H6V073;F2VNJ6;F1AQL5;E3SWG7;D7NP83;D7NNR3;C6K4H4;B8Y1X8;A0A1C3MVT8;A0A141AZ64;A0A0X7YKU5;A0A0X7YIV2;A0A0K0KR91;A0A0G2R0R0;A0A0E3DD29;A0A0A7C820;A0A0A7C729;Q000J8;K9LC23;I6QU03;D7NPL4;D5FHR2;Q9TQG6;Q9TQ28;Q9TQ26;Q9TPV5;Q9TPS9;I3QHR2;H8XVX1;H6V077;G1EPH5;F6KRP7;D6ML07;D2DKV2;C9E848;C6K4E4;B1PL02;A0A0G2R0V1;A0A0E3DD74;Q9TQF3;Q9TQF2;G1EP75;F8RHD8;F8R126;F2VNF1;E5D6K2;E3SWG9;D7NQU0;D6MLP4;D6MLN5;D6ML13;D5FHK0;D5FHH3;C7C5G4;C0M140;B8Y6A7;B5ATU8;B5ATU6;A0A109VDK6;A0A0X7YR78;A0A0N7A477;A0A0A7C5G0;Q208P6;Q1G4P0;I6QU20;I3UI62;H2BE91;G1ENE6;G0X8R3;F2VNJ3;F2VNI6;E5G0Y5;D7NSP6;D7NNS3;D7NNN5;D7NNN1;D7NNN0;D7NNM8;D7NNM7;D7NNM2;D6MLH8;D6MLH5;D6MLH3;D6MLH2;D6MLH1;D5L999;D2JZZ8;D1MEQ1;A7E1B9;A5Z1D4;A0A186VN36;A0A0E3DD51;A0A0A7C830;A7M780;T2ET92;T1WE98;S6CRG7;Q45NE1;Q0GE97;J7RE54;I3VB22;E7BBA3;E0WMV3;D5GU49;A0A1C3L6B7;A0A0K2GUM3;A0A078BRA4;A0A076VF41;A0A110BH75;A0A0G3EHK9;E0WN92;I2GUK1;I7A6W0;I3TBB9;G9FTJ8;W1IAW1;E9ABI3;E1Y6M4;R9UR01;Q95IG6;Q1EPW2;Q0GC70;M9TIT3;M4VSN7;G8FV57;D5H3W3;D5H3W2;A5PHT4;A4URF2;N1NV67;M5EF56;H6SFV4;C5J3U2;A0A0N9QHU8;A7MAP2;W6JNQ2;Q6IUZ4;B5A9M9;A0A140T975;Q860B4;A4URH6;Q9GJ45;H6SHQ4;F6IR58;F6IQT0;F6IR40;F6IR39;U5YKD6;F6IQY7;F6IQY6;U5YJM7;F6IQY3;F6IQX9;F6IQX8;U5YMJ8;U5YJL3;F6IR32;F6IR31;X5MI18;A0A061DD14;W0UTP4;Q9GJ43;V6A6U0;Q7YQ33;E3Q1L4;A0A0S4XRX2;X5M4Z2;Q9GJ44;Q5RJ27;B5TZV4;A0A0U5QLK5;A0A0U5PUN7;A0A0S4XRU2;A0A0S4XRJ0;A0A0S4XR13;Q8MGZ1;C9EIW0;S6AP35;P10314		
228	A0A024R0P9;O96008;K7EJ57	TOMM40	214870000
229	B3KNF6;B4DR61;P61619;B3KME8	SEC61A1	214160000
230	E5KLJ7;E5KLM1;E5KLJ5;E5KLK1;E5KLJ9;E5KLL9;O60313;E5KLM2;E5KLJ6;E5KLK2;E5KLK0;E5KLM0	OPA1	212010000
231	A0A140VK11;Q9H078;H0YGM0;Q7Z777	CLPB	211460000
232	Q96AG4	LRRC59	208170000
233	Q8NC51;D3DQ70;Q63HR1;Q5VU21;D3DQ69	SERBP1;DKFZp686P17171	207440000
234	**P82914;B4DYW3;D3DPS9;Q59EA6**	**MRPS15**	**206050000**
235	P47985;P0C7P4	UQCRFS1;UQCRFS1P1	205300000
236	P54707	ATP12A	204530000
237	P07814;Q3KQZ8;V9GYZ6;B4DKX5;H6WCP5	EPRS	204430000
238	D3YTB1;A0A024R2G7;F8W727;P62910	RPL32	204210000
239	A0A024R1U4;P51148;K7ERI8;K7ERQ8;F8VVK3;K7ENY4	RAB5C	203890000
240	Q8TCJ2	STT3B	203610000
241	P24390;Q96H29;A0A024QZT7;M0R1Y2;P33947	KDELR1;KDELR2	202480000
242	CON__P08779;P08779	KRT16	201850000
243	O94874	UFL1	200740000
244	Q9NRK6;Q6ZMF8	ABCB10	198780000
245	Q969V3;B2RA56;K7EMW4;K7ENM2;A0A0C4DGP7	NCLN	198220000
246	P56537	EIF6	196410000
247	C9J4Z3;P61513;M0R0A1;Q6P4E4;E9PEL3;M0R2L6;G5E9R3	RPL37A	194910000
248	O75396	SEC22B	191220000
249	Q9BQQ5;E9PLL6;Q6NZ52;P46776;E9PJD9	L27a;RPL27A	190050000
250	R4SBI6;P07099;Q6FGZ3	EPHX1	189710000
251	A0A024RB87;P61224;Q5U0C3;A8KAH9;P62834;E7ESV4;A0A0J9YXB3;F5H7Y6;A6NIZ1;F5H004;A0A075B6Q0;F5GX62;B7ZAY2;Q9BXV4;F5H4H0;F5GYH7;F5H077;F5GWU8;F5H491;F5H0B7;F5H500;F5H823;B7ZB78;F5GZG1;F5H6R7;F5GYB5	RAP1B;RAP1A	186500000
252	Q6ZRP7;B3KY64	QSOX2	185530000
253	G3V325;B4DJ38;Q3ZB84;A4D273;O75127;Q3SYP6;B3KMD7	ATP5J2-PTCD1;PTCD1	184140000
254	A0A024R5H0;O75531;B2R4V4	BANF1	183430000
255	**Q96EL3**	**MRPL53**	**182220000**
256	Q6NUK1;B4E290;B7ZB41	SLC25A24	181900000
257	A0A024R467;Q9Y276;Q53EX1;A8JZZ8;Q53RT4;C9J8G3	BCS1L	180940000
258	Q99442;F8WF48;A0JLN5;R9WWI7;F8WCJ7;D3DNQ1	SEC62;TLOC1	178200000
259	A2TJK5;Q5JWS0;H0Y5K5;Q9Y282;A6PVJ3;H0Y621;B4DV36	ERGIC3	177810000
260	Q9BTT5;Q16795;A8K4V2	NDUFA9	177560000
261	Q5JRA6;A0A0A0MRH6	MIA3	177300000
262	**P82673;H0YG82**	**MRPS35**	**176900000**
263	A0A024R0G0;Q96S66;A0A024R095	CLCC1	176390000
264	**Q9H2W6**	**MRPL46**	**175740000**
265	B4DSV8;B4DPG9;Q9H3K2;B4DNL0;Q6FIA7;Q658I8	GHITM;DKFZp566C0746	175350000
266	I3L0N3;B7Z5J7;P46459;B4DGR3	NSF	174850000
267	A8K4M4;Q96G23;Q5SZE1;Q5SZE3;H0YKH6;Q5SZE4;H0YNU7;Q5SZE2	CERS2	174020000
268	Q53ZR1;P55011;G3XAL9;B7ZM24	SLC12A2	173580000
269	Q5QNZ2;Q53GB3;Q08ET0;A8K4W2;P24539	ATP5F1;hCG_39985	171270000
270	A0A024R670;A0A087WUM0;P57105;A0A087X1F5;A0A087WYV9	SYNJ2BP	169430000
271	Q96ER9;A0A024R2V4	CCDC51	169280000
272	Q9HC07;B3KNQ2;V9GY93	TMEM165	167080000
273	A0A024RBE7;P42167;G5E972;A0A024RBH7;Q59G12	TMPO	166640000
274	Q8IZ29;Q8IWP6;P68371;Q8N6N5;B3KML9;P04350;B4DJ43;B4DE77	TUBB2C;TUBB4B;TUBB4A	165390000
275	Q9HC39;Q9HBB9;I3L2C7;P57678;Q8WUM5	GEMIN4	164120000
276	Q71U36;Q1ZYQ1;Q13748;Q53GA7;F5H5D3;Q9BQE3;Q6PEY2;Q9UQM3;B4DQK4;B7Z1K5;Q8N532;C9J2C0;Q9NY65	TUBA1A;TUBA2;TUBA3C;TUBA1C;TUBA3E;TUBA8	163730000
277	Q13308;Q59FV9	PTK7	163340000
278	A0A024R845;P61106;X6RFL8	RAB14	162510000
279	Q8TEM1	NUP210	160130000
280	Q6P4E1;A8K4R1	CASC4	159710000

281	Q9P2B2	PTGFRN	159670000
282	B4DH58;A0A087WU53;Q9H0U3;Q96SP2	MAGT1	158590000
283	P60866;E5RIP1;E5RJX2	RPS20	158580000
284	Q53FA5;P60468;S4R3B5	SEC61B	154400000
285	A0A0C4DGS5;Q08379	GOLGA2	152300000
286	A0A024RB17;A0A024RB16;Q9BSJ8;B3KY56;B3KMV5	FAM62A;ESYT1	151930000
287	A0A024R7N2;Q9HD20;A0A024R7P3	ATP13A1	151300000
288	Q96DP0	N/A	150350000
289	Q14257;A8MXP8;H0YL43	RCN2	148720000
290	B4DPK2;Q9NVH1;B4DGD5	DNAJC11	148480000
291	Q7Z434	MAVS	148430000
292	Q8N5K1;I3L1N9	CISD2	147880000
293	V9HWE1;P08670;Q53HU8;B0YJC4;B3KRK8	HEL113;VIM	147330000
294	P51648;J3QRD1;Q59H65;Q68D64	ALDH3A2;DKFZp686E23276	147170000
295	A8K321;B4DZ55;Q6ZXV5	TMTC3	146120000
296	E1NZA1;Q92616;A0A024RBS1	PRIC295;GCN1L1	145710000
297	D3DP46;P61009	SPCS3	144880000
298	Q6LEU2;A3KLL5;P05026;B7Z9S8;A6NGH2;V9GYR2	ATP1B1	143960000
299	O75844;B3KNM6	ZMPSTE24	143170000
300	A0A0S2Z591;O00165;A0A0S2Z565;E9PIQ7;Q5VYD6	HAX1	141720000
301	A8K0D2;A0A024R5F7;Q9UBM7;X5DNI9;B4E1K5;E9PM00;X5DRD7	DHCR7	141120000
302	Q9P0I2;C9JLM9	EMC3	141040000
303	Q08378	GOLGA3	140330000
304	J3KNF8;Q5HYD9;H3BUX2;O43169;D6RFH4	CYB5B;DKFZp686M0619	139160000
305	Q96IX5	USMG5	138310000
306	Q5JR94;P62241;Q5JR95;Q9BS10	RPS8	136950000
307	Q8NBL9;B2RBB2;Q96S52;B4DLL0	PIGS	136800000
308	A0A0S2Z382;A0A0S2Z3G3;Q9UBX3;B4E1E9;A0A0S2Z3I3;F6RGN5	SLC25A10	136480000
309	Q14571	ITPR2	135630000
310	C9JXB8;C9JNW5;V9HW01;P83731	RPL24;HEL-S-310	134310000
311	**Q9BYN8**	**MRPS26**	**133970000**
312	Q9NP72;B7Z4P9;A0A087X163;B7Z5V3;H0Y6T8	RAB18	133210000
313	**A0A0S2Z5D2;Q53G62;A0A0S2Z563;A0A0S2Z5H0;Q9Y2Q9;E5RGC7;H0YAT2;H7C5V3;E5RFH3**	**MRPS28**	**132920000**
314	**Q8IY71;I3L0E3;Q9Y2R5;E9PE17**	**MRPS17**	**132230000**
315	Q9NX47	N/A	132180000
316	C9J9K3;A0A024R2P0;A0A0C4DG17;P08865;Q96RS2;A0A024R7P5;F8WD59	RPSA;LOC388524	130370000
317	Q8TDR3;Q8NEH0;Q8IYV2;Q9UHI6;E9PJ60	DDX20	129080000
318	P35610;B1APM4;B7ZAT6	SOAT1	128960000
319	Q6FHJ5;O14828	SCAMP3	127980000
320	P08754	GNAI3	127570000
321	Q96N83;B7ZKQ8;O00592	PODXL	124900000
322	**A8K7J6;Q86TS9;G3V3U6;G5E9P5**	**MRPL52**	**124090000**
323	**A0A024R0H2;O15235**	**MRPS12**	**123550000**
324	Q9H3N1;B4DZX7	TMX1;TXNDC	123070000
325	CON__Q86YZ3;Q86YZ3	HRNR	121990000
326	A0A193DRS0;A0A0A8JCD0;Q59GR1;O15118;A0A0S2A5C8;K7EQ23	NPC1	120890000
327	P23396;Q53G83;E9PL09;H0YEU2;E9PPU1;Q9NQS8	RPS3	120420000
328	A0A024RDG6;Q14108	SCARB2	118170000
329	A0A024R1N1;P35579;A0A0U4BW16;Q86XU5	MYH9	116110000
330	L0R5D5;Q9BUB7	TMEM70	116090000
331	Q9UBV2	SEL1L	115550000
332	A0A0A6YYA0;Q9Y3B3;B4E2C1;Q3B7W7	TMED7	115540000
333	O75489;Q9UF24;Q53FM7	NDUFS3;DKFZp586K0821	115310000
334	Q96IR1;B2R491;P62701;Q53HV1	RPS4X	114850000
335	A0A024R9K7;Q9NPA0;H0YDT8;H0YDX2	C15orf24;EMC7	114570000
336	Q14204	DYNC1H1	114120000
337	P62269	RPS18	113340000
338	B4DMF5;E9KL48;P00367;B4DMG8;Q53GW3;B3KT18;A0A140VK14;P49448	GLUD1;GLUD2	112790000
339	Q7Z4X2;Q9NX14	NDUFB11	112680000
340	B7Z2R9;B4E2S7;P13473;H0YCG2;B4DF49	LAMP2	112180000
341	Q13190;E9PNU4;B4DKR0	STX5;STX5A	111740000
342	P67809;H0Y449;Q6PKI6;Q7KZ24;A0JLU4;Q2VIK8	YBX1	110600000
343	A0A024R277;O15269;Q6NUL7;Q59EQ4	SPTLC1	109730000
344	Q9Y487;Q8TBM3	ATP6V0A2	109030000
345	Q53X12;Q5CZH6;Q93050;Q53ET5;B7Z641;B7Z2A9;B7Z2J9	DKFZp686N0561;ATP6V0A1	108610000
346	C9J406	IMMT	107940000
347	H0Y5B4;H7BZ11;J3KQN4;P83881;R4GN19	RPL36A;RPL36A-HNRNPH2	105620000
348	Q5HYI8;C9JXM3;F8WF50;F8WDC7	RABL3	105140000
349	H0Y9V7;B4E2Q0;P98194;B4E295;Q59G44	ATP2C1	104670000
350	Q969S3	ZNF622	104600000
351	B2R8A2;A0A024R7M0;Q9BVK6	TMED9	103720000
352	A0A024R0R7;Q9H9S5;M0QYV8	FKRP	103540000

353	O15173	PGRMC2	102840000
354	A0A024R7G7;Q96K37;H7C1I0	SLC35E1	102580000
355	O43819	SCO2	102030000
356	P78527	PRKDC	101700000
357	H7BXY3;A0A024R2T6;Q7L2E3	DHX30	98998000
358	Q9HCU5;A8K813;Q05DB2;B5MC98	PREB	98897000
359	Q99720;B4DR71;A2A3U5	SIGMAR1;hCG_20471	98564000
360	Q9Y639;Q9UFM8;Q9Y499	NPTN;DKFZp566H1924	98130000
361	A0A0S2Z433;O43181	NDUFS4	97973000
362	Q96ME4;J3KQ48;Q9Y3E5	PTRH2	97925000
363	A0A0S2Z3H2;O96005;A0A0S2Z3H6	CLPTM1	97730000
364	Q14BN4;H7C3M8;H7BZK0	SLMAP	97677000
365	G3V0I5;E5KNH5;P49821;Q53G70;Q96ID4;B4DE93;B4DUN7;E9PMX3	NDUFV1	97152000
366	B4DEA8;P49748;B3KPA6;Q53HR2	ACADVL	96750000
367	Q02218;E9PCR7;E9PDF2;A0A0D9SFS3;B4DF00;B4DH65;B4DZ95;B4E3E9;E9PFG7;B4DK55;A2VCT3;A2VCT2	OGDH	95950000
368	Q86SF2;H0YAH3	GALNT7	95934000
369	Q8TAD4;Q9BY48;Q9H9X0;Q9BTR6	SLC30A5	95771000
370	Q9P032	NDUFAF4	95464000
371	B3KMV8;O75746	SLC25A12	95450000
372	Q6IBK3;A8K769;A0A140VK92;O15127	SCAMP2	95374000
373	**O60783;B2R4A5**	**MRPS14**	**95289000**
374	F8W7C6	RPL10	95202000
375	Q8IXI2;H7BXZ6	RHOT1;TMEM91	94346000
376	Q9NTJ5;E9PGZ4;B4DVV3	SACM1L	94171000
377	P27708;Q53SY7;F8VPD4	CAD	93462000
378	A8K8B7;Q14409;P32189	GK3P;GK	93144000
379	B4DFL1;A0A024R713;P09622;E9PEX6;B4DMK9	DLD	93040000
380	Q969N2;B7Z3L1;B7Z1F1;B7ZAP3;B7Z1N3	PIGT	92971000
381	Q8NE86;S4R468	MCU	91968000
382	Q9HDC9;H0Y512	APMAP	91181000
383	B3KVJ8;Q96RY8;P51798;B7Z9L3;H0Y2M6;Q2VPA2;B3KUD9;B3KXZ3;Q9BSM4;Q9BRN4;B4E3N4	CLCN7	89622000
384	Q9UHA4;Q53FH6	LAMTOR3	89271000
385	A2A2G4;Q9Y672;B4DHV8;S4R350	ALG6	88316000
386	Q7Z2K6;E7ER77;D3DRI3	ERMP1;KIAA1815	88071000
387	A8K492;P56192;B4DF61;B4E0E9	MARS	87994000
388	P62277;J3KMX5	RPS13	87290000
389	B7Z4S4;A0A1B0GVW0;O75787;A0A1B0GTB0;A0A1B0GVB9;A0A1C7CYW4;A0A1B0GWJ8;H7C3E1;B7Z1I9;A0A1B0GTU8;A0A1B0GUT7;A0A1B0GVC7;B7Z413;A0A1B0GU12;A0A1B0GWD6;A0A1B0GVI9	ATP6AP2	87268000
390	B3KN15;Q7LGA3	HS2ST1	85697000
391	A0A024R576;O95159;E9PQ47;E9PNY1;E9PQA5	ZFPL1	85582000
392	A0A024RB01;P08648;A8K6A5;B2R627	ITGA5	85400000
393	A0A024R918;O75063	FAM20B	84796000
394	Q2M1J6	OXA1L	84148000
395	B4DS66;H7C463	IMMT	83960000
396	B7Z9D0;Q8NCM9;B7Z2R7;B7Z2A7;Q5T8D3;X6RDD7;Q5T8E0	KIAA1996;ACBD5	83729000
397	M0R210;P62249;A0A087WZ27;M0R3H0	RPS16	83462000
398	Q9NVH0;B3KP95	EXD2	82567000
399	Q70UQ0	IKBIP	82555000
400	P02786;G3V0E5	TFRC	82012000
401	A4D2P2;A4D2P1;A4D2P0;P63000;A0A024R9T5;P60763;J3KSC4;J3QLK0;B1AH77;B1AH78;B1AH80;A0A024R1P2;P15153	RAC1;hCG_20693;RAC3;RAC2	81709000
402	P25398	RPS12	81037000
403	O43815;Q3B874	STRN	80946000
404	A0A024RC97;Q9BVG9;E9PS47;E9PLE4	PTDSS2	80137000
405	O15400;B4DH37	STX7	79914000
406	Q01650;Q96QB2	SLC7A5;lat1	79781000
407	Q8IVF2	AHNAK2	79539000
408	**Q9NZE8;D3YTC1**	**MRPL35**	**78476000**
409	A2RRP1;H0Y5G7;G1UI26	NBAS	78311000
410	H7C0D5;Q9BSR8	YIPF4	78256000
411	Q6LEU0;Q86Y82;B1AJQ6;B4DSZ1	STX12	77899000
412	**A0A024R8D4;Q9Y399;Q5T8A0**	**MRPS2**	**77580000**
413	I3L3P7;B2R4W8;P62244;I3L246;A8K7H3;H3BN98	RPS15A;hCG_1994130	77575000
414	Q7Z518;A8K413;A0A087WXC5;A0A024R4B3;E7ESZ7;O95299;Q53SW4;Q59FM0	NDUFA10	77533000
415	P35580	MYH10	77462000
416	P13073;Q86WV2;H3BPG0;H3BN72;H3BNV9	COX4I1	77372000
417	B5MCR8;Q6NXT4;B3KU87	SLC30A6	76164000
418	F8W914;Q6IPN0	RTN4	75441000
419	B7Z7Q4;Q8WZA1;B7ZAT4;B7Z7F2	POMGNT1	75353000
420	B4DZZ8;B4DVK8;A0A024RCX7;Q92504;A2AAT0	SLC39A7	74584000
421	B4DDK9;Q10469	MGAT2	74445000
422	Q549N5;Q9Y5M8;H7C4H2	SRPRB	74186000
423	Q8WXD5	GEMIN6	73385000
424	Q96HY6;A0A0A0MRX2	DDRGK1	73355000
425	A0A024RCZ1;Q8NC56	LEMD2	73256000

426	F8W0P7	ATP5B	72913000
427	A8YXX5;Q9Y374;A4FVA6;A0A024RD08;A0A024RCX4;Q9NZJ7;H0Y8C3;Q8IW90	PIG60;MTCH1	72620000
428	B3KR70;Q15904;Q8NF19;A0A0C4DGX8;B4DWM8	ATP6AP1;FLJ00383	72326000
429	B3KN05;B2RBE0;A0A024R497;O95573;B3KMA6	ACSL3	72169000
430	CON_Q3MHN2		72064000
431	Q6IBP2;Q6FHB5;B3KSE0;P30519;Q53HF1;A0A087WT44;I3L159;I3L1F5	HMOX2	71965000
432	A1L0T0;M0R026;Q59GP4	ILVBL	71865000
433	A0A140VKD1;Q9Y3Q3;Q53HR4;Q9UMB6;G3V1J9;F5H4M7;B4E277	TMED3	71745000
434	A0A0A0MS29;C9JHF5;H7C433	MFF	71595000
435	A0A024QZN7;Q9NZ45	C10orf70;CISD1	71426000
436	Q5JP53;Q5SU16;P07437;B7ZAF0;B4DY90;Q6LC01;Q5ST81;B7ZAK1;B4E052;B4DQN9;Q1KSF8;B4DMU8;A0A024QZU2;Q96B85;B4DXZ5;O43209	TUBB;XTP3TPATP1;TUBB2B	71296000
437	B4DDH8;Q96N66	MBOAT7	71006000
438	Q6NZ55;A8K4C8;P26373;J3QSB4	RPL13	70764000
439	O60830;V9GYS0	TIMM17B	70602000
440	O00425	IGF2BP3	70551000
441	B4DLH2;Q8N357;B4DS67	C2orf18;SLC35F6	70023000
442	V5J3L2;G0XQ39;Q13586;E9PNJ4;H0YDB2	STIM1	70022000
443	P61026;Q53T70	RAB10	69613000
444	Q92643;A6NEM5;B1AK81	PIGK	69531000
445	Q13948;Q3LIA3	CUX1;Nbla10317	69388000
446	B3KNK4;B3KM95;O95674	CDS2	69367000
447	A0A075X6P1;Q53ZV6;H9A7H1;D7P652;D7P639;D7P626;B8X5X6;B2XIN1;A0A023REG7;A0A023QG09;X5CM76;X5CKG0;X5CI32;X5CF88;X5CBQ3;X5BYA7;X5BWL7;X5BWF0;X5BVZ3;X5BVA2;X5BV52;X5BPC3;X2JJ49;W8DRA6;W8DIL7;W8DCA6;W8DBU7;W8DBM7;W8DAS2;W8D9V0;W8D9F9;W8D8R1;W0C6Q7;W0C3F1;V9PAU1;V9PAR5;V9PA42;V9NA48;V9N990;V9N6Q0;V9N6J1;V9N5T7;V9N4K8;V9M765;V9K141;V9JYL6;V9JXJ3;V9JTH7;V9JMS4;V9JLL5;V9JJF5;V9JJ03;V9JCX3;V9JCN2;V9J4Q5;V9J1H0;V9IVP1;V9IVA7;V5L8C9;V5L865;V5L835;V5L812;V5JRZ3;V5JQE6;V5JM76;V5JLM6;V5JHW3;U5ZC31;U5Z7S3;U5KP70;U3M3X4;U3M2W8;U3LRZ3;U3LRI3;U3LQT8;U3LC53;U3LC10;U3LAH9;U3L687;U3L5J7;U3L4U4;U3L3U6;U3L3J4;U3L346;U3KX27;U3KWL2;T1SXJ9;T1STG4;T1SS69;T1Q7F5;T1Q6Q4;T1Q687;T1Q5V7;T1PZR2;T1PZM5;S5RMH6;S5RLG1;S4V8X0;S4STV3;S4SQT8;R9YBR2;R9YAG1;R9Y968;R9Y8C8;R9Y676;R9Y628;R9Y5T9;R9Y599;R9Y546;R9Y4N0;R9Y4H2;R9Y499;R9Y3W8;R9Y2F5;R9Y2A0;R4I9Z4;R4I9L1;Q9B303;Q9B301;Q9B2Z7;Q9B2Y4;Q9B2Y2;Q9B2Y1;Q9B2X2;Q9B2W1;Q9B2V4;Q9B2V3;Q9B2V1;Q9B1R0;Q9B1F8;Q9B105;Q9B0V1;Q8WCX8;Q8WCX1;Q8WCW9;Q8WCW7;Q8WCW4;Q8WCW2;Q8WCW1;Q8W946;Q8W8U1;Q8HNR2;Q8HG24;Q8HG21;Q8HG20;Q8HG18;Q8HAS6;Q85KZ0;Q85KW1;Q85KU7;Q85KT3;Q85KS1;Q85HM4;Q7YEG3;Q7YEF9;Q7YEF0;Q7YEE5;Q7YED7;Q7YCH1;Q7YCG8;Q7YCG0;Q7YCE8;Q7YCE2;Q7YCC4;Q7Y823;Q7Y7F0;Q7Y6Z2;Q7GXT4;Q7GWT3;Q7GWL6;Q6WQ97;Q6VIZ4;Q6VIX6;Q6VID5;Q6VI79;Q6VHD5;Q6RS00;Q6RRR0;Q6RQI4;Q6RPF2;Q6RNL1;Q6RNJ0;Q6RMM5;Q6RMF4;Q6PZ35;Q5XTE4;Q5XTD1;Q5XT79;Q5XS00;Q5XRG8;Q5XRC9;Q5SB14;Q5SAM1;Q5S9U8;Q5S9S2;Q5S938;Q5S8W0;Q4ZFF5;Q4VFD3;Q4VFC2;Q4VFA5;Q4GW31;Q4GW05;Q4GVZ2;Q4GVS7;Q4GVA8;Q4GUX8;Q4GUE6;Q4GUC0;Q4GTI4;Q4GSD1;Q4GQ64;Q4GNT3;Q4GMK4;Q4GLM9;Q4GL73;Q4GJP0;Q4GJ06;Q4GI57;Q4GI18;Q4GHL2;Q4GHG0;Q4GG68;Q4GFX7;Q4GF15;Q4GEN5;Q4GE79;Q4GDK8;Q4GF669;Q4F656;Q4F5V2;Q4F5R3;Q4F568;Q4F4X2;Q4F4F8;Q4F454;Q4F3W3;Q4F2Y8;Q4F2K8;Q4F2F6;Q4F200;Q4F1S2;Q4F0F4;Q4F050;Q4EZT3;Q4EZS0;Q4EZP4;Q4EZ36;Q4EYP3;Q4EY48;Q4EXY9;Q4EXW4;Q4EXU5;Q4EXP2;Q4EXM9;Q4EWD7;Q3S9H4;Q306C1;Q305W9;Q2LHU9;Q2LHB7;Q2LH26;Q2L743;Q2HKQ7;Q2HKK5;Q2HJQ6;Q27H51;Q27H25;Q1ZY31;Q1W0U7;Q1ADM1;Q1ADK8;Q15II4;Q15ID2;Q15HM4;Q15HL1;Q15HH2;Q15HE6;Q15H42;Q15GZ0;Q15GW4;Q0ZK24;Q0ZFK3;Q0ZFC5;Q0Z7P8;Q0Z7K9;Q06V50;Q06UH9;Q06UC7;N0BU90;M1LMB0;M1LK27;L7XZG8;L7XZ93;L7XYG0;L7XWB1;L7XTW6;L7XTK6;L7XRG1;L7XQ59;L7XPB1;L7XM56;L7XLF4;L7XHT9;L7XH80;L7XEQ0;L7XCA5;L7SC04;L7NV51;L0E7U5;K9R3W5;K9MWA7;K9M4G7;K9JT28;K7WG69;K4GXW9;J7HWP4;J7HV84;J7HU51;J7HR49;J7HPX5;J7HKD4;J7HJU9;I7A0A7;I6QHH7;I6MMN1;I3QAV0;I3QA79;I3Q509;I3Q447;I3Q320;I3Q2U2;I3Q196;I3Q043;I3PY41;I3PXT7;I3PXI3;I3PXH0;I3PX66;H9T7P9;H9T617;H9T5H2;H9T3K9;H9T1U8;H9SZZ8;H9SWI9;H9SSA7;H9SR93;H9SQF7;H9SQD1;H9SKV8;H9SHU2;H9SFH3;H9SFG0;H9S8U6;H9SSW3;H9SS5;H9S0P3;H9RY26;H9RWA2;H9RNB6;H9RGG5;H9RF34;H9RCL3;H9R7X5;H9QLC2;H9QH53;H9QGG9;H9QG52;H9QF64;H9QDZ8;H9Q5T8;H9Q5E5;H9PUZ2;H9PUS7;H9PRH0;H9PRE4;H9PR79;H9PMN1;H9PHH4;H9PF29;H9PDH0;H9PBX4;H9P8K4;H9P3L2;H9P242;H9P066;H9NYJ4;H9NS19;H9NQZ2;H9NQH3;H9MSR5;H9MRH3;H9MN27;H9M4T1;H9M4P2;H9M4B2;H9M486;H9M473;H9LPV9;H9LPC0;H9LP57;H9LLT6;H9EBJ0;H9E7S7;H9A8F9;H9A7D2;H9A7B9;H9A780;H7BSQ4;H6WHV4;H6WGQ1;H6TWG9;H6TWF6;G9LMU8;G9LMS2;G9LMI1;G9LLT4;G9LIH7;G9LHQ4;G9LGV5;G9LGE9;G9LG84;G9LG32;G9LFG1;G9LF70;G9LEM5;G9LE82;G9LE56;G9LDN7;G9LDI5;G9LCZ0;G9LCV1;G9LCR2;G9LBA5;G9LB01;G9LAW2;G9IFS0;G9IFA1;G9IER9;G9IE74;G9AZW2;G5D8R2;G5D8Q2;G5D8N9;G5D8L3;G5D8K0;G5D8H4;G5D8E8;G5D831;G5D818;G5D7W6;G4W654;G4W5W3;G4W5R1;G4W5P8;G3CA17;G1FHS3;G0XP03;F8VAF6;F6N669;F2WIK7;F2WGS0;F2WFF2;F1KL67;F1DNK3;F1DMW9;F1DMK2;F1CIP3;F1B6V0;F1B5I2;F1AZ42;F1AX03;F1AKK4;F1AK74;F1AIH6;E9NZ96;E9NKM2;E9NJS3;E9LCI3;E9LB52;E9LAN3;E9L8H9;E9K900;E9JWJ0;E7E4L2;E7E3Z1;E7E2X7;E7E2S5;E7E2R2;E7CM12;E7CLW0;E7BKC7;E5LMD0;E5EXH0;E5EXE4;E5E1U5;E5E1Q6;E5E148;E5E135;E5E0X0;E5DYU2;E5DYP0;E5DYH5;E5DY71;E5DY58;E5DY45;E5DY19;E3W716;E3T7C0;E2JKY3;E2J0Z7;E2FPE6;E2FPA7;E0Y565;E0Y4S2;D9N004;D8L3H5;D7PAQ6;D6R4M5;D6R4G0;D6N5T8;D6N3K8;D6C1N2;D6C0C7;D6C010;D6BZU5;D6BZF2;D6BYR8;D5MBN5;D5M955;D5M8J7;D5M834;D5I8I3;D5I7G9;D3YLI0;D2KR88;D2K1I3;C9EJ80;C9D603;C9D5A6;C9D515;C8YFD1;C8YFB8;C8YDI1;C8YDE2;C8YB23;C8Y7R6;C8Y2D1;C8XZF4;C8XVB1;C7SKZ0;C7SJI3;C7B2Y6;C7AB27;C7AAY8;B9EFN7;B9EFL1;B9EFD3;B9EF68;B9EES5;B9EEN6;B9ED27;B9ED14;B8YQJ5;B8Y0K8;B8XZ47;B8XYT0;B8X5Y9;B8X5N5;B8X540;B8RFZ7;B8RFQ6;B8RF22;B7ZJ75;B7U6Z8;B7TNG1;B7TCV9;B4YFW0;B4YCP0;B4YCD8;B3VEC2;B3GTF2;B2ZHA4;B2YBC2;B2Y9E6;B2XQI6;B2XPU3;B2XNF1;B2XMC8;B2XL89;B2XKZ8;B2XKN1;B2XKK5;B2XK88;B2XK23;B2XJG6;B2XJ88;B2XIC7;B2XHU6;B2XH89;B2XH11;B2XGP4;B2XFN4;B2XEY8;B2XEX5;B2WRM8;B2MZA0;B2KLX4;B2D667;B2D465;B2D400;B2D3J4;B2D322;B2CB44;B1NU71;B0Z7B4;B0Z723;B0EWF8;A9UJI6;A8RC27;A8JMW8;A8JL28;A7XT63;A7XSF3;A7LFH4;A7IZ50;A6ZHZ3;A6ZHU1;A6ZH91;A6ZH65;A6ZH52;A6ZGN4;A6ZGM1;A6ZGF9;A6ZFS5;A6ZFN6;A6ZFM3;A6ZFH1;A6ZF67;A6ZCT8;A6ZBM3;A6ZB41;A6Z9T7;A6Z7E2;A6Z7A3;A6Z638;A6Z5B5;A6Z477;A6Z1E0;A6Z0J2;A6YZQ6;A6YZ48;A6YXC5;A6YWH7;A6YUU5;A6YTU4;A4ZYN0;A4ZN07;A4ZMW9;A4ZMU3;A4ZMH6;A4ZM22;A4ZLT3;A4ZLL8;A4ZLE0;A4ZLC7;A4ZLB4;A4ZLA1;A4ZL49;A4ZL36;A3R0P4;A3R0N1;A3R0L8;A1Z550;A1Z4K5;A1Z4H9;A1Z4G6;A1E1L3;A1DVU9;A1DVN4;A1DV00;A1DTY1;A1DTP0;A1DTE9;A1DTD6;A1DT71;A1DSY0;A1DSV4;A1DSU1;A1DSK0;A1DSD5;A0SBQ0;A0SBN6;A0SBJ7;A0SBH1;A0SB29;A0S952;A0S939;A0S8Q9;A0S8I1;A0S4F9;A0S481;A0S302;A0S2X6;A0A1B1PER2;A0A1B1II68;A0A1B1II15;A0A1B0Z3L4;A0A1B0W5P9;A0A1B0W3R8;A0A1B0W1E7;A0A1B0VZQ7;A0A143FYP8;A0A143FYJ8;A0A141ZT86;A0A141ZT08;A0A141ZSQ4;A0A1	ND5;NADH5;ndh5;MT-ND5	69055000

#	Protein IDs	Gene	Value
	41ZRB0;A0A140DIT4;A0A140DHV9;A0A109Q807;A0A0Y0K9C3;A0A0X9RUW8;A0A0X8DQV3;A0A0S1S8G0;A0A0R6NC07;A0A0R6NAY1;A0A0R6NAX4;A0A0R6NA86;A0A0R4RWY3;A0A0R4RWT8;A0A0R4RUV0;A0A0R4QNV0;A0A0R4QHI3;A0A0R4QEQ9;A0A0R4Q191;A0A0R4PXT6;A0A0N7G638;A0A0N6YP85;A0A0N6YN55;A0A0N6YMJ0;A0A0N6W203;A0A0K1HQP7;A0A0H4D2V1;A0A0G2URD1;A0A0G2UNX2;A0A0G2UJS2;A0A0G2UIK6;A0A0G2UI99;A0A0E3X8V0;A0A0E3T339;A0A0E3T281;A0A0E3T1X7;A0A0E3D705;A0A0D4WR40;A0A0D4WQW8;A0A0D4WQI1;A0A0D4WPH0;A0A0D4WNW9;A0A0D4BJS5;A0A0B6C660;A0A0A7HII9;A0A0A0PJS4;A0A097QFR9;A0A097QEC5;A0A097QA13;A0A097Q961;A0A097Q6P5;A0A097Q5J3;A0A097Q432;A0A097Q1F5;A0A097Q025;A0A097PZZ1;A0A097PYE7;A0A097PWW3;A0A097PW46;A0A096YCN7;A0A096YCI4;A0A096X6L2;A0A096X404;A0A096X3C9;A0A096WZC6;A0A096WXJ5;A0A096WVU0;A0A096WSU0;A0A096WPE3;A0A096WP35;A0A096WK30;A0A096WDB2;A0A096WCN3;A0A096WAH6;A0A096WAC6;A0A096W8J6;A0A096W882;A0A096VW26;A0A096VTC1;A0A076L3M9;A0A075CBC2;A0A075CA07;A0A068C1Y8;A0A068BZI1;A0A068BZ12;A0A068BYG7;A0A068BY57;A0A068BXB4;A0A068BVM3;A0A068BUU2;A0A068BTP6;A0A059SEV9;A0A059SDA4;A0A059S9U8;A0A059RZW9;A0A059RYJ7;A0A059RXT6;A0A059RXC6;A0A059RVW9;A0A059RUF6;A0A059RUA6;A0A059RS62;A0A059RRD7;A0A059RQE3;A0A059RQ72;A0A059RPI5;A0A059RP84;A0A059RP21;A0A059RNJ9;A0A059RNF7;A0A059RMV2;A0A059RMA0;A0A059RLJ1;A0A059RJA1;A0A059RIW6;A0A059RHF0;A0A059RH77;A0A059RD49;A0A059RBG0;A0A059QY45;A0A059QUY8;A0A059QR29;A0A059QQT9;A0A059QQG5;A0A059QQ42;A0A059QQ07;A0A059QPV5;A0A059QP43;A0A059QLA4;A0A059QKL2;A0A059QJ14;A0A059QH44;A0A059QH09;A0A059QFE7;A0A059QB82;A0A023R4U6;A0A023QVC6;A0A023QVA6;A0A023QUA7;A0A023QSS7;A0A023QS10;A0A023QKL5;A0A023QKD1;A0A023QGG0;A0A023QFH0;A0A023QEQ5;A0A023Q7K9;A0A023Q7H6;A0A023Q756;A0A023Q6D2;A0A023I9A5;A0A023I985;A0A023I918;A0A023I900;A0A023I8N5;A0A023I8L7;A0A023I8I7;A0A023I890;A0A023I885;A0A023I807;A0A023I7Z4;A0A023I7R3;A0A023I7R1;A0A023I7N8;T2HLH6;B1W6B2;P03915;A0A0A0PVC5;A0A0A0PQ79;A0A0A0PSC0;A0A0A0PVA5;A0A0A0PMH4;A0A0A0PMP8;A0A0N6YPC3;H9M4C5;A0A059RIX9;Q8HG23;Q8HG22;Q54111;V9J2G5;T1Q5Q5;R9YBG4;R9YB64;R9Y7Y5;R9Y6Z7;R9Y6E0;R9Y550;R9Y4F5;Q9B1M0;Q7YEE0;Q6VKL7;L7XD10;I6N513;I3Q2G2;H9SVQ3;H9E7Y3;H9E7J0;H9E7B2;H9E799;H9E786;G9LGK1;G9LGH5;G5D7V3;F2WH76;F1B816;E5DYL4;D6R4X9;A8QTM8;A1DVT6;A0A096WF12;A0A059RXE4;A0A059RX43;A0A059RS22;A0A059RHT6;A0A059RE98;A0A059QPL7;A0A059QIR2;A0A023QQ40;R9Y4B7;Q7YEE9;L7XV85;J7HPA7;H9PIQ3;H9MQS6;G9LMC9;G9LCA6;B8XYI9;B2WRG3;A0A1B0W5J6;A0A141ZSL5;A0A141ZQA9;A0A0R6N9S2;A0A0E3DJI4;A0A097PXG7;A0A059RS89;A0A059RIX6;A0A059RHM0;A0A059QNC6;X2CH62;R9Y259;Q6VIF3;Q0ZF73;H9STM5;H9RVX2;H9RLB8;H9RK52;H9R0D6;H9QXX8;H9PV83;H9PMJ2;H9PBJ4;H9LNU2;G3LZE0;E2DG88;D0UTS7;A8JMI8;A6ZF93;A6ZE30;A3FP67;A1DTC3;A1DT97;A0S9B7;A0A097Q5V5;A0A059S4S4;A0A059R0K6;A0A059QWC3;A0A023Q8X7;V9JLZ2;V9J3G5;V5L8Q9;U3LBY0;U3LAU0;U3L8P2;T1Q773;R9Y440;Q8WCY9;Q85KW4;Q7YEF2;Q6RMK4;Q4GMF2;Q4F604;Q4F5X8;Q4F5W5;Q4EWF0;L7XYW1;L7SAT6;L7P4C4;K7WBF9;I3Q548;H9S9F4;H9R273;H9Q414;H9PDW3;H9MMA4;H9M499;H9LRM7;H9LMD8;H6TVN3;H6TVI1;G9LM25;G9LLG7;G9LLB5;G9LJ35;G9LIZ6;G9LIG4;G9LI60;G9LI08;G9LEU0;G9LEI6;G9LEE7;G9LDT9;G9LDL1;G9LDJ8;G9IFC7;F2WJ65;F2WII1;F2WIG8;F2WIC9;F2WI64;F2WG10;F2WFN0;F2WFG5;F2WF35;F2WF09;F2WEV7;F2WEU4;F2WET1;F2WEB2;F2WE21;F1B6A5;F1AK87;E9LCJ6;E5QAB6;E5FF97;C8Y8P1;C7SJN5;C7B3F5;B8XYL5;B8X5V0;B6E908;B2XL11;B2KM00;B2D4D0;A8JMR6;A8JL93;A3R0K5;A3R0J2;A0SBB9;A0S556;A0S468;A0A141ZQE8;A0A0S1S5N9;A0A0N6YP77;A0A0K1HQL6;A0A097Q0R3;A0A097PX07;A0A096VYN4;A0A076MIL9;A0A075C751;A0A059RSY8;A0A023QTY8;A0A023QSL8;A0A023Q6E7;A0A1B0W1F8;Q8HG19;E5E1J1;X5CNW6;W0C7J9;V9N397;V9J4S4;V5L8Q1;R9Y487;R9Y3R3;R9Y247;Q9B2Z9;Q9B2Z5;Q7YCF6;Q7YCD9;Q7YCD7;Q7Y6H2;Q6RS27;Q4F340;J7HLE4;I3QB80;H9SXY3;H9S0A0;H9QHJ6;H9PY99;H9E8A0;H6WJ33;H6WIS9;G9LED4;F2YMB8;E9NKP8;E9L8Q7;E9JYF1;E5EXP8;E2CZ46;C9DF68;C9D4X6;C8YGS5;C8YGM3;C8Y4J8;B2XQL2;B2XPM8;B2XH24;B2KMS3;B2D6E5;A6Z901;A6YVZ7;A4ZMY2;A4GYN5;A0A140DHA1;A0A0E3M488;A0A0E3GKZ3;A0A096X0V2;A0A096WB60;A0A096VZ02;A0A088FX07;A0A076LB70;A0A075C8A0;A0A068BS35;A0A059S704;A0A059RKB7;A0A059QPB1;A0A023I954;A0A023I8C1;A0A023I7H2;F2WEL6;Q2LHG9;A0A059RTM1;F2WHS1;F2WG62;A0A0D4L4T2;A0A0N7BBQ4;A0A0N7BB88;A0A0N7B9C5;A0A0A0PWB3;A0A0A0PQM4;A0A0A0PQC8;F2WH89;A0A141ZQW7;A0A023Q8L4;H9SZP4;A7IYY2;A0A023QV97		
448	Q8N4P8;Q53GS0;D2CFK9;Q9BZE4;B4DHR2;O60747	GTPBP4	68960000
449	A0A024RB08;A0A087WU02;Q9HC06;Q96RQ1;H0YI50;F8VPA6;F8W0R1	ERGIC2;RLN3	68760000
450	O95140;B7Z3H8	MFN2	68627000
451	Q99808	SLC29A1	68405000
452	**A0A024R3R0;Q7Z7F7;X6R631;X6RIW1**	**MRPL55**	**68221000**
453	**P51398;V9GZ03;V9GYL9**	**DAP3**	**66599000**
454	Q13445	TMED1	66580000
455	G5E994;Q5VW38;B7ZL93;A8KAM7	GPR107	66507000
456	A0A024R957;Q8NFQ8	TOR1AIP2	66269000
457	C4N9M8;Q9NUM3	SLC39A9	66187000
458	Q9H089	LSG1	66043000
459	A0A0B4J1Z1;B4DEK2;C9JAB2;Q16629;Q8NB80	SRSF7	65625000
460	A0A024R006;Q9UBU6	FAM8A1	65373000
461	A0A024R9D2;Q86UE4;E5RJU9	MTDH	65050000
462	B4E054;A0A024R7X3;A0A024R7U9;Q9UI12;G3V126;Q8TF11;B3KUZ7	ATP6V1H	63920000
463	B7Z829;B7ZLA9;Q9C0E8;B7Z7F5	KIAA1715;LNP	63660000
464	Q969Z3;F6V6Z1	N/A	63324000
465	P35606	COPB2	62120000
466	A0A024R8P8;P63173;J3KT73;J3QL01;J3KSP2	RPL38	61672000
467	B7ZLC9;Q8TEQ6	GEMIN5	60958000
468	A0A024RBX2;Q9NWZ8	FAM51A1;GEMIN8	60597000
469	Q53HS1;Q9NRG9;B4DDU7;F8VZ44;H3BU82	AAAS	59950000
470	A0A024R9U3;Q9NX40;D6RG39;D6RIT9;D6RDK6;D6RBN5	OCIAD1	59764000
471	Q6P4A7	SFXN4	59232000
472	P33908	MAN1A1	58989000
473	**C9JJ19;P82930;A4UCR9**	**MRPS34**	**58989000**
474	P30048;Q53HC2	PRDX3	58452000
475	H0YNP1;O94923;B3KML4	GLCE	57558000
476	A0A0S2Z583;Q8TC12;A0A0S2Z575;G3V2G6;B3KQ19;H0YIZ8;G3V234;H0YJ46	RDH11	57448000
477	B2RAF3;A0A024R2Y2;Q12893	TMEM115	57255000
478	Q96BW9;A0A0G2JQ92	TAMM41	57243000
479	B3KN59;B3KM36;O95816	BAG2	56409000

480	Q8NBU5;B4E2J1	ATAD1	56390000
481	A0A0C4DGH0;B4DK26;Q5ZPR3;A8K9J6;A8K6Q6;H0YL10	CD276	56021000
482	H0YEN5;P15880;Q8J014;Q6IPX5;Q3KQT6;Q8N5L9;Q9BSW5;I3L404;E9PM36;E9PQD7;O60249;E9PMM9	RPS2;rps2	55484000
483	O00767;Q59GX7	SCD	55030000
484	P11717;Q59EZ3	IGF2R	54930000
485	F8W930;Q9Y6M1;B4DKT5	IGF2BP2	54737000
486	A8KAH1;P48651;Q9BSY0	PTDSS1	54599000
487	A0A024R313;Q68CQ7;C9JA13;C9J880	GLT8D1	54436000
488	B3KNN9;Q13740;F5GXJ9;B4DX43	ALCAM	54409000
489	**B4DP77;A0A024RD03;P82664**	**MRPS10**	**54371000**
490	A0A0S2Z4Y5;Q5QPK2;H0Y368;O60762;Q5QPJ9	DPM1	54189000
491	P62906;Q1JQ76;A0A024RCW3	RPL10A	53989000
492	Q59G75;P41252;A0A0A0MSX9;Q7Z3U5;Q6P0M4;B4DVX2	IARS;DKFZp686L0869	53901000
493	Q8WY22	BRI3BP	53226000
494	Q53GQ0;B4DWS6;D3DR22;B3KQJ0;A0A1B0GV93;A0A1B0GVY6	HSD17B12	53173000
495	A5PKX5;Q16706	MAN2A1	52814000
496	A8K287;O00161;H3BM38;H3BNE1;H3BR18;H3BPJ0;A0A024R9R8	SNAP23	52703000
497	B4DPL8;A8K0S7;U3KPU7;Q6IBR9;A0A024R3H9;U3KQS2;A0A024R3L1;O43826;U3KQL4;B4DUH2;A0A024R3F7	SLC37A4	52591000
498	D6RF48;Q9P2W9;D6RC71	STX18	52583000
499	E9PJK1;E9PRJ8;H0YDL9;H0YDJ9;A0A024RCB7;E9PIF1;A6NMH8;P60033	CD81	52484000
500	**Q9Y3D3;A6ND22**	**MRPS16**	**52327000**
501	A0A024R9P6;Q96TC7;B3KUI4;H0YMB1	FAM82C;RMDN3	52156000
502	P49411	TUFM	52101000
503	A0A024R9L0;Q9Y375;H0YL22;H0YNN4;H0YNB7	NDUFAF1	51536000
504	Q53YE7;Q53EZ0;P21397;Q49A63	MAOA	51303000
505	Q53G69;O43615;Q9UPE4;M0QXU7	TIMM44;hTIM44	51240000
506	B2R7M1;F5GYQ1;P61421;J3QL14;R4GN72;B7Z6L9;B7Z788	ATP6V0D1	51222000
507	A0A087WVQ6;Q00610	CLTC	51119000
508	Q6FHM2;P62879;C9JIS1;C9JXA5;C9JZN1;E7EP32	GNB2	50862000
509	A8K5N3;Q8IUH4	ZDHHC13	50846000
510	Q9BXK5;A0A087WTL4;A0A087WX97;B2RB43;E9PDD6	BCL2L13	50754000
511	Q546E0;A8K8P8;Q9BYC5;A5PLL2;G3XAD2	FUT8	50299000
512	B4DKS0;A0A024R0H1;P53985;B2R6A5	SLC16A1	50167000
513	A6QKW0;A0A024R9W7;P57088;D6RAA6	SHINC3;TMEM33	50030000
514	A0A087WUD3;A0A024RDJ1;Q9NRP0	DC2;OSTC	49975000
515	O43909;E7ET85	EXTL3	49956000
516	J3KN66;A0A0A0MSK5;Q5JTV8	TOR1AIP1	49909000
517	Q7KZN9;B4DQM2	COX15	49597000
518	B2R7M3;A0A024QZY1;Q13155;A8MU58;F8W950	JTV1;AIMP2	49479000
519	B4E240;Q92575;B3KTD5	UBXN4	49041000
520	F5GXX5;P61803;Q53G02;F5H895;A0A0B4J239	DAD1	48787000
521	Q96LR7	C2orf50	48760000
522	B3KTL0;Q4ZIN3;U3KPY4	TMEM259	48589000
523	Q9HBR0	SLC38A10	48517000
524	A0A140VJG8;P21964;B8XPJ7;B8XPJ8;E7EMS6;E7EUU8	COMT	48213000
525	E7EQ72;B4DP27;Q6FHT8;Q15363;F5GX39	TMED2;RNP24	48066000
526	A0A024R292;Q06136;K7ERC8	FVT1;KDSR	47927000
527	Q53Y03;O43402;M0R1B0	COX4NB;EMC8	47899000
528	R4GMX5;R4GN83	BSG	47606000
529	Q9BTX1;B4DZG6	NDC1	47542000
530	E9PIZ0;C9JST7;A6NGW1;A8K509;O95070	YIF1A	47496000
531	Q9H1C7	CYSTM1	47324000
532	O75225;B3KW79;A0A024RA40;Q9H3G5;Q9NZ90;C9JLV0;H7C0X5	CPVL	46662000
533	Q499Z2;Q96L58	B3GALT6	46620000
534	Q86YI5;A0A024R3D8;P10515;B4DJX1;E9PEJ4;H0YDD4;B4DLQ2;B4DS43	DLAT	46519000
535	Q86T03;G3V5T5;H0YJ90	TMEM55B	46162000
536	M0QZ12;Q96CP6;B3KUH3;B3KQF7	GRAMD1A	45803000
537	Q12797	ASPH	45652000
538	Q9BQ95;J3KTF5	ECSIT;ZNF428	45346000
539	A0A024R8S5;P07237;B4DLN6;B4DUA5;H7BZ94;B4DNL5;H0Y3Z3;I3L398;Q96C96	P4HB	45202000
540	Q9Y5Z9	UBIAD1	44466000
541	A0A0A0MST8;E9PFN4;B5M450;C9JRP1;Q9Y6M7;H7C3C4	SLC4A7	43949000
542	Q59FD2;G3V599;A0A193H6U5;O15320;Q96PC5;Q4G155	CTAGE5;MIA2	43732000
543	Q8TBT6;P08574	CYC1	43346000
544	C9JA08;Q96D46;B3KT11;B4DKU1;B3KMN5	NMD3	43045000
545	P10606;Q6FHM4;Q6FHJ9	COX5B	42854000
546	P80723	BASP1	42635000
547	A0A087X2D0;B2R6F3;P84103	SFRS3;SRSF3	42612000
548	Q12904;B4DNK3	AIMP1	42518000
549	A0A024R6H1;O15270;H0YJV2	SPTLC2	42405000
550	Q9P0J0;U3KQP3;B4DEZ3;K7EJE1;E7ENQ6;B4DQP1	NDUFA13	42341000
551	Q9NP58;H7BXK9;A0A024R436	ABCB6	42318000
552	A0A024RDV5;A0A024RDT9;Q9Y2H6;G5E9X3	FNDC3A	41956000
553	Q56VL3	OCIAD2	41794000
554	Q9HB00;Q08554	DSC1	41082000

555	B4DSA4;Q7KZA3;Q53FU1;P22830;Q5TZY0	DKFZp686P18130;FECH	41045000
556	Q9Y6H1;Q5T1J5	CHCHD2;CHCHD2P9	40921000
557	A0A0C4DGQ8;Q6IAN0;J3QLJ8;J3KRS1	DHRS7B	40828000
558	**Q9NQ50**	**MRPL40**	**40524000**
559	Q14643;A0A024R2E1;A0A024R2I2	ITPR1	40412000
560	E9PNW8;Q9H600;B2RDG1;Q8WVX9	FAR1	40226000
561	Q9NV96;B4DIF5;B4DDK3	TMEM30A	40060000
562	Q9UKV5;Q1RN03;A0A024R6R5	AMFR;hCG_1811773	40055000
563	P13639;B4DPU3;Q8TA90	EEF2	39702000
564	Q8NBJ5	COLGALT1	39482000
565	B4E0N6;Q969X5	ERGIC1	39481000
566	B0AZV0;Q9Y3F4;H0YH33	STRAP	39415000
567	Q8IY95	TMEM192	39399000
568	A0A140VKE9;Q13409;B4DPZ3;Q59GU5;E7EQL5;E7EV09	DYNC1I2	39166000
569	**A0A075B746;P82921**	**MRPS21**	**39144000**
570	Q5T749	KPRP	38786000
571	Q86XL3	ANKLE2	38752000
572	Q6XYC5;J3KPT4;Q9H4I3;A0A024R500	RP3-402G11.12;TRABD	38511000
573	P54136;B4DXW6	RARS	38142000
574	Q5HYG8;A0A024RB99;V9HW06;Q53ET4;P34897;B4E1G2;B4DJQ3;B4DW25;B4DP88;Q5BJF5;B4DJ63;B4DWA7;B4DLV4;H0YIZ0;G3V2Y4	DKFZp686P09201;SHMT2;HEL-S-51e	38117000
575	Q53G40;B7Z6Q5;P16278;Q53H18;E7EQ29;B7Z5H9	GLB1	38087000
576	A0A024RBY9;P53701;Q68D50	HCCS;DKFZp779I1858	37911000
577	Q59EK6;A0A140VJY2;Q12931;Q9BV61;Q53FS6;Q53G55;Q8N9Z3;K0A7K7;Q5CAQ4;I3L0K7	TRAP1	37707000
578	A0A0S2Z472;A8KAH7;A0A024R2W3;P13861	PRKAR2A	37706000
579	Q6NXR8;P61247;A8K4W0;D6RG13;B7Z3M5;E9PFI5;D6RAT0;H0Y8L7;H0Y9Y4;D6RB09;D6RAS7;D6R9B6	RPS3A	37536000
580	P15924;Q4LE79	DSP;DSP variant protein	37397000
581	V9HWJ0;B4DJ30;Q14697;F5H6X6;B4DSM6;A0A024R592;B4DIW2	HEL-S-164nA;GANAB	37354000
582	A0A024R061;P51809;B2R6P4;B4DIH9;A0A024R074;B4DE96	SYBL1;VAMP7	37087000
583	Q9H840	GEMIN7	36912000
584	Q9H0U4;Q6FIG4;E9PLD0;Q9H1C9	RAB1B	36813000
585	A0A024R4H0;Q02809;B4DGN8;B2R5M9	PLOD1	36655000
586	B2RBR9;Q14974;J3KTM9;B7Z752;B7Z5M1	KPNB1	36240000
587	A0A024RD80;P08238;B4DMA2;B4DGL0;Q6PK50	HSP90AB1	36209000
588	Q6N075;F8VV69	MFSD5	36090000
589	B7Z8E7;Q13438;Q9BR60	OS9	36017000
590	B4E1S3;B2R9T9;Q9BVC6	TMEM109	35893000
591	Q53HS0;A8K3A8;P47897;Q96AW5;A0A1B0GVU9;B4DNN3;Q9H3A5;Q9BUZ3;B4DDN1	QARS	35717000
592	Q6LET6;A0A024RAX2;P10620;F5H7F6;F5H6X2	MGST1	35693000
593	Q6ZPD9;K7ELH8	DPY19L3	35608000
594	B4DEN5;B3KQQ7;A0A024R5F9;O43505	B3GNT6;B3GNT1	35177000
595	A0A024R9Z1;Q8N353;Q9NUM4;F2Z3N7;C9JZ87	TMEM106B	34688000
596	Q8NBT6;Q5JPC1;Q9HC21;J3KSI7;J3QL84;J3KS44;J3QLV3;J3KRY6	DKFZp667O1614;SLC25A19	34526000
597	B7Z587;P17152	TMEM11	34132000
598	H0YCR6;E9PN88;E9PMA1;E9PK19;B3KX82;Q86TM6	SYVN1	34031000
599	**B4DLN1**	**MRPL12**	**33684000**
600	A0A024R8U8;Q8WVQ1;K7EN15	CANT1	33511000
601	Q6I9U3;P20645;F5GX30;Q53GY9;B2R6S2;F5GXE0;F5GXU0;F5H883;Q96AH2	M6PR	33286000
602	Q969P0;C9J8Z4	IGSF8	33135000
603	G3XAN4;Q6FHU7;Q6FHL3;A8K032;Q15629	TRAM1	33087000
604	Q5CAQ5;V9HWP2;P14625;B4DU71;Q59FC6;B4DHT9	TRA1;HEL-S-125m;HSP90B1	32910000
605	Q6ZMG9	CERS6	32755000
606	P23229	ITGA6	32711000
607	B4DUQ1;A0A024R228;Q6IBN1;Q5EC54;P61978;B4DFF1;B3KU16;Q5T6W2	HNRNPK;HNRNPK	32701000
608	B3KW74;B7Z6T7;A8K2S7;A0A024RE02;Q8NBM4	PHGDHL1;UBAC2	32650000
609	Q8N4D4;Q9NQ11;Q8NBS1	ATP13A2	32291000
610	A0A024R972;P11047	LAMC1	31875000
611	Q02413	DSG1	31872000
612	Q5SZR4;B3KPI5;B4DZR8;F6TB26;Q9Y2W6	TDRKH	31866000
613	C9J5X1;P08069	IGF1R	31856000
614	A0A0S2Z514;Q6PML9;B2R745;A0A024R9W8;B4DSU2	SLC30A9	31649000
615	E9PCW1;B4DQA8;K7EJC8;A8K5R6;O95249;F6RU00;Q96QI9;G5E9T8	GOSR1	31484000
616	B4DPP0;A6NNI4;G8JLH6;P21926;F5GXT1;Q56CY1;A0A087WU13;B4DK09	CD9;BTCC-1	31265000
617	A0A067XG54;Q8NB49	ATP11C	31156000
618	Q0D2M2;B2R4S9;A8K9J7;A0A024RCL8;A0A024RCJ9;A0A024QZZ7;I6L9F7;U3KQK0;B4DR52;Q99880;Q99879;Q99877;Q93079;Q5QNW6;P62807;P58876;P57053;O60814;A0A024RCJ2;Q8N257;Q16778;P33778;P23527;P06899;Q96A08	HIST1H2BC;HIST1H2BK;HIST1H2BN;HIST1H2BD;HIST1H2BM;HIST1H2BL;HIST1H2BH;HIST2H2BF;H2BFS;HIST1H2BJ;HIST3H2BB;HIST2H2BE;HIST1H2BB;HIST1H2BO;HIST1H2BA	31019000
619	E7ESU6;D6R9Q7;A0A024QZR9;Q8NBW4;D6RER8;D6RG31;D6RHF5	SLC38A9;FLJ90709	30733000

620	B3KPP7;A8K140;A0A024R438;Q7Z3C6;B4DYN3;H7C152	ATG9A	30186000
621	Q59E88;Q53G26;Q96EY1;B3KM81	DNAJA3	30077000
622	D3DVL7;B4DU42;Q969Z0;B3KRS4;B3KMT3;B3KM73	TBRG4	29461000
623	B1Q2B0;Q6ZNB6	URCC5;NFXL1	29431000
624	P53621	COPA	29411000
625	E5RJY1;E7ESM1;B7Z5Z7;B7Z4H0;B3KWB2;B7Z505;Q8N959;B3KU62;A0A024R9I3;Q597H1;Q53EU7;Q92597	NDRG1;TRG14	29271000
626	A0A024R9I0;P21283;E7EV59;B7Z593	ATP6V1C1	28955000
627	A0A024R7I3;P61006	RAB8A	28939000
628	Q86X52;B4DLD0	CHSY1	28926000
629	Q96D53;A0A024R0Q9;M0R001	ADCK4	28785000
630	Q5VV42	CDKAL1	28664000
631	Q58F09;Q13724;C9J8D4;A8K9K4	GCS1;MOGS	28411000
632	Q59GF1;P04920;Q9UEY4;Q9UEY5;Q9UEY6;Q99654;Q8TAG3;Q6PJY3	SLC4A2	28140000
633	Q5HYK3;F8VVX6;F8VP53;F8VVW7	COQ5	27776000
634	Q6IBG5;F8VPF3;F8W1R7;J3KND3;G8JLA2;G3V1V0;B7Z6Z4;P60660;F8VZU9;G3V1Y7;F8W180;H0YI43	MYL6;PDE6H	27663000
635	Q9Y2Q5	LAMTOR2	27555000
636	A0A024RDY0;O00410;B4E0R6;H0Y8C6;E7ETV3;B3KWG6	RANBP5;IPO5	27539000
637	A0A024R5X7;O76031;Q9H072	CLPX;DKFZp586J151	27218000
638	A0A024R3U8;Q8WWC4	FLJ22555;C2orf47	27021000
639	P29966;Q6NVI1	MARCKS	26937000
640	L7RXH0;A5YM53;P06756	ITGAV	26919000
641	Q8NCI4;E7EWV1;Q5H8A4;E7EM50;D6RFE8	PIGG	26874000
642	P84157	MXRA7	26739000
643	A0A024RCQ4;B4DJS6;Q99942;A0A140TA09	RNF5	26591000
644	Q5TZX9;A8K6M4;Q9UEU0;B2RE64	VTI1B	26501000
645	A0A024R3P1;O15121	DEGS1	26351000
646	A0A024R3N9;Q8IW92;Q8NCG3	LOC89944;GLB1L2	26291000
647	O00116;B7Z3Q4;A0A1B0GWA2;B7ZAC5;Q53SG6	AGPS	26234000
648	P17301	ITGA2	26037000
649	A0A024RAA0;Q969V5;B7Z8S4;B4DE24	C1orf166;MUL1	25998000
650	P50990;Q53HU0;Q7Z759	CCT8	25871000
651	Q86TM7;Q6P184;Q3SX58;A0A140VJI4;B4DEH1;Q9P2X0	DPM3	25507000
652	A0A024R716;Q9H0V1;H7C268	FLJ13576;TMEM168	25497000
653	Q86UT6;B7Z889	NLRX1	25481000
654	Q6Y1H2	PTPLB	25419000
655	Q6ICV6;P78381;A0A0U1RR61;A6NGW4;A0A0U1RRG4;A6NFI1;B4DE15	SLC35A2	25225000
656	K7ESE6;Q9BUM1	G6PC3	25078000
657	H3BQ24;X5DRB9;X5D9F0;D9MXF4;Q9Y2M0;X5D7V8	FAN1	24947000
658	E7EN73;B2RBC8;Q8IZA0;C9J519	KIAA0319L	24561000
659	E5RFT4;Q8N4L2;E5RJC2;E5RIP9;E5RIY0	TMEM55A	24508000
660	H7C0X4;Q92685;B4DS50;C9J7S5	ALG3	24354000
661	Q5SZ82;A0A087WXU0;Q9NWS8;Q9H5X7	RMND1	24231000
662	C9JAG1;G1UI38;Q8WU57;C9J9I1;A0A087WW58;Q9C0D9	EPT1;SELI	24221000
663	Q99735	MGST2	24171000
664	A0A024R5K8;P50454;B4DN87;A8K259;E9PR70;E9PPV6;E9PNX1;E9PK86;E9PMI5	SERPINH1	24100000
665	P06213;Q86WY9	INSR	23668000
666	A0A0A0MRK6;Q13505;A0A0C4DFQ1	MTX1	23663000
667	Q8TEQ8	PIGO	23493000
668	E9PF19;A0A0S2Z5F3;Q8N2L6;B2RB52;Q9Y4P3;B4DY50;Q96E41;B4DY59;A0A0S2Z5C1	TBL2	23336000
669	Q8NEN9	PDZD8	23204000
670	H7C1U8;Q9BUR5;A0A0J9YWW6;G3V1B6	APOO	23090000
671	A0A024R9C1;P11940;A0A087WTT1;E7EQV3;B4DZW4;E7ERJ7;B4DQX0;B3KT93;A0A024R9E2;H0YAR2	PABPC1	23037000
672	A0A087WVF8;A0A0A0MRM0;A0A0A0MRM1;A0A087WX83;A0A075B749;Q5VU43;E9PQG4;A0A0A0MRL8;A0A0A0MRL9;E9PL24;A0A0C4DFQ0	PDE4DIP	22879000
673	B4DRD7;H3BRU6;F8VZX2;Q15366;F8W0G4;F8VXH9;F8W1G6;B4DLC0;J3QT27;Q5MJP6;E9PFP8;P57721	PCBP2;PCBP3	22155000
674	A0A140TA86;Q5XKP0;K7EIR2;A0A140TA84	QIL1;C19orf70	21931000
675	Q6GYA4;Q9BQE4;A0A182DWI4;E9PN30	SELS;VIMP	21898000
676	Q8N2F6;H7BXQ8;C9J5N7	ARMC10	21716000
677	Q9NRX5	SERINC1	21551000
678	X5CMH5;Q59H06;Q5JNW1;A0A0G2JLV0;A0A087WYD6;Q03519;Q9UQ60;Q9UP03;A0A140T9S0;B4DS72;E7ENX8;Q9UMW6	TAP2;TAP2-G	21361000
679	B4E0E1;B2R5W3;A0A024R3T8;P09874	PARP1	20975000
680	Q53G71;V9HW88;P27797;B4DHR1;K7EJB9;B4E2Y9	HEL-S-99n;CALR	20932000
681	P50991;A8K3C3;B7Z9L0;B7Z2Z8;B7Z2F4	CCT4	20743000
682	E9PG40;A0A140VJC8;P05067;H7C0V9;B4DJT9;A0A0A0MRG2;B4DGD0;B4DQM1;B4DM00;B4DMD5	APP	20613000
683	A8K6H9;A0A024R0W3;Q96QD8;F8VUY8	SLC38A2	20547000
684	A8KA68;O43462	MBTPS2	20508000
685	M4QHP2;Q92508	PIEZO1	20392000
686	B3KSR0;Q5SVS4;A0A087WWR9;E5RIW6;B3KTE8	SLC25A30	20285000
687	A0A0S2Z4Y4;A0A0S2Z5H3;Q14677	CLINT1	19952000
688	G3XAI2;P07942;Q8TAS6	LAMB1	19922000
689	A0A090N7U2;A0A024RA81;X6RM59;Q9H0P0;B9A035	NT5C3;NT5C3A	19908000
690	B7Z6W6;K7ERN2;Q5NKU1;B2R736;A0A024R7C1;P32942	ICAM3;hCG_2033729	19692000

691	O00411;Q4G0F4;Q59E91;B4DZE5	POLRMT	19638000
692	F8W7Q4;Q96A26	FAM162A	19367000
693	K7EK00;Q96ND0;K7ERQ2	FAM210A	19240000
694	**Q4U2R6;M0R176;A0A087WU28;A0A0B4J2C1**	**MRPL51**	**19189000**
695	K7EQX8;Q6ZR64;K7EPS4	MXRA7	19012000
696	B7Z7P4;X5CKB3;B2R9F3;A0A140T9T7;A0A0S2Z5A6;Q03518;Q6QWC1;Q6QWC0;A0A0S2Z4R8	TAP1	18863000
697	Q9Y394;A0A087X0Z7;H0YJ66;H0YJE4	DHRS7	18831000
698	A0A0S2Z4W7;K7ELL7;B4DJQ5;A0A0S2Z4D8;A0A024R7F1;P14314;A0A0C4DGP4	PRKCSH	18732000
699	F5H6E2;B7Z3E5;O00159;I3L4D4;I3L501;I3L3Y6;I3L204;B7Z9C0	MYO1C	18426000
700	Q53RX3;Q9HBH5	RDH14	18350000
701	B3KUZ8;A0A024R6W0;P00505;A8K482	GOT2	18078000
702	Q9UKX3;Q14905	MYH13;MYH7	17868000
703	CON__Q04695;Q04695;F5GWP8;K7EPJ9;Q14666	KRT17	17836000
704	Q9H6H4;E5RGS2;B4DYB6	REEP4	17771000
705	A0A0S2Z487;A0A024R1X8;P14923	JUP	17645000
706	Q86SK9;Q9BSN4	SCD5	17516000
707	Q8N8J7	C4orf32	17381000
708	P62280;M0QZC5	RPS11	17110000
709	CON__Q5D862;Q5D862	FLG2	17052000
710	A0A0S2Z5C8;A0A0S2Z5B1;A0A0S2Z5Z7;A0A0S2Z534;Q15043;E5RIP4;E5RFT1	SLC39A14	16945000
711	Q9NUL7	DDX28	16555000
712	A0A0G2JNW7;Q9Y666;B4DZD0	SLC12A7	15721000
713	F8VWB0;B7Z9M2;A0A0X8GKR4;P49281;F8VZL6;F8W154;F8W1C0;F8W1F2;F8W1P7	SLC11A2	15548000
714	A0A140VJQ4;P04181	OAT	15522000
715	A0A0G2JN29;A0A087X117;Q15155;A0A0G2JP90;A0A087WW46	NOMO1	15468000
716	F8VVY0;F8VXH1;F8VUW9;F8VV39;F8VS54;F8VWX0;F8W0L1;F8VZ66;F8VV47;F8VWY4;F8VVE5;F8VRD2;B2RE34;A0A024R136;Q9H0H5;Q9BZ74	RACGAP1;FKSG42	15449000
717	B3KVN0;B4DKW1;Q0P512;Q59GX2;P11166	SLC2A1	15379000
718	J3KQ45;F8W8W7;O43493	TGOLN2	15360000
719	E9PJ42;B4E0E0;Q5BJD5	TMEM41B	14895000
720	B4DTS6;P48960;B4E336;B3KUI0	CD97	14841000
721	B3KQT9;V9HVY3;P30101;B3KQT2;B4DDM1;B4DJ98	HEL-S-269;PDIA3	14427000
722	K7EJE8;K7EKE6;B3KU28;Q2VPA0;B3KXS5;E5KMI6;P36776;B4DPX0	LONP1	14245000
723	Q13501;E7EMC7;E3WH17;E9PFW8;E3W990;B4DE82;B4E3V2	SQSTM1;SQSTM1-ALK	14159000
724	A4D110	LOC401309	14092000
725	A0A0A0PZ76;A0A0A0PMV0;A0A0A0PWW8;A0A0A0PMJ8;A0A0A0PV27;A0A0A0PMS4;A0A0A0PVF3;X2C0J7;X2C0J3;X2C0I9;X2C0V5;X2C0I6;A0A0A0PXN1;A0A0A0PXR7;A0A0A0PYV6;A0A0A0PSE8;A0A0A0PWY2;A0A0A0PPX2;A0A0A0PU97;A0A0A0PRG6;A0A0A0PPE7;A0A0A0PPV1;X2CLX6;V9N931;V9M958;V9K2Q7;V9JR71;V9JDL3;V9JBQ6;V9J6I9;V9J4J6;V9J1G8;U5Z977;U5Z8L9;U3L5W2;T1Q6P2;T1Q6I5;T1Q524;R9Y8B2;Q9B302;Q9B2Y0;Q9B2U4;Q9B1K4;Q9B0M9;Q8WCX7;Q8HG31;Q8HG29;Q8HAZ5;Q8HAX7;Q7YEG7;Q7YCE9;Q7YCC3;Q7Y668;Q7GXW8;Q7GWZ6;Q7GRU6;Q6VLM1;Q6VKJ8;Q6VII9;Q6RRP1;Q6RRL4;Q6RR68;Q6RMK3;Q5XRX3;Q5XRI0;Q5S9S1;Q541N0;Q4ZEJ2;Q4GSE3;Q4GN61;Q4GLZ5;Q4GIS7;Q4GE26;Q4G7B0;Q4F694;Q4F4P8;Q4F4M2;Q4F3Y8;Q4F290;Q4F0F3;Q4F0B4;Q4EWR6;Q305Y1;Q305V5;Q305R6;Q2HLE2;Q20CU2;Q0ZEY1;Q0G8P9;L7YIF0;L7XZW0;L7XUF6;L7XU16;L7XJA6;L7S6V9;L7S6N1;L7NVW1;L7NV95;K7WVK8;K7WBE4;K4GXX7;J7LLQ9;J7HR70;J3RFY3;J3RF73;J3QZS3;I3Q2Q4;I1SYL0;H9SWX0;H9SS69;H9SPJ6;H9SCA6;H9SBJ6;H9S7N1;H9S313;H9QNZ6;H9QNX0;H9QLS9;H9QH02;H9QE77;H9Q8L4;H9Q1I1;H9PPP7;H9PHK1;H9P7D9;H9P0H1;H9NZ79;H9NWC8;H9LLK6;H9E7R9;H9E7L7;H9E7J1;H7BU52;H6TVT6;G9LKY6;G9LKQ8;G9LGV6;G9LGM8;G9LFR6;G9LF58;G9LCN7;G9B0P8;G9AZH0;G5D8P0;G5D8K1;G4W466;G4W036;G3M8K8;G3M3S3;G3CA57;G3CA18;G3C9Z2;G1JVH5;F6N1U0;F6MZF8;F2WG63;E9LAG9;E9L8Y6;E9L8W0;E9JWL7;E5QBL9;E5KYG1;E5KYE8;E5KYD5;E5E1V9;E5DYD7;E5DY72;E5DY33;E5DY20;D8L5G9;D6R5P0;D6C1N3;D2KI69;C9D643;C8YCT5;C8YC64;C8YA62;C8XWK4;C8XV66;C7B3B7;B8RC54;B8R3C2;B4YG26;B4YG13;B4YBV7;B3VLA5;B2Y8L1;B2XQV4;B2XHG7;B2D5P9;B2D3W3;B1W9K7;B0Z776;A7XTS4;A7LER5;A6ZHJ2;A6ZGV0;A6ZDH3;A6ZBM4;A6Z1T4;A6YZJ2;A6YXL7;A6YXB3;A6YX87;A6YWD9;A4ZMD8;A1DVP8;A1DVF7;A1DUW2;A0S9S4;A0A143FYP7;A0A141ZT09;A0A141ZSL6;A0A141ZSC5;A0A141ZRQ4;A0A141ZRI9;A0A141ZRG3;A0A141ZQW8;A0A141ZQP0;A0A109QTL5;A0A0X9TT95;A0A0U2DZT5;A0A0P0K707;A0A0N7AHK7;A0A0N6YMM8;A0A0G2UR40;A0A0G2UP70;A0A0E3M0M8;A0A0E3JV88;A0A0D4WPD0;A0A097Q4B7;A0A097Q221;A0A096WNH2;A0A096W049;A0A075X6N0;A0A075C7T2;A0A068C695;A0A068BPU9;A0A059S6I0;A0A059RR87;A0A059RNZ2;A0A059RMZ8;A0A059RJ10;A0A059RI68;A0A059RG71;A0A059RBF9;A0A059QTJ2;A0A059QQW3;A0A059QPR0;A0A059QLG0;A0A059QF73;A0A023R5S7;A0A023R385;A0A023QQE5;A0A023QFF6;A0A023Q568;A0A023I8P3;A0A023I8N0;A0A023I852;B9EEZ1;B9ECT7;A0A023I7W4;P03923	ND6;NADH6;MT-ND6	13993000
726	C9JPX5;C9JKL2;A0A024RA89;O95772	STARD3NL	13935000
727	K7W4U9		13825000
728	B5MDE0;Q96AA3;C9JP01	RFT1	13488000
729	A1A508;Q86W20;B1AN99;Q8N2U3;Q7Z5F4;P35030	PRSS3;PRSS1	13435000
730	A0A0S2Z523;E5KRX5;Q15526;A0A087WYS9	SURF1	13415000
731	F5GXW6;O95415	BRI3	13098000
732	A0A0S2Z4V6;O76024	WFS1	12909000
733	Q8N4V1	MMGT1	12692000
734	Q9BWS2;S4R3V8;Q86X29	LSR	12049000
735	E5KSY5;Q96RR1;Q9H6V3	PEO1;C10orf2	11951000
736	A8K948		11804000
737	A0A087X0B7;A0A0K0K1I8;Q5SQN1;U3KPT7;A0A087X2J6;H0Y627;H7C3C7	SNAP47	11608000
738	P18827;Q53H42;E9PHH3;H7C1K4;B4DRQ9	SDC1	11346000
739	P49454	CENPF	11173000
740	D6RBS5;Q8IZ81	ELMOD2	11129000
741	Q13393;F8WBV7;C9IY79;Q59EA4	PLD1	11099000
742	A0A0C4DG33;O43933;B4DER6;Q96S70	PEX1;PEX1R633Ter	11027000
743	A0A024R8B5;Q86YN1	DOLPP1	10976000

7. Supplementary

744	K7EQ91;B4DWH6;Q13433	SLC39A6	10510000
745	A0A0A0MTI6;B4DSC2;B3KWH9;A0A024RD35;Q9NYP7	ELOVL5	10433000
746	Q96AJ9	VTI1A	10004000
747	A0A024RAM0;Q92973	TNPO1	9970200
748	Q14126	DSG2	9523900
749	F8W8C2;Q9HBM0	VEZT	9517400
750	F8VNT9;F8VV56;F8W022;F8VWK8;W6A4U0;A0A024RB05;P08962	CD63	9507900
751	B4DV31;P56589;Q7Z6V3	PEX3	9239800
752	Q9HAV0;A8K3F6	GNB4	9157700
753	Q8WUD1;Q5HYI5;B4DUD4	RAB2B;DKFZp313C1541	8974200
754	Q5RKT7;B2RDW1;P62979;Q8WYN9	RPS27A;HEL112	8896400
755	A0A024RD41;Q9ULC3	RAB23	8793200
756	D3DSR9;Q6FH58;B5BU36;O14763;B7Z3M7;Q7Z2I8;B7Z588	TNFRSF10B;DKFZp686A24188	8681200
757	P35243	RCVRN	8539800
758	F8W120;F8VWX5;F8VVN7;F8W098;H0YIA4;A0A087WYD4;Q9BVX2	TMEM106C	8516000
759	L7RRS0;O00443;E9PPP3;A0A0C4DGF9;B4DRX6;B4DG55	PIK3C2A	8484600
760	J3QQN7;Q8N9F7;J3KTA9	GDPD1	8415300
761	F6SFZ6;B7Z6W8;Q99571;B7Z1K8;H0YF70;B7Z1M5;F5GZQ9;B7Z4R5	P2RX4	8334500
762	Q4VB24;B2R984;A3R0T8;A3R0T7;P16403;P10412;P16402	HIST1H1E;HIST1H1C;HIST1H1D	8245200
763	Q8NHS3	MFSD8	8201700
764	Q8WV19	SFT2D1	8071500
765	A0A024R991;Q8N8Y2	ATP6V0D2	7816800
766	E3UPC4;U3Q010;A0A060GZE8;Q9BD09;Q7YNX6;O19784;A0A0A8R710;V5NQ98;V9N3G5;V9N366;S4W2N6;R9R086;R9QZB6;Q8MHN5;Q8HWT6;Q8HWT3;Q8HWR1;Q704P8;Q6UFS6;Q5MBP4;Q306H7;Q27I54;Q27I53;Q209I0;P79560;M9ZD80;M9PNR4;M9PAL4;M9PAK4;M9PAG4;M9PAB9;M9PA47;M9PS2;M9P9R4;M9P9L8;M9P9J0;M9P933;M9P8Z8;M9P8U4;M9P8J0;M4NBW4;K7X4C9;K7WRG4;K7P5T5;K7P5M6;K7P569;J9PW14;J9PVC1;J7K6Q7;J7K1D0;J7K1C0;J7JXQ5;J7JXQ4;J7JWP0;J7JPG5;I7AYB0;I7API8;I6ZTR2;I6ZTQ5;I6NXG5;I6NVT1;I6M559;H6UV85;H2BDQ9;H2BDQ5;G9I2N0;G9HWB2;G3DR70;G3D6G7;G3D6E5;G1EQJ5;G1EQG2;G1EQE1;G1EQD4;G1EQC9;G1EQ93;G1EQ54;G1ENU0;G1ENR1;G1ENQ9;G1ENQ3;G1ENQ2;G1ENN3;G1ENN1;G1EMU9;G1EMT4;G1EGZ5;G0ZML1;G0ZMK7;G0Z8E8;G0X8S9;G0X8S4;F8TI97;F8SY73;F8SKY0;F8RHI7;F8R8L6;F8R8L5;F6KRY8;F6KRV9;F4YU79;F2X645;F2VP92;F2VP89;F2VNU7;F2VNU6;F2VNU5;F2VNP9;F1CCJ8;F1AQR4;F1AQP5;F0V6C0;E5DCP8;E3SWM8;E3SWK1;E3SGC4;E2D5T1;E2D5R6;E0YTM9;E0YTM8;E0X613;E0WN37;E0WBQ6;D7NR17;D7NR10;D7NP53;D7NP46;D7NP41;D7NP15;D7NNW1;D7NNV5;D7NNV4;D6MLG5;D6MLE8;D6MLC5;D6MLC3;D6MLC1;D6MLB4;D6MLB1;D6MLA3;D6ML96;D6ML92;D6MKX8;D6MKW5;D6MKV9;D6MKV2;D6MJK5;D6MJH7;D6C6H0;D6C6A8;D5M8B6;D5FZR5;D5FZM3;D3Y5Z6;D3U761;D3U751;D3U416;D3U3Q7;D3U3Q2;D3U3P5;D3U3N9;D3U3N8;D3U3N6;D2XUR0;D2U832;D2DKK1;D0EP72;C9WES9;C8CHF4;C8CHB2;C8C3Y9;C7FDW2;C7FDT8;C6K4K5;C6JSY7;C5J041;C5J038;C5J036;C5J034;C5J008;C5IZZ4;C5IZY7;C5IZY4;C5IZW8;C5IZW4;C5IZV7;C5IZM1;C1L373;C1KJK5;C0M127;C0KK00;C0KJZ6;C0KJZ5;C0KJZ2;C0KJX7;C0KJX6;C0KJX1;C0KJX0;B9VR41;B5B8Y6;B2Z8W3;B1A653;B0I562;A2BCY2;A2BCX4;A2BCX1;A2BCW8;A2BCW4;A1JVF1;A0A186VNV8;A0A186VNE5;A0A186VNC0;A0A186VN82;A0A180H5L0;A0A172W5K2;A0A141AZE6;A0A141AZC0;A0A140FAI1;A0A120GWC3;A0A0N7A4X6;A0A0N7A4R9;A0A0K0KSC4;A0A0K0KRM7;A0A0K0KRM5;A0A0K0KRA4;A0A0K0KR94;A0A0G2R108;A0A0G2R0Z7;A0A0G2R0Z3;A0A0G2R0Y5;A0A0E3DDJ1;A0A0E3DDH0;A0A0E3DDG2;A0A0E3DDF6;A0A0E3DCX3;A0A0E3DCE9;A0A0E3DCD9;A0A0E3DCD0;A0A0D5CC74;A0A0A7C973;A0A0A7C803;A0A0A7C7Z0;A0A0A7C5X4;A0A0A7C511;A0A0A7C4S5;A0A0A7C4N6;A2IBK3;X5MNS9;W0GBJ0;U3RCQ8;T2AUP2;S5TCP9;S5DTD0;S5DTC5;S5DMX7;S5DMX2;S5DL77;S5DL69;S5DHW1;S5DHV5;S5DHI7;S5DHI0;Q5EFR2;N1NV66;L0GD23;I7KE77;H6UWQ4;H2ALZ8;G1UK10;G1UK09;F8LFQ0;F2XI51;F2XI50;F2XI48;F2XI47;F2XI46;E9RJS7;E1Y7F8;E1XUP7;E0WMV4;D6QTC4;B9WPX4;A0A0N9M6F5;A0A0H5BMM5;V5NQU1;F5A4J4;D9UAZ4;C8C9X1;A0A089WV06;V5NSS6;V5NSS3;V5NSS0;V5NR98;V5NR93;V5NR91;V5NQT6;V5NQQ8;V5NQA0;F6IQA6;F6IQA5;F6IQA4;F6IQA3;F6IQA2;F6IQA1;F6IQA0;F6IQ99;F6IQ98;F6IQ97;F6IQ96;F6IQ95;F6IQ94;F6IQ93;H9TV74;C0KXH1;Q7YNW6;K4RH56;D7GN71;D3XQC2;C9E8V2;C9E8V1;C7EXL8;A0ZY49;A0A1C3PI40;A0A1C3PI27;A0A1C3PHT1;A0A1C3PHN3;A0A173ADA7;A0A173AD42;A0A0U5Q1S9;A0A0S4T1F2;A0A0B7NXW5;A0A090KM67;A0A090KEY9;P30499;D3U740;C0M121;G0X8S5;E0YTP1;D6ML94;D6MJK7;C0KJZ9;A0A0K0KSB7;A0A0E3DDE3;I7DE59;F2XI49;A0A1C3PHT4	HLA-C;HLA-Cw;HLA;MHC	7806700
767	B4DWZ5;O43772	SLC25A20	7632400
768	Q9BSK2;D6RB26;D6RCF5;F6SDC8;Q96CQ1	SLC25A33;SLC25A36	7489300
769	P60602	ROMO1	7435200
770	I3L4N6;B4DF30;Q9UP95	SLC12A4	7378600
771	E9PF31;O94788	ALDH1A2	7318500
772	A0A024RA32;Q9NS00;C9JDX1;C9K0C8	C1GALT1	7318200
773	A6QRH7;Q5HY75;D3DWX8;P98173	FAM3A	7173300
774	Q9UIL3;Q53S60;B4DZQ8;B4DYQ0;O95342	ABCB11	7111100
775	A0A024R491;Q9GZY8	C2orf33;MFF	7055600
776	C9JPV1;B4E140;Q59GD7;A0A087WYN0;A0A024R2N0;A0A087WY96;P31641	SLC6A6	6750100
777	B4DTV1;B4E3I5;A0A024R3N3;A0A140VJE9;Q06481	APLP2	6675500
778	B4DKK1;A0A087WV67;A0A087WT23;O00124	UBXN8	6536700
779	G3V1B8;H0YEB6;O60232	SSSCA1	6456000
780	O75592;H7C3U4	MYCBP2	6170700
781	A0A087WZA9;A0A024R4K9;A0A087X266;Q9BXJ8	TMPIT;TMEM120A	5765500
782	D6RDM3;D6R9S7;D6RHE3;D6RDB0;Q96GZ6	SLC41A3	5744200
783	G5EA29;H0YEL0;O14893	GEMIN2	5526600
784	J3QRM4;D6RAB89;D6RBB0;Q6FGN0;A0A024R068;A0A024R0A4;O60683	PEX10	5453500
785	CON_P35908		5422500
786	A0A024RBP7;Q53EP9;A8K546;Q8TCT6	UNQ1887;SPPL3	5344100
787	V6A6E5	HLA-C	4817900
788	S4R386;Q6P9H1;B1ANB7;A8K841;Q8TDD5	MCOLN3	4618200
789	Q9NXV2	KCTD5	4405300

790	B9A054;A0A024R455;Q8TEB9	RHBDD1	4036500
791	B4DHJ7;Q53HF4;F6RP06;Q66K24;A0A0J9YW18;Q6NVY4;Q12983	BNIP3	4022700
792	Q5VZM0;Q7L523	RRAGB;RRAGA	3827100
793	Q9H617;Q5U3C3	RP13-360B22.2;TMEM164	3751300
794	Q9NWQ8	PAG1	3685500
795	D3DWC4;Q86VZ5;E6ZCI6;E6ZCI7;C0MHM2;B4DJU2	TMEM23;SGMS1	3606000
796	P32856	STX2	3216700
797	Q86WV6	TMEM173	3091900
798	B4E2E5;E9PHV5;P28290	SSFA2	3045800
799	F8VQW0;F8VX73;F8VPI1;F8W201;F8W086;F8VR05;B7Z984;F8VQQ5;F8VSI7;F8VVJ4;B7Z5Y9;B3KWE3;A0A024R0Z5;P55061	TMBIM6;TEGT	2621800
800	E9PPF9;E9PLD2;B2RAQ5;A0A0S2Z5H6;B4DRE5;Q9H019;E9PPQ0;C9JF50;E9PLU1;E9PRK5;B3KPT5	MTFR1L	2427900
801	Q92522	H1FX	2307500
802	A0A087WYR0;P09132;A0A087WWU9	SRP19	2205400
803	Q9H1C4	UNC93B1	2168400
804	E7EPW5;G3XAH9;E9PCV1;B7Z4U3;B7Z4L1;A8K8K7;E7ENZ9;C9JU30;B7Z573;E7EPD9;H7BXS2;X5DRA0;Q9NRC1	ST7	2167700
805	B4DJ17;A0A024QZ44;A0A024QZ15;Q96NT5	HCP1;SLC46A1	1945200

Supp. Table 2: MS-analysis of fraction 11 from a 5-30% sucrose gradient (lysate of mitoplasts was separated). 55S proteins (green), 80S proteins (grey).

#	Majority protein IDs	Gene names	LFQ intensity 11
1	V9HW26;P25705;K7EK77	HEL-S-123m;ATP5A1	2.5913E+11
2	V9HW31;P06576;H0YH81;F8W079	HEL-S-271;ATP5B	2.5513E+11
3	CON__P00761	N/A	2.4029E+11
4	A0A024QZT0;P45880;A0A024QZN9;A0A0A0MR02;B4DKM5	VDAC2	1.1038E+11
5	A0A024R3X4;P10809;B3GQS7;B7Z597;B7Z5E7;B7Z4F6	HSPD1	90695000000
6	E5KNY5;P42704;B4DSR0	LRPPRC	90435000000
7	P21796;B3KTS5	VDAC1	68574000000
8	Q16891;B9A067;B4DQY2;B4DT20	IMMT	65985000000
9	Q9Y277;E5RJN6;E5RHZ6	VDAC3	63628000000
10	Q9BZE1;S4R369	MRPL37	51859000000
11	A8K401;P35232;Q6PUJ7;Q6FHP5;Q53FV0;C9JW96;C9JZ20;E7ESE2;E9PCW0	PHB;HEL-S-54e	48906000000
12	E9KL44;P40939;B4DRH6	HADHA	41375000000
13	Q99623;J3KPX7;F5GY37;B4DW05;F5GWA7;F5H3X6	PHB2	40885000000
14	A0A024QZ30;P31040;D6RFM5;B3KT34;Q00QF12;A0A087X1I3;B4DYN5	SDHA	40308000000
15	B4DL14;B4DFE6	N/A	37247000000
16	G5E9W7;G5E9V5;P82650;Q8NBL6;Q59GX8;A8K9Y7	MRPS22	34276000000
17	P22695;H3BRG4;H3BSJ9	UQCRC2	34264000000
18	Q86YI5;A0A024R3D8;P10515;B4DJX1;E9PEJ4;H0YDD4;B4DS43;B4DLQ2	DLAT	33632000000
19	Q9Y3B7;Q53G19	MRPL11	31234000000
20	Q96DV4	MRPL38	30257000000
21	Q9P015;B2R739;E5RIZ4;E5RHF4	MRPL15	29814000000
22	Q96EY7;B2RDU4	PTCD3	28795000000
23	Q9NYK5;C9JG87	MRPL39	28251000000
24	A8K5D5;P49406;B4DIG4;S4R3W9	MRPL19	27588000000
25	P31930	UQCRC1	27169000000
26	Q6I9V5;P12236;Q59EI9	SLC25A6	27123000000
27	P55084;B4DY96;F5GZQ3;B4DDC9;D6W539;B5MD38	HADHB	24869000000
28	H0Y9G6;E7ETU7;B4DKM0;P09001;B4DW56;D6RC14;E9PF06	MRPL3	23754000000
29	Q9BYD1;E5RJI7	MRPL13	23330000000
30	Q5T9A4;Q9H834;Q8N3E6	ATAD3B;DKFZp761L1023	22617000000
31	P82933;Q86WV4	MRPS9	21731000000
32	Q9BUN6;Q53H77;Q9NP92;Q53GN7	MRPS30	20537000000
33	P82663;E7EPW2	MRPS25	20225000000
34	P82675	MRPS5	20124000000
35	Q8N5N7	MRPL50	20073000000
36	A0A024R578;Q13405;H0YDP7;Q59GE9	MRPL49	19964000000
37	Q9BYD2;Q5SZR1	MRPL9	19829000000
38	Q92665	MRPS31	19360000000
39	Q5T653;A0A024RD44;C9IY40	MRPL2	18914000000
40	Q9NX20;E9PI14	MRPL16	18695000000
41	Q7Z2W9;B4DXI4;F5H7V8;A0A024R5G7	MRPL21	18156000000
42	E7ESL0;J3KQY1;Q9NWU5	MRPL22	17770000000
43	B7Z4V2;V9HW84;P38646;Q8N1C8;B7Z1V7;B7Z4T3	HEL-S-124m;HSPA9	17627000000
44	A0A087X2D5;B4DEF8;Q9BRJ2;A0A0G2JMS5;A0A087WU62	MRPL45	17406000000
45	A0A024R8L0;J3QLS3;Q9Y2R9;J3QKW2;J3QQS1;J3KSI8	MRPS7	17330000000
46	Q13084;A2IDC6;Q4TT37;A2IDC7	MRPL28	17114000000
47	A0A024R473;Q9H9J2	MRPL44	16966000000
48	P51398;V9GZ03;V9GYL9;V9GYJ9;V9GYA7;V9GZ61	DAP3	16927000000
49	A4D1N4;C9JRZ6;Q9NX63;F8WAR4;B7Z1X9	CHCHD3	16636000000
50	A0A024RAJ1;Q92552;G5EA06;D6RH20;B4DT94;Q6PKB3;D6RJC7	MRPS27	16553000000
51	A0A024R7C5;Q9BYD3;K7ES61;X6RAY8;K7ELQ0	MRPL4	16265000000
52	Q9Y3D9;J3QLR8	MRPS23	15822000000
53	P48047;Q53HH2;H7C0C1	ATP5O	15016000000
54	P05141;Q6NVC0	SLC25A5	14690000000
55	P82673;H0YG82	MRPS35	14654000000
56	B1AL05;Q8N983;H0Y6Y8;H0YBU8	MRPL43	14637000000
57	A0A024RCB2;Q16540;B2R9J4;A6NJD9;A8MVT4;A8MYK1;H7C2P7	MRPL23	14560000000
58	Q9UJZ1;A0A087WYB4;Q6ZNW0	STOML2	14239000000
59	Q9NVI7	ATAD3A	14229000000
60	A0A024RD78;Q6P1L8	MRPL14	13864000000
61	Q9NQ50	MRPL40	13498000000
62	Q96A35;X6RJ73	MRPL24	13462000000
63	Q9Y512	SAMM50	13415000000
64	H6VRG0;H6VRF8;H6VRG1;P04264;H6VRG3;CON__P04264;H6VRF9	KRT1	13065000000
65	C9JJ19;P82930;A4UCR9	MRPS34	13063000000
66	E5KLJ7;E5KLJ5;E5KLM1;E5KLL9;E5KLK1;E5KLJ9;E5KLJ6;O60313;E5KLM2;E5KLM0;E5KLK2;E5KLK0	OPA1	12801000000
67	Q8NCF7;A0A024RBE8;B2RE88;A0A024RBH9;Q00325;Q53HC3;F8VVM2	SLC25A3	12800000000
68	Q9NVS2;Q5QPA5	MRPS18A	12793000000
69	Q8IY71;I3L0E3;Q9Y2R5;E9PE17	MRPS17;hCG_1984214	12694000000
70	Q8IXM3	MRPL41	12591000000
71	A4D1V4;Q9BYC8	MRPL32	12583000000

72	P63261;B4E3A4;B4DVQ0;I3L3I0;I3L1U9	ACTG1	12397000000
73	P30049	ATP5D	12040000000
74	O95202;D3DVQ1	LETM1	11899000000
75	F5H702;Q96GC5;F5H8D0	MRPL48	11866000000
76	P07919;Q567R0;A0A096LP55	UQCRH;UQCRHL	11767000000
77	Q9P0M9;D6RAN8;H7C5U8	MRPL27	11747000000
78	O00330;B2R673	PDHX	11682000000
79	Q59EK6;A0A140VJY2;Q12931;Q9BV61;Q53G55;Q53FS6;K0A7K7;Q8N9Z3;Q5CAQ4;I3L0K7	TRAP1	11592000000
80	O75947	ATP5H	11431000000
81	Q9HD33	MRPL47	11420000000
82	Q9BYN8	MRPS26	11419000000
83	Q8TBT6;P08574	CYC1	11279000000
84	Q2TB59;A0A024R0C3;Q13423;E9PCX7	NNT	11062000000
85	Q86W17;Q53ZX9;Q53ZX8;Q53ZX7;Q45KI0;H0Y8D1;Q6PK75;A6XMV8;Q5NV56;Q3SY20;Q3SY19;CON__P07477;A0A0J9YYC8;A0A087WW55;Q7Z5F3;E7EQ64;A6XMV9;Q8NHM4;P07478;P07477	PRSS1;PRSS2;TRY8;PRSS3P2	10705000000
86	Q9H2W6	MRPL46	10604000000
87	K7EKE6;K7EJE8;B3KU28;B3KXS5;P36776;Q2VPA0;E5KMI6;B4DPX0	LONP1	10412000000
88	Q6IBR0;P04843;Q96HX3;Q53EP4;B4DL99;B7Z4L4;B4DNJ5	RPN1	10151000000
89	A0A024R0P9;O96008	TOMM40	9968800000
90	P47985;P0C7P4	UQCRFS1;UQCRFS1P1	9656700000
91	P35527;CON__P35527;K7EQQ3	KRT9	9647500000
92	A0PJ79;Q9BYD6;H0Y8N7	MRPL1	9485400000
93	Q96HS1	PGAM5	9280700000
94	A0A024R467;Q9Y276;Q53EX1;A8JZZ8;Q53RT4	BCS1L	9273600000
95	O75306;B7Z792;Q53HG2	NDUFS2	9221000000
96	A0A024R0H2;O15235	MRPS12	9186400000
97	Q9BYC9	MRPL20	9077400000
98	Q53FX9;P82912;Q53GJ8;H0YL99	MRPS11	9067500000
99	Q96EL3	MRPL53	9041200000
100	B0S7P4;Q9Y676;A0A0G2JIC6;B4DFG6	MRPS18B	8860200000
101	Q8TAE8;Q7LAX7	GADD45GIP1	8850200000
102	Q9Y3D3;A6ND22	MRPS16	8786100000
103	P05023;B7Z3V1	ATP1A1	8159600000
104	Q96EL2	MRPS24	7860000000
105	A4D1U5;Q53H12;E9PC15;B4E2Z8;E9PG39;B4DR72;A0A0G2JLG5	FLJ10842;AGK	7798200000
106	A8K9D2;Q9H0U6	MRPL18	7733600000
107	Q07021;A8K651	C1QBP	7669000000
108	O75489;Q9UF24;Q53FM7	NDUFS3;DKFZp586K0821	7569200000
109	Q9NRX2;E9PKV2	MRPL17	7512500000
110	Q9H9B4;D6RFI0;S4R2X2;D6RDG7	SFXN1	7479300000
111	D3DUJ0;Q8TA92;Q9Y4W6	AFG3L2	7375200000
112	Q8TCC3;B8ZZV5	MRPL30	7270200000
113	Q9Y6C9;Q53G34	MTCH2	7002200000
114	E5KRK5;P28331;B4DJ81	NDUFS1	6873400000
115	A0A024R3R0;Q7Z7F7;X6R631	MRPL55	6811100000
116	O60783;B2R4A5;Q96Q61	MRPS14	6700100000
117	J3KS15;Q14197	ICT1	6567500000
118	Q8IXI1;H3BST5;I3L2C6	RHOT2	6531700000
119	P21912;A0A087WWT1	SDHB	6500200000
120	P49411	TUFM	6488000000
121	J3KPP0;A0A024RBG3;Q9Y6G3;S4R360;S4R2Z7	MRPL42	6472300000
122	Q9NRK6;Q6ZMF8	ABCB10	6108500000
123	A0A024R8D4;Q9Y399;Q5T8A0	MRPS2	5969400000
124	H7BXY3;A0A024R2T6;Q7L2E3	DHX30	5955400000
125	Q53GR7;Q9UJS0;B7Z2E2	SLC25A13	5908800000
126	Q08ET0;A8K4W2;P24539;Q5QNZ2;Q53GB3	hCG_39985;ATP5F1	5763600000
127	B2RE46;P04844	RPN2	5568500000
128	Q0VAB1;A0A024R0M6;Q3ZCQ8;M0R2F8;M0R0C3;M0R003	TIMM50	5558300000
129	P82914;B4DYW3;D3DPS9;Q59EA6	MRPS15	5431400000
130	A0A024R7J4;M0R226;Q9BQ48	MRPL34	5420700000
131	A0A0S2Z5D2;A0A0S2Z563;A0A0S2Z5H0;Q9Y2Q9;Q53G62;H0YAT2;H7C5V3;E5RGC7;E5RFH3	MRPS28	5376000000
132	A8K5H7;Q96TA2;Q96I63;Q9Y2Q2;Q9NQ51	YME1L1;FTSH	5164100000
133	B4DEH0;Q7Z7H8	MRPL10	5098000000
134	Q9H845;Q9H9W4;H0Y8Z9;Q9BUX5;Q59FN3	ACAD9	4962500000
135	B4DP77;A0A024RD03;P82664	MRPS10	4947200000
136	A4D0W4;Q9UDR5;F8WAH1;F8WE53	AASS	4902500000
137	CON__P13645;P13645	KRT10	4715400000
138	A0A140VK11;Q9H078;H0YGM0;Q7Z777	CLPB	4642100000
139	X2D546;X2D544;X2D537;X2D4V5;X2D4V3;X2D4U5;X2D4K6;X2D4F2;X2D4E2;X2D4D6;X2D3Z8;X2D3Z7;X2D3Z6;H9E7F7;A0A059QM31;H9E7P8;A0A059RTG7;A0A059QNV4;E2DTL8;A0A1B1PEQ8;H9E7W2;G3CA49;K7WVJ5;H9E7T7;X5C6M5;X5BKA4;X2CK15;W8DFH5;W8D4U9;W8D1X2;V9K571;V9JPM6;V9J3S1;U5Z9R9;U5Z487;U3LSI8;T1SWS8;T1Q632;S4STI1;R9Y412;Q9B2U8;Q9B138;Q8WCW3;Q8HNR1;Q85KS0;Q7Y6M3;Q7Y626;Q6VJJ3;Q6VJD8;Q6VIG7;Q6RQ80;Q6RNN7;Q6RKW8;Q6R0V6;Q5XRW8;Q5SB08;Q5SAP1;Q5S971;Q4GW12;Q4GQP0;Q4GHE1;Q4GCZ4;Q4GCG2;Q4F4V6;Q305H0;Q19MP7;Q15HH9;Q0Z7S0;Q0Z7J0;Q06TE6;L7XQ86;L7XMG0;K9M370;J7HPF9;J7FG21;I6UIH6;I6PZI4;I6PRP7;I6N6Q6;I3Q4M2;I3	cox2;COX2;COII;MT-CO2	4353500000

	PYD8;I2E7Z7;H9S868;H9S5Y2;H9S054;H9RV93;H9RJL3;H9RF01;H9RD12;H9RAX1;H9QLC8;H9QH59;H9Q9T5;H9PWQ9;H9PMX8;H9MK30;H9M675;H9LMC2;H9E7D1;G9LG51;G9LB98;G8JF18;G5D8Q5;G4W3U1;F2WJ84;F2WI31;F2WGV2;F1CIN6;F1AZF2;F1AZ87;E9P659;E7E4E0;E7CNQ9;E7CM18;E5FWC0;E5EWR3;E5EWL4;E5E1V1;E5E1A6;E2JFC4;E0AF97;D2IKF4;C8Y3Q5;C8XWJ6;C5H6M4;C5H6M3;C5H6K7;C5H6K6;C5H6K5;B5M7M0;B3DE06;B2XP28;B2XL43;B2XIR3;B2WRY8;B1W855;A7LFA2;A7LF11;A6ZHA9;A6ZFK3;A6ZF47;A6ZEU4;A6Z3M5;A1Z455;A0SA07;A0S3T1;A0S2P1;A0A1B1PEN9;A0A1B0W3A7;A0A1B0W1P0;A0A1B0W0T5;A0A143G082;A0A143FZ56;A0A0R6NEC0;A0A0N6YNR7;A0A0E3JSF1;A0A0E3JG40;A0A0D4WSL8;A0A0B5E697;A0A068IXK4;A0A059SAH5;A0A059S8A4;A0A059S2S6;A0A059S242;A0A059RVU8;A0A059RUP9;A0A059RTZ6;A0A059RRR2;A0A059RR09;A0A059RQT0;A0A059RQQ2;A0A059RQI1;A0A059RPV8;A0A059RP05;A0A059RNV8;A0A059RMK0;A0A059RLH3;A0A059RKX5;A0A059RKP1;A0A059RJF0;A0A059RIZ2;A0A059RIQ8;A0A059RI85;A0A059RI53;A0A059RFY4;A0A059R1T0;A0A059QVH0;A0A059QTW9;A0A059QS59;A0A059QQA7;A0A059QPY9;A0A059QPU3;A0A059QPE9;A0A059QPE7;A0A059QLX8;A0A059QI72;A0A023QZ25;A0A1B0W1E4;A0A059RUZ1;H9STE0;P00403;Q14XT3;V9JD22;Q8HNR6;Q7YEH2;Q0Z7D8;L7NVC9;G8JE99;G5D8N2;G5D8K6;G5D8J3;G5D8C8;G5D863;G4W3M6;C5H6M8;B3GUF3;A0A1B0VYS2;A0A0D4WQL7;A0A0D3MLN1;A0A097PWY7;A0A059RRG1;A0A059RQ10;W8DBX9;U3L556;Q7YCE6;Q5SA98;Q4GCC3;Q4EZD4;Q0Z7F1;Q09U41;N0BMC4;K7X9X2;H9T3W9;H9SA70;G9LKX8;G9LHJ5;E5E079;E5DZN4;D1G421;C8Y3G4;C5H6M7;C5H6M5;B2CB37;A0A0P0C1B5;A0A0D4WR75;A0A097Q0T5;A0A068BY99;A0A059RSL1;A0A059RNF8;X2C841;R9Y478;H9RKS9;H9RA87;E5EWG2;C5H6L3;B2XHT9;A0A059RZV1;A0A059RX67;A0A059RHY7;A0A059QPT6;A0A059QPR4;X2D4T8;K7WG81;H9E7B8;H9E779;A0A1B1PEM6;S4UQ76;Q9B1F9;Q4F6A2;Q4EYL1;L7YNE0;H9SYF8;H9RJM6;G9C8L9;E9LAG1;E2JJS5;D7NUN3;D5M8T1;D3YPT7;D2K1G3;B2XHF9;B0Z6W4;A7LDC6;A6Z6E8;A6YXV0;A4ZKZ0;A1Z4V2;A0S0W7;A0A141ZQJ3;A0A141ZQA2;A0A0E3D6T2;A0A097PYA5;A0A097PX98;A0A068BTX8;A0A068BST3;A0A068BP29;A0A023QRX9;A0A023QCZ2;Q0Z7K3;V9J3C6;V9J128;A6YW54;A0A059RIK5;A0A059RHR2;D3WYY8;B2YKU2;X2D541;H9E7E4;H9T056;G9LAZ4;B2XPS3;Q8HQB7;H9E792;A6YWD1;A0A059QTV7		
140	I3L1P8;Q6IBH0;Q02978	SLC25A11	4346900000
141	Q9GZT3;A0A087WUN7;H0YJ40;G3V4X6;G3V2S9;H0YJW7	SLIRP	4312600000
142	O00411;Q4G0F4;Q59E91;B4DZE5	POLRMT	4175700000
143	Q9NVH1;B4DPK2;B4DGD5	DNAJC11	4027600000
144	D2Y6Y7;D3WYZ0;A0A098CMI8;A0A098CL94;A0A098CL77;A0A098CJX4;Q14XY3;A0A0D4WP22;A6ZHM2;K7WIJ6;A0A059QQB7;A0A075X6H8;A0A075X6V9;A6ZGJ0;G9LC49;A0A0Y0GJV2;X5CJR1;X5CIF1;X5CFG7;X5CDZ8;X5BZD6;X5BWE9;X5BW47;X5BSQ0;X5BSN2;X2CNL3;X2C587;W8DFC5;W8DBL0;W8D9J2;W8D8V4;W8D5L5;W8D5F7;W8D2P9;W5VMK3;W0C8M5;W0C6Y6;W0C6A8;V9NAZ0;V9N8I7;V9N5U4;V9N4L5;V9K6C5;V9K4I6;V9K052;V9JTU3;V9JF96;V9JB23;V5JTX2;V5JSZ5;V5JSF4;V5JS27;V5JQM7;V5JMC8;V5JH69;V5JGY5;U5YWI5;U5YV11;U5YSN6;U5L389;U5L326;U5KQ12;U5KPX6;U3LUU5;U3LS18;U3LRA8;U3LQN5;U3LCA2;U3LBN0;U3LBH8;U3LBD0;U3L924;U3L4G0;U3L3I1;U3L335;T2HJH9;T1WUI6;T1SXS5;T1SWT7;T1SUY8;T1STW0;T1STR3;T1STG6;T1SSU2;T1SSS1;T1Q6J8;S5SA44;S5S9I7;S4V2L4;S4UQD8;S4SQC6;R9ZRI6;R9ZPP1;R9ZP27;R9Y9G5;R9Y9A7;R9Y9A2;R9Y5X7;R9Y4V1;R9Y4G7;R9Y3L7;R9Y256;R9UCI0;R4IBN0;R4IA57;R4I9Q0;R4I9N7;Q9B2W7;Q9B2V5;Q9B2U2;Q9B1L8;Q9B1K9;Q9B1D3;Q9B1A9;Q9B185;Q8WCX3;Q8WCX0;Q8WCW5;Q8WCV8;Q8M7T2;Q8HNQ5;Q8HBV1;Q85KZ2;Q85KY8;Q85KV7;Q85KU2;Q85KT4;Q85KR7;Q85KR5;Q7YEG6;Q7YEG4;Q7YEF3;Q7YEE6;Q7YED8;Q7YED4;Q7YED3;Q7YED2;Q7YCH3;Q7YCG6;Q7YCD5;Q7YCD1;Q7Y843;Q7Y788;Q7Y6X6;Q6VLT0;Q6VLP4;Q6VL11;Q6VKS1;Q6VJI3;Q6VJ77;Q6VIX0;Q6VHW2;Q6VHL0;Q6VHB0;Q6VHA0;Q6UG00;Q6RRX7;Q6RRV0;Q6RRA9;Q6RQW5;Q6RQU7;Q6RQR1;Q6RQ23;Q6RNJ5;Q6RNI4;Q6RNG3;Q6RMK9;Q6RLU8;Q6RLS1;Q6RKY6;Q6RKX7;Q6R0Z3;Q5XSM6;Q5XS83;Q5SB97;Q5SB58;Q5SAZ3;Q5SAH4;Q5SA70;Q5S9N8;Q5S9J9;Q5S9H3;Q5S9G0;Q5S956;Q4ZFD4;Q4ZFC1;Q4ZEL1;Q4ZEI5;Q4ZEE6;Q4VGD2;Q4VFU7;Q4VFM9;Q4VFK9;Q4VFF2;Q4VFB5;Q4GV61;Q4GUH7;Q4GU60;Q4GT85;Q4GSG2;Q4GSE9;Q4GRN9;Q4GR70;Q4GR31;Q4GQZ2;Q4GQS7;Q4GQR4;Q4GQ17;Q4GPN7;Q4GPF9;Q4GMY9;Q4GM79;Q4GL52;Q4GKN3;Q4GK64;Q4GJ37;Q4GIK5;Q4GH61;Q4GFR7;Q4GFI9;Q4GFH6;Q4GEP0;Q4GE32;Q4GDK0;Q4GDG1;Q4GD70;Q4G992;Q4G8Y8;Q4G8X5;Q4F6K4;Q4F5T1;Q4F5R8;Q4F5G4;Q4F5F1;Q4F4Z6;Q4F4R7;Q4F4F0;Q4F4D7;Q4F459;Q4F407;Q4F3S9;Q4F3R6;Q4F2Y0;Q4F296;Q4F0V2;Q4F0F9;Q4F0E6;Q4EZ28;Q4EYS4;Q4EYJ6;Q4EXV0;Q4EXN4;Q4EXI2;Q4EXG9;Q4EXF6;Q4EWS2;Q4EWN3;Q3S988;Q2LHW7;Q2LH31;Q2HLG7;Q2HLF6;Q2HL94;Q2HL42;Q27GX8;Q15IZ5;Q15IL5;Q15IK2;Q15GW9;Q0ZK81;Q0ZK68;Q0ZFG9;Q0ZFE3;Q0ZEN3;Q0Z7R3;Q0Z7K1;Q0Z7G2;Q0VXH8;Q0VW08;Q0VV46;Q09U65;Q06UF8;Q06U80;L7YL59;L7YKA8;L7Y075;L7XTN8;L7XLN7;L7XKE8;L7XJ25;L7SRW4;L7SKU1;L7SDL5;L7P4X9;L7NVL6;L7NV50;L7NV23;K9R230;K9MX48;K9M3B9;K7WVK3;K4GY12;J7K441;J7HTA3;J7HST1;J7HR34;I7D8P0;I6R7U9;I6MMM6;I6MDZ8;I3Q8L5;I3Q6Q2;I3Q644;I3Q4T9;I3Q4R3;I3Q468;I1E4I7;I0B6N6;H9T7A2;H9T776;H9T6E2;H9T5P5;H9T335;H9T0U2;H9SZG1;H9SY95;H9STU8;H9STS2;H9SRX2;H9SRS0;H9SR23;H9SP73;H9SNR7;H9SHT7;H9SH14;H9SF77;H9SEJ3;H9SDV9;H9SBL6;H9S9Y1;H9S8D5;H9S385;H9S0I6;H9RZ95;H9RY47;H9RVR5;H9RTM9;H9RQ86;H9RQ40;H9RN98;H9RLD9;H9RKF1;H9RJH6;H9RHH4;H9RCN4;H9RCE3;H9RB12;H9R9T3;H9R203;H9QWE0;H9QVF2;H9QVC6;H9QTU3;H9QSY1;H9QRR5;H9QRN9;H9QQA8;H9QPX8;H9QP16;H9QLE3;H9QJB5;H9QH48;H9QEH5;H9QD83;H9QBC0;H9QA54;H9Q9E4;H9Q2V6;H9Q2F0;H9Q0D5;H9PYL1;H9PTZ9;H9PQV7;H9PQP2;H9PNM7;H9PLI6;H9PI66;H9PFC8;H9PCV7;H9P592;H9P4K8;H9P4E3;H9P4A4;H9P1N1;H9P0H8;H9P048;H9NZ34;H9NXQ3;H9NTE5;H9NSN5;H9NRK8;H9NRA4;H9NQF5;H9MSB7;H9MN09;H9MIG0;H9M442;H9M3X7;H9LRH8;H9LPU2;H9LP54;H9LLS3;H9LLP7;H9LL75;H9LKN6;H9LKK9;H9LJM3;H9LH24;H6WIT7;H6WHW2;H6WHI2;H6WH00;G9LMV6;G9LLL4;G9LLD6;G9LKE8;G9LI16;G9LGW3;G9LGH0;G9LFU9;G9LES2;G9LE51;G9LC88;G9LBA0;G9LB87;G9IES7;G9B0G4;G8JD62;G5D8J5;G4W2G2;G4W1R5;G4W1K0;G4W157;G4W0D4;G4VZS6;G4VZQ0;G4VZM4;G4VZ16;G3C9Y6;G1JYS7;F8VBB0;F8V4U1;F8V422;F8V3Y3;F6N1T4;F6K6M4;F5BA93;F2YWM7;F2WIP1;F2WIH6;F2WID7;F2WI85;F2WHZ4;F2WHS9;F2WGR5;F2WGM6;F2WGK0;F2WGE8;F2WG57;F2VPX4;F1CIQ1;F1CIE7;F1B850;F1B837;F1B824;F1B811;F1B7N7;F1B6U5;F1B5V5;F1AZB5;F1AZ37;E9P7C2;E9P6Q2;E9P2Y5;E9NKT2;E9NJY3;E9NA19;E9LCR9;E9K9C5;E9JXI6;E7E3U7;E7E3S1;E7E3A2;E7E2Y5;E7CPM3;E5QCD4;E5QBE8;E5LR28;E5KYE2;E5FWR5;E5FWN9;E5F549;E5EXA0;E5E1V3;E5E1S7;E5E1Q1;E5E143;E5E0W5;E5E0V2;E5E0T9;E5E0Q0;E5E0L1;E5E0I5;E5E0C0;E5E094;E5E042;E5E003;E5DZZ0;E5DYSE5;E5DZS5;E5DYX6;E5DYK9;E5DYI3;E5DYF7;E5DYE4;E5DY40;E3W6H4;E2JKH1;E2JKF8;E2J3Y5;E2FQ77;E2DGN9;E2DG83;E1B4I5;E1AXS4;D9MZX0;D9MYY6;D8L4E5;D8L3N5;D8L392;D8L327;D8L1J0;D7SF29;D7PAH3;D7P9M4;D7P9H2;D7P9F9;D7P9D3;D7NUP8;D7NMC1;D7NMA8;D7NM56;D6R7T3;D6R6F7;D6R5S3;D6R5P7;D6N7S2;D6N624;D6N5X2;D6N474;D6N3H7;D6BZN8;D6BZD4;D5K701;D5I8G5;D5I8A0;D5I7X0;D5I7T1;D3KD25;D3KAZ0;D2Y572;D1G3Z7;D0VDU7;D0V1V0;D0UTX4;D0UTW1;D0UTS2;C9D6E1;C9D637;C9D5T3;C9D5C7;C8YI12;C8YHY6;C8YGB4;C8YFB3;C8YDR7;C8YCE9;C8Y6T6;C8Y5J4;C8Y3L8;C8Y0Y2;C8Y007;C8XV28;C8XV02;C8CCZ1;C8CCX8;C7SJ	ATP6;atp6;MTATP6;ATPase6;MT-ATP6	3898100000

	U5;C7SJA0;C7B333;C7AAU4;C5MN37;C0LU52;C0LJY4;B9U5I9;B9EFX3;B9EFL9;B9EEV9;B9EDY4;B9EDU5;B8XZR3;B8XYH1;B8X5R9;B8X4J0;B8RFM5;B8R3B7;B7ZIX9;B7TPA5;B7TCM6;B6RGC6;B5M880;B5M7X6;B5M7I3;B4YG72;B4YD67;B4YBC1;B4YBA8;B3DE99;B3DE47;B2Z680;B2Z592;B2YAA3;B2Y9P5;B2Y9B5;B2XQ41;B2XNN7;B2XM45;B2XKS8;B2XKN9;B2XKM6;B2XK18;B2XI44;B2XHM6;B2XHD6;B2XGZ3;B2XG09;B2XFD8;B2XEZ6;B2XER9;B2XEL7;B2XEH8;B2WS29;B2MZ69;B2MZ39;B2MYP5;B2MXH9;B2KLZ5;B2KLT0;B2KLM8;B2KLD7;B2D5C6;B2D4T1;B2D3Q0;B2D398;B2D0N3;B2CB39;B2CB26;B1PI24;B1NUN5;B1NTU9;B0EWL8;A8WF83;A8WDK6;A8R1T6;A8QTE5;A8QT67;A8JLH9;A7XUC2;A7XTZ0;A7XTK2;A7XSM8;A7LDA2;A6ZIR4;A6ZHP8;A6ZG24;A6ZFB4;A6ZF88;A6ZEV9;A6ZET3;A6ZEL8;A6ZCZ8;A6Z7G3;A6Z7D7;A6Z6R7;A6Z698;A6Z659;A6Z571;A6Z4T0;A6Z2Z4;A6YYN7;A6YXS6;A6YX94;A6YWX8;A6YW69;A6YW31;A6YVS8;A6YVQ2;A6YVN9;A6YUU0;A6YUS7;A6YUI6;A5JYK3;A4ZYE7;A4ZM68;A4ZM04;A4ZLL3;A4ZLA9;A4LB80;A4GYN0;A4GWW2;A3R0R5;A3FPA1;A1Z519;A1Z4L3;A1Z4G1;A1Z4E8;A1Z496;A1E1T6;A1E1E3;A1DVF1;A1DV99;A1DTI3;A1DTA5;A0SCX3;A0SBX2;A0SBS0;A0S590;A0S525;A0S3X2;A0S3K5;A0S2V8;A0S2R9;A0S2H8;A0S2B3;A0S1G1;A0S0Z5;A0S0T0;A0A1B2RCV6;A0A1B1PER3;A0A1B1PEP3;A0A1B1PEM5;A0A1B1PEM2;A0A1B0W9M1;A0A1B0W800;A0A1B0W6X2;A0A1B0W5Q2;A0A1B0W446;A0A1B0W2H6;A0A1B0VZK8;A0A1B0VYI1;A0A1B0VY34;A0A167L959;A0A143FZ00;A0A143FYU0;A0A143FYN5;A0A143FYL2;A0A141ZTF9;A0A141ZRV0;A0A141ZRP8;A0A141ZQA4;A0A140DII8;A0A140DFM4;A0A109QFB8;A0A0X8DB89;A0A0S3IUU7;A0A0S3CR60;A0A0S1VVC4;A0A0S1S5W2;A0A0R6NAJ0;A0A0R4RWH1;A0A0R4RTL7;A0A0R4RET0;A0A0R4QTT8;A0A0R4QGQ9;A0A0R4QEB8;A0A0R4Q8V5;A0A0R4PX07;A0A0N9Q9K1;A0A0N7APK3;A0A0N6YMR1;A0A0N6YMF5;A0A0K1HR82;A0A0K1HQC4;A0A0G2T4D3;A0A0E3X7Q1;A0A0D4WSH3;A0A0D4WPX0;A0A0D4BLN4;A0A0D4BKT5;A0A0B5H1L7;A0A0A0QMI3;A0A097QD97;A0A097QCA4;A0A097QB54;A0A097Q610;A0A097Q3M6;A0A097Q3H9;A0A097Q1W7;A0A097Q1B9;A0A097PZD5;A0A097PYS3;A0A097PYQ8;A0A097PY54;A0A096YAI4;A0A096Y961;A0A096Y7G3;A0A096WX18;A0A096WTX2;A0A096VZZ3;A0A096VY74;A0A096VTP9;A0A076MLZ1;A0A075X6V4;A0A075QVS9;A0A075QTM4;A0A075C9B0;A0A075C8F1;A0A075C811;A0A075C7X8;A0A075C7R9;A0A068CCX5;A0A068CBC4;A0A068C9R9;A0A068C3D5;A0A068C1D0;A0A068BYY3;A0A068BXU9;A0A068BUX7;A0A068BUM1;A0A068BQR7;A0A068BNY9;A0A068BKC1;A0A060BKR4;A0A059VCQ6;A0A059S7N3;A0A059S701;A0A059S1D9;A0A059RXE0;A0A059RW04;A0A059RVW3;A0A059RUY3;A0A059RU34;A0A059RTL6;A0A059RTC0;A0A059RS84;A0A059RRH2;A0A059RR79;A0A059RPU4;A0A059RP18;A0A059RNJ2;A0A059RNF3;A0A059RND0;A0A059RMA1;A0A059RL82;A0A059RKH8;A0A059RJ29;A0A059RIS0;A0A059RIN6;A0A059RHU8;A0A059RHL4;A0A059RGC7;A0A059QWC2;A0A059QSI6;A0A059QR71;A0A059QR26;A0A059QQZ9;A0A059QQT5;A0A059QPL3;A0A059QLY9;A0A059QLQ9;A0A059QJ47;A0A059QIY9;A0A059QGJ9;A0A023R5M9;A0A023QZN9;A0A023QYE6;A0A023QW19;A0A023QTT5;A0A023QMV4;A0A023QLJ8;A0A023QHY5;A0A023QGP6;A0A023QFT6;A0A023QEV0;A0A023QEM9;A0A023QE67;A0A023QD05;A0A023Q9F0;A0A023Q7H2;A0A023Q788;A0A023Q2S3;A0A023I989;A0A023I930;A0A023I8Y9;A0A023I8R5;A0A023I8J4;A0A023I8F6;A0A023I889;A0A023I7V4;A0A023I7N7;A0A023I7L8;A0A023I7H5;B2Z4U9;B1PIH2;A0A096VTU4;P00846;W8D860;V9M6K4;V5JPE6;U3KWA8;Q7Y802;Q4ZF95;Q1ZY36;L7SA60;J7HRK4;H9SAF0;H9P6L0;F2WHK1;E9K908;D8L3B8;D6C298;B2YBN4;B1W8I7;A6ZB88;A0SB36;A0A0E3T137;A0A0E3D7F5;A0A096W0M4;A0A096VYY1;A0A096VW93;A0A059RLI7;A0A023I8F1		
145	A0A0C4DGS1;A0A024RAD5;P39656	DDOST	3757700000
146	P82932	MRPS6	3652100000
147	A0A0A0MRK6;Q13505;A0A0C4DFQ1	MTX1	3624200000
148	P51970;B7Z768	NDUFA8	3425200000
149	A0A024R4X0;P00387;B1AHF3;Q6ZVI6	CYB5R3	3334500000
150	Q9P0J0;B4DEZ3;K7EJE1;E7ENQ6;B4DQP1	NDUFA13	3280400000
151	A0A024R4H0;Q02809;B2R5M9;B4DGN8	PLOD1	3267400000
152	V9HWB4;P11021	HEL-S-89n;HSPA5	3260500000
153	G3V0I5;E5KNH5;P49821;Q53G70;Q96ID4;B4DE93;B4DUN7	NDUFV1	3230100000
154	A0A024R5X7;O76031;Q9H072	CLPX;DKFZp586J151	3192600000
155	P30837;B4DLJ0	ALDH1B1	3078100000
156	A0A024RBX9;P08559;Q53GE3;A5YPB6	PDHA1	2997900000
157	Q9BTT5;Q16795;A8K4V2	NDUFA9	2949200000
158	A4D1T3;Q3KRB4;Q9Y291;C9JBY7	MRPS33	2938700000
159	P35908	KRT2	2913400000
160	Q9BSF4	C19orf52	2894600000
161	B4DFL1;A0A024R713;P09622;E9PEX6;B4DMK9	DLD	2846800000
162	P30048;Q53HC2	PRDX3	2773300000
163	A0A024R6C9;P36957;Q6IBS5;Q86SW4;Q86TQ8;Q86TW7	DLST	2759800000
164	F5GZS6;J3KPF3;P08195;B4E2Z3;A0A024R599	SLC3A2	2701200000
165	A0A0S2Z591;O00165;Q5VYD6	HAX1	2685200000
166	A8K7J6;Q86TS9;G3V3U6	MRPL52	2645000000
167	P11177;C9J634	PDHB	2634300000
168	G3V325;B4DJ38;Q3ZB84;A4D273;O75127;Q3SYP6;B3KMD7	ATP5J2-PTCD1;PTCD1	2580000000
169	Q6NUK1;B7ZB41;B4E290	SLC25A24	2578000000
170	A8K761;O96000;H3BPJ9;H3BV16	NDUFB10	2556300000
171	Q3MIH3;P62987;M0R2S1	UBA52	2553100000
172	P27824	CANX	2455200000
173	D3DVL7;B4DU42;Q969Z0;B3KRS4;B3KMT3;B3KM73	TBRG4	2451900000
174	B4DLN1;B4E1E9	N/A	2436300000
175	Q96ER9;A0A024R2V4	CCDC51	2427900000
176	Q8TAS0;P36542	ATP5C1	2425900000
177	Q9UHQ9;H7C0R7	CYB5R1	2402800000
178	Q8TB01;Q6NWZ1;A0A024RBH2;Q07065;B3KVX6	CKAP4	2312100000
179	P12532;F8WCN3;B4DFE8;E9PCP8;B4DH34	CKMT1A;CKMT1B	2309700000
180	A0A0S2Z2Z3;O75027;A0A087WW65;B4DGL8;B3KM98	ABCB7	2307400000
181	Q547S8;Q16134;B4DEQ0;A7UNU5	ETFDH	2305400000
182	Q7Z518;A8K413;A0A087WXC5;A0A024R4B3;E7ESZ7;O95299;Q53SW4	NDUFA10	2279900000
183	B4DMF5;E9KL48;P00367;B4DMG8;Q53GW3;B3KT18;A0A140VK14;P49448	GLUD1;GLUD2	2272900000

184	Q71UA6;Q15758;M0QXM4;Q59ES3;B4DE27;M0QX44	SLC1A5	2244200000
185	Q2M1J6;S4R3Q9;J3KNA0;Q15070;E7EVY0	OXA1L	2228400000
186	B3KY51;Q8NC60	NOA1	2197600000
187	Q9P032	NDUFAF4	2160700000
188	Q9NPL8;C9JU35	TIMMDC1	2058400000
189	A0A140VJX1;P24752	ACAT1	2045900000
190	A0A087WVM4;B7ZM99;Q6UB35;B2RD24	MTHFD1L	2009200000
191	Q9BU61	NDUFAF3	1993900000
192	Q96IX5	USMG5	1989000000
193	Q9NZE8	MRPL35	1947800000
194	Q567R6;A4D1U3;Q04837;A0A0G2JLD8;E7EUY5;B7Z268;C9K0U8	SSBP1	1897500000
195	Q5JP53;Q5SU16;P07437;B7ZAF0;B4DY90;Q5ST81;Q6LC01;Q9BUU9;B4E052;B7ZAK1;B4DQN9;B2R6L0;Q9BVA1;Q13885;B4DMU8;Q1KSF8;Q96B85;B4DXZ5	TUBB;TUBB2B;TUBB2A;XTP3TPATP1	1880600000
196	F8W7Q4;Q96A26;E9PH05;B4DF97	FAM162A	1760400000
197	P13073;H3BPG0;H3BN72;H3BNV9	COX4I1	1698800000
198	B3KT06;B3KPS3;P68363;A8JZY9;P68366;B4DDU2;F8VVB9	TUBA1B;TUBA4A	1675500000
199	A0A024RA60;Q9GZY4;B3KUH1;C9JA07	FLJ10803;COA1	1624600000
200	A0A087WYF7;Q6UXV4;A0A087WUX8;Q68DW4	APOOL;DKFZp779P1227	1601900000
201	A0A140VJK2;Q53T76;P43304;A8K1Z2;B7Z601	GPD2	1576000000
202	P54709;D3DNF9	ATP1B3	1570500000
203	A0A024RDH9;Q9Y3D5;H0YAG5;D6RCM2	MRPS18C	1527300000
204	P82921;A0A075B746	MRPS21	1520700000
205	B4DY23;Q54A51;P35613;B4DNE1;A0A087X2B5;I3L192;A0A087WUV8	hEMMPRIN;BSG	1500400000
206	L0R5D5;Q9BUB7	TMEM70	1466800000
207	A0A140VK29;Q9HCC0;D6RD67	MCCC2	1426500000
208	A0A024R9U3;Q9NX40;D6RG39;D6RIT9;D6RDK6;D6RBN5	OCIAD1	1422300000
209	Q9BQ95;K7EPL5	ECSIT	1358900000
210	E9PJH7;Q9H936;A0A0D9SEI9;A0A0D9SFE1;A0A024RCA6;K4DIB8;K4DIA8;E9PS95	SLC25A22	1354800000
211	B7Z9F3;O75431;C9JNK6;B3KM74;C9JAZ1	MTX2	1329200000
212	Q9NSE4;A8K5W7	IARS2	1323700000
213	Q96DP0	N/A	1312300000
214	B4DVB7;A0A024R3S3;Q8NI60;Q5T7A2;B4DN23;B4DED1;A1L377	CABC1;ADCK3	1311600000
215	Q13850;B1AH87;P30536;Q8N730	TSPO;PBR	1309700000
216	O75616;J3QSB2;J3QRV9	ERAL1	1294100000
217	Q9NWS8;Q5SZ82;A0A087WXU0	RMND1	1270800000
218	P18077;C9K025;F8WBS5;F8WB72	RPL35A	1256600000
219	A8K8B7;Q14409;P32189	GK3P;GK	1255400000
220	Q5HYD9;H3BUX2;J3KNF8;O43169;D6RFH4	DKFZp686M0619;CYB5B	1243600000
221	A0A0S2Z3L2;P16615;H7C5W9	ATP2A2	1240300000
222	Q9UDW1;Q9P012;Q9NZY4	UQCR10	1231300000
223	P30050;Q59FI9;D3DS95	RPL12;hCG_21173	1203400000
224	Q8N766	EMC1	1195500000
225	A0A024R670;A0A087WUM0;P57105;A0A087X1F5;A0A087WYV9	SYNJ2BP;SYNJ2BP-COX16	1188600000
226	Q96EH3	MALSU1	1175000000
227	A0A024RB87;P61224;E7ESV4;A0A0J9YXB3;F5H7Y6;A6NIZ1;F5GX62;F5H823;B7ZB78;F5GZG1;F5H004;B7ZAY2;Q9BXV4;F5H6R7	RAP1B	1145300000
228	A0A0A0971;Q9NYY8;B3KMB8	KIAA0971;FASTKD2	1131400000
229	A0A024R9L0;Q9Y375;H0YL22;H0YNN4;H0YNB7	NDUFAF1	1125800000
230	Q6P4A7	SFXN4	1122800000
231	A0A024RBY9;P53701;Q68D50	HCCS;DKFZp779I1858	1109700000
232	Q6IBC4;O75380;D6RBT3	NDUFS6	1102600000
233	A0A075X8B5;H9E785;A0A059QSR8;A0A141ZSL4;A0A141ZQA8;Q1ZY32;X5CDJ3;X5BLB3;W0C568;V9N9T2;V9N9H0;V9N518;V9JFH6;V9J5G3;V9J548;V9J0Z6;V9IZQ9;V5JGF7;U5ZDA5;U5YYT3;U5YXJ5;U5YT86;U3LDR4;U3L8P3;U3L6U8;T2HMQ7;T1Q5B1;T1Q517;S5RPJ8;S5RLC1;R9Y4Q4;R9Y4D9;R9Y457;R9Y323;R9Y0J8;Q9B2Y7;Q9B2Y5;Q9B2X8;Q9B2X6;Q9B2W5;Q9B2W2;Q9B1S7;Q9B0T8;Q8WCZ0;Q8W8T1;Q8HNR0;Q8HG25;Q8HCA7;Q8HB66;Q85KY1;Q7YEE1;Q7YCF7;Q7YCD8;Q7YCC8;Q7Y891;Q7Y7S0;Q7GSH8;Q6VLU5;Q6VL53;Q6VI80;Q5XTH1;Q5XRD0;Q5SAV0;Q5S8X4;Q541L8;Q4GR66;Q4GQY8;Q4GQ65;Q4GJP1;Q4GJM8;Q4GI32;Q4GGG0;Q4GE93;Q4G8Y4;Q4G822;Q4F6A9;Q4F2K9;Q4F0N3;Q4F0G8;Q4EWT1;Q305P2;Q305M9;Q305J0;Q305G4;Q2LHT7;Q2LHB8;Q2L718;Q20CX0;Q1W0W1;Q06T62;L7XVX3;L7XPG1;L7XNH9;L7XL84;L7SDG0;L7NVW2;K9M3N5;K7WII4;K7WG77;I6QD14;I6PNE4;I3Q2C2;I3Q1M5;I3Q1J9;I3Q0R3;I3PZE5;H9T2B6;H9SV05;H9RSM7;H9REP0;H9RBN7;H9R171;H9R0S8;H9R0H4;H9QUS2;H9QH13;H9Q5H0;H9Q5A5;H9PF15;H9PAU6;H9P9L7;H9P619;H9NQH2;H9MW73;H9M485;H9LKR2;H9LHT0;H9EC08;H9E7P1;H9E7L5;H9E7I9;H9E7B1;H9E798;H9A727;H6TX00;G9LMZ9;G9LHQ3;G9LGD5;G9LGA9;G9LFX9;G9LFL2;G9LCN5;G8JB22;G3CA55;G3CA03;G3C9Z0;G1FK64;F8RZZZ;F8RZC1;F2WMZ9;F2WJ90;F2WII0;F2WIG7;F2WIF4;F2WFX0;F2WFC5;F2WE98;F2WE72;F1B7S4;F1B6R0;F1B6B7;F1B678;F1B5Y7;E9P678;E9NKJ3;E9N9V8;E7E4R3;E7E4D3;E5DZE9;E5DYG1;E5DY18;E2J0J0;E2CZ45;E0Y551;E0Y476;E0AG48;D8L3G1;D7SF85;D7NV19;D7NMF1;D6R6Z6;D6R6M6;D6R6G1;D6R5X9;D6C3P6;D6C3M0;D6C1H9;D5K6X9;D5I7Q9;D5I7I1;D2KR58;D2KLI0;D2K1N4;D2K1J5;C9D5S4;C9D5R1;C8YIQ0;C8YD76;C8YCK5;C8Y972;C8Y7K0;C8Y200;C7SMD4;C7SJN4;C7SJJ5;C7B389;B8X5N4;B6ULE4;B4YGU7;B4YBV5;B3GUI8;B3GRN7;B2YA81;B2Y993;B2Y8X6;B2XQV2;B2XQ96;B2XLK5;B2XLC7;B2XJG5;B2XIK4;B2XHT2;B2XEX4;B2KLY6;B2D666;B2D3T4;B2CB95;B2CB43;B1W8J1;B1NU70;B0Z774;A8JMY0;A8JMA7;A6ZHN9;A6ZHM6;A6ZHA3;A6ZGQ9;A6ZER1;A6ZBX6;A6Z4U7;A6Z2B4;A6YWL5;A4ZYF1;A4ZMU2;A4ZMM7;A4ZML4;A4ZMK1;A4ZLX0;A4ZLD9;A4ZLA0;A4ZL74;A4ZL22;A3R0J1;A1Z4C6;A1DV51;A1DUY6;A1DU19;A1DTS8;A0SA68;A0A1B1CX94;A0A143FYP3;A0A141ZT85;A0A140DI23;A0A140DGM9;A0A140DFM8;A0A0R6NAE0;A0A0R4QFI1;A0A0N6YQL0;A0A0N6YMQ4;A0A0N6YMG8;A0A0N6W1U7;A0A0G2UNT8;A0A0G2UI58;A0A0E3T501;A0A0E3T380;A0A0D4WPF4;A0A0D4WPA9;A0A0D4WP47;A0A0D3RJ62;A0A097QFQ1;A0A097PWY9;A0A096YC52;A0A096Y9Q3;A0A096WW63;A0A096WLM0;A0A096WE11;A0A096WBE5;A0A088FS66;A0A075CA14;A0A059S4N3;A0A059S1L1;A0A059S0W6;A0A059RYR9;A0A059RXA6;A0A059RU63;A0A059RTL2;A0A059	ND4;ndh4;NADH4;MT-ND4	1094400000

	RSB1;A0A059RRX9;A0A059RRD2;A0A059RQW2;A0A059RQ43;A0A059RPR4;A0A059RND1;A0A059RN57;A0A059RN05;A0A059RMH3;A0A059RL10;A0A059RKV7;A0A059RIC1;A0A059RI30;A0A059RHV6;A0A059RHA5;A0A059RBT2;A0A059RB77;A0A059R902;A0A059R8T0;A0A059R372;A0A059QWE2;A0A059QW16;A0A059QV08;A0A059QUW1;A0A059QQY2;A0A059QQI6;A0A059QPD2;A0A059QNU0;A0A059QNP1;A0A059QM57;A0A059QLZ1;A0A059QD15;A0A059QAQ3;A0A023QWK0;A0A023QVM5;A0A023QUC2;A0A023QTW4;A0A023QT03;A0A023QQQ9;A0A023QNG3;A0A023QHD1;A0A023QGC0;A0A023QGA7;A0A023Q9G1;A0A023Q6X3;A0A023Q6C7;A0A023I905;B9EES4;B9EEM2;B9EED1;B9EDU9;B9EDF6;B9EDE3;B9ECU8;I7GQD9;P03905;Q4GG69;U5ZC24;T1Q5T0;T1Q5L1;R4IA33;Q9B300;Q7Y7B0;Q6WQ46;Q6VHV8;Q4GI58;Q15HM5;K9R3M7;J7HWK6;E5E147;C8YCP4;B2XIN0;B2XG13;B1W861;A0A143FZ36;A0A0E3X973;A0A0D4WSX9;A0A097QEL5;A0A068BXG7;A0A059RRN19;A0A059RH27;A0A059QQ89;A0A059QP87;A0A023Q9X5;U3LCU1;U3L9L1;U3L8Y8;U3L6N6;U3L6H7;U3L372;S4UQT8;Q9T9Y1;Q9B188;G9LLY5;G5D8N8;G4W3B5;G4W2Y5;G4W2C7;E9LBP6;B1NUU1;B1NUQ2;A6ZF01;A4ZLL7;A0S2T6;A0S2M1;A0A141ZRQ2;H9PDG9;G9LNW0;C9D583;A0A143FYQ0;A0A141ZT07;A0A059RV41;A0A059RTX8;A0A059RMQ2;A0A059QR61;R9Y2B9;Q8WCY0;L7NVA1;H9E7M8;H9E7G3;G5D8E7;G5D869;G5D804;G5D7X8;G5D7V2;B5M7S8;A4ZKZ6;A0A0K1HQ73;A0A075X788;A0A059RVT1;A0A059RQP3;A0A059RLS4;A0A059QTU3;A0A059QH26;B9EDW2;B9ECT5;D8VCQ0;Q2LHW3;F2WNE2;A0A141ZQX9;A0A0E3JSF5;A0A0E3JG42;A0A059QPY2;A0A075X860;A0A075X6Q0;A0A075X6T1;A0A059RKZ9		
234	Q0QEW2;H0YHA7;A0A024QZD1;J3QQ67;Q07020;G3V203;F8VUA6;F8VYV2;B4DDY5;A0A075B7A0	RPL18	1090100000
235	Q5VVD0;P62913;Q08ES8;Q5VVC8;Q5VVC9	RPL11	1073900000
236	J3QTA6;Q9BRQ6;J3QTB2;H0Y922	CHCHD6	1051700000
237	E9PN17;O75964	ATP5L	1050100000
238	A0A024R3J7;P46977	hCG_2032701;STT3A	1041500000
239	B3KMV8;O75746	SLC25A12	1036100000
240	Q02218;E9PCR7;E9PDF2;A0A0D9SFS3;B4DF00;B4DH65;B4DZ95;B4E3E9;E9PFG7;B4DK55;A2VCT3;A2VCT2	OGDH	1032100000
241	Q53G69;O43615;Q9UPE4;M0QXU7	TIMM44;hTIM44	1030100000
242	Q6NZ55;A8K4C8;P26373;J3QSB4	RPL13	1020000000
243	C9J406	IMMT	1018800000
244	Q53HW2;Q53HK9;A8K4Z4;A0A024RBS2;P05388;Q6NSF2;F8VWS0;F8VU65;B4E3D5;F8VW21;F8VZS0;Q8NHW5;F8VQY6;F8VPE8;F8VRK7;G3V210	RPLP0;RPLP0P6	994310000
245	Q7RU05;Q99595;A0PJ74	TIM17A;TIMM17A	985930000
246	Q9NVV4	MTPAP	985810000
247	A8K4V4	N/A	981780000
248	Q6FHM2;P62879;C9JXA5;C9JIS1;C9JZN1;E7EP32	GNB2	971770000
249	P05091;Q53FB6;B4YAH7	ALDH2	959200000
250	Q53ZV6;H9A7H1;D7P652;D7P639;D7P626;B8X5X6;B2XIN1;A0A023REG7;A0A023QG09;X5CM76;X5CKG0;X5CI32;X5CF88;X5CBQ3;X5BYA7;X5BWL7;X5BWF0;X5BVZ3;X5BVA2;X5BV52;X5BPC3;X2JJ49;W8DRA6;W8DIL7;W8DCA6;W8DBU7;W8DBM7;W8DAS2;W8D9V0;W8D9F9;W8D8R1;W0C6Q7;W0C3F1;V9PAU1;V9PAR5;V9PA42;V9NA48;V9N990;V9N6Q0;V9N6J1;V9N5T7;V9N4K8;V9M765;V9K141;V9JYL6;V9JXJ3;V9JTH7;V9JMS4;V9JLL5;V9JJF5;V9JJ03;V9JCX3;V9J1H0;V9IVP1;V9IVA7;V5L8C9;V5L865;V5L835;V5L812;V5JRZ3;V5JQE6;V5JM76;V5JLM6;V5JHW3;U5ZC31;U5Z7S3;U5KP70;U3M3X4;U3M2W8;U3LRZ3;U3LRI3;U3LQT8;U3LC53;U3LC10;U3LAH9;U3L687;U3L5J7;U3L4U4;U3L3U6;U3L3J4;U3L346;U3KX27;U3KWL2;T1SXJ9;T1STG4;T1SS69;T1Q7F5;T1Q6Q4;T1Q687;T1Q5V7;T1PZR2;T1PZM5;S5RMH6;S5RLG1;S4V8X0;S4STV3;S4SQT8;R9YBR2;R9YAG1;R9Y968;R9Y8C8;R9Y676;R9Y628;R9Y5T9;R9Y599;R9Y546;R9Y4N0;R9Y4H2;R9Y499;R9Y3W8;R9Y2F5;R4I9Z4;R4I9L1;Q9B303;Q9B301;Q9B2Z7;Q9B2Y4;Q9B2Y2;Q9B2Y1;Q9B2X2;Q9B2W1;Q9B2V4;Q9B2V3;Q9B2V1;Q9B2U1;Q9B1R0;Q9B1F8;Q9B105;Q9B0V1;Q8WCX8;Q8WCX1;Q8WCW9;Q8WCW7;Q8WCW4;Q8WCW2;Q8WCW1;Q8W946;Q8W8U1;Q8HNR2;Q8HG24;Q8HG21;Q8HG20;Q8HG18;Q8HAS6;Q85KZ0;Q85KW1;Q85KU7;Q85KT3;Q85KS1;Q85KR4;Q7YEG8;Q7YEG3;Q7YEF9;Q7YEF0;Q7YEE5;Q7YED7;Q7YCH1;Q7YCG8;Q7YCG0;Q7YCE8;Q7YCE2;Q7YCC4;Q7Y823;Q7Y7F0;Q7Y6Z2;Q7GXT4;Q7GWT3;Q7GWL6;Q6WQ97;Q6VIZ4;Q6VIX6;Q6VID5;Q6VI79;Q6VHD5;Q6RS00;Q6RRR0;Q6RQI4;Q6RPF2;Q6RNL1;Q6RNJ0;Q6RMM5;Q6RMF4;Q6PZ35;Q5XTE4;Q5XTD1;Q5XT79;Q5XS00;Q5XRG8;Q5XRC9;Q5SB14;Q5SAM1;Q5S9S2;Q5S938;Q5S8W0;Q4ZFF5;Q4VFD3;Q4VFC2;Q4VFA5;Q4GW31;Q4GW05;Q4GVZ2;Q4GVS7;Q4GVA8;Q4GUX8;Q4GUE6;Q4GUC0;Q4GTI4;Q4GSD1;Q4GQ64;Q4GNT3;Q4GMK4;Q4GLM9;Q4GL73;Q4GJP0;Q4GJ06;Q4GI57;Q4GI18;Q4GHL2;Q4GHG0;Q4GG68;Q4GFX7;Q4GF15;Q4GEN5;Q4GE79;Q4GDK8;Q4G9U5;Q4F669;Q4F656;Q4F5V2;Q4F5R3;Q4F568;Q4F4X2;Q4F4F8;Q4F454;Q4F3W3;Q4F2Y8;Q4F2K8;Q4F2F6;Q4F200;Q4F1S2;Q4F0F4;Q4F050;Q4EZS0;Q4EZP4;Q4EZ36;Q4EYP3;Q4EY48;Q4EXY9;Q4EXW4;Q4EXU5;Q4EXP2;Q4EXM9;Q4EWD7;Q3S9H4;Q305W9;Q2LHU9;Q2LHB7;Q2LH26;Q2L743;Q2HKQ7;Q2HKK5;Q2HJQ6;Q27H51;Q27H25;Q1ZY31;Q1W0U7;Q1ADM1;Q1ADK8;Q15II4;Q15ID2;Q15HM4;Q15HL1;Q15HH2;Q15HE6;Q15H42;Q15GZ0;Q15GW4;Q0ZK24;Q0ZFK3;Q0ZFC5;Q0Z7P8;Q0Z7K9;Q06V50;Q06UH9;Q06UC7;N0BU90;M1LMB0;M1LK27;L7XZG8;L7XZ93;L7XYG0;L7XWB1;L7XTW6;L7XTK6;L7XRG1;L7XQ59;L7XPB1;L7XM56;L7XLF4;L7XHT9;L7XH80;L7XEQ0;L7XCA5;L7SC04;L7NV51;L0E7U5;K9R3W5;K9MWA7;K9M4G7;K9JT28;K7WG69;K4GXW9;J7HWP4;J7HV84;J7HU51;J7HR49;J7HPX5;J7HKD4;J7HJU9;I7A0A7;I6QHH7;I6MMN1;I3QAV0;I3QA79;I3Q509;I3Q447;I3Q320;I3Q2U2;I3Q196;I3Q043;I3PY41;I3PXT7;I3PXI3;I3PXH0;I3PX66;H9T7P9;H9T617;H9T5H2;H9T3K9;H9T1U8;H9SZZ8;H9SWI9;H9SSA7;H9SR93;H9SQF7;H9SQD1;H9SKV8;H9SHU2;H9SFH3;H9SFG0;H9S8U6;H9S5W3;H9S5A5;H9S0P3;H9RY26;H9RWA2;H9RNB6;H9RGG5;H9RF34;H9RCL3;H9R7X5;H9QLC2;H9QH53;H9QGG9;H9QG52;H9QF64;H9QDZ8;H9Q5T8;H9Q5E5;H9PUZ2;H9PUS7;H9PRH0;H9PRE4;H9PR79;H9PMN1;H9PHH4;H9PF29;H9PDH0;H9PBX4;H9P8K4;H9P3L2;H9P242;H9NYJ4;H9NS19;H9NQZ2;H9NQH3;H9MSR5;H9MRH3;H9MN27;H9M4T1;H9M4P2;H9M4B2;H9M486;H9M473;H9LPV9;H9LPC0;H9LP57;H9LLT6;H9EBJ0;H9E7S7;H9A8F9;H9A7D2;H9A7B9;H9A780;H7BSQ4;H6WHV4;H6WGQ1;H6TWG9;H6TWF6;G9LMU8;G9LMS2;G9LMI1;G9LLT4;G9LIH7;G9LHQ4;G9LGV5;G9LGE9;G9LG84;G9LG32;G9LFG1;G9LF70;G9LEM5;G9LE82;G9LE56;G9LDN7;G9LDI5;G9LCZ0;G9LCV1;G9LCR2;G9LBA5;G9LB01;G9LAW2;G9IFS0;G9IFA1;G9IER9;G9IE74;G9AZW2;G5D8R2;G5D8Q2;G5D8N9;G5D8L3;G5D8K0;G5D8H4;G5D8E8;G5D831;G5D818;G5D7W6;G4W654;G4W5W3;G4W5R1;G4W5P8;G3CA17;G1FHS3;G0XP03;F8VAF6;F6N669;F2WIK7;F2WGS0;F2WFF2;F1KL67;F1DNK3;F1DMW9;F1DMK2;F1CIP3;F1B6V0;F1B5I2;F1AZ42;F1AZ03;F1AKK4;F1AK74;F1AIH6;E9NZ96;E9NKM2;E9LCI3;E9LB52;E9LAN3;E9L8H9;E9K900;E9JWJ0;E7E4L2;E7E3Z1;E7E2X7;E7E2S5;E7E2R2;E7CM12;E7CLW0;E7BKC7;E5LMD0;E5EXH0;E5EXE4;E5E1U5;E5E1Q6;E5E148;E5E135;E5E0X0;E5DYU2;E5DYP0;E5DYH5;E5DY71;E5DY58;E5DY45;E5DY19;E3W716;E3T7C0;E2JK	ND5;NADH5;ndh5;MT-ND5	950260000

	Y3;E2J0Z7;E2FPA7;E0Y565;E0Y4S2;D9N004;D8L3H5;D7PAQ6;D6R4M5;D6R4G0;D6N5T8;D6N3K8;D6C1N2;D6C0C7;D6C010;D6BZU5;D6BZF2;D6BYR8;D5MBN5;D5M955;D5M8J7;D5M834;D5I8I3;D5I7G9;D3YLI0;D2KR88;D2K1I3;C9EJ80;C9D603;C9D5A6;C9D515;C8YFD1;C8YFB8;C8YDI1;C8YDE2;C8YB23;C8Y7R6;C8Y2D1;C8XZF4;C8XVB1;C7SKZ0;C7SJI3;C7B2Y6;C7AB27;C7AAY8;B9EFN7;B9EFL1;B9EFD3;B9EF68;B9EES5;B9EEN6;B9ED27;B9ED14;B8YQJ5;B8Y0K8;B8XZ47;B8XYT0;B8X5Y9;B8X5N5;B8X540;B8RFZ7;B8RFQ6;B8RF22;B7ZJ75;B7U6Z8;B7TNG1;B7TCV9;B4YFW0;B4YCP0;B4YCD8;B3VEC2;B3GTF2;B2ZHA4;B2YBC2;B2Y9E6;B2XQI6;B2XPU3;B2XNF1;B2XMC8;B2XL89;B2XKZ8;B2XKN1;B2XKK5;B2XK88;B2XK23;B2XJG6;B2XJ88;B2XIC7;B2XHU6;B2XH89;B2XH11;B2XGP4;B2XFN4;B2XEY8;B2XEX5;B2WRM8;B2MZA0;B2KLX4;B2D667;B2D465;B2D400;B2D3J4;B2D322;B2CB44;B1NU71;B0Z7B4;B0Z723;B0EWF8;A9UJI6;A8RC27;A8JMW8;A8JL28;A7XT63;A7XSF3;A7LFH4;A7IZ50;A6ZHZ3;A6ZHU1;A6ZH65;A6ZH52;A6ZGN4;A6ZGM1;A6ZGF9;A6ZFS5;A6ZFN6;A6ZFM3;A6ZFH1;A6ZF67;A6ZCT8;A6ZBM3;A6ZB41;A6Z9T7;A6Z7E2;A6Z7A3;A6Z638;A6Z5B5;A6Z477;A6Z1E0;A6Z0J2;A6YZQ6;A6YZ48;A6YXC5;A6YWH7;A6YUU5;A6YTU4;A4ZYN0;A4ZN07;A4ZMW9;A4ZMU3;A4ZMH6;A4ZM22;A4ZLT3;A4ZLL8;A4ZLE0;A4ZLC7;A4ZLB4;A4ZLA1;A4ZL49;A4ZL36;A3R0P4;A3R0N1;A3R0L8;A1Z550;A1Z4K5;A1Z4H9;A1Z4G6;A1E1L3;A1DVU9;A1DVN4;A1DV00;A1DTY1;A1DTP0;A1DTE9;A1DTD6;A1DT71;A1DSY0;A1DSV4;A1DSU1;A1DSK0;A1DSD5;A0SBQ0;A0SBN6;A0SBJ7;A0SBH1;A0SB29;A0S952;A0S939;A0S8Q9;A0S8I1;A0S4F9;A0S481;A0S302;A0S2X6;A0A1B1PER2;A0A1B1II68;A0A1B1II15;A0A1B0Z3L4;A0A1B0W5P9;A0A1B0W3R8;A0A1B0VZQ7;A0A143FYP8;A0A143FYJ8;A0A141ZT86;A0A141ZT08;A0A141ZSQ4;A0A141ZRB0;A0A140DIT4;A0A140DHV9;A0A109Q807;A0A0Y0K9C3;A0A0X9RUW8;A0A0X8DQV3;A0A0S1S8G0;A0A0R6NC07;A0A0R6NAY1;A0A0R6NAX4;A0A0R6NA86;A0A0R4RWY3;A0A0R4RWT8;A0A0R4RUV0;A0A0R4QNV0;A0A0R4QHI3;A0A0R4QEQ9;A0A0R4Q191;A0A0R4PXT6;A0A0N7G638;A0A0N6YP85;A0A0N6YN55;A0A0N6YMJ0;A0A0N6W203;A0A0K1HQP7;A0A0H4D2V1;A0A0G2URD1;A0A0G2UNX2;A0A0G2UJS2;A0A0G2UIK6;A0A0G2UI99;A0A0G2RGN3;A0A0E3X8V0;A0A0E3T339;A0A0E3T281;A0A0E3T1X7;A0A0E3D705;A0A0D4WR40;A0A0D4WQW8;A0A0D4WQI1;A0A0D4WPH0;A0A0D4WNW9;A0A0D4BJS5;A0A0B6C660;A0A0A7HII9;A0A0A0PJS4;A0A097QFR9;A0A097QEC5;A0A097QA13;A0A097Q961;A0A097Q6P5;A0A097Q5J3;A0A097Q432;A0A097Q1F5;A0A097Q025;A0A097PZZ1;A0A097PYE7;A0A097PWW3;A0A097PW46;A0A096YCI4;A0A096X6L2;A0A096X404;A0A096X3C9;A0A096WZC6;A0A096WXJ5;A0A096WVU0;A0A096WSU0;A0A096WPE3;A0A096WP35;A0A096WK30;A0A096WDB2;A0A096WCN3;A0A096WAH6;A0A096WAC6;A0A096W8J6;A0A096W882;A0A096VW26;A0A096VTC1;A0A076L3M9;A0A075CBC2;A0A075CA07;A0A068C1Y8;A0A068BZI1;A0A068BZ12;A0A068BYG7;A0A068BY57;A0A068BXB4;A0A068BVM3;A0A068BUU2;A0A068BTP6;A0A059SEV9;A0A059SDA4;A0A059S9U8;A0A059RZW9;A0A059RYJ7;A0A059RXT6;A0A059RXC6;A0A059RVW9;A0A059RUF6;A0A059RUA6;A0A059RS62;A0A059RRD7;A0A059RQE3;A0A059RQ72;A0A059RPI5;A0A059RP84;A0A059RP21;A0A059RNJ9;A0A059RNF7;A0A059RMV2;A0A059RMA0;A0A059RLJ1;A0A059RJA1;A0A059RIW6;A0A059RHF0;A0A059RH77;A0A059RD49;A0A059RBG0;A0A059QY45;A0A059QR29;A0A059QQT9;A0A059QQG5;A0A059QQ42;A0A059QQ07;A0A059QPV5;A0A059QP43;A0A059QLA4;A0A059QKL2;A0A059QJ14;A0A059QH44;A0A059QH09;A0A059QFE7;A0A059QB82;A0A023R4U6;A0A023QVC6;A0A023QVA6;A0A023QUA7;A0A023QSS7;A0A023QS10;A0A023QKL5;A0A023QKD1;A0A023QGG0;A0A023QEQ5;A0A023Q7K9;A0A023Q7H6;A0A023Q756;A0A023Q6D2;A0A023I9A5;A0A023I985;A0A023I918;A0A023I900;A0A023I8N5;A0A023I8L7;A0A023I8I7;A0A023I890;A0A023I885;A0A023I807;A0A023I7Z4;A0A023I7R3;A0A023I7R1;A0A023I7N8;T2HLH6;B1W6B2;P03915;A0A0A0PVC5;A0A0A0PQ79;A0A0A0PSC0;A0A0A0PVA5;A0A0A0PMH4;A0A0A0PMP8;A0A0N6YPC3;A0A075X6P1;H9M4C5;Q8HG23;Q8HG22;Q541I1;Q7YEE9;L7XV85;J7HPA7;H9PIQ3;H9MQS6;G9LMC9;G9LCA6;B8XYI9;B2WRG3;A0A1B0W5J6;A0A141ZSL5;A0A141ZQA9;A0A0R6N9S2;A0A0E3DJI4;A0A097PXG7;A0A059RS89;A0A059RIX6;A0A059RHM0;A0A059QNC6;V9J2G5;T1Q5Q5;R9YBG4;R9YB64;R9Y7Y5;R9Y6Z7;R9Y6E0;R9Y550;R9Y4F5;Q9B1M0;Q7YEE0;Q6VKL7;L7XD10;I6N513;I3Q2G2;H9SVQ3;H9E7Y3;H9E7J0;H9E7B2;H9E799;H9E786;G9LGK1;G9LGH5;G5D7V3;F2WH76;F1B816;E5DYL4;D6R4X9;A8QTM8;A1DVT6;A0A096WF12;A0A059RXE4;A0A059RX43;A0A059RS22;A0A059RHT6;A0A059RE98;A0A059QPL7;A0A059QIR2;A0A023QQ40;V9JCN2;V9J4Q5;R9Y2A0;Q5S9U8;Q4EZT3;Q306C1;H9P066;E9NJS3;E2FPE6;A6ZH91;A0A1B0W1E7;A0A059QUY8;A0A023QFH0;X2CH62;R9Y259;Q6VIF3;Q0ZF73;H9STM5;H9RVX2;H9RLB8;H9RK52;H9R0D6;H9QXX8;H9PV83;H9PMJ2;H9PBJ4;H9LNU2;G3LZE0;E2DG88;D0UTS7;A8JMI8;A6ZF93;A6ZE30;A3FP67;A1DTC3;A1DT97;A0S9B7;A0A097Q5V5;A0A059S4S4;A0A059R0K6;A0A059QWC3;A0A023Q8X7;V9JLZ2;V9J3G5;V5L8Q9;U3LBY0;U3LAU0;U3L8P2;R9Y440;Q8WCY9;Q85KW4;Q7YEF2;Q6RMK4;Q4GMF2;Q4F604;Q4F5X8;Q4F5W5;Q4EWF0;L7XYW1;L7SAT6;L7P4C4;K7WBF9;I3Q548;H9S9F4;H9R273;H9Q919;H9Q414;H9PDW3;H9MMA4;H9M499;H9LRM7;H9LMD8;H6TVN3;H6TVI1;G9LM25;G9LLG7;G9LLB5;G9LJ35;G9LIZ6;G9LIG4;G9LI60;G9LI08;G9LEU0;G9LEI6;G9LEE7;G9LDT9;G9LDL1;G9LDJ8;G9IFC7;F2WJ65;F2WII1;F2WIG8;F2WIC9;F2WI64;F2WG10;F2WFG5;F2WF35;F2WF09;F2WEV7;F2WEU4;F2WET1;F2WEB2;F2WE21;F1B6A5;F1AK87;E9LCJ6;E5QAB6;E5FF97;C8Y8P1;C7SJN5;C7B3F5;B8XYL5;B8X5V0;B6E908;B2XL11;B2KM00;B2D4D0;A8JMR6;A8JL93;A3R0K5;A3R0J2;A0SBB9;A0S556;A0S468;A0A141ZQE8;A0A0S1S5N9;A0A0N6YP77;A0A0K1HQL6;A0A097Q0R3;A0A097PX07;A0A096VYN4;A0A076MIL9;A0A075C751;A0A059RSY8;A0A023QTY8;A0A023QSL8;A0A023Q6E7;A0A059RIX9;Q8HG19;E5E1J1;X5CNW6;W0C7J9;V9N397;V9J4S4;V5L8Q1;R9Y487;R9Y3R3;R9Y247;Q9B2Z9;Q9B2Z5;Q7YCF6;Q7YCD9;Q7YCD7;Q7Y6H2;Q6RS27;Q4F340;J7HLE4;I3QB80;H9SXY3;H9S0A0;H9QHJ6;H9PY99;H9E8A0;H6WJ33;H6WIS9;G9LED4;F2YMB8;E9NKP8;E9L8Q7;E9JYF1;E5EXP8;E2CZ46;C9DF68;C9D4X6;C8YGS5;C8YGM3;C8Y4J8;B2XQL2;B2XPM8;B2XH24;B2KMS3;B2D6E5;A6Z901;A6YVZ7;A4ZMY2;A4GYN5;A0A140DHA1;A0A0E3M488;A0A0E3GKZ3;A0A096X0V2;A0A096WB60;A0A096VZ02;A0A088FX07;A0A076LB70;A0A075C8A0;A0A068BS35;A0A059S704;A0A059RKB7;A0A059QPB1;A0A023I954;A0A023I8C1;A0A023I7H2;Q2LHG9;T1Q773;F2WFN0;F2WEL6;F2WHS1;F2WG62;A0A0D4L4T2;A0A059RTM1;R9Y4B7;A0A0N7BBQ4;A0A0N7BB88;A0A0N7B9C5;A0A1B0W1F8;A0A0A0PWB3;A0A0A0PQM4;A0A0A0PQC8;A7IYY2;A0A023QV97;H9SZP4;F2WH89;A0A141ZQW7;A0A023Q8L4		
251	A8K5I0;A0A0G2JIW1;P0DMV9;P0DMV8;Q59EJ3;B4DNT8;B4DWK5;B4DI39;B4DFN9;B4E1S9;B4E388;B4DVU9;V9GZ37;B3KTT5;B4DNX1	HEL-S-103;HSPA1B;HSPA1A	948660000
252	Q9NX47	N/A	947340000
253	P62917;B4DVG7;E9PKU4;E9PKZ0;G3V1A1	RPL8	939900000
254	Q59GY2;P36578;B4DMJ6;B4DFI6;H3BM89;Q53G74;B4DMJ2	RPL4	938870000
255	K7EIR2;A0A140TA84;A0A140TA86;Q5XKP0	C19orf70;QIL1	936490000
256	P54886	ALDH18A1	932990000
257	A4D2P2;A4D2P1;A4D2P0;P63000;A0A024R9T5	RAC1;hCG_20693	927610000
258	B7Z587;P17152	TMEM11	925430000
259	A0A0S2Z514;Q6PML9;A0A024R9W8;B2R745;B4DSU2	SLC30A9	912880000

260	O60568;B3KQQ3;Q9UG85	PLOD3;DKFZp564O1822	910710000
261	A0A024R814;P18124;A8MUD9	RPL7	906140000
262	Q9Y584	TIMM22	905090000
263	E9PH64;Q9Y6M9;B7Z7N1;E7EWZ0;E9PF49;Q9UQS5	NDUFB9	897750000
264	A0A024R3U8;Q8WWC4;H7C0V0	FLJ22555;C2orf47	895270000
265	P62424;Q9BY74;Q5T8U2;Q5T8U3	RPL7A;RP-L7a	881400000
266	Q9P035;H3BPZ1;H3BS72	HACD3	874240000
267	Q6P161	MRPL54	867450000
268	A0A0S2Z5U6;Q96C36;A0A087WTV6;A0A024R3Q9;A0A087WZR9;J3KR12;Q4W8W1;B4DQK8	PYCR2;P5CR2	859370000
269	Q9Y2Z4;H0YHS6	YARS2	839470000
270	Q7Z4X2;Q9NX14	NDUFB11	826070000
271	Q7L8L6;B4DWZ8	FASTKD5	825420000
272	Q4U2R6;A0A087WU28;A0A0B4J2C1	MRPL51	815410000
273	Q9H857	NT5DC2	812920000
274	O14925;Q5SRD1;B4DDK6;B1APJ0;B7ZB25;B4DI18	TIMM23;TIMM23B	805050000
275	E4W6B6;B2R4D8;A0A024R1V4;P61353;K7ELC7;K7EQQ9	RPL27	776180000
276	Q9NUL7	DDX28	772660000
277	Q6IPW4;Q6IB76;E7EPT4;P19404;Q9UEH5;A8K750	NDUFV2	761140000
278	Q549C5;Q9NS69;Q53GB0	MST065;TOMM22	760390000
279	A3KMH1	VWA8	757030000
280	E5KTM5;Q8WVM0;A8K0B9	TFB1M	756640000
281	V5IRT4;Q9BRT2;Q5TAQ0	UQCC2	755930000
282	Q8NBU5;B4E2J1	ATAD1	751320000
283	A0A024R325;Q96I99;Q3ZCW5;E9PDQ8;B7Z2D5	SUCLG2	744070000
284	A8YXX5;A4FVA6;A0A024RD08;A0A024RCX4;Q9NZJ7;Q9Y374;H0Y8C3;Q8IW90	PIG60;MTCH1	738010000
285	Q9UI09;Q53HG1;F8VRD8	NDUFA12	736550000
286	Q969M1;Q9H9G4;B7Z4T8	TOMM40L	732670000
287	P56134;Q53FE1	ATP5J2	730260000
288	Q14204	DYNC1H1	729340000
289	O95140;B7Z3H8;A6NLD2	MFN2	728900000
290	O95831;E9PMA0;A0A140VK04	AIFM1	724620000
291	Q9BW92	TARS2	717570000
292	Q6LES8;E5KSX8;E5KSU5;Q00059;H7BYN3	TFAM	706670000
293	E9KL35;P63244;J3KPE3;D6RAC2;H0YAF8;H0Y8W2;D6RHH4;D6R9Z1;H0YAM7;D6R9L0;D6REE5;D6RFX4;B4DVD2	GNB2L1	705500000
294	B4DH58;A0A087WU53;Q9H0U3;A8MUP5;Q96SP2	MAGT1	699020000
295	B4DS66;H7C463	IMMT	693990000
296	P39023;Q8TBW1;Q96QL0;H7C422;Q9NY85;G5E9G0;B3KS36;B5MCW2;Q49AJ9;Q9BT63;H7C3M2	RPL3;rpl3	689170000
297	Q59E88;Q53G26;Q96EY1;B3KM81	DNAJA3	688490000
298	B2R6K4;A0A024R056;P62873;F6UT28;B1AKQ8;Q71UM6;B3KVK2	GNB1	685730000
299	Q6PI78	TMEM65	675010000
300	Q5VT66;H7BYZ9	N/A	670360000
301	H7C1U8;Q9BUR5;G3V1B6	APOO	662310000
302	B3KTM6;A2RUM7;Q59GX9;P46777;Q5T7N0	RPL5	657540000
303	Q8NBJ5	COLGALT1	656640000
304	Q86Y39;K7EQ77;K7EK78;K7EP35;K7EMT4	NDUFA11	655730000
305	E5RI99;A0A024R9D3;P62888;E5RJH3	RPL30	653600000
306	D6RAN4;Q53Z07;P32969;H0Y9V9;B4E1M5;E7ESE0;B4DLV8;Q2NKY6	RPL9	650410000
307	A0A0S2Z382;A0A0S2Z3G3;Q9UBX3;A0A0S2Z3I3;F6RGN5	SLC25A10	648010000
308	B4DKS0;A0A024R0H1;P53985;B2R6A5	SLC16A1	642220000
309	Q5T160;H0UI22	RARS2;RARSL	640120000
310	A0A024R6U3;O75208;B4DIV2;H3BNT2;H3BPY0;H3BSJ5	hCG_2025883;COQ9	629410000
311	Q6IBH6;P61254;J3QRI7;J3QQQ9;J3QQV1;J3QRC4;J3KTJ8;A0A024RBF6	RPL26;hCG_26523	622790000
312	Q53G17;O00217;E9PKH6;A0A024R5K3;E9PPW7;E9PN51;F8W9K7;B4DYI3	NDUFS8	621770000
313	A0A0S2Z693;Q96RQ3;E9PHF7;F5GYT8;E9PG35;G5E9X5	MCCC1	620880000
314	Q6IB11;O00264	PGRMC1	619850000
315	Q8NBX0	SCCPDH	617480000
316	Q96AG4	LRRC59	614970000
317	J3KPT4;Q9H4I3;Q6XYC5;A0A024R500	TRABD;RP3-402G11.12	613590000
318	Q8NBT6;Q5JPC1;Q9HC21;J3KSI7;J3QL84;J3KS44;J3QLV3;J3KRY6	DKFZp667O1614;SLC25A19	608870000
319	P20674;H3BNX8;H3BRM5;H3BV69	COX5A	603810000
320	B4DSV8;B4DPG9;Q9H3K2;Q6FIA7;B4DNL0;Q9Y6G2	GHITM	601420000
321	A8K1K8;Q9BVV7	C18orf55;TIMM21	579390000
322	A8K7N0;E7EPB3;A0PJ62;B7Z6S8;P50914;A8K3Q9	RPL14	578780000
323	A8K9B2;Q9H9P8;C9JVN9	L2HGDH	578380000
324	D3DR65;O75477;B2RDK6;B4DPN7	SPFH1;ERLIN1	573510000
325	A7E2D8;Q68DH9;A0A024R968;P23634;A8K8U3	ATP2B4;DKFZp686M088	562240000
326	Q7KZN9	COX15	553580000
327	P51571;A6NLM8	SSR4	553180000
328	D3DPC4;Q53R41	FLJ21901;FASTKD1	548180000
329	Q9H300;F8WCQ4;C9JNP8;H7C0U0	PARL	542500000
330	Q8NE86	MCU	537180000
331	A0A087WXM6;J3QQT2;J3KRX5;A0A024R261;A0A0A6YYL6;P18621;J3QLC8;A0A0A0MRF8;J3KRB3;A0A087WWH0;J3QS96;A0A087WY81	RPL17;hCG_24487;RPL17-C18orf32	537040000
332	A0A0S2Z433;O43181	NDUFS4	533560000

333	O95168;F2Z3P9;C9JXQ9	NDUFB4	526410000
334	Q96I51;A0A087WT38	WBSCR16	524350000
335	Q7LD69;O75251;F5H5N1;B7Z1U1;A8K0V6;Q8NAS7;Q9H3K5;A0A087WXF6;A0A087WTI3;F5GXJ1	NDUFS7	522760000
336	Q9NX00	TMEM160	520610000
337	P46199;Q6P1N2;Q8IWH1;H7C213	MTIF2	518810000
338	B4E0L2;Q8NFF3;A0A0A0MRG8;A8K7S8;A0A0S2Z391;A0A0S2Z319;Q16611;Q5HCI0;B3KRK7;B4DEB4	BAK;BAK1;DKFZp686D0345	515030000
339	Q53GB9;A0A024R8Z1;Q5VV89;O14880;Q5VV87	MGST3	512630000
340	I6L975;Q3SXM5	HSDL1	505350000
341	Q9Y6H1;Q5T1J5	CHCHD2;CHCHD2P9	502190000
342	B3KQF0;A0A0S2Z5M1;Q9UGP8;B3KNE7	SEC63	497220000
343	Q5JTZ9	AARS2	496950000
344	J3QL56;O75880	SCO1	496850000
345	Q32Q12;Q6FHN3;P22392;J3KPD9;E7ERL0;O60361	NME1-NME2;NME2;NME1;NME2P1	494270000
346	O60830;V9GYS0	TIMM17B	482350000
347	Q6IAX2;P46778;Q59GK9	RPL21	472460000
348	O00469;E7ETU9;B4DHG3	PLOD2	466150000
349	Q8IXI2;H7BXZ6	RHOT1	466030000
350	V9HW35;P30044	HEL-S-55;PRDX5	460750000
351	Q6IPT9;Q6IPS9;Q53HR5;Q53HQ7;Q53HM9;Q53GE9;Q53G85;P68104;A8K9C4;Q6IPN6;Q53GA1;Q5VTE0;B4DNE0;Q96RE1;A0A087WVQ9;Q8IUB0;B4DV42;Q53HR1;A0A087WV01;Q9H2I7;Q53G89;Q96C29;Q8TBL1;Q6P082;Q96CD8;Q6P4C9;Q504Z0;Q9NZS6;Q16577;Q05639	EEF1A1;EEF1A1P5;EEF1A1L14;PTI-1;EEF1A2	457550000
352	A0A024R745;Q16718;F8WAS3;A0A087X1G1;H7BYD0	NDUFA5	451990000
353	A0A024R9K7;Q9NPA0;H0YDT8;H0YDX2	C15orf24;EMC7	450830000
354	P78527	PRKDC	445820000
355	Q9UQ90	SPG7	445720000
356	Q5JR94;P62241;Q5JR95;Q9BS10	RPS8	440600000
357	Q96BQ5	CCDC127	439750000
358	B3KM34;O75439;Q96CP5;G3V0E4;A8K1E9;B4DM90;Q9UG64;B3KQ85	PMPCB;DKFZp586I1223	438520000
359	Q6NUM7;A0A024R640;Q9NUQ2	AGPAT5	430970000
360	Q14165;F5H1S8	MLEC	425670000
361	P11182;Q5VVL7;B4E1Q7	DBT	420700000
362	Q96CS3	FAF2	420660000
363	Q8TBK5;Q8N5Z7;A0A024RBK3;Q9HBB3;Q02878;B2R4K7;B4DRX3	RPL6	417600000
364	Q8TCJ2	STT3B	416120000
365	Q0D2M2;B2R4S9;A8K9J7;A0A024RCL8;A0A024RCJ9;A0A024QZZ7;I6L9F7;U3KQK0;B4DR52;Q99880;Q99879;Q99877;Q93079;Q5QNW6;P62807;P58876;P57053;O60814;A0A024RCJ2;Q16778;P33778;P23527;P06899;Q96A08;Q8N257	HIST1H2BC;HIST1H2BI;HIST1H2BK;HIST1H2BN;HIST1H2BD;HIST1H2BM;HIST1H2BL;HIST1H2BH;HIST2H2BF;H2BFS;HIST1H2BJ;HIST2H2BE;HIST1H2BB;HIST1H2BO;HIST1H2BA;HIST3H2BB	415350000
366	Q9NUF9;Q13232;H3BPR2	c371H6.2;NME3	415260000
367	Q96BW9;A0A0G2JQ92	TAMM41	404040000
368	E7ETY2;Q13428;B4DRA2;J3KQ96	TCOF1	402140000
369	Q9E29;E5RIY4;E5RIK9	MTERF3	399850000
370	Q3KRB6;Q9NVA1;B1AKV3;F6UTR7;B1AKV3;B7Z314;Q59FR0;B1AKV2;B1AKV6	UQCC;UQCC1	389290000
371	Q96CU9;B4DXM1;B4DI59;B4DQI0	FOXRED1	386860000
372	B0ZBD0;Q8WVX7;P39019	RPS19	382090000
373	O75394	MRPL33	381250000
374	F5GXX5;P61803;Q53G02;F5H895;A0A0B4J239	DAD1	381030000
375	Q96A33	CCDC47	378450000
376	F5GX99	CLPB	371590000
377	CON__P02533;P02533	KRT14	371420000
378	K7ERI7;Q7Z4W8;P35268;K7EP65;K7EKS7;K7ELC4;K7EMH1;K7EJT5	RPL22	369620000
379	Q9HC36;I3L443	RNMTL1	368060000
380	Q9UG56;A0A024R1K5;B4DPS3;H0Y7P7;B1AKM8;B1AKM6	PISD	366060000
381	Q5HYK3;F8VVX6;B4DP72	COQ5	364350000
382	A0A024R3R5;Q14739	LBR	364240000
383	Q8IVS2	MCAT	363440000
384	Q9NZJ6	COQ3	362980000
385	Q9H3N1;B4DZX7	TMX1;TXNDC	360880000
386	A0A0S2Z3L0;P13804;A0A0S2Z3M4;H0YLU7;H0YK49;H0YL12;H0YNX6;H0YKF0	ETFA	360350000
387	A0A024RAA0;Q969V5;B7Z8S4;B4DE24	C1orf166;MUL1	359030000
388	Q9UNM1;P61604;B8ZZL8;A0A024R3X7;S4R3N1	EPFP1;HSPE1;HSPE1-MOB4	358260000
389	B3KNF6;B4DR61;P61619;B3KQ68;F8W776;Q8TC24;Q9H9S3	SEC61A1;SEC61A2	357880000
390	Q9H061;E9PI90	TMEM126A	355070000
391	Q7L0Y3;C9JVB6	TRMT10C	350880000
392	Q96NB2;A0A1B0GX61;R4GMW0;A0A0C4DGR6	SFXN2	347570000
393	Q6YN16;B2R923;A0A024R159;B4E136;B4DWC7	HSDL2	347170000
394	C9J3L8;C9J5W0;B2R6N9;E9PAL7;C9IZQ1;P43307	SSR1	346960000
395	A0A0A8K8N9;Q4G0I0;H3BP47	URLC5;CCSMST1;C16orf91	345860000
396	Q9P2B2	PTGFRN	342820000
397	A3KPC7;A0A024RAS2;Q08AJ9;B2R5B3;A4FTV9;A0A024R017;A0A0U1RR32;A0A0U1RRH7;Q99878;Q96KK5;Q9BTM1;Q16777;Q93077;Q7L7L0;Q6FI13;P20671;P0C0S8;P04908;H0YFX9;B4E0B3;C9J0D1;B2R5B6;Q71UI9;P0C0S5;Q96QV6;P16104	HIST1H2AH;H2AFJ;HIST1H2AB;HIST1H2AK;HIST1H2AC;HIST1H2AJ;HIST2H2AC;HIST3H	342390000

		2A;HIST2H2AA3;HIST1H2AD;HIST1H2AG;H2AFV;H2AFZ;HIST1H2AA;H2AFX	
398	A0A0G2JNZ2;A0A0G2JPP5;Q14160;A0A0G2JMS7	SCRIB	341020000
399	Q96D53	ADCK4	339820000
400	A0A024QZN7;Q9NZ45	C10orf70;CISD1	335990000
401	Q6L8Q7;F6T1Q0	PDE12	333490000
402	B4DKN9;Q5JR08;A0A024R324;A0A024R0I3;P61586;P08134;Q5JR07;C9JNR4;E9PQH6;C9JX21;Q5JR05;Q9BVT0	RHOC;RHOA;hCG_2043376;ARHA	333450000
403	B2RA56;Q969V3;K7EMW4;K7ELZ9;A0A0C4DGP7	NCLN	328200000
404	A0A024R4M8;Q8NBN7;B2RDH1;G8JLA1	RDH13	326570000
405	Q53HG5;A8K4K9;Q15006	EMC2	324150000
406	A0A024R1U4;P51148;K7ERI8;K7ERQ8;F8VVK3;K7ENY4	RAB5C	324140000
407	Q02543;M0R3D6;M0R1A7;M0R117;B4DM74;Q53HD3;B2R4C0;B4DM94;B4DUV3;M0R0P7;Q32XH3	RPL18A	317590000
408	C9J9K3;A0A024R2P0;A0A0C4DG17;P08865;Q96RS2;A0A024R7P5	RPSA;LOC388524	314650000
409	O14561;H3BNK3	NDUFAB1	305260000
410	A0A024R886;O95900	TRUB2	303740000
411	O43819	SCO2	300370000
412	J3KN36;P69849;Q5JPE7;Q1LZN2	NOMO3;NOMO2	299160000
413	P29966;Q6NVI1	MARCKS	292370000
414	B3KUD0;A0A024RAE5;Q53S58	MGC10993;TMEM177	291750000
415	A0A024R2F9;Q9BTV4;Q8TEP9;A0A0S2Z5N2	TMEM43;FLJ00144	287260000
416	A0A024RB99;V9HW06;P34897;Q53ET4;Q5HYG8;B4DJQ3;B4E1G2;Q5BJF5;B4DP88;B4DWA7;B4DJ63;B4DW25;B4DLV4;H0YIZ0;G3V2Y4	SHMT2;HEL-S-51e;DKFZp686P09201	286890000
417	B4DP48;Q8IUX1;E9PKZ9;E9PJQ6;E9PKZ7	TMEM126B	285560000
418	A0A0S2Z3S5;A0A0S2Z3H8;P63092;Q5JWF2;B0AZR9;Q5FWY2;Q14455;O60726;A0A0A0MR13	GNAS;GSA	283550000
419	Q86UT6;B7Z889	NLRX1	275580000
420	L0R6D7;Q96EX1;E5RH51	C1orf212;SMIM12	275060000
421	A0A024R8Z9;Q6PI48;A8K4A8;Q9H9J7;Q9NVT8	DARS2	274800000
422	A0A0S2Z3H3;P12235;A8K787;V9GYG0;A0A0S2Z359;Q59EP7	SLC25A4	273570000
423	Q969Y2	GTPBP3	270490000
424	A8K9T3;P33121;E7EPM6;B4E0R0;B7Z3Z9	ACSL1	268240000
425	Q14257;A8MXP8	RCN2	267510000
426	A8K337;Q86VU5;R4GNF4	COMTD1	259620000
427	P15531	NME1	254920000
428	O75600	GCAT	254520000
429	P60866;E5RJX2;E5RIP1	RPS20	252770000
430	Q6FG42;Q32Q14;O95182;Q6IB89;M0R0N0	NDUFA7	251940000
431	P23396;Q53G83;E9PL09;E9PPU1;F2Z2S8;H0YCJ7;A7E2S3;Q9NQS8;H0YEU2	RPS3	251350000
432	Q8N0V3	RBFA	250870000
433	P08754	GNAI3	246710000
434	Q9Y2Z9;A0A0D9SFJ1	COQ6	245220000
435	A0A024RD80;P08238;B4DMA2;B4DGL0;Q6PK50	HSP90AB1	244650000
436	O15439;O75555;A8K2Q2;Q59GY6	ABCC4;MOAT-B	238870000
437	B4DRR0;CON__P02538;A8K2I0;A0A0S2Z428;P02538;CON__P48668;P48668;B4DRU6;B2R853;B4DWU6;B4DRY0	KRT6A;KRT6C	237370000
438	Q5CAQ5;V9HWP2;P14625;Q59FC6;B4DU71	TRA1;HEL-S-125m;HSP90B1	236560000
439	E9PJK1;E9PRJ8;H0YDL9;H0YDJ9;A0A024RCB7;E9PIF1;A6NMH8;P60033	CD81	236160000
440	Q9NVT9;E5RJ86	ARMC1	235890000
441	P42766;F2Z388;A0A024R866;A4D2M5	RPL35;LOC154880	231410000
442	O75323	GBAS	228170000
443	A0A0S2Z5V5;A0A0S2Z5L8;Q9H7H0;G3V353;G3V4P2;G3V3X6	METTL17	227670000
444	A8K0D2;A0A024R5F7;Q9UBM7;X5DNI9;B4E1K5;E9PM00;X5DRD7	DHCR7	227300000
445	A0A090N7U2;A0A024RA81;X6RM59;Q9H0P0;B9A035	NT5C3;NT5C3A	225170000
446	P62249;M0R210;A0A087WZ27;M0R3H0;Q6IPX4	RPS16;ZNF90	223970000
447	Q8WUK0;B4DGK8	PTPMT1	223650000
448	P62906;Q1JQ76	RPL10A	221760000
449	O15091	KIAA0391	221640000
450	A0A024RDH8;P49207	RPL34	219450000
451	B3KSN3;Q8N1X3;Q9NUT2	ABCB8	218430000
452	I3L072;A0A024R8P4;Q9BSJ5;B7Z7E5	C17orf80	214240000
453	M0QWZ7;Q9NP81;M0R2C6;B4DXB9;B4DJM9	SARS2	213770000
454	B3KN09;Q9Y2C4	EXOG	209250000
455	Q96RL7;A0A024R238;A0A024R223	VPS13A	206560000
456	A0A024R1N1;P35579;A0A0U4BW16;Q86XU5	MYH9	204250000
457	A0PJW6	TMEM223	203490000
458	Q6FHM4;P10606;Q6FHJ9	COX5B	200050000
459	Q9UII2	ATPIF1	199860000
460	Q6P087;A8K773;C9JM75;H7C454	RPUSD3	195500000
461	A0A140VJQ4;P04181;Q59HE2	OAT	192300000
462	P49748;B3KPA6;Q53HR2;B4DEA8;B3KPX1	ACADVL	185960000
463	A0A024R1E4;Q9UDX5;B5MC22;H7C417	MTP18;MTFP1	183420000
464	C9JXB8;C9JNW5;V9HW01;P83731	RPL24;HEL-S-310	183000000
465	Q6NXR8;A8K4W0;P61247;D6RG13;D6RAT0;B7Z3M5;D6RB09;E9PFI5;H0Y9Y4;H0Y8L7;D6R9B6;D6RAS7	RPS3A	181100000
466	A6QKW0;A0A024R9W7;P57088;D6RAA6	SHINC3;TMEM33	181080000

467	Q5QTS3;P40429;Q9BSQ6;Q53H34;M0QYS1;Q8J015;Q0VGL3	RPL13A;RPL13a	179870000
468	B7ZL88;Q8N8Q8	COX18	178640000
469	B7ZBH1;P56537;F8WD20;B4DJH0;A0A0B4J1Y7;F8WDS6	EIF6	177060000
470	B3KM21;Q5RI15	FAM36A;COX20	176940000
471	Q9BSY0;A8KAH1;P48651	PTDSS1	174950000
472	A4D1E9;C9J8R7;C9JNI1	GTPBP10	171200000
473	Q969Z3;F6V6Z1	02. Mrz	170560000
474	Q13724;Q58F09;C9J8D4;A8K9K4	MOGS;GCS1	169690000
475	B4DDB9;A0A087WUC6;E9PI68;Q15005;E9PL01;H0YE04	SPCS2	166340000
476	A0A024R0K4;B4DNR0;Q9NW81;M0QZP7;M0QZC4;K7EIV4;B4DFT4;B7ZAJ8	FLJ10241;ATP5SL	161720000
477	Q59FM5;P29992;K7EL62	GNA11	160730000
478	Q9P0I2;S4R3U9;C9JLM9	EMC3	160030000
479	B2R728;A0A024RDQ9;P30825;A0A0A8K9B7	SLC7A1	158160000
480	Q9HD23;B4DSN2;A0A0A0MQX2	MRS2	156620000
481	A0A024R6I3;Q53GF9;P49755;G3V2K7;B4DL12	TMED10	155590000
482	Q9HDC9;H0Y512	APMAP	154310000
483	A0A024R8M0;Q14344;B4DWV9	GNA13	152220000
484	Q8N5K1;I3L1N9;D6RCF4	CISD2	147350000
485	A0A024R2Q4;P61313;E7EQV9;E7ENU7;B4DLP4;E7EX53	RPL15	144020000
486	Q9HAV0;A8K3F6	GNB4	135560000
487	A8K900;U3KQ69;E9PI62;B3KWF9	MTG1	135250000
488	Q9H7Z7;B3KPZ2;A6NHH0;B4DWP1	PTGES2	135190000
489	B4DSA4;Q7KZA3;Q53FU1;P22830;Q5TZY0	DKFZp686P18130;FECH	134780000
490	B4DK94;E9PH70;Q9ULH0;B4DGY1;H0Y8E4	KIDINS220	125300000
491	Q05DB2;Q9HCU5;A8K813;B5MC98	PREB	121750000
492	A0A140VK65;P21281;B4DFM5;B4DQI9	ATP6V1B2	118770000
493	CON__P13647;P13647;B4E1T1;B4DL32	KRT5	118130000
494	E7D7X9;A0A024R8U9;P32322;E2QRB3;E7D7Y0;A0A1B2JLU7;J3KQ22;Q8TBX0;J3QKT4;J3QL24;B7Z8T1	PYCR1	117450000
495	Q53RX3;Q9HBH5	RDH14	116910000
496	A0A087X2D0;B2R6F3;P84103	SRSF3;SFRS3	116480000
497	Q49AG2;B4DDR7;Q9Y3A6	TMED5	113910000
498	E1NZA1;Q92616;A0A024RBS1	PRIC295;GCN1L1	113270000
499	B3KX11;Q59H77;P49368;Q2TU64;B4DUR8	CCT3	112720000
500	P61026;Q53T70	RAB10	112530000
501	F8VZA2;B7Z7F8;B2RCH7;Q6P1Q0;F8VP71;F8VVQ3;H0YIV5;F8W1Z2;B7Z7E4	LETMD1	111130000
502	CON__Q86YZ3;Q86YZ3	HRNR	100700000
503	A0A0S2Z366;Q5T4U5;Q5HYG7;P11310;B7Z9I1;B4DWX6;B4DJE7;B4DVE0	ACADM;DKFZp686M24262	100230000
504	Q96DV6;A2A3R6;P62753;A2A3R5;A2A3R7	RPS6	99092000
505	P50991;A8K3C3;B7Z9L0;B7Z2Z8;B7Z2F4	CCT4	83818000
506	A6NEM5;Q92643	PIGK	81471000
507	P36551	CPOX	68832000
508	Q96IR1;Q53HV1;B2R491;P62701	RPS4X	60676000
509	A8K1C7;A0A024R892;Q8IWT6	LRRC8A	47109000
510	B3KNH1;A0A024R8D2;Q6P1M0	SLC27A4	16345000

Supp. Table 3: MS-analysis of 633 pmol purified 55S mitoribosomes. Mitoribosomal proteins are highlighted in green, 80S ribosomal proteins in grey.

#	iBAQ 2h	Majority protein IDs	Gene names
1	31.70956	P08559	PDHA1
2	31.26657	P11177	PDHB
3	30.7823	P52815	MRPL12
4	29.87173	Q13405	MRPL49
5	29.75307	P10515	DLAT
6	29.74124	Q9BQC6	MRPL57
7	29.62305	Q9Y2R9	MRPS7
8	29.54736	O75394	MRPL33
9	29.39901	Q96EL3	MRPL53
10	29.3973	Q8N983	MRPL43
11	29.38837	Q8IXM3	MRPL41
12	29.28654	Q9BYD1	MRPL13
13	29.2693	Q9Y3B7	MRPL11
14	29.24692	Q6P1L8	MRPL14
15	29.24425	P82663	MRPS25
16	29.23649	Q9NX20	MRPL16
17	29.20464	Q13084	MRPL28
18	29.17657	Q96BP2	CHCHD1
19	29.1049	Q9Y3D3	MRPS16
20	29.07969	Q14197	ICT1
21	29.05064	Q9BYC9	MRPL20
22	29.03438	Q9P015	MRPL15
23	29.02078	Q9H0U6	MRPL18
24	28.98972	Q9NRX2	MRPL17
25	28.96947	Q9H2W6	MRPL46
26	28.96782	Q9BYC8	MRPL32
27	28.9526	Q9NWU5	MRPL22
28	28.87596	Q9Y676	MRPS18B
29	28.83936	Q96A35	MRPL24
30	28.81635	Q9BYN8	MRPS26
31	28.81048	Q9BZE1	MRPL37
32	28.80858	Q96GC5	MRPL48
33	28.78628	Q9Y6G3	MRPL42
34	28.75675	Q9BQ48	MRPL34
35	28.64034	P82914	MRPS15
36	28.62774	Q9NVS2	MRPS18A
37	28.60601	P82930	MRPS34
38	28.60523	Q8N5N7	MRPL50
39	28.58484	Q96DV4	MRPL38
40	28.58212	Q9BYD6	MRPL1
41	28.56627	Q9BYD2	MRPL9
42	28.56376	Q9Y3D9	MRPS23
43	28.53916	Q9Y399	MRPS2
44	28.48316	P82650	MRPS22
45	28.47816	Q9P0M9	MRPL27
46	28.45411	Q9NYK5	MRPL39
47	28.38072	Q9HD33	MRPL47
48	28.37886	Q92552	MRPS27
49	28.33994	Q9NQ50	MRPL40
50	28.33313	Q9NP92	MRPS30
51	28.2961	Q5T653	MRPL2
52	28.28352	P09001	MRPL3
53	28.22683	P82675	MRPS5
54	28.2243	P82921	MRPS21
55	28.19676	P51398	DAP3
56	28.16557	P82932	MRPS6
57	28.11466	P49406	MRPL19
58	28.07311	P82933	MRPS9
59	28.02512	Q9BRJ2	MRPL45
60	28.00072	Q9H9J2	MRPL44
61	27.95604	P82673	MRPS35
62	27.93365	Q7Z2W9	MRPL21
63	27.92926	Q8TCC3	MRPL30
64	27.82899	Q96EY7	PTCD3
65	27.74957	Q7Z7F7	MRPL55
66	27.69511	P82912	MRPS11
67	27.62366	Q8TAE8	GADD45GIP1
68	27.53408	Q9BYD3	MRPL4
69	27.45654	O00330	PDHX
70	27.44987	Q4U2R6	MRPL51
71	27.44134	Q9Y2R5	MRPS17
72	27.41296	Q16540	MRPL23

73	27.38311	Q7Z7H8	MRPL10
74	27.36328	Q9GZT3	SLIRP
75	27.27932	O15235	MRPS12
76	27.15374	O60783	MRPS14
77	27.14034	Q96EL2	MRPS24
78	26.99442	P42704	LRPPRC
79	26.87479	Q15120	PDK3
80	26.84002	Q6P161	MRPL54
81	26.78905	P82664	MRPS10
82	26.77744	Q9Y2Q9	MRPS28
83	26.49886	Q9NZE8	MRPL35
84	26.48342	Q92665	MRPS31
85	26.42084	P25705	ATP5A1
86	25.94862	Q9NWT8	AURKAIP1
87	25.86252	Q9Y291	MRPS33
88	25.64417	P06576	ATP5B
89	25.40454	P56385	ATP5I
90	25.38703	Q07020	RPL18
91	25.29158	Q15118	PDK1
92	25.11985	O75947	ATP5H
93	25.02901	Q04837	SSBP1
94	24.97215	P24539	ATP5F1
95	24.94244	P09622	DLD
96	24.87905	P62805	HIST1H4A
97	24.83557	P42766	RPL35
98	24.79054	Q99880;Q99879;Q99877;Q93079;Q5QNW6;Q16778;P62807;P58876;P57053;P33778;P23527;P06899;O60814;Q8N257;Q96A08	HIST1H2BL;HIST1H2BM;HIST1H2BN;HIST1H2BH;HIST2H2BF;HIST2H2BE;HIST1H2BC;HIST1H2BD;H2BFS;HIST1H2BB;HIST1H2BO;HIST1H2BJ;HIST1H2BK;HIST3H2BB;HIST1H2BA
99	24.7755	O75964	ATP5L
100	24.65327	P30049	ATP5D
101	24.64559	P47813;O14602	EIF1AX;EIF1AY
102	24.50118	Q99878;Q96KK5;Q9BTM1;Q16777;Q93077;Q7L7L0;Q6FI13;P20671;P0C0S8;P04908;Q71UI9;P0C0S5;Q8IUE6;Q96QV6;P16104	HIST1H2AJ;HIST1H2AH;H2AFJ;HIST2H2AC;HIST1H2AC;HIST3H2A;HIST2H2AA3;HIST1H2AD;HIST1H2AG;HIST1H2AB;H2AFV;H2AFZ;HIST2H2AB;HIST1H2AA;H2AFX
103	24.47933	P36542	ATP5C1
104	24.44683	Q9P0J6	MRPL36
105	24.41944	P55084	HADHB
106	24.37252	P61353	RPL27
107	24.34962	P18859	ATP5J
108	24.25379	P62241	RPS8
109	24.24205	Q9Y3U8	RPL36
110	24.24031	P40939	HADHA
111	24.23191	P62888	RPL30
112	24.15846	P35268	RPL22
113	24.13759	P48047	ATP5O
114	24.09321	Q02878	RPL6
115	23.98233	P62917	RPL8
116	23.92016	P62906	RPL10A
117	23.8447	Q9H307	PNN
118	23.84412	Q9BV38	WDR18
119	23.78716	P62913	RPL11
120	23.6904	P61513	RPL37A
121	23.6621	P50914	RPL14
122	23.66112	P62910	RPL32
123	23.62945	P46776	RPL27A
124	23.61639	P62750	RPL23A
125	23.53683	P46778	RPL21
126	23.53647	P18077	RPL35A
127	23.48898	P61254;Q9UNX3	RPL26;RPL26L1
128	23.48198	P46777	RPL5
129	23.47098	Q96IX5	USMG5
130	23.46239	P62424	RPL7A
131	23.43644	Q5VTU8;P56381	ATP5EP2;ATP5E
132	23.43352	Q96EH3	MALSU1
133	23.43059	P35232	PHB
134	23.35097	P36957	DLST
135	23.34584	Q7L2E3	DHX30
136	23.31769	P05387	RPLP2
137	23.25983	P49207	RPL34
138	23.24811	P10809	HSPD1
139	23.23065	P62851	RPS25
140	23.2076	P26373	RPL13
141	23.15202	P38646	HSPA9
142	23.09917	P12236;P12235	SLC25A6;SLC25A4
143	23.04647	P27635;Q96L21	RPL10;RPL10L
144	23.02401	P30050	RPL12
145	22.95026	Q92522	H1FX

146	22.91803	P18124	RPL7
147	22.91055	P25398	RPS12
148	22.89464	P03928	MT-ATP8
149	22.84031	P62753	RPS6
150	22.81839	Q5SSJ5	HP1BP3
151	22.81173	Q00325	SLC25A3
152	22.8041	Q969Q0;P83881	RPL36AL;RPL36A
153	22.75719	Q96HS1	PGAM5
154	22.70172	P61313	RPL15
155	22.70085	Q99623	PHB2
156	22.62776	P56134	ATP5J2
157	22.53825	P62263	RPS14
158	22.43288	Q15119	PDK2
159	22.39362	P36578	RPL4
160	22.36666	Q5VTE0;P68104;Q05639	EEF1A1P5;EEF1A1;EEF1A2
161	22.33786	P62899	RPL31
162	22.31976	P39019	RPS19
163	22.30958	P62266	RPS23
164	22.28608	P32969	RPL9
165	22.25825	Q9P2P6	STARD9
166	22.24658	P15880	RPS2
167	22.15026	P84103	SRSF3
168	22.1456	Q86TS9	MRPL52
169	22.14071	P18621	RPL17
170	22.08771	A4D1E9	GTPBP10
171	22.05441	P84098	RPL19
172	21.99317	P05388;Q8NHW5	RPLP0;RPLP0P6
173	21.97715	P60866	RPS20
174	21.96677	P40429;Q6NVV1	RPL13A;RPL13AP3
175	21.96109	Q96E11	MRRF
176	21.95649	P00846	MT-ATP6
177	21.818	P63244	GNB2L1
178	21.74041	P83731	RPL24
179	21.73554	Q6NXT2;Q71DI3;Q16695;P84243;P68431	H3F3C;HIST2H3A;HIST3H3;H3F3A;HIST1H3A
180	21.71104	P23396	RPS3
181	21.45091	P39023	RPL3
182	21.42332	P62854;Q5JNZ5	RPS26;RPS26P11
183	21.33887	P63173	RPL38
184	21.28709	P63261;P60709	ACTG1;ACTB
185	21.26327	P61247	RPS3A
186	21.24226	P62269	RPS18
187	21.2089	O43491	EPB41L2
188	21.19538	Q15070	OXA1L
189	21.19123	P46781	RPS9
190	21.17292	P35659	DEK
191	21.15993	P46779	RPL28
192	21.05874	P67809;Q9Y2T7;P16989	YBX1;YBX2;YBX3
193	21.03523	P82909	MRPS36
194	20.99479	Q9Y3D5	MRPS18C
195	20.97379	P62249	RPS16
196	20.94999	Q9HC36	RNMTL1
197	20.8833	Q7Z6M4	MTERF4
198	20.87395	O00411	POLRMT
199	20.79313	O95900	TRUB2
200	20.78469	P16403;P10412;P16402	HIST1H1C;HIST1H1E;HIST1H1D
201	20.74238	P08865	RPSA
202	20.73298	Q96CB9	NSUN4
203	20.70616	Q9UDW1	UQCR10
204	20.69183	P49411	TUFM
205	20.6696	Q96C36	PYCR2
206	20.5996	Q02218	OGDH
207	20.46294	P62829	RPL23
208	20.42039	P46199	MTIF2
209	20.38416	Q8N0V3	RBFA
210	20.35971	P55265	ADAR
211	20.31761	Q13243;Q13247;Q08170	SRSF5;SRSF6;SRSF4
212	20.26774	P62277	RPS13
213	20.13308	Q5T9A4	ATAD3B
214	20.10034	P62701	RPS4X
215	20.0458	Q16718	NDUFA5
216	20.02594	P62244	RPS15A
217	19.92483	Q96H55	MYO19
218	19.89239	Q16656	NRF1
219	19.82672	P11171;Q9H4G0	EPB41;EPB41L1
220	19.82616	P21796	VDAC1
221	19.78526	Q12849	GRSF1

222	19.76408	Q08380	LGALS3BP
223	19.59909	Q8TEM1	NUP210
224	19.37922	Q16891	IMMT
225	19.3342	Q9Y2J2	EPB41L3
226	19.30566	P08708	RPS17
227	19.28688	O75616	ERAL1
228	19.21966	P30086	PEBP1
229	19.04346	Q02543	RPL18A
230	18.98387	Q9Y4F1	FARP1
231	18.90457	Q8IYB8	SUPV3L1
232	18.75825	Q9NUL7	DDX28
233	18.60266	P46782	RPS5
234	18.49884	P45880	VDAC2
235	18.38254	Q96I51	WBSCR16
236	18.29244	Q02978	SLC25A11
237	18.10585	P13637	ATP1A3
238	18.03666	Q96E29	MTERF3
239	17.97141	Q9HCC0	MCCC2
240	17.89723	Q9UDR5	AASS
241	17.87616	P27694	RPA1
242	17.72314	Q9H845	ACAD9
243	17.62913	O75306	NDUFS2
244	17.45523	O76021	RSL1D1
245	17.4416	Q9Y305	ACOT9
246	17.36521	Q9NYY8	FASTKD2
247	17.26059	Q9NVV4	MTPAP
248	17.21731	Q9BU76	MMTAG2
249	17.16133	Q8NC60	NOA1
250	17.06118	P05023;P50993	ATP1A1;ATP1A2
251	16.99976	Q8IVS2	MCAT
252	16.81315	Q96CM3	RPUSD4
253	16.65843	O75489	NDUFS3
254	16.5989	Q9UJS0;O75746	SLC25A13;SLC25A12
255	16.36441	P43304	GPD2
256	15.99577	P19338	NCL
257	15.0789	Q08AE8	SPIRE1

Supp. Table 4: MS-analysis data of fraction 2 and 3 of mL44⁻/⁻R FLAG-IP eluate separated by sucrose density gradient centrifugation.

#	iBAQ L44R_2	iBAQ L44R_3	Majority protein IDs	Gene names
1	29.75097	27.7999	Q9H9J2	MRPL44
2	28.99197	28.56446	P50796	N/A
3	28.28299	29.56085	Q07021	C1QBP
4	27.22325	27.14307	Q99880;Q99879;Q99877;Q93079;Q5QNW6;P62807; P58876;P57053;O60814;Q96A08	HIST1H2BL;HIST1H2BM;HIST1H2BN; HIST1H2BH;HIST2H2BF;HIST1H2BC; HIST1H2BD;H2BFS;HIST1H2BK;HIST 1H2BA
5	26.61779	27.07755	P62805	HIST1H4A
6	26.29889	26.43744	Q99878;Q96KK5;Q9BTM1;Q16777;Q93077;Q7L7L0; Q6FI13;P20671;P0C0S8;P04908;Q71UI9;P0C0S5;Q 6QV6;P16104	HIST1H2AJ;HIST1H2AH;H2AFJ;HIST2 H2AC;HIST1H2AC;HIST3H2A;HIST2H 2AA3;HIST1H2AD;HIST1H2AG;HIST1 H2AB;H2AFV;H2AFZ;HIST1H2AA;H2 AFX
7	25.67481	26.08361	Q8N983	MRPL43
8	25.61583	25.33797	P60709	ACTB
9	25.59719	25.69795	P62987;P62979;P0CG47;P0CG48	UBA52;RPS27A;UBB;UBC
10	25.416	26.416	Q9Y6G3	MRPL42
11	25.25879	25.21308	Q71DI3;Q16695;P84243;P68431;Q6NXT2	HIST2H3A;HIST3H3;H3F3A;HIST1H3 A;H3F3C
12	24.84484	24.80799	P62937	PPIA
13	24.64075	24.48603	P04406	GAPDH
14	24.60332	24.78157	Q7Z2W9	MRPL21
15	24.28828	24.5484	Q9BYC9	MRPL20
16	24.05937	24.33354	P07737	PFN1
17	23.91534	24.09208	P68371;P04350	TUBB4B;TUBB4A
18	23.64735	23.62355	P06733	ENO1
19	23.45425	23.60738	Q9BQE3;P68363;Q71U36;P0DPH8;P0DPH7;P68366; Q6PEY2	TUBA1C;TUBA1B;TUBA1A;TUBA4A;T UBA3E
20	23.40549	23.15734	P38646	HSPA9
21	23.39754	23.27668	P62258	YWHAE
22	23.38851	23.32045	P06702	S100A9
23	23.30939	23.33142	Q5VTE0;P68104;Q05639	EEF1A1P5;EEF1A1;EEF1A2
24	23.18299	22.5302	Q8TEJ3	SH3RF3
25	23.17217	22.91727	Q5T749	KPRP
26	23.1553	24.68148	Q8N5N7	MRPL50
27	23.14238	23.15447	P05109	S100A8
28	23.10575	22.4267	P81605	DCD
29	22.96224	23.04609	P16403;P10412;P16402	HIST1H1C;HIST1H1E;HIST1H1D
30	22.94924	20.32356	P0DOX5;P01857	IGHG1
31	22.89099	22.79858	P00338	LDHA
32	22.78985	21.28421	P10809	HSPD1
33	22.72121	22.82893	Q5T2N8;Q5T9A4;Q9NVI7	ATAD3C;ATAD3B;ATAD3A
34	22.69799	21.22776	Q9P0W8	SPATA7
35	22.53055	21.08544	P30048	PRDX3
36	22.48141	22.6091	P05387	RPLP2
37	22.41119	21.77028	P06703	S100A6
38	22.38809	22.46954	P00558	PGK1
39	22.37838	22.01114	P26447	S100A4
40	22.29027	22.5858	P35908	KRT2
41	22.24118	21.06612	P14618	PKM
42	22.18544	22.2357	P07355;A6NMY6	ANXA2;ANXA2P2
43	22.17785	21.71846	P23490	LOR
44	22.09223	22.17889	P07437	TUBB
45	22.05857	21.70578	P60842;Q14240	EIF4A1;EIF4A2
46	22.03443	22.19934	Q32P51;P09651	HNRNPA1L2;HNRNPA1
47	21.99307	21.88498	P11021	HSPA5
48	21.97656	21.89404	P10599	TXN
49	21.91017	18.19282	Q9NZT1	CALML5
50	21.79685	22.071	Q02413	DSG1
51	21.77604	21.21567	A2NJV5;A0A0A0MRZ7;A0A075B6S2;A0A075B6S6;A 0A075B6P5;A0A087WW87;P06310;P01615;P01614	IGKV A18;IGKV2D-26;IGKV2D- 29;IGKV2D-30;IGKV2D-28;IGKV2-40
52	21.76166	0	Q9UMR3	TBX20
53	21.65827	20.87912	Q5T750	XP32
54	21.5775	21.11496	P06748	NPM1
55	21.55548	21.16638	P14174	MIF
56	21.50988	21.46389	P07195	LDHB
57	21.50019	21.4764	P08238	HSP90AB1
58	21.28923	21.40883	P14923	JUP
59	21.27162	21.42075	P22626	HNRNPA2B1
60	21.25534	21.18526	P62829	RPL23
61	21.23567	21.37231	P06454	PTMA
62	21.18247	20.34722	P06576	ATP5B
63	21.18132	18.02659	P61978	HNRNPK
64	21.177	20.70767	Q01469	FABP5
65	20.97883	21.22917	P11142;P54652	HSPA8;HSPA2
66	20.90713	17.38591	P35321;P22528	SPRR1A;SPRR1B
67	20.90588	17.62335	Q5VTQ0	TTC39B
68	20.90014	20.7725	Q06830	PRDX1

69	20.87493	19.30981	P31943	HNRNPH1
70	20.82811	20.72742	P01834;P0DOX7	IGKC
71	20.65211	16.65285	Q8TF66	LRRC15
72	20.62872	0	Q7Z6M4	MTERF4
73	20.62203	0	Q15208	STK38
74	20.58921	22.03446	P42704	LRPPRC
75	20.58435	20.67582	P31151	S100A7
76	20.55487	0	Q8N4Q1	CHCHD4
77	20.47368	20.70033	Q08554	DSC1
78	20.38248	20.52936	Q07020	RPL18
79	20.37029	20.61863	P15924	DSP
80	20.30986	20.08926	P31944	CASP14
81	20.21975	20.02662	P27797	CALR
82	20.19689	20.00388	P05141;P12236;P12235	SLC25A5;SLC25A6;SLC25A4
83	20.15301	16.7499	Q52LG2	KRTAP13-2
84	20.07822	19.50961	P22531;Q96RM1;P35326;P35325;P22532;Q9BYE4	SPRR2E;SPRR2F;SPRR2A;SPRR2B;SPRR2D;SPRR2G
85	20.03429	19.99493	Q86TJ2	TADA2B
86	19.99645	20.81206	P61626	LYZ
87	19.94489	17.00185	A4D1E9	GTPBP10
88	19.94407	14.04712	P98175	RBM10
89	19.80702	19.30577	P40926	MDH2
90	19.78155	19.80458	Q6ZVX7	NCCRP1
91	19.73569	20.05735	P47929	LGALS7
92	19.67716	20.32454	P07910;P0DMR1;O60812;B7ZW38;B2RXH8	HNRNPC;HNRNPCL4;HNRNPCL1;HNRNPCL3;HNRNPCL2
93	19.64408	19.12729	P30101	PDIA3
94	19.63382	0	Q3LI77	KRTAP13-4
95	19.63314	20.15351	P58557	YBEY
96	19.55268	19.10329	O00148;Q13838	DDX39A;DDX39B
97	19.54336	21.1322	Q8N257;Q16778;P33778;P23527;P06899	HIST3H2BB;HIST2H2BE;HIST1H2BB;HIST1H2BO;HIST1H2BJ
98	19.53345	20.02499	P17066;P48741	HSPA6;HSPA7
99	19.51002	20.00881	P0DP25;P0DP24;P0DP23	N/A
100	19.49806	18.56503	Q8IUC0	KRTAP13-1
101	19.44243	19.66308	P0DOX6;P01871	IGHM
102	19.43693	17.82009	P12273	PIP
103	19.43553	18.82128	A6NIE6	RRN3P2
104	19.40252	19.43311	P84103;Q16629	SRSF3;SRSF7
105	19.40129	19.8147	P16949	STMN1
106	19.37568	19.33893	P25311	AZGP1
107	19.36954	0	Q9BYR6	KRTAP3-3
108	19.34895	17.82706	P05089	ARG1
109	19.32733	19.50133	P39023	RPL3
110	19.30401	19.43906	Q96P63	SERPINB12
111	19.25863	17.3067	Q9BVA1;Q13885	TUBB2B;TUBB2A
112	19.23659	14.69343	Q96CB9	NSUN4
113	19.21124	19.4037	Q15517	CDSN
114	19.17726	18.74304	Q08188	TGM3
115	19.14068	20.7766	Q9BYD3	MRPL4
116	19.06442	17.74714	P04792	HSPB1
117	19.0615	17.43575	P01876	IGHA1
118	19.06121	17.29643	P23588	EIF4B
119	19.03389	19.68475	P14625	HSP90B1
120	19.01702	19.58542	Q13835	PKP1
121	18.98846	0	Q9Y2H1	STK38L
122	18.98008	15.31295	P62249	RPS16
123	18.94895	20.56402	P04259	KRT6B
124	18.93088	15.21777	Q9NQ50	MRPL40
125	18.8388	18.05277	Q96FQ6	S100A16
126	18.83037	18.58083	P30041	PRDX6
127	18.63612	0	P49411	TUFM
128	18.61479	19.07726	P08670	VIM
129	18.61414	18.05463	Q9Y2S7	POLDIP2
130	18.46965	0	Q15233	NONO
131	18.45129	15.66983	Q9H2W6	MRPL46
132	18.41378	16.31003	Q9HCY8	S100A14
133	18.40728	17.20448	Q6UB35	MTHFD1L
134	18.39477	0	P23526	AHCY
135	18.38368	18.32382	P63244	GNB2L1
136	18.35022	16.52794	P62917	RPL8
137	18.29648	18.59226	Q96SI9;Q12906	STRBP;ILF3
138	18.29235	17.73079	P22735	TGM1
139	18.28771	16.11933	Q99729	HNRNPAB
140	18.22034	17.80152	Q13867	BLMH
141	18.08892	17.33516	P62241	RPS8
142	17.99733	19.67211	P01040	CSTA

143	17.97651	18.21665	P31327	CPS1
144	17.96195	14.7601	Q9BXW7	CECR5
145	17.93526	0	Q9UQ80	PA2G4
146	17.84567	17.44152	P07237	P4HB
147	17.81265	0	Q13765;E9PAV3	NACA
148	17.79023	15.29785	P52597	HNRNPF
149	17.78033	0	P67809	YBX1
150	17.76694	16.47351	P13489	RNH1
151	17.75042	17.37696	Q99714	HSD17B10
152	17.7411	16.8572	P22392;P15531;O60361	NME2;NME1;NME2P1
153	17.73965	0	P12277	CKB
154	17.73443	15.72853	P61247	RPS3A
155	17.71827	18.79306	P30084	ECHS1
156	17.69493	16.55844	Q13185;P83916	CBX3;CBX1
157	17.65655	15.56727	P29508;P48594	SERPINB3;SERPINB4
158	17.64878	17.06687	P36578	RPL4
159	17.6416	0	P04181	OAT
160	17.63687	18.56763	P50914	RPL14
161	17.5813	15.36448	P25705	ATP5A1
162	17.5654	17.08742	P62857	RPS28
163	17.54525	0	Q16134	ETFDH
164	17.54435	0	Q8NHW5;P05388	RPLP0P6;RPLP0
165	17.49576	0	Q86U42	PABPN1
166	17.48219	18.17192	P00966	ASS1
167	17.47833	16.93468	O76031	CLPX
168	17.45282	15.45128	O75439	PMPCB
169	17.44071	19.48703	P19338	NCL
170	17.38119	0	P50991	CCT4
171	17.37984	16.60562	P62266	RPS23
172	17.32254	17.94037	P60174	TPI1
173	17.31717	0	P50990	CCT8
174	17.3131	17.79506	Q96QA5	GSDMA
175	17.29221	18.17908	Q01105;P0DME0	SET;SETSIP
176	17.27994	0	P23396	RPS3
177	17.27876	17.9398	Q00839	HNRNPU
178	17.26123	0	Q13253	NOG
179	17.22863	18.31725	P07339	CTSD
180	17.21077	0	O75223	GGCT
181	17.20151	0	P21796	VDAC1
182	17.18437	0	P19957	PI3
183	17.17172	19.1253	P55209;Q99733	NAP1L1;NAP1L4
184	17.15116	16.62156	Q58FF6	HSP90AB4P
185	17.09476	18.26151	P63104	YWHAZ
186	17.05123	14.71794	P31947	SFN
187	17.01433	0	P63261	ACTG1
188	17.00547	0	P01860	IGHG3
189	16.95742	0	O00231	PSMD11
190	16.89688	17.73925	P07196	NEFL
191	16.84512	0	O75390	CS
192	16.79271	0	P36957	DLST
193	16.77957	0	B2RPK0;P09429	HMGB1P1;HMGB1
194	16.77571	16.4064	P0DPA2	N/A
195	16.6937	0	P02787	TF
196	16.68236	17.63396	P84085;P84077;P61204;P18085	ARF5;ARF1;ARF3;ARF4
197	16.65564	14.8008	P38159;Q96E39	RBMX;RBMXL1
198	16.57805	0	P14866	HNRNPL
199	16.54656	15.45494	P09622	DLD
200	16.49659	0	P22234	PAICS
201	16.46609	0	O43175	PHGDH
202	16.45306	15.84975	P23528	CFL1
203	16.40065	0	P82663	MRPS25
204	16.36567	0	P78371	CCT2
205	16.33317	16.96815	Q8WVV4	POF1B
206	16.27997	17.18853	P61604	HSPE1
207	16.27832	0	Q9Y285	FARSA
208	16.2495	16.82786	P23284	PPIB
209	16.23628	15.59581	Q9BYD1	MRPL13
210	16.19871	17.79544	O75380	NDUFS6
211	16.10501	0	Q15750	TAB1
212	16.08417	17.87213	P02545	LMNA
213	16.05486	15.99214	Q8TDY2	RB1CC1
214	16.00018	17.33228	P04040	CAT
215	15.97116	13.88322	Q16610	ECM1
216	15.9679	0	P68133;P68032;P63267;P62736	ACTA1;ACTC1;ACTG2;ACTA2
217	15.90195	0	P11177	PDHB
218	15.84735	16.00233	P04075	ALDOA

219	15.80406	0	P17987	TCP1
220	15.70479	0	Q99832	CCT7
221	15.6839	0	Q12931	TRAP1
222	15.564	0	P52907;P47755	CAPZA1;CAPZA2
223	15.50786	0	P08559	PDHA1
224	15.50199	16.251	P0DMV9;P0DMV8	HSPA1B;HSPA1A
225	15.49101	0	Q9Y697	NFS1
226	15.4128	0	P40227	CCT6A
227	15.36208	0	Q99623	PHB2
228	15.31359	18.27876	P46821	MAP1B
229	15.23444	16.29004	P05783	KRT18
230	15.22581	0	Q8WWY3	PRPF31
231	15.03798	14.16992	Q10713	PMPCA
232	14.96862	0	P28482;P27361	MAPK1;MAPK3
233	14.83743	0	P02788	LTF
234	14.66634	15.72563	Q13263	TRIM28
235	14.60084	0	Q6UWP8	SBSN
236	14.43762	0	Q9P258	RCC2
237	14.39861	0	Q12849	GRSF1
238	14.28482	16.54249	P04083	ANXA1
239	14.2109	0	P42357	HAL
240	14.0892	0	Q9P270	SLAIN2
241	13.54774	15.20166	P27824	CANX
242	13.16219	0	Q8IVV2	LOXHD1
243	0	22.99774	Q96K30	RITA1
244	0	20.84866	Q13162	PRDX4
245	0	20.52373	P59666;P59665	DEFA3;DEFA1
246	0	19.15973	P02452	COL1A1
247	0	17.80826	O75531	BANF1
248	0	17.41568	P60866	RPS20
249	0	17.40291	P32119	PRDX2
250	0	16.8881	P15880	RPS2
251	0	16.5354	P08865	RPSA
252	0	16.39689	P01859;P01861	IGHG2;IGHG4
253	0	16.36441	Q86VM9	ZC3H18
254	0	16.2717	P62244	RPS15A
255	0	16.24552	Q08211	DHX9
256	0	16.16111	Q8NBS9	TXNDC5
257	0	16.15143	P27348;Q04917;P31946;P61981	YWHAQ;YWHAH;YWHAB;YWHAG
258	0	16.12089	P62913	RPL11
259	0	15.92539	Q13813	SPTAN1
260	0	15.84336	P30044	PRDX5
261	0	15.67052	P68871;P02042	HBB;HBD
262	0	15.61105	P29373	CRABP2
263	0	15.544	P52272	HNRNPM
264	0	15.43482	P34897;P34896	SHMT2;SHMT1
265	0	15.38033	P07900	HSP90AA1
266	0	15.35346	O60313	OPA1
267	0	15.1926	P82650	MRPS22
268	0	15.11939	P30876	POLR2B
269	0	15.1176	Q14257	RCN2
270	0	13.47991	Q9UH99	SUN2

8. Acknowledgements

At first, I want to thank Dr. Ricarda Richter-Dennerlein who provided me with the opportunity to work on this interesting project. Thank you for your great supervision, your advices regarding lab work, data presentation and writing and for your motivation when I struggled during mitoribosome isolations.

Next, I owe many thanks to the members of my thesis advisory committee: Prof. Dr. Marina Rodnina and Prof. Dr. Blanche Schwappach. Thank you for all your good suggestions and the challenging discussions during my thesis advisory committee meetings, which helped me to improve my scientific work. Especially, I also want to thank Prof. Dr. Heike Krebber for being my new second referee due to Prof. Dr. Schwappachs movement to Hamburg. In addition, I owe many thanks to Prof. Dr. Michael Meinecke, Prof. Dr. Ralph Kehlenbach and Prof. Dr. Henning Urlaub for agreeing to be in my extended examination board.

I thank Prof. Dr. Marina Rodnina for sharing her expert knowledge and her advice during establishing sucrose gradients and ribosome isolation protocols. Furthermore, I want to thank Dr. Ekaterina Samatova for helpful discussions and Sandra Kappler for giving me hands-on experience in ribosome purification procedures.

I owe many thanks to our collaborators Prof. Dr. Henning Urlaub and Dr. Andreas Linden for MS-analysis of my samples. Additionally, I thank Monika Raabe and Uwe Pleßmann for sample preparation prior mass spectrometry. I want to thank Lukas Schulte and Uma Lakshmi Dakshinamoorthy for their help to figure out the perfect sucrose concentration for mitoribosome isolations.

I would like to thank the GGNB and the SFB860 for providing support during my pregnancy. In addition, I would like to thank the GGNB office for their constant help regarding questions of the doctoral program. I owe many thanks for practical support during my pregnancy and maternity leave to Anna Teegen and Joana Oschwald. Thank you for casting uncountable gels for me. I could not have managed without you.

Many big thanks are going to all members of the research group of Dr. Ricarda Richter-Dennerlein. Especially, I want to thank Elena Lavdovskaia for helpful discussions and Mandy Mai, Franziska Nadler and Emely Steube for their help during ribosome isolation! Also, I am thankful to Dr. Cong Wang and Dr. Sven Dennerlein for many advices during the last years. I thank Amanda Ernst for proofreading this thesis. Last but not least, I want to thank my family for their constant support during my whole life and for taking care of Rosa, which enabled me to write this thesis. Stefan, thank you for always being there for me and Rosa for being the joy of my life! This thesis would not have been possible without you!

9. Curriculum Vitae

Elisa Hanitsch

Contact

Marienstr. 12
06844 Dessau-Roßlau

⌨ elisa.hanitsch@gmail.com

Profile

Born in 1990
in Lutherstadt Wittenberg

Name at birth: Kolander

Married, one daughter

Education

PhD Student
University Medical Center - Göttingen, Institute for Cellular
Biochemistry, Supervisor: Dr. Ricarda Richter-Dennerlein
$\qquad$ 10/2016 – 11/2020

Master Molecular Medicine
Georg-August-University Göttingen,
Degree: Master of Science (1.46)
$\qquad$ 10/2014 – 04/2016

Bachelor Biotechnology
Ernst-Abbe-Hochschule Jena,
Degree: Bachelor of Engineering (1.3)
$\qquad$ 10/2011 – 07/2014

Medical studies
Martin-Luther-University Halle-Wittenberg,
Degree: Preliminary medical examination
$\qquad$ 2008 – 2011

A-level
Europagymnasium „Walther Rathenau" Bitterfeld-Wolfen.
Grade: 1.4
$\qquad$ 2002 – 2008

Publications

Hanitsch, E., and Richter-Dennerlein, R. (2020). Biogenese der mitochondrialen
Proteinsynthesemaschine. BioSpektrum 26, 16–19.

Lavdovskaia, E., **Kolander, E.**, Steube, E., Mai, M.M.Q., Urlaub, H., and Richter-
Dennerlein, R. (2018). The human Obg protein GTPBP10 is involved in mitoribosomal
biogenesis. Nucleic Acids Res. 46, 8471–8482.